

**Cellular and molecular dynamics of splenic myeloid
cells during blood-stage malaria**

Katharina Mael

ORCID ID:

0009-0007-4879-032X

from Adenau, Germany

Submitted in total fulfilment of the requirements of the joint
degree of Doctor of Philosophy (PhD)

of

The Medical Faculty

The Rheinische Friedrich-Wilhelms-Universität Bonn

and

The Department of Microbiology and Immunology

The University of Melbourne

Bonn/Melbourne, 2024

Performed and approved by the Medical Faculty of The Rheinische Friedrich-Wilhelms-Universität and The University of Melbourne

1. Supervisor: Prof. Dr. Elvira Mass

2. Supervisor: Prof. Dr. Rayk Behrendt

Co-Supervisor: Dr. Lynette Beattie

Co-Supervisor: Prof. Dr. William Heath

Month and year of original thesis submission: 03/2024

Month and year of the oral examination: 10/2024

Institute in Bonn: Life & Medical Sciences Institute (LIMES)

Director: Prof. Dr. Waldemar Kolanus

Table of Contents

Abbreviations	VII
List of Tables	IX
List of Figures	X
Abstract	XII
Declaration	XIV
Preface	XV
Acknowledgements	XVI
List of Publications	XXVI
1 Introduction	1
1.2 Hematopoiesis.....	2
1.3 Macrophage ontogeny.....	4
1.3.1 Waves of macrophage development	4
1.3.1.1 Primitive hematopoiesis: first wave	5
1.3.1.2 Definitive hematopoiesis: second wave	5
1.3.1.3 Definitive hematopoiesis: third wave	5
1.3.2 Models to study macrophage ontogeny.....	7
1.3.2.1 Fate-mapping of HSC-derived cells	8
1.3.2.2 The double-fatemapper	10
1.4 Macrophages in infection and inflammation	13
1.5 The spleen.....	15

1.6 Splenic macrophages and functions	16
1.6.1 Splenic red pulp macrophages	17
1.6.1.1 Regulation of iron homeostasis by splenic red pulp macrophages	19
1.6.1.2 The CD163 receptor and hemoglobin uptake	21
1.6.2 Splenic marginal zone macrophages and marginal metallophilic macrophages	23
1.6.3 Splenic white pulp macrophages	24
1.7 Malaria.....	25
1.7.1 <i>Plasmodium</i> life cycle	26
1.7.1.1 Hemozoin	28
1.7.2 The bone marrow as a reservoir for <i>Plasmodium</i> parasites	29
1.7.3 <i>Plasmodium</i> clearance in the spleen	30
1.7.4 Human malaria	33
1.7.5 Chloroquine	34
1.7.6 Murine malaria	36
1.7.6.1 <i>P. chabaudi</i>	36
1.7.6.2 <i>P. yoelii</i>	37
1.7.6.3 <i>P. berghei</i>	38
1.8 <i>Plasmodium</i> clearance by splenic red pulp macrophages	38
1.9 Models to study the functional role of specific macrophage subtypes	40
1.9.1 Genetic depletion of the CD163 receptor	41
1.9.2 Genetic depletion of Lxra	42
1.10 Macrophages and T cell activation upon blood-borne infections.....	43
1.11 Vaccines	46
1.12 The viral infection model of lymphatic choriomeningitis virus.....	47
1.13 Aims.....	48
1.13.1 Aim 1: Characterization of developmental origin and phenotypic identity of splenic macrophage subpopulations	48

1.13.2 Aim 2: Characterization of the cellular and molecular changes amongst splenic macrophage subpopulations when challenged with blood-stage malaria	49
1.13.3 Aim 3: Genetic depletion of the CD163 receptor or marginal zone macrophages during a <i>P. chabaudi</i> infection to study the respective relevance and impact on malaria progression	52
1.13.4 Aim 4: Follow the dynamics of myeloid and lymphoid cells in the bone marrow and blood, which compensate for the loss of effector cells in peripheral tissues during a blood-stage malaria infection	54
2 Materials and Methods	55
2.1 Materials	55
2.1.1 Devices	55
2.1.2 Consumables	56
2.1.3 Reagents and Buffers	57
2.1.4 Antibodies	59
2.1.5 Mouse strains	62
2.1.5.1 PCR reagents	62
2.1.6 Pathogens	62
2.1.7 Software	63
2.2 Methods	64
2.2.1 Experimental animals	64
2.2.1.1 Breeding	64
2.2.1.2 Genotyping	64
2.2.1.3 Generation of a CD163-depletion mouse model	66
2.2.2 Tamoxifen inducible fate-mapping	68
2.2.3 Malaria	69
2.2.3.1 Infection of experimental animals from donor	69
2.2.3.2 Parasitemia	69
2.2.3.3 Chloroquine treatment	71
2.2.4 LCMV	72
2.2.5 Organ isolation	72
2.2.6 Flow Cytometry	72
2.2.6.1 Preparation of spleen tissue	72

2.2.6.2. Preparation of bone marrow.....	73
2.2.6.3 Preparation of blood.....	74
2.2.6.4 Analysis of flow-cytometry data.....	75
2.2.7 Preparation of spleen tissue for imaging.....	75
2.2.7.1 Preparation of tissue for cryo-section.....	75
2.2.7.2 Antibody staining.....	75
2.2.7.3 Microscopy and image analysis.....	76
2.2.7.4 Immunohistochemistry (H&E).....	76
2.2.8 Iron assay.....	77
2.2.9 Single-cell RNA-sequencing.....	78
2.2.9.1 Sorting of CD64 ⁺ macrophages.....	78
2.2.9.2 Single-cell library preparation and single-cell RNA-sequencing.....	78
2.2.9.3 Single-cell data alignment, read processing, data analysis and annotation.....	79
3 Results.....	81
3.1 Identification and ontogeny of splenic macrophage populations.....	81
3.1.1 Splenic macrophage ontogeny.....	85
3.2 The dynamics of splenic myeloid cells during blood-stage malaria.....	90
3.2.1 Loss of splenic CD163 ⁺ RPM upon <i>P. chabaudi</i> infection.....	93
3.2.2 Loss of splenic CD163 ⁺ RPM upon malaria infection.....	99
3.2.3 Parasite clearance by chloroquine and respective impact on splenic CD163 ⁺ RPM.....	102
3.2.4 CD163 ⁺ RPM dynamics in a viral infection model.....	104
3.2.5 Ontogeny of splenic macrophages in malaria.....	105
3.2.6 Characterization of the transcriptional profile of splenic macrophages and changes upon a <i>P. chabaudi</i> infection via single-cell RNA-sequencing.....	112
3.3 Genetic depletion of CD163 receptor or macrophage populations in the splenic marginal zone and respective impact on malaria progression.....	124
3.3.1 Genetic depletion of the CD163 receptor and relevance for the maintenance and recovery of the splenic architecture in malaria.....	124

3.3.2 The impact of the depletion of splenic marginal zone and marginal metallophilic macrophages on malaria progression.....	129
3.4 The cellular dynamics in the bone marrow and blood during blood-stage malaria	135
3.4.1 Stem- and progenitor cells in the bone marrow during blood-stage malaria	135
3.4.2 Circulating immune cells in the blood during blood-stage malaria.....	138
4 Discussion	141
4.1 Characterization of splenic macrophages	141
4.1.3 Conclusions regarding aim 1	148
4.2 Characterization of cellular and molecular changes of splenic macrophages upon malaria infection	149
4.2.1 Ontogeny and phenotype of splenic red pulp macrophages upon malaria infection and other perturbations	149
4.2.1.3 Cure of <i>Plasmodium</i> infection does not recover CD163 expression on RPM	162
4.2.1.4 Splenic RPM dynamics upon viral perturbations.....	163
4.2.1.5 Mechanisms of CD163 loss	165
4.2.2 Ontogeny and phenotype of splenic macrophages in the marginal zone and white pulp upon <i>P. chabaudi</i> infection.....	169
4.2.2.1. Marginal zone macrophages and marginal metallophilic macrophages	169
4.2.2.2 White pulp macrophages	172
4.2.3 Conclusions regarding aim 2	174
4.3 Delineating macrophage interaction and signaling pathways in malaria via the genetic depletion of receptors or sub-populations.....	175
4.3.1 Genetic depletion of the CD163 receptor on macrophages in the context of <i>P. chabaudi</i> infection	175
4.3.2 Depletion of Lxra-dependent macrophages in the splenic marginal zone in the context of <i>P. chabaudi</i> infection	178

4.3.3 Conclusions regarding aim 3	180
4.4 The cellular dynamics in the bone marrow and blood during blood-stage malaria	181
4.4.1 Adaptation of stem- and progenitor cells in the bone marrow to blood-stage infection with <i>P. chabaudi</i>	181
4.4.2 The impact of <i>P. chabaudi</i> blood-stage malaria on circulating immune cells in the blood	183
4.4.3 Conclusions regarding aim 4	185
5 Conclusion	186
References	188

Abbreviations

BM	bone marrow
BSA	bovine serum albumin
CLP	common lymphoid progenitor
CMF	common myeloid progenitor
CRISPR	clustered regularly interspaced short palindromic repeats
Ctrl	control
DAPI	4',6-diamidino-2-phenylindole, diacetate
DFM	double-fatemapper
DNA	deoxyribonucleic acid
DTR	diphtheria toxin receptor
E	embryonic day
EDTA	ethylenediaminetetraacetic acid
EMP	erythro-myeloid progenitor
FACS	fluorescence-activated cell sorting
FBS	fetal bovine serum
g	gram
GM-CSF	granulocyte-macrophage colony stimulating factor
GMP	granulocyte-monocyte progenitor
GO	gene ontology
h	hour
H&E	hematoxylin and eosin
HMGB1	high mobility group box protein 1
HSP	heat shock protein
i.p.	intraperitoneal
IF	immunofluorescence
IFN	interferon
IL	interleukin
KO	knockout
LCMV	lymphatic choriomeningitis virus
LPS	lipopolysaccharide
LT-HSC	long-term hematopoietic stem cell
Lxr	liver X receptor

VIII

M-CSF	macrophage colony stimulating factor
MARCO	macrophage receptor with collagenous structure
MEP	megakaryocyte-erythroid progenitor
MerTK	Mer tyrosine kinase
MHC	major histocompatibility complex
min	minute
MMM	marginal metallophilic macrophages
MPP	multipotent progenitor
MPS	mononuclear phagocyte system
MZM	marginal zone macrophages
NGS	normal goat serum
PBS	phosphate-buffered saline
P.chab	<i>Plasmodium chabaudi</i>
PCR	polymerase chain reaction
PFU	plaque forming unit
pMac	pre-macrophage
PPAR γ	proliferator-activated-receptor- γ
RBC	red blood cells
RNA	ribonucleic acid
ROS	reactive oxygen species
RPM	red pulp macrophages
RS	rat serum
RT	room temperature
ST-HSC	short-term hematopoietic stem cell
tdT	tdTomato (red fluorescent protein)
TGF- β	transforming growth factor beta
TLR	toll-like receptor
UMAP	uniform manifold approximation and projection
UV	ultra violet light
VCAM-1	vascular adhesion molecula-1
WPM	white pulp macrophages
WT	wildtype
YFP	yellow fluorescent protein
YS	yolk sac

List of Tables

Table 1: Anti-malaria drugs.....	34
Table 2: PCR Master-Mix.....	65
Table 3: PCR Primer for genotyping.....	65
Table 4: PCR program.....	66
Table 5: PCR primer to test the introduction of loxP-sites into the CD163 gene	67
Table 6: Hematoxylin and eosin staining.....	77

List of Figures

Figure 1: Hematopoiesis.	3
Figure 2: Macrophage development.....	6
Figure 3: The Cre-loxP system for genetic fate-mapping.	8
Figure 4: The double-fatemapper model.	12
Figure 5: Splenic macrophages.....	17
Figure 6: CD163 receptor mechanism.	22
Figure 7: Plasmodium life cycle.....	28
Figure 8: Developmental origin of splenic macrophages.	49
Figure 9: Cellular and molecular changes amongst splenic macrophages upon a malaria infection.	51
Figure 10: Genetic depletion of CD163 and Lxra respectively to study functional impacts on malaria progression.	53
Figure 11: Genetic knockout of CD163.....	67
Figure 12: Tamoxifen treatment.....	68
Figure 13: Gating strategy to determine parasitemia. . Error! Bookmark not defined.	
Figure 14: Blood smear.	71
Figure 15: Sorting gate.....	78
Figure 16: Quality control of single-cell RNA-sequencing data.	80
Figure 17: Relevant marker to distinguish splenic macrophages.....	82
Figure 18: Identification of splenic macrophages via UMAP.....	83
Figure 19: Gating strategy for splenic macrophages.....	84
Figure 20: HSC-derived origin of splenic macrophages.....	85
Figure 21: The double-fatemapper.	87
Figure 22: Developmental origin of splenic RPM.	89
Figure 23: The <i>P. chabaudi</i> malaria model.....	92
Figure 24: Loss of CD163 ⁺ RPM in <i>P. chabaudi</i> malaria.....	95
Figure 25: Expression of macrophage-specific markers in the spleen upon malaria with <i>P. chabaudi</i>	97
Figure 26: Dynamics of splenic marginal metallophilic macrophages, marginal zone macrophages and white pulp macrophages in <i>P. chabaudi</i> malaria infections.	99
Figure 27: Loss of CD163 expressing RPM in malaria.	101

Figure 28: Parasite clearance with chloroquine does not rescue CD163 expression on RPM..... 103

Figure 29: Viral infections cause a reduction, but not loss of splenic CD163⁺ red pulp macrophages..... 105

Figure 30: Quantification of HSC-derived circulating monocytes and splenic macrophages in malaria. 107

Figure 31: Quantification of HSC-derived and EMP-derived splenic red pulp macrophages in malaria. 109

Figure 32: Quantification of HSC-derived and EMP-derived splenic macrophages in malaria..... 111

Figure 33: UMAP-clustering of CD64⁺ sorted cells. 113

Figure 34: Feature plots showing expression of relevant macrophage genes for splenic macrophages..... 115

Figure 35: Assignment of UMAP clusters to splenic macrophage populations. 118

Figure 36: Differentially expressed genes in splenic red pulp macrophages populations upon malaria infection. 119

Figure 37: Gene ontology analysis of different splenic macrophages..... 121

Figure 38: Subclustering of red pulp macrophages and comparison of differentially expressed genes. 123

Figure 39: Impact of the absence of the CD163 receptor on splenic architecture and parasitemia in malaria. 126

Figure 40: The absence of CD163 impacts the splenic marginal zone in malaria... 128

Figure 41: Spleen tissue in the absence of macrophages in the splenic marginal zone and impact of a *P. chabaudi* infection..... 130

Figure 42: The impact of the absence of splenic marginal zone macrophage populations on the splenic architecture and cellularity during a malaria infection... 132

Figure 43: The absence of macrophages in the splenic marginal zone and impact on the splenic architecture upon *P. chabaudi* infection..... 134

Figure 44: Quantification of stem- and progenitor cells in the bone marrow during a malaria infection. 137

Figure 45: Quantification of lymphoid and myeloid immune cells in the blood during a malaria infection. 139

Abstract

The spleen is a secondary lymphoid organ with the essential function of maintaining blood homeostasis through its function as a filtering system. Aberrant erythrocytes and infectious particles are recognized and eliminated by specialized phagocytes, the splenic macrophages, that reside in the spleen. These splenic macrophages have different specializations and phenotypes dependent on their sub-tissular niche of residence. To date, four different macrophage subtypes have been identified in distinct splenic compartments: red pulp macrophages (RPM), marginal metallophilic macrophages, marginal zone macrophages and white pulp macrophages. The ontogeny and function of these different splenic macrophages is incompletely understood. Here, novel fate-mapping models were developed to discover new biology on the fate and function of the splenic macrophage populations during steady-state and in the context of parasitic or viral infection. With high-dimensional flow cytometry and immunofluorescent imaging, a so far unrecognized CD163⁺ RPM subpopulation that develops early during embryogenesis was identified. The CD163 receptor is responsible for uptake of free heme and thereby prevents oxidative stress in the tissue. To understand the functional role of the CD163 receptor on RPM, mice were challenged with blood-stage malaria infection, and the dynamics of the splenic macrophage populations studied. As part of the natural course of infection, *Plasmodium* parasites cause erythrolysis and the release of free heme. Upon challenge with blood-stage malaria, CD163⁺ RPM disappeared seven days after infection with *P. chabaudi*, *P. bergheii*, and *P. yoelii*, while CD163⁻ RPM were completely replenished by monocyte-derived macrophages. The splenic architecture was disrupted during acute-phase malaria, and the distinct anatomical zones of red and white pulp, which harbor different macrophage subpopulations, were dissolved. However, while the splenic architecture recovered after the resolution of infection, the spatiotemporal myeloid cell dynamics and functions remained altered. Longitudinal studies, including chloroquine treatment to achieve sterile control of infection, revealed that CD163⁺ RPM did not recover after 90 days, when the tissue largely returned to its homeostatic state. Using single-cell RNA-sequencing, two distinct cluster of RPM were identified with differential expression of CD163 in the steady-state. The annotated CD163⁺ RPM cluster remained 90 days after *P. chabaudi* infection, but CD163 expression was almost absent compared to expression observed in naïve mice,

indicating a persistence of this macrophage population per se, but an inability of these cells to express CD163 after parasite exposure. The failure to express CD163 after infection was also observed in viral infection-models and caused a partial loss of the CD163⁺ RPM population, that does not recover to steady-state numbers long-term. To test the function of the CD163 receptor, *CD163*^{-/-} mice were infected showing that CD163 had no impact on the control of parasitemia but lead to an abrogated regeneration of the structure of the marginal zone. In contrast, genetic deficiency of marginal zone macrophages resulted in increased parasitemia during the acute phase of the infection. In summary, this study presents a comprehensive ontogenetic and functional map of splenic macrophage populations and provides evidence that the tight interplay of RPM and marginal zone macrophages is important to resolve malaria infection.

Declaration

The work presented in this thesis was conducted at The Rheinische Friedrich-Wilhelms-Universität Bonn and The University of Melbourne in the laboratories of Prof. Elvira Mass (Life & Medical Sciences Institute in Bonn, Germany) and Prof. William Heath (Peter Doherty Institute in Melbourne, Australia).

I hereby declare that:

- (i) This thesis comprises only my original work towards the degree of Doctor of Philosophy (PhD), except where indicated in the Preface
- (ii) Due acknowledgement has been made in the text to all other material used;
and
- (iii) This thesis is fewer than the maximum word limit in length, exclusive of tables, bibliographies and appendices.

Bonn, 7th of March, 2024



Katharina Maue

Preface

I acknowledge the important contributions of others to the experiments and figures presented in this thesis:

Daria Hirschmann (University of Bonn & University of Melbourne) performed the quantification of the total iron content in the spleen tissue (Figure 24, F).

Dr. Lynette Beattie (University of Melbourne, Peter Doherty Institute) performed the ELISA for quantification of soluble CD163 (Figure 27, D).

Takahiro Asatsuma, Dr. Yannick Alexandre and Dr. Thomas Burn (University of Melbourne, Peter Doherty Institute) provided spleen tissue of their LCMV experiments. Dr. Lynette Beattie (University of Melbourne, Peter Doherty Institute) performed the flow cytometry experiment on week 20 after LCMV infection (Figure 29).

Dr. Nelli Blank-Stein (University of Bonn, LIMES Institute) performed the single-cell RNA-sequencing procedure (10x Genomics) of the sorted cells and analyzed the aligned data set to provide the figures of the sequencing data. Dr. Lisa Maria Steinheuer (University of Bonn, Institute for Experimental Oncology,) aligned the sequencing data to a mouse reference genome (Chapter: 3.2.6 Characterization of the transcriptional profile of splenic macrophages and changes upon a *P. chabaudi* infection via single-cell RNA-sequencing).

I acknowledge the Boehringer Ingelheim Fonds for their fellowship during my PhD.

Acknowledgements

There is only one constant element in immunity, whether innate or acquired, and that is phagocytosis. The extension and importance of this factor can no longer be denied

-Elie Metchnikoff-

My journey into the macrophage world began a long time ago, when Prof. Dagmar Wachten, my former supervisor at the caesar institute, introduced me to Elvira, who was successfully completing her postdoc in the group of Prof. Frederic Geissmann at the Memorial Sloan Kettering Cancer Center in New York at that time. But it was not then that our paths have crossed. Elvira already became a professor by the time I arrived in the Geissmann group for my internship. My fascination for the macrophage universe however was ignited. Coming back to Heidelberg, I joined the group of Prof. Rodewald, who had collaborated with Prof. Geissmann before. But I was still eager to gain more experience in the macrophage field. It was by the time I arrived in Melbourne for an internship in the group of Prof. Ian Van Driel that Elvira told me about her new collaboration with Prof. William Heath and Dr. Lynette Beattie within the IRTG program and set up a meeting between Lynette and me. This was basically where the journey of my PhD began and I was thrilled and excited, because I was confident to have a very supportive network of excellent supervisors.

The important thing in science is not so much to obtain new facts, as to discover new ways of thinking about them

-William Bragg-

Elvira was my mentor and inspiration. Already when I first met her, I was impressed by her career and achievements. She is an amazing scientist and thinks ahead of time, which reflects on the projects that run in her lab.

You have always supported me, motivated me and taught me. I learned a lot from you, starting from prepping tiny organs from mouse embryos, through analysis of flow data and writing project proposals. Your comments and feedback have been valuable to advance my way of thinking and approaching scientific projects and writing. I appreciate the time you have invested into my education and the way you have always encouraged and supported me. Your enthusiasm and ideas made me leave every

meeting with a long list of work, but also very motivated. You have always been available, understanding and interested in the project. Thank you for this amazing journey through my PhD.

A good teacher can inspire hope, ignite the imagination and install a love of learning

-Brad Henry-

I consider myself very lucky that I had two amazing supervisors during my PhD. Lynette was my Melbourne supervisor and a true inspiration. Next to her scientific career, she raised two beautiful children and has always put lots of effort into teaching her students well. I truly enjoyed our monthly meetings; you have always been interested in the project, discussing the data and you brought up new ideas. You gave me a very warm welcome when I arrived in Melbourne – picking me up at the airport in the middle of the night. Thanks to you I was able to run experiments within no time. Thanks for your support, for your comments and feedback, for our nice conversations, for your time and for your interest and encouragement.

Nothing in life is to be feared, it is only to be understood. Now is the time to understand more, so that

we may fear less

-Marie Curie-

Thank you so much Bill for having me in your lab. Knowing that I was already in good hands with Elvira and Lynette, you still have always been available when needed and showed constant interest in my project, gave me feedback and joined our meetings for lively discussions about the data and the progress of the project. Thank you very much for your support and interest.

Our greatest weakness lies in giving up. The more certain way to succeed is always to try just one

more time

-Thomas Edison-

I further want to convey my appreciation to Prof. Linda Wakim, the chair of my Melbourne PhD-committee and Prof. Shalin Naik, as an external member of my

committee. I always enjoyed our meetings. Both are great scientists, who simulated scientific discussions and broad along new ideas and perspectives for the project and were always very supportive. I consider myself very lucky that I had such a great committee during my PhD.

In addition, I would like to thank my TAC-committee in Bonn for the fruitful meetings and helpful discussions: Prof. Natalio Garbi, Prof. Christian Kurts and Prof. Wolfgang Kastenmüller, as well as Prof. Rayk Behrendt, who became my second examiner.

Special thanks also to the whole IRTG-team for making this program and the organization possible. Thanks to Prof. Christian Kurts and Prof. Sammy Bedoui. Especially thanks to Sandra Rathmann, Lucie Delforge and Dr. Marie Greyer, who always supported the students, answered questions, organized meetings and helped us with bureaucratic obstacles.

I was also happy to meet amazing students within the program and share a nice time during meetings, retreats and social events. And it was great to even meet some familiar faces again: Andreas, Markus and Lena.

Thank you so much to Conny, Maria and Dagmar. They are the caring good heart of the lab and take care of so many things in the background to support us. Maria's extraordinary management skills give structure to the lab. Conny, you are the good soul of the lab, always being so supportive and helpful, you significantly contribute to the success of the projects in the lab. I appreciate your kindness and support and am really happy that our paths have crossed again.

A very big "thank you" to the whole GRC-team at the LIMES institute. Maria and Joachim who have always supported me and made it possible to start malaria experiments in our facility. Stephan, who generated a new mouse line for my project. And all animal care takers, who ensured everything ran smooth behind the scenes.

Thank you to the IT-team, Michael and Tom, who helped me with several technical challenges.

I acknowledge the 'Histologisches Labor' of the Bonn university clinics for preparing paraffin sections and staining them with hematoxylin and eosin. The facility is funded by the German Research Foundation (Deutsche Forschungsgemeinschaft, DFG) under Germany's excellence strategy (EXC2151 – 390873048).

I acknowledge the core facilities of the Peter Doherty institute:

The Imaging core facility (BOMP), who introduced me to their confocal microscope systems. They maintain the microscopes and I was able to acquire images of stained spleen tissue.

The flow cytometry core facility, especially Alexis, who introduced me into their Aurora system. They maintain the flow cytometers and I was able to acquire labeled spleen cells.

The animal facility and animal care takers, who introduced me into their guidelines and techniques and took care of the mice.

I thank Prof. Kevin Couper (Lydia Becker Institute of Immunology and Inflammation, University of Manchester, UK) for sending aliquots the *Plasmodium* species *P. chabaudi*, *P. yoelii* and *P. berghei* (originating from Prof. William Heath group at the PDI, Melbourne), which were expanded and used in this study.

I thank Prof. Florent Ginhoux (ITIC – University of Paris – Saclay) for sharing the *Ms4a3^{FlpO}* mouse with us.

I thank the group of Prof. Marc Bajenoff (Immunology Center of Marseille CIML, France) for providing the CD163-ATTO antibody for immunofluorescent labeling of fixed spleen tissue, which they have produced in their laboratory.

I acknowledge the Boehringer Ingelheim Fonds for their fellowship and funding during my PhD. They have provided helpful seminars and regular meetings to advance my scientific skills. In addition, I was able to make new friends in the scientific community with a diverse research focus. Special thanks to Claudia, Stephan, Marc, Anna and the whole team.

Anything is possible when you have the right people there to support you

This brings me to a lot of people who are close to my heart and who have accompanied me on this journey and left their footprints in my life. Within the last 3.5 years I was facing some of the biggest challenges of my life and I would not have been able to go through all of them without those wonderful people around me.

Happiness is – working with great people

Much later and much shorter than initially expected, was my stay at the Peter Doherty Institute in Melbourne. But I had the great pleasure to meet amazing people in the lab, who let me enjoy every day. They gave me a very warm welcome and we enjoyed coffee breaks and scientific discussions. Thank you, Shirley, Thiago, Jeff and Daniel from the Heath lab. And thanks to Marcel and Helena from the IRTG program, who were always amazing company.

Good friends are like stars – you don't always see them, but you know they are always there

Not only was my time in Melbourne a great scientific experience, but also it allowed me to find amazing new friends. Jules I met already during my very first time in Melbourne for an internship. We had crazy and fun times together, but also my Columbian Joujou became a dear friend to me. Likewise, Daniella, I met her at the Bio21 Institute and we stayed in touch ever since, she even visited me in Heidelberg and met my friends. Melissa, Alex and Sozaf are friends who found a place in my heart in no time with their warm and caring nature. We (the moja pendejos) share our passion for climbing and had memorable trips together. I hope to see you again soon.

Work made us colleagues, but our sarcasm, inspiring conversations and sharing the same challenges

made us friends

A PhD brings along many personal and work-related challenges - being surrounded by people I felt comfortable with, made me enjoy coming to the lab every day. Thank you, Maria, Hao, Linda, Aya, Kerim and Seyhmus as well as Marie who joins me for her master-thesis and our motivated students Theresa and Hannah.

And when you can't go back you have to worry only about the best way of moving forward

-The Alchemist-

Especially thanks to Daria, who after several years of malaria-solitude joined me on this project. She is a talented scientist full of ideas. Thank you, Nikola, my flow-hero and happy person. Sharing jokes and discussing life with you was always joyful. Iva, I miss your company and positive energy, your kindness, supportiveness and empathy, I am thankful to have you in my life.

Good friends help you to find important things when you have lost them

...your smile, your hope and your courage

Thanks to my dear friend Eliana, we met already during our studies in Heidelberg working as waitresses and I believe it was fate that brought us together again and I have no doubt that your lovely nature will always be part of my life. You mean so much to me and I can always count on you. Thanks for being so caring.

Thanks also to mia amica Alice, you became a dear friend in no time. Your honest and caring nature and your enthusiasm for new adventures made the past year with you very beautiful and memorable. Thanks, that your glittery smile was supporting me every day while writing this thesis ;-)

Friendship improves happiness and ablates misery,

by doubling our joys and dividing our grief

Marina, I think life has connected us in many ways. Sharing our sorrow made us grow so close together and made the pain a little less, because we always had each other. You are a dear friend to me, who cares so much about other people and always brings joy and happiness into my life. Thanks for being such a supportive and lovely friend. Many thanks to Nelli (my appreciation would of course fill more than one page ;-P). She is a dedicated and very talented scientist (even though she sometimes doesn't know this by herself). Ever since we completed our apprenticeship, I never wanted to let go of you ;-) The happier I was that we became colleagues again when I started my PhD. You are a dear friend to me, who is always caring and supportive and honest, which I appreciate very much. "Nie mehr Fastelovend – ohne dich"

Many of you have caught me when I was falling, supported me, made me believe in myself and stand up again, this has formed bonds that I will never forget and want to express my deepest appreciation.

Home is where stories begin

I learned to appreciate the true value of 'home' again, while I was writing this thesis. Home it not a place, it is the people. Thank you so much to my WG: Soffi, Lukas, Chris and Thomas for caring and checking on me. Thank you to Sophie, for keeping me healthy with vitamin C and happy with 9 hugs per day. I want to express my deepest appreciation towards Ronja, she has caught me and supported me and pushed me to get through this. Thanks for the 'motivation-calendar' with so much love and handcraft – you cheered up every day for me and became a very important person in my life. Also many thanks to Laura, who has already been a dear friend to me, before moving in together. You have helped me and cheered me up and filled places with new memories. I miss you here in Bonn.

Best memories are those about the time we have spent together

Thank as well to my Mensa-gang. Rob and Freddy you made my Friday-lunches an entertaining highlight. Thanks for your company, the jokes and laughter. Thank you Rob, you have always been a dear, understanding and caring friend when I needed you. And thanks to Dennis, who joined this crew and many others and became a very dear, fun and supportive friend to me.

Many people walk in and out of your life,

but only true friends will leave footprints in your heart

Thanks to my dear cousins Jenny and Jessy, my godchild Zoe, my aunt Erika, as well as my good friends Bob and Leon. I feel lucky to have such a loving family in my life. Through ups and down, happy and cozy times, I enjoyed your company - love you.

It is only with the heart that one can see rightly, what is essential is invisible to the eye

-The little prince-

This brings me now to the people who have accompanied me on the way to start this PhD. Tabea was the first friend I made, when I started my masters in Heidelberg and we have shared many adventures together – our internship in Boston, our travels in Costa Rica and of course lots of cake and study time.

Thanks as well to Carina, Esti, Nehemiah and Tomi. I met them during my internship in the Geissmann group and they inspired me to study macrophages.

Being honest may not get you a lot of friends but it will always get you the right ones

Back in Heidelberg also Branko, Niko, Anni and Larissa from the Rodewald group have supported my scientific career in the macrophage world and became my friends. After an internship with Larissa and Kay, I completed my master thesis with Anni and Katrin. I have learned a lot from all of you and enjoyed the time in the lab. Especially socializing with Crschsch-Deadline was sometimes challenging, but no matter if behind the sorter or under a desk, I found all their hiding spots ;-)

Truly great friends are hard to find, difficult to leave and impossible to forget

During my masters in Heidelberg, I also met Domi and Flo, my best buddies. We shared fun times in Untere in Heidelberg or in the streets of New York, had nice hikes and coffees breaks or social events together. Thanks for the hugs and laughter, for the chaos and the fun – I miss you a lot in my everyday life.

True friends are never apart,

maybe by distance but never by heart

With four people I have started this journey in the first place. I met Ruth, Franzi, Alina and Ilka in the first weeks of my bachelors and we became very close friends, study-buddies and travel-buddies. Though none of us was planning to do a PhD at that time, we all took the same route in the end ^^ I appreciate your company, your empathy and support, your warm and caring nature. I know I can always count on you and I love you very much.

The secret of life, though, is to fall seven times and to get up eight times

-The Alchemist-

This brings me now to the friends that have accompanied me on my outdoor adventures and share the same passion for mountains, nature and sports. Ansgi, Henning and Susi are my mountainbike-buddies and close friends. Thank you for being so lovely and warm-hearted. Thanks Henning for proof-reading and highlighting every "geschützter Trennstrich" for me ^^ Schluffili, you have literally carried me when needed, ever since we met during our apprenticeship – thank for always being such a good friend.

Good times and crazy friends make the best memories

My passion for outdoor sports especially starts with climbing. It is fundamentally based on the trust in your climbing partner. This trust leads to the formation of a close bond and friendship. Thanks to Angi, Anne, Denis, Gregor, Roland, Flo, Koen and many more that I can always rely on you and know that you will catch me if I fall. Thanks, Denis for all the amazing adventures. Thanks, Angi and Anne for the climbing-girl-power. Thanks Gregor and Roland for amazing trips and laughter.

A best friend is someone who tells you the truth even when you don't want to hear it

This brings me to my three closest friends. Franci, I appreciate having you in my life. I appreciate your honesty and your caring nature. You have been through heartbreaks and tears with me and were always by my side to support me. Not only do we share our passion for climbing and biking and had many adventures together, I can also share my thought and feelings with you and you are always understanding and tell me honestly what is on your mind. Love you Franci-Schneekanone and wish you always good health ;-P Thanks to you and Davidino for your friendship.

A best friend isn't someone who is just always there for you. It is someone who understands you a bit more than you understand yourself

Lisa thank you so much for always being by my side and supporting me, for drying my tears and cheering me up, for motivating me and always being honest with me. I know

that you always have the best in mind for me and you are amongst the people closest to my heart. After living together in Heidelberg, we both made our Australian adventure come true together. Thanks for all the amazing memories and many more to come. Love you. (And thanks a lot of course for proof-reading - I am amazed by your skills and how you spotted so many tiny things in no time).

*There are friends and there is family,
and then there are friends that became family*

Anna, I think there are no words to describe our bond and friendship. You are my soulmate, the best friend one can ever wish for. You have been by my side almost my entire life now and you have never let me down, you lifted me up when I was down, you encouraged me when I felt weak, you made me smile, you gave me confidence and brought me joy. Without you I'm incomplete and I wouldn't be who I am today. Countless memories, full of laughter and happiness – thanks for every moment and many more to come. Love you.

Family is like branches on a tree, we all grow in different directions, but our roots keep us all together
Papa-Lillemaule, Mama-Brenntetan, Buderherzi-Hannes, ich danke euch von ganzem Herzen, dass ihr mich zu dem Menschen gemacht habt, der ich heute bin, dass ihr an mich geglaubt und mich immer unterstützt habt, meine Träume zu verwirklichen. Ich hab euch von ganzem Herzen lieb und bin euch sehr dankbar. Meine Familie sind meine Wurzeln und meine Flügel. Danke auch an Julia und Marco.

My parents and my brother have been the solid rocks in my life. I can always count on you and you have supported me in any possible way and motivated me to complete this PhD, even though you all had to face one of the most existential crisis in life, when our hometown got flooded. You made me believe that broken things can be rebuilt and that one should never give up. As long as we have each other we can face all the challenges in the world.

List of Publications

Mauel K, Mass E (2023) Fate-mapping of hematopoietic stem cell-derived macrophages. *Tissue-resident macrophages*: 139-148. doi: 10.1007/978-1-0716-3437-0_9

Kayvanjoo AH, Splichalova I, Bejarano DA, Huang H, Mauel K, Makdissi N, Heider D, Balzer NR, Osei-Sarpong C, Baßler K, Schultze JL, Uderhardt S, Kiermaier E, Beyer M, Schlitzer A, Mass E (2023) Fetal liver macrophages contribute to the hematopoietic stem cell niche by controlling granulopoiesis. *Biorxiv* (preprint). doi: 10.1101/2023.02.21.529403

Huang H, Splichalova I, Balzer N, Seep L, Franco Taveras E, Radwaniak C, Acil K, Mauel K, Blank-Stein N, Makdissi N, Zurkovic J, Kayvanjoo A, Wunderling K, Jessen M, Yagmour M, Ulas T, Schultze JL, Liu Z, Ginhoux F, Beyer M, Thiele C, Hasenauer J, Wachten D, Mass E (2023) Developmental programming of Kupffer cells by maternal obesity causes fatty liver disease in the offspring. *Nature* (preprint). doi: 10.21203/rs.3.rs-3242837/v1

1 Introduction

Macrophages are innate immune cells that were discovered in the 19th century by Elie Metchnikoff (Gordon, 2016; Underhill *et al*, 2016; Mechnikov, 1988) and belong to the mononuclear phagocyte system (MPS). This system comprises a family of professional phagocytes, including macrophages, monocytes and dendritic cells. These cells are distributed through various organs and play crucial roles for the maintenance of tissue homeostasis (Summers *et al*, 2020). Furthermore, cells belonging to the MPS function as a first line of defense towards infections (Hume, 2008).

In that regard, monocytes circulate in the blood and can extravasate into the tissue at the site of infection for differentiation. Macrophages are responsible for the engulfment and digestion of foreign substances and pathogens, while dendritic cells have an important role in the presentation of antigens to T cells for the initiation of an adaptive immune response (Guilliams *et al*, 2014). The coordinated activity of mononuclear phagocytes in the body contributes to immune surveillance, tissue repair and maintenance of homeostasis. Understanding the role of these mononuclear phagocytes is essential to comprehend immune responses and the progression of diseases and eventually to support the development of strategies to selectively enhance treatments for infectious and inflammatory diseases.

However, the classification of the MPS has been challenged with novel discoveries. Many characteristics of monocytes, macrophages and dendritic cells are overlapping, making the distinction between those cell types challenging. Therefore, a novel classification was suggested, that primarily identified cellular identities based on their ontogeny and secondarily takes their location, function and phenotype into consideration (Guilliams *et al*, 2014).

1.2 Hematopoiesis

Hematopoiesis describes the generation of blood cells and occurs in the bone marrow (BM) in adulthood (Figure 1). It is a critical process that ensures proper functioning of the immune system and oxygen transport in the body (Rieger & Schroeder, 2012).

Long-term hematopoietic stem cells (LT-HSC) comprise the top of the hematopoietic hierarchy. They have the unique ability to give rise to all different types of blood cells, but this process must be tightly regulated to prevent diseases and maintain the capacity to provide functional cellular output throughout life. LT-HSC typically remain quiescent to protect them from damage associated with cell division, such as DNA-damage and they expand only to maintain the HSC pool (Wilson et al, 2008).

Short-term hematopoietic stem cells (ST-HSC), in contrast, deliver more output to the downstream hematopoietic system. They are discriminated from LT-HSC by the loss of CD150 expression (Kim et al, 2006) and give rise to a variety of multipotent progenitor populations (MPPs). MPPs represent an intermediate stage in the differentiation of stem cells to specialized cell types. MPPs have the ability to differentiate into specific cell lineages (Busch et al, 2015). All immature multipotent cells characteristically express c-Kit and Sca-1 (Rieger & Schroeder, 2012).

Downstream of the MPP lineages, the hematopoietic system branches into erythropoiesis, myelopoiesis and lymphopoiesis. The common lymphoid progenitors (CLP) specifically give rise to cells of the adaptive immune system - to T cells and B cells (Kondo, 2010).

Common myeloid progenitors (CMP) branch into different subsets of myeloid cells. On the one hand megakaryocyte-erythroid progenitors (MEP) give rise to erythrocytes and megakaryocytes. On the other hand, CMP differentiate into granulocyte-monocyte progenitors (GMP), which give rise to monocytes and granulocytes. Granulocytes comprise mostly neutrophils, but also eosinophils and basophils, while monocytes in turn can give rise to macrophages (Rieger & Schroeder, 2012).

GMP are involved in the host defense system against infections with pathogens because they give rise to innate cells that play key roles during early-stage infectious or inflammatory challenges. The differentiation and development of GMPs is tightly regulated by cytokines and growth-factors, such as granulocyte-macrophage colony stimulating factor (GM-CSF) and interleukins (IL) (Rieger et al, 2009).

The hematopoietic system can rapidly adapt to changes. When encountering a systemic infection, a shift towards GMP lineages and an enhanced output of monocytes and neutrophils is detected within hours (Chiba et al, 2018). Adhesion molecules are upregulated at the site of infection, where recruited cells can extravasate. Once monocytes have entered the tissue and receive further stimuli, they can differentiate into macrophages to immediately repress foreign organisms (Trzebanski & Jung, 2020).

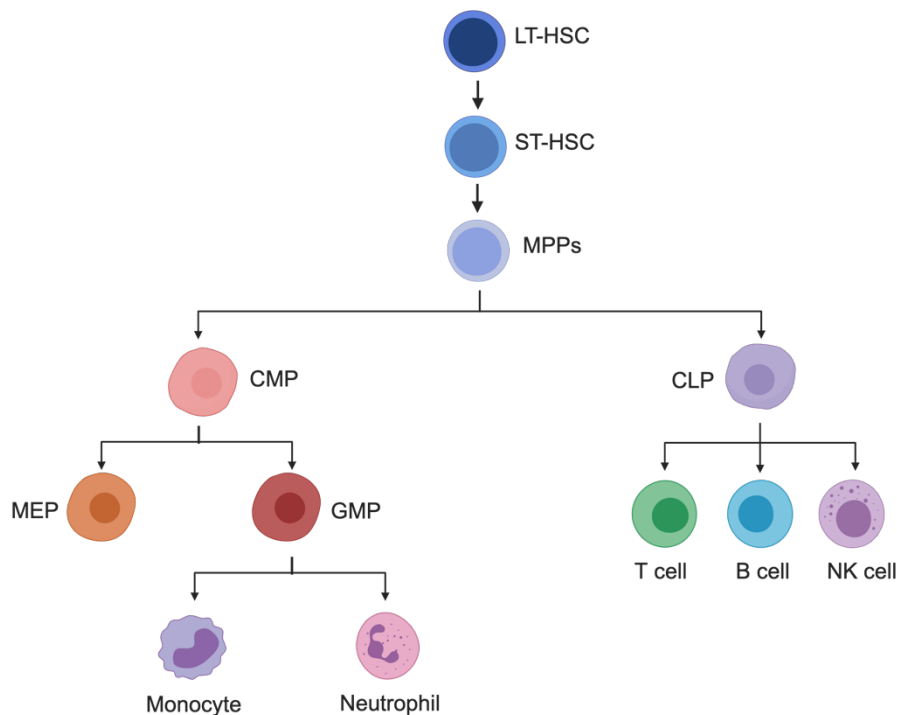


Figure 1: Hematopoiesis. Long-term hematopoietic stem cells (LT-HSC) reside in the bone marrow and give rise to short-term hematopoietic stem cells (ST-HSC), which in turn can differentiate into multipotent progenitor populations (MPP). MPPs give rise to more committed progenitors, the common myeloid progenitors (CMP) and the common lymphoid progenitors (CLP). The later can

differentiate into T cells, B cells and NK cells. CMP give rise to either megakaryocyte-erythroid progenitors (MEP) or to granulocyte-monocyte progenitors (GMP). The GMP can differentiate into monocytes and neutrophils.

1.3 Macrophage ontogeny

Macrophages are innate immune cells that monitor for pathogens, engulf and digest microbes and cell debris, and are thus vital for tissue homeostasis (Gentek et al, 2014). While most immune cells are derived from HSCs, it was long believed that tissue macrophages also originated from BM-derived monocytes that differentiated in the tissue. About a decade ago, the prevalent understanding of monocyte-derived macrophages was revised through the discovery of resident macrophages that arise from erythro-myeloid-progenitors (EMP) in the yolk sac (YS), before the onset of definitive hematopoiesis (Gomez Perdiguero et al, 2015). These HSC-independent macrophages colonize the developing organs during embryogenesis. They are long-lived and self-maintain in adult tissues through local proliferation, mostly independent of circulating BM-derived cells (Hoeffel & Ginhoux, 2018). This is supported by parabiosis studies which found that the majority of myeloid cells in the brain, lung, peritoneum and spleen proliferate locally and do not depend on monocyte recruitment (Parwaresch & Wacker, 1984).

1.3.1 Waves of macrophage development

Hematopoietic cell development in the mouse embryo occurs in several waves and at multiple anatomic locations (Waas & Maillard, 2017) (Figure 2).

1.3.1.1 Primitive hematopoiesis: first wave

Primitive hematopoiesis starts at embryonic day (E) 7.5 with the detection of erythroid progenitors in the extra-embryonic mesoderm layer of the YS. This wave can give rise primitive erythroid progenitors for oxygenation and embryonic macrophages for defense (Palis, 2016; Palis *et al*, 1999). But primitive hematopoiesis is transient and rapidly replaced by definitive hematopoiesis.

1.3.1.2 Definitive hematopoiesis: second wave

During the subsequent second wave starting at E8.5, multipotent EMPs emerge. EMPs are generated upon an endothelial-to-hematopoietic transition in the YS and have the potential to differentiate into monocytes, granulocytes, megakaryocytes, mast cells, erythrocytes and macrophages. EMPs colonize the fetal liver between E8.5 and E10.5. In the YS and fetal liver, they upregulate the expression of *Tnfrsf11a* and differentiate into a *Cx3cr1*-expressing pre-macrophage (pMac) precursor that is distinct from monocytes (Mass *et al*, 2016). EMPs and pMac expand in the YS and fetal liver before entering the blood stream to migrate into the embryonic tissues where they give rise to most tissue-resident macrophages (Mass, 2018; Mass & Gentek, 2021; Stremmel *et al*, 2018). This transient hematopoietic wave that generates long-lived cells, is considered as HSC-independent hematopoiesis. In many tissues EMP-derived macrophages self-maintain throughout life, with minimal contribution of HSC-derived cells, for example microglia in the brain (Ginhoux *et al*, 2013), Kupffer cells in the liver and Langerhans cells in the epidermis (Kanitakis *et al*, 2011; Schultze *et al*, 2019).

1.3.1.3 Definitive hematopoiesis: third wave

Definitive hematopoiesis is initiated when HSCs, characterized by their self-renewal capacity, emerge in the aorta-gonad-mesonephros (AGM) region at E10.5 (Kissa & Herbomel, 2010). The AGM is derived from the mesoderm germ layer. From the AGM region, the generated HSCs migrate to the fetal liver at

around E12.5. In the fetal liver HSC expand and can differentiate into all blood cells. Around E15.5 the presence of HSCs is detected in the spleen, but does not deliver significant hematopoietic output (Christensen *et al*, 2004).

Before birth, the BM cavity is formed and definitive hematopoiesis shifts from the fetal liver to the BM at E17.5. HSC-derived cells from the BM will replace most cells originating from previous hematopoietic waves, with the exception of macrophages and a few other immune cell types, such as mast cells (Gentek *et al*, 2018; Li *et al*, 2018). The replacement of EMP-derived tissue macrophages by HSC-derived cells varies between organs. For example, the Spi-C dependent red pulp macrophages in the spleen become successively replaced by HSC-derived monocytes during adulthood (Liu *et al*, 2019). These HSC-derived monocytes have differentiated from Ms4a3-positive myeloid cells, which in turn originate from Cxcr4-expressing HSC (Werner *et al*, 2020; Liu *et al*, 2019). Those monocytes can enter tissue niches and differentiate into macrophages.

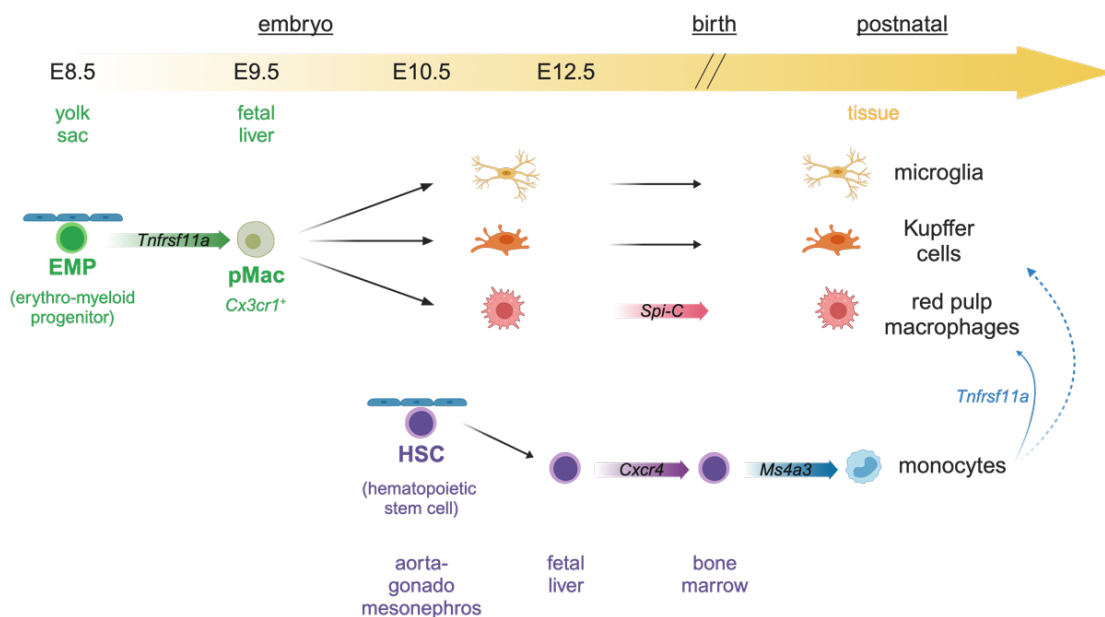


Figure 2: Macrophage development. Erythro-myeloid progenitors (EMP) in the yolk sac upregulate the expression of *Tnfrsf11a*, while giving rise to pre-macrophages (pMac) that express *Cx3cr1* and migrate to the fetal liver around embryonic day 9.5 (E9.5). Those pMac migrate to the developing organs and give rise to tissue macrophages, e.g. microglia in the brain, Kupffer cells in the liver or red pulp macrophages in the spleen. Organ specific cues lead to the upregulation of tissue specific factors, e.g. red pulp macrophages specifically upregulate *Spi-C*. At E10.5 definitive hematopoiesis starts in the aorta-gonad-mesonephros and at

E12.5 the hematopoietic stem cells (HSC) migrate to the fetal liver. At birth, hematopoiesis has shifted to the bone marrow. Stem cells characteristically express *Cxcr4* and when hematopoietic progenitors give rise to monocytes, they upregulate *Ms4a3*. Dependent on the organ, monocytes replace the EMP-derived macrophages during adulthood.

1.3.2 Models to study macrophage ontogeny

Current knowledge about macrophage ontogeny as well as the function of EMP- and monocyte-derived macrophages is mostly based on genetic fate-mapping studies. To target distinct myeloid lineages under steady state conditions and study macrophage development and function, the Cre/loxP system has emerged as an important tool, thereby enabling site-specific recombination to generate conditional knockout or genetic fate-mapping models (Álvarez-Aznar *et al*, 2020). Using this system, gene activity can be controlled in a spatiotemporal manner in almost all tissues of the mouse to study gene function and cell ontogeny.

The Cre-enzyme is a site-specific recombinase that is derived from bacteriophages. This recombinase recognized and catalyzes the recombination at a specific DNA sequence, the loxP-site. This loxP-site is a short 34 bp palindromic sequence, which is separated by a core region. The Cre-recombinase binds loxP-sites and induces site-specific recombination (Kim *et al*, 2018).

The Cre-loxP-system is a precise and controllable method for genetic manipulation. Introduction of the Cre-recombinase gene into the promoter region of a cell lineage-specific gene allows for Cre-recombinase expression only in cells that have committed to specific lineage identity or even a specific cell type (Kim *et al*, 2018).

To study the ontogeny of cells, loxP-sites are introduced into the ubiquitously expressed *Rosa26* locus. The whole genetic cassette that is integrated comprises a stop-codon, that is flanked by loxP-sites and followed by a genetic sequence

that encodes a fluorescent protein. Thus, only upon Cre-recombinase expression and activity, are the loxP-sites recombined and the stop-codon excised, allowing for expression of a fluorescent protein (Figure 3). Cells that express the fluorescent reporter can be followed with fluorescent microscopy or flow cytometry (Hutter, 2006). This is a powerful tool, but pitfalls can emerge from misinterpretations by assuming absolute Cre-specificity and -efficiency without adequate controls or by neglecting effects on the endogenous locus upon transgene insertion (Mass, 2018). Also, non-specific recombination can lead to unintended genetic changes at off-target sites.

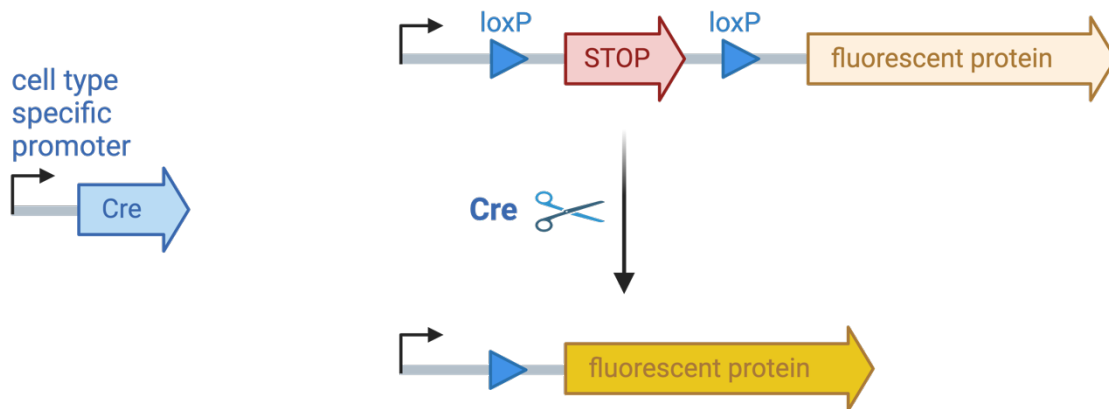


Figure 3: The Cre-loxP system for genetic fate-mapping. Cre-recombinase is expressed under the control of a cell type specific promoter. The enzyme recognizes loxP-sequences in the genome and catalyzes site-specific cleavage. Thereby the stop codon in front of a fluorescent reporter gene is removed and the fluorescent protein is expressed.

1.3.2.1 Fate-mapping of HSC-derived cells

An example use of the Cre-loxP system for genetic fate-mapping is the inducible *Cxcr4*^{CreERT2}; *Rosa26*^{LSL-tdTomato} mouse model (Mauel & Mass, 2024). In this system, the Cre-recombinase is expressed under the control of the *Cxcr4* gene promoter. *Cxcr4* is expressed by LT-HSC at the top of the hematopoietic hierarchy

(Werner *et al*, 2020) and thus all subsequent progenitor populations will express tdTomato. Additionally, Cre-recombinase activity in this model is inducible. The Cre-sequence is fused with a mutant form of the estrogen receptor ligand-binding domain sequence. When expressed, the estrogen receptor binds to tamoxifen, a drug that can be administered to the animals at specific times. In the absence of tamoxifen, the fusion of the Cre-recombinase to the estrogen receptor, sequesters the Cre-recombinase in the cytoplasm and prevents Cre-mediated recombination events in the nucleus. Upon administration of tamoxifen, the Cre-recombinase can translocate to the nucleus and mediate loxP-specific recombination events (Monvoisin *et al*, 2006; Mauel & Mass, 2024).

In the *Cxcr4*^{CreERT2}; *Rosa26*^{LSL-tdTomato} mouse model, Cre is expressed under the control of the *Cxcr4* promoter element and Cre-activity is temporally controlled through the administration of tamoxifen (Werner *et al*, 2020). Upon the administration of tamoxifen, all HSC-derived progeny is labeled with the fluorescent reporter. A discrepancy in the labeling efficiency between myeloid and lymphoid cells exists, meaning that while almost all myeloid cells in the blood are labeled, the fluorescent reporter is only detected in approximately 40 % of the lymphoid cells after one month (Werner *et al*, 2020), likely due the longevity of some circulating T and B cell populations. Following the labeling of cells shortly after a tamoxifen pulse provides insights into the immediate recruitment of cells derived from HSCs into a tissue. However, this does not offer conclusive evidence regarding the persistence or longevity of those labeled cells within the tissue microenvironment. Instead, when HSCs at the top of the hematopoietic hierarchy are labeled with this model and subsequently their progeny is examined over an extended period of time, a comprehensive description of the kinetics and long-term engraftment potential of HSC-derived cells within the tissue can be generated.

There is a broad literature about fate-mapping studies, but the chosen timepoint for the readout after tamoxifen administration differs (Feil *et al*, 2014). This is a limitation when interpreting the data.

1.3.2.2 The double-fatemapper

A combination of fate-mapping of both EMP- and HSC-derived lineages within the same mouse proposes a solution to limitations observed with the *Cxcr4^{CreERT2}; Rosa26^{LSL-tdTomato}* mouse model. Labeling of both EMP-derived and HSC-derived precursor cells with different fluorophores allows tracing of the origin and the temporal dynamics and longevity of postnatal macrophages. To generate this sort of model, two different recombinase enzymes were combined; the previously described Cre-recombinase and the FlpO-recombinase, which each recognize and cleave different genetic target sequences.

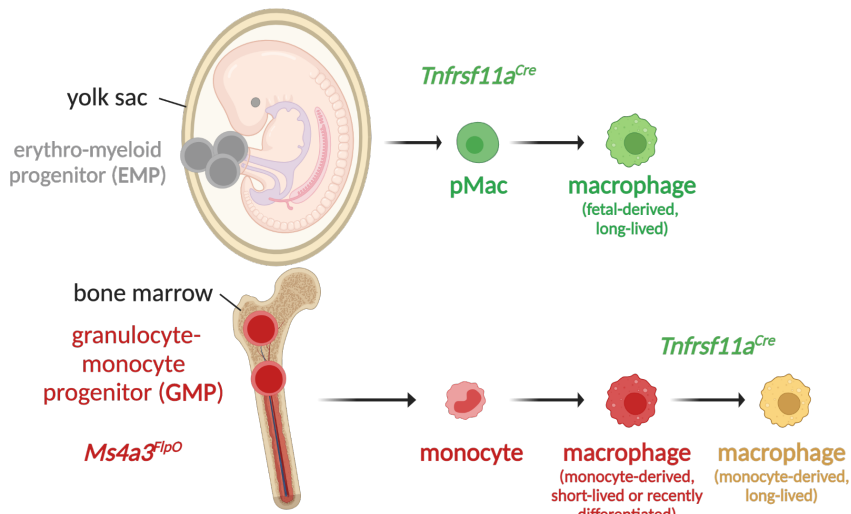
The FlpO-recombinase is derived from *Saccharomyces cerevisiae* and specifically recognizes a genetic sequence called an *frt*-site (Dan *et al*, 2022). The *frt*-target sites are inserted in the ubiquitously expressed *Rosa26* locus. An *frt*-site is followed by a stop-codon and another *frt*-site in front of a fluorescent reporter gene. Without FlpO-recombinase activity, the stop codon terminates transcription and the reporter is not expressed. FlpO-recombinase expression leads to the target site recognition and enzymatic cleavage of the DNA at the *frt*-sites. Thereby, the stop codon is removed and the polymerase can transcribe the fluorescent reporter protein (Humphreys & DiRocco, 2014).

In the double-fatemapper model, both recombinase enzymes are constitutively expressed, but each under the control of a distinct, lineage-specific promoter. To specifically target the macrophage lineage, the discovery of the TNF receptor superfamily member 11a (*Tnfrsf11a*), a transmembrane protein receptor that activates the NFκB pathway, was a major breakthrough in the field (Mass *et al*, 2016). *Tnfrsf11a* expression is a hallmark of EMP-derived macrophage precursors that colonize the developing embryo (Jacome-Galarza *et al*, 2019), and thus, can be used as a specific Cre-driver for long-lived, tissue-resident macrophages. On the other hand, *Ms4a3* was identified as specific marker, expressed by HSC-derived granulocyte-monocyte progenitors (Liu *et al*, 2019). The *Ms4a3* promoter is only active in cells downstream of the GMP-lineage and can therefore induce FlpO expression in monocytes and consequently in monocyte-derived macrophages (Liu *et al*, 2019).

In the *Tnfrsf11a^{Cre}; Rosa26^{LSL-YFP}; Ms4a3^{FlpO}; Rosa26^{LFL-tdTomato}* (double-fatemapper [DFM]) model, *Ms4a3*-driven FlpO-recombinase activity induces the expression of the fluorescent reporter protein tdTomato in HSC-derived progenitors, and *Tnfrsf11a*-driven Cre-recombinase activity induces the expression of the fluorescent reporter yellow fluorescent protein (YFP) in EPM-derived progenitors. Importantly, *Tnfrsf11a* is a core macrophage gene, so it is also upregulated by HSC-derived monocytes after they extravasate into tissues, differentiate into macrophages, and become resident. Thus, HSC-derived cells that have differentiated into long-lived tissue macrophages will express both YFP and tdTomato within this model, while short-lived or freshly differentiated cells will be only tdTomato-positive (Figure 4, A).

This novel approach enables the differential labeling of EMP- and HSC-derived macrophages within the same mouse. In adult organs, this model yields insight about the longevity of tissue macrophages. Macrophages that only express YFP in adults originated from YS-derived EMPs and self-maintain through local proliferation. All cells that are derived from HSCs in the BM express tdTomato. These cells can extravasate and differentiate into short-lived macrophages that are frequently replaced or have not completed their differentiation. Only HSC-derived macrophages that are long-lived also express YFP with tdTomato (Figure 4, B). These dynamics can change during aging and the contribution of EMP- versus HSC-derived cells to the pool of macrophages differs between tissues. This can be precisely delineated with the DFM-model.

A



B

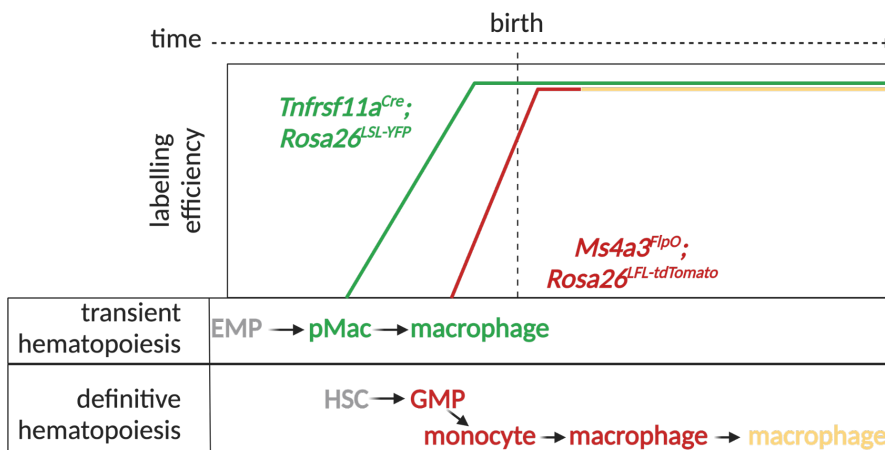


Figure 4: The double-fatemapper model. (A) Schematic representation of macrophage ontogeny. *Tnfrsf11a^{Cre}; Rosa26^{LSL-YFP}; Ms4a3^{FlpO}; Rosa26^{LFL-tdTomato}* mouse model: EMP-derived macrophages express *Tnfrsf11a* (green) and BM-derived GMPs and monocytes express *Ms4a3* (red). Each lineage specific gene induces the expression of a fluorescent reporter: YFP in EMP-derived cells (green) and tdTomato in BM-derived cells (red). BM-derived cells upregulate *Tnfrsf11a* (thus YFP), when they differentiate into long-lived macrophages and become positive for both fluorescent reporter (B) Temporal resolution of macrophage ontogeny. During embryogenesis, transient hematopoiesis gives rise to EMP, which differentiate into macrophages independent of the contribution of HSC-derived cells. At birth definitive hematopoiesis gives rise to monocyte-derived macrophages, that in some tissues replace the EMP-derived macrophages over time.

1.4 Macrophages in infection and inflammation

Macrophages are innate immune cells that present a high degree of plasticity and can change their phenotype in response to environmental stimuli (Ponzoni *et al*, 2018). They play a critical role in maintaining the homeostasis of the whole body. Macrophages clear cellular debris and metabolic waste, mediate antimicrobial defense, promote immune tolerance and maintain iron homeostasis through the phagocytosis of red blood cells (RBC) (Willekens *et al*, 2005; Scott & Guilliams, 2018). Macrophages are found in all organs, with most tissues harboring only a minor fraction of monocyte-derived macrophages in the steady state, while the majority of tissue macrophages originate from EMPs. The phagocytes form networks to support tissue function through the production of growth factors and via phagocytosis of dying cells. They are amongst the first cells to encounter pathogens and thus play an important role in the onset and progression of various diseases (Mass & Lachmann, 2021). The demonstration that tissue-resident and recruited macrophages represent different developmental lineages hints towards their non-redundant function in the steady state and in disease (Mass & Gentek, 2021). It can be assumed that the plasticity and functionality of macrophages is not only determined by environmental cues, but also by their ontogeny, which should be considered in the context of immune-therapy approaches (Gomez Perdiguero *et al*, 2015).

YS-derived precursor cell differentiation is driven by a core macrophage transcriptional program. Once the precursors migrate into the tissues, their specification is completed through the expression of tissue-specific transcriptional regulators early during embryogenesis (Mass, 2018; Gomez Perdiguero *et al*, 2015). It is therefore conceivable that YS-derived macrophages have functions during steady-state and inflammation that are distinct from HSC-derived monocytes, which differentiate into short-lived macrophages and are often characterized by a more inflammatory phenotype (Werner *et al*, 2020). Recruited macrophages originate and renew from BM-derived monocytes that extravasate into the tissue and mature. The recruitment of circulating monocytes

is increased upon inflammation, resulting in increased macrophage counts in infected and inflamed tissue (Mass, 2018). Isolated BM-derived macrophages express more pro-inflammatory markers compared to YS-macrophages *in vitro* (Yosef *et al*, 2018). However, it cannot be assumed that EMP-derived macrophages are pro-regenerative and anti-inflammatory, while monocyte-derived macrophages are pro-inflammatory (Seidman *et al*, 2020). Macrophages from both origins play a role in advancing and resolving tissue inflammation and infection across diverse diseases. The variety of macrophage subsets and their adaptability could account for the varied functional responses observed in the context of different diseases (Wen *et al*, 2021). For example, the differential impact of splenic macrophage populations on malaria progression and parasite clearance is assumed to be crucial, but still poorly elucidated.

Many macrophages display a diverse range of phenotypes in reaction to various physiological and pathological triggers (Gentek *et al*, 2014). Their ability to adapt to local stimuli and exhibit different phenotypes and functions in response to changing physiological demands is a remarkable feature (Okabe & Medzhitov, 2016; Mosser *et al*, 2020). The dysregulation of their polarization has been implicated in numerous diseases (Gordon & Plüddemann, 2017). Through either the expression of, or the response to inflammatory cytokines, like IFN γ and TNF α , as well as reactive oxygen species (ROS), macrophages play an important role in antimicrobial responses. However, when hyperactivated this can also lead to inflammation and tissue damage (Shapouri-Moghaddam *et al*, 2018). On the contrary, the expression of anti-inflammatory cytokines, such as IL-10 can contribute to tissue repair, but may also result in fibrosis if dysregulated (Hu *et al*, 2021; Gordon & Plüddemann, 2017). Emerging screening approaches, targeting the identification of bioactive compounds and targets for macrophage reprogramming or activation, aim to reverse pathological polarizations and functions (Hu *et al*, 2021).

1.5 The spleen

The spleen is a secondary lymphoid organ located at the left side of the abdomen, behind the stomach, but has no direct connection to the lymphatic vessels. Instead, the spleen collects antigens from the blood and is involved in the immune response to blood-borne infection. The bulk of the spleen is composed of the red pulp, with a large volume of venous sinuses, being responsible for the characteristic red appearance. The red pulp is the site where old or aberrant RBCs are disposed. Splenic macrophages along the sinus endothelium filter abnormal erythrocytes out of the blood, while young and flexible cells pass through the endothelial cells of the splenic sinuses (Kapila *et al*, 2023).

Lymphocytes surround the arterioles that run through the spleen and form isolated areas of the white pulp, where humoral and cell-mediated pathways are activated to generate immune responses (Cesta, 2016). Germinal centers that contain B cells are found in the white pulp regions and are surrounded by T cells. An area that is called the marginal zone surrounds those lymphoid follicles. Blood-borne pathogens and antigens can be filtered from the blood by macrophages and dendritic cells within the marginal zone (Murphy & Weaver, 2018). These professional antigen presenting cells can present antigens from infectious agents to T cells and B cells in the white pulp. B cells in turn start to proliferate in the germinal centers and produce opsonizing antibodies (Bronte & Pittet, 2013). Opsonization is important for the clearance of microbes and intra-erythroid parasites by phagocytes (Kapila *et al*, 2023).

Not only does the spleen support the breakdown of old RBC, it is also a reservoir of blood and plays a role in hematopoiesis, as the organ can compensate for hemolysis and support the BM via extramedullary hematopoiesis (Kapila *et al*, 2023).

For several medical conditions, including a trauma that leads to the disruption of the spleen or diseases that lead to an enlargement of the spleen, splenectomy is a powerful therapeutic procedure. However, although the spleen is an organ that

is not essential for survival, patients that have undergone splenectomy surgery have a higher risk for subsequent overwhelming infections and long-term cardiovascular complications (Weledji, 2014). Housing a significant component of the mononuclear phagocyte system, the absence of the spleen can cause predisposition to various bacterial infections, such as *Streptococcus* or *Neisseria* infections (Brender *et al*, 2005).

Using mouse models to study the spleen during infectious diseases yields valuable insight into the organ function, but structural differences between the spleen of humans and rodents must be considered. One major difference is that a capillary sheath of endothelial cells, pericytes and stromal cells that surrounds capillaries and arterioles, is present in humans but absent in rodents (Steiniger, 2015).

1.6 Splenic macrophages and functions

Macrophages have functions relevant to homeostasis, immune responses, tissue repair, antigen presentation and the control of infections. However, the specific manifestation of those functions depends on the respective organ and tissue niche that they exist in (Schultze *et al*, 2019). Splenic macrophages of different origins occupy and adapt to different micro-anatomical niches within the spleen (A-Gonzalez & Castrillo, 2018) and are specialized to conduct organ-specific functions, including the control of hematopoietic cell turnover, especially of erythrocytes (Gordon & Plüddemann, 2017). To date, four distinct macrophage subtypes are described to populate different anatomical niches of the spleen (Figure 5). The highly phagocytic red pulp macrophages (RPM) are found in the splenic red pulp. The lymphocyte rich white pulp area is where the splenic white pulp macrophages (WPM) are located. Splenic red pulp and white pulp are separated by the marginal zone. The splenic marginal zone is populated by two distinct macrophage subtypes: the marginal zone macrophages (MZM) are located along the marginal sinus, facing the red pulp, while marginal metallophilic

macrophages (MMM) line the marginal sinus at the boarder of the white pulp (A-Gonzalez & Castrillo, 2018).

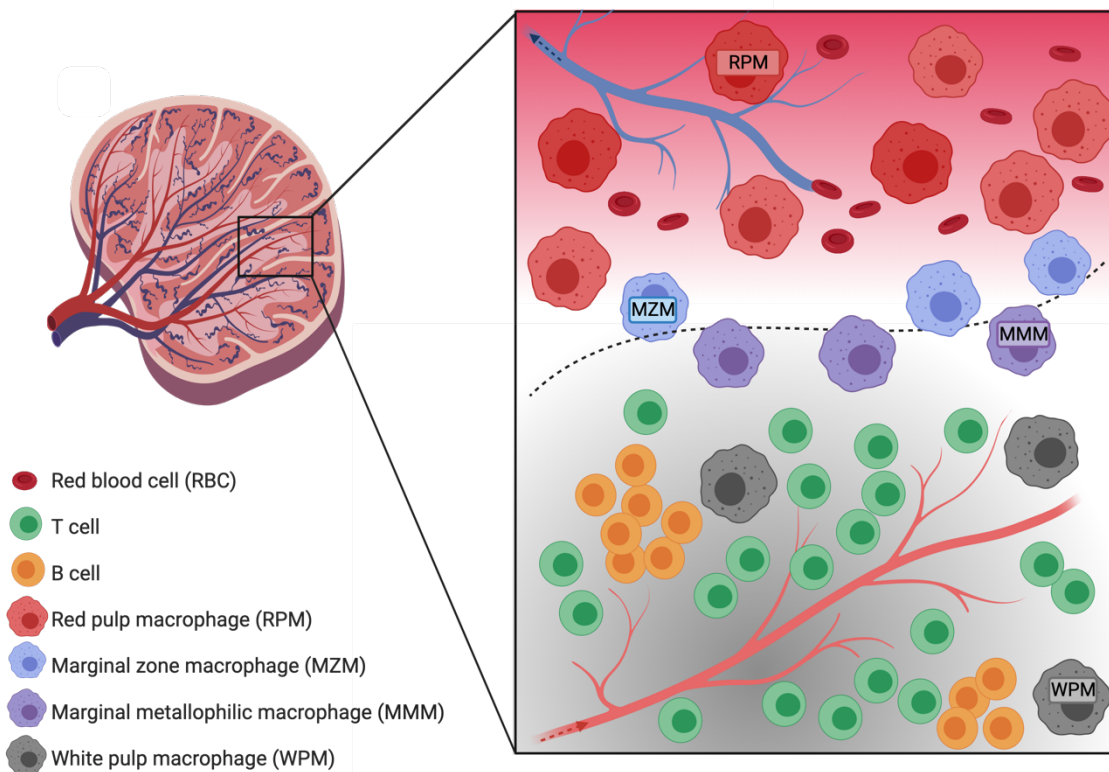


Figure 5: Splenic macrophages. At least four distinctive macrophage populations can be identified in the spleen. The red pulp macrophages (RPM) locate in the splenic red pulp. Marginal zone macrophages (MZM) and marginal metallophilic macrophages (MMM) line the marginal zone. White pulp macrophages (WPM) are in the B cell and T cell rich white pulp area.

1.6.1 Splenic red pulp macrophages

Amongst splenic macrophages, only those that populate the red pulp express the characteristic F4/80 glycoprotein in high levels on their plasma membrane. They develop during fetal stages with minimal contribution of monocyte-derived cells. However, after macrophage depletion, BM-derived monocytes can repopulate the splenic red pulp with F4/80⁺ macrophages (Schulz *et al*, 2012). It was described

that HSC-derived monocytes contribute to the adult pool of splenic RPM, but the precise dynamics of precursor cells and the contribution of EMP- versus HSC-derived cells to the splenic red pulp macrophages (RPM) in the steady-state has not been completely determined (Lavin *et al*, 2015). The best known function of splenic RPM is the clearance of debris, pathogens and erythrocytes that are trapped in the red pulp sinusoids and stromal network (A-Gonzalez & Castrillo, 2018). They are equipped with the machinery to process heme and iron after the uptake of senescent erythrocytes: RPM express high levels of Spi-C, CD163, heme-oxygenase-1 and ferroportin (Ganz, 2016). In short, the CD163 receptor binds a hemoglobin-haptoglobin complex, which facilitates downstream degraded of heme by heme-oxygenase-1 and the resulting free iron can be exported via ferroportin. There is evidence for a different mechanism of erythrocyte elimination by splenic RPM, which involves the exposure of phosphatidylserine on the outer membrane of shrinking erythrocytes, similar to apoptotic cells (Lang *et al*, 2012). But these erythrocytes are believed to be recognized by a different subset of phagocytes in the spleen (Larsson *et al*, 2016).

Recently, proliferator-activated-receptor γ (PPAR γ) has been identified as an important factor for the development of iron-recycling macrophages (Okreglicka *et al*, 2021). With a genetic depletion-model, Okreglicka *et al* (2021) showed that RPM lose the expression of signature genes, related to erythrocyte clearance and iron recycling. PPAR γ -deficiency caused a reduction of vascular cell adhesion molecule-1 (VCAM-1) expression, which is critical for the development of RPMs and thus had a severe impact on splenic RPM counts.

Splenic RPM further play a role in immunological functions. They respond to inflammatory stimuli and parasitic infections through the production of large amounts of type I interferons (Kim *et al*, 2012). *In vitro* studies of co-cultures of RPM with CD4 T cells hint towards an implication of RPM on the differentiation of T cells towards a regulatory phenotype (regulatory T cells) (Kurotaki *et al*, 2011).

RPM confer two main protective functions during blood-borne infections: they phagocytose pathogens from the circulation, and they activate the immune system. Therefore, they are equipped with a variety of pattern-recognition receptors (Borges Da Silva *et al*, 2015). Toll-like receptor 4 (TLR) binds bacterial lipopolysaccharide (LPS) and induces the expression of pro-inflammatory genes. TLR-4 and TLR-2 have been described to interact with *Plasmodium* parasite structures and TLR-9 can recognize bacterial or parasitic DNA (Parroche *et al*, 2007).

1.6.1.1 Regulation of iron homeostasis by splenic red pulp macrophages

Splenic RPM are specialized for the recycling of iron. They act as scavengers for heme and take up damaged RBC and recycle the iron that is released. In a homeostatic state, this iron is predominantly used for the production of hemoglobin in new erythrocytes (Ganz, 2016). An adult human contains approximately 4 g of iron, of which 2.5 g is bound in heme within erythrocytes and approximately 1 g is stored in hepatocytes and macrophages in the liver and spleen (Ganz, 2016). Splenic macrophages play a key role in the maintenance of iron homeostasis, digestion of erythrocytes, and extraction of heme. In the human body, an erythrocyte passes the spleen approximately every 20 min and is subjected to a quality check by the macrophages. Macrophages monitor erythrocytes for opsonization with antibodies, decreased deformability and loss of the self-antigen CD47 (Buffet *et al*, 2011). One macrophage ingests approximately 1 erythrocyte per day. Erythrophagocytosis can be enhanced during hemolytic diseases, but this can cause damage to the splenic macrophages (Kondo *et al*, 1988). Upon a high demand for erythrophagocytosis and iron recycling, a transient population of monocyte-derived macrophages has been described in the liver, which delivers iron to hepatocytes (Theurl *et al*, 2016). This specific transient macrophage population was not detected in the spleen upon hemolytic events, which is otherwise the major organ responsible for erythrophagocytosis and iron recycling. Erythrophagocytosis can further be enhanced by mild genetic abnormalities, such as the sickle cell trait, which can

be advantageous. It can for example protect the carrier from malaria, because enhanced clearance of abnormal erythrocytes also mediates faster removal of parasitized erythrocytes (Mohandas & An, 2012).

RPM are characterized by an enhanced expression of proteins that are involved in hemoglobin uptake (e.g. CD163), heme breakdown (e.g. hemo-oxygenase-1) and iron export (e.g. ferroportin). Heme-oxygenase-1 catalyzes the degradation of heme to iron, carbon monoxide and biliverdin. The expression of the enzyme is enhanced upon oxidative stress. The important role of hemo-oxygenase-1 is highlighted by the fact that even hematopoietic stem and progenitor cells express it to be protected from oxidative damage by free heme (Liu *et al*, 2023). Severe hemolysis induced during pathological states, such as sickle cell disease, ischemia reperfusion and malaria leads to increased amounts of free heme, which is toxic and can cause severe injuries to organs, tissues and cells. Free heme catalyzes the covalent crosslinking of proteins and their aggregation. Heme then further catalyzes the formation of cytotoxic lipid peroxide, which can damage the DNA through oxidative stress. Since heme is lipophilic, it can intercalate into membranes and damages the lipid bilayer and cellular organelles. Prolonged exposure to free heme can induce vascular inflammation and lead to renal failure and arteriosclerosis (Kumar & Bandyopadhyay, 2005). Thus, the function of heme-oxygenase, which is predominantly expressed by macrophages is crucial to prevent oxidative damage in tissues and organs. Myeloid cell differentiation towards anti-oxidant, iron-recycling macrophages is therefore favored upon hemolytic events to restore homeostasis. The heme-activated transcription factors Spi-C and PPAR γ regulate the replenishment of erythrophagocytic macrophages in adaptation to hemolysis-related tissue toxicity (Haldar *et al*, 2014).

While RPM have the capacity to store iron in their cytoplasm, the export of iron into the bloodstream is mostly mediated by the transporter protein ferroportin. The expression of ferroportin is tightly regulated by the hepatic hormone hepcidin. During inflammation, IL-6 leads to an increased expression of hepcidin, which

can bind to ferroportin and induce endocytosis of the transporter. This sequesters iron inside the macrophage. This function is important for macrophages to act as effectors in the antimicrobial defense of the host, because they can employ these mechanisms to deprive microbes of iron and thereby contain infections (Ganz, 2016).

Iron is an essential trace element and its bioavailability is crucial for many microbes and pathogens. During the acute phase of an infection, IL-6 mediated reduction of iron availability can eventually lead to the development of anemia and iron availability thus requires tight regulation (Liu *et al*, 2023). In addition, neutrophils that are recruited to the site of infection, can secrete lactoferrin, which captures free iron (Wong *et al*, 2009).

1.6.1.2 The CD163 receptor and hemoglobin uptake

Efficient clearance of extracellular hemoglobin is important to prevent oxidative stress. Upon erythrolysis, hemoglobin is released and its heme and iron components can form harmful ROS (Etzerodt & Moestrup, 2013). The uptake of hemoglobin is mediated by the CD163 receptor, which is expressed by mature tissue-resident macrophages (Fabriek *et al*, 2009). CD163 is a glycoprotein receptor on the plasma membrane and belongs to the scavenger receptor cysteine-rich protein family (Schaer *et al*, 2007).

Mechanistically, the CD163 receptor has a high affinity towards the hemoglobin-haptoglobin complex and mediates the uptake via endocytosis (Skytthe *et al*, 2020; Schaer *et al*, 2006). The cargo is delivered to the endosome, processed and transported to the enzyme heme-oxygenase for further degradation into biliverdin, carbon monoxide and free iron (Yang & Wang, 2022), while the receptor is recycled back to the plasma membrane surface (Figure 6). This circumvents heme toxicity and triggers anti-inflammatory responses (Etzerodt *et al*, 2014). High levels of expression of CD163 on the surface of macrophages is characteristic in tissues that respond to inflammation. Through the scavenging of oxidative hemoglobin, the receptor contributes to anti-inflammatory responses. There is increased evidence that CD163

expression is increased in acute and chronic inflammatory disorders (Etzerodt & Moestrup, 2013). CD163 expressed on the cell surface of macrophages, can be cleaved by inflammation responsive proteases, such as Adam17. The cleavage restricts hemoglobin uptake and prevents iron supply to intracellular pathogens (Fabriek *et al*, 2005). Soluble CD163 further plays a role in the resolution of inflammation. In humans, soluble CD163 is proposed as a biomarker, because it reflects macrophage activation during inflammation and relates to disease severity (Møller *et al*, 2017; Yap *et al*, 2023).

Increased serum levels of CD163 and a larger number of CD163 expressing macrophages were detected in patients with septic shock (Kjærgaard *et al*, 2014; Weaver *et al*, 2007). Animal studies in CD163-deficient mice showed decreased survival rates after LPS injection. In the deficient mice, inflammatory cytokines were more abundant, while IL10 was downregulated (Fujiwara *et al*, 2020).

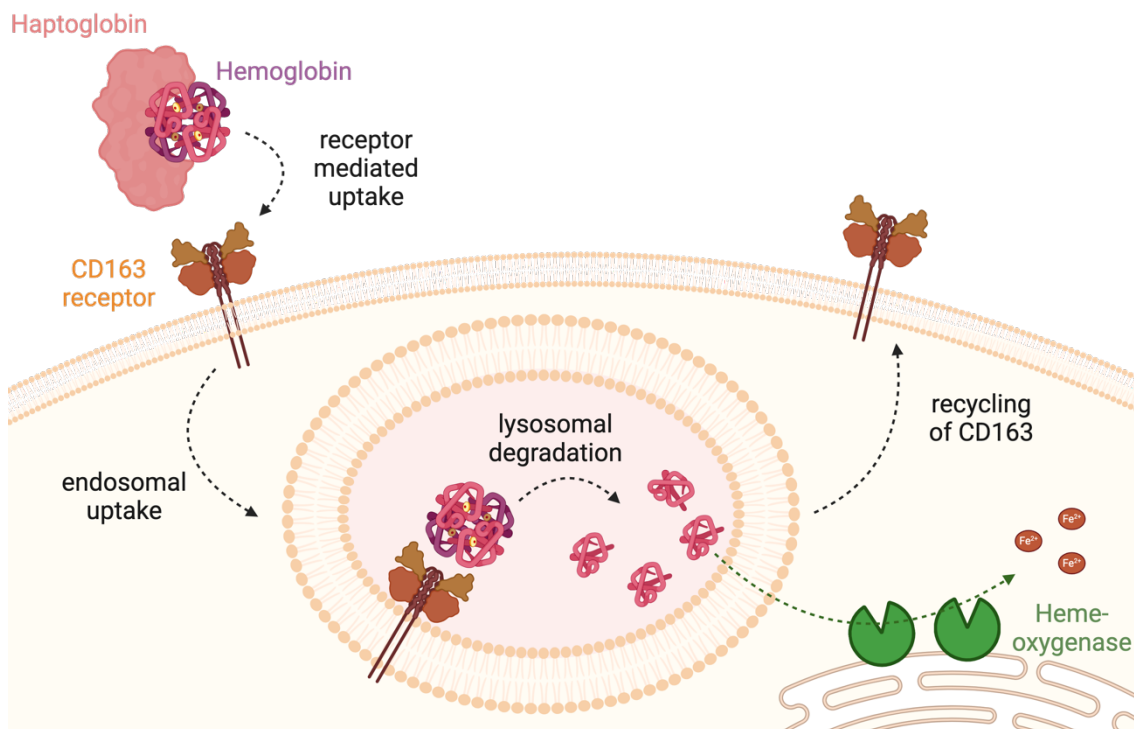


Figure 6: CD163 receptor mechanism. Hemoglobin-complexes bind to the CD163 receptor on the cell membrane, which mediates uptake into the endosome and degradation of hemoglobin by lysosomal enzymes. Heme-oxygenase on the endoplasmic reticulum catalyzes further degradation of heme-peptides to recover

iron. The CD163 receptor is recycled and fuses with the cell membrane to mediate further transport.

Other cellular mechanisms for the uptake of heme and iron also exist. Iron ions can bind to transferrin forming a complex, which induces internalization when bound to the transferrin receptor. The transferrin receptor is therefore one of the major iron-carrier proteins (Testa *et al*, 1993). In the gut, heme carrier protein 1 mediates the uptake of dietary heme in the small intestine and facilitates the transport of heme to enterocytes (Le Blanc *et al*, 2012).

1.6.2 Splenic marginal zone macrophages and marginal metallophilic macrophages

Macrophages in the splenic marginal zone are located at the interface between the red pulp and the lymphocyte-rich white pulp. Their strategic location provides an environment that is suitable for the recognition of blood-borne antigens (A-Gonzalez & Castrillo, 2018). They are described to be involved in the clearance of blood-borne bacteria, such as *Streptococcus pneumoniae* (Kang *et al*, 2004) and the phagocytosis of parasites, such as *Leishmania* (Gorak *et al*).

Macrophages in the marginal zone depend on the nuclear receptor Lxra and express the scavenger receptor MARCO at high levels (A-Gonzalez *et al*, 2013). The splenic marginal zone contains special endothelial cells that line the marginal sinus and express MadCAM1. But different from the equivalent structures in the lymph nodes, these cells do not form vessels but instead form a line that surrounds the white pulp area. Splenic MMM are in close association with the marginal sinus and co-exist with an outer layer of MZM. This makes the splenic marginal zone a unique microenvironment, where two phenotypically and functionally distinct macrophage subtypes co-exist (A-Gonzalez & Castrillo, 2018). However, speculations about the distinctive functions of MMM and MZM

are difficult, because most genetic mouse models do not specifically deplete only one subtype. Characteristically, MMM express high levels of CD169 and MZM typically show high expression of SIGNR1. These markers are however rapidly internalized when the cells are isolated from the spleen for *in vitro* studies (A-Gonzalez & Castrillo, 2018; A-Gonzalez et al, 2013).

It has been described that MMM are involved in the clearance of viruses (Vanderheijden *et al*, 2003) and take up antigens for presentation to CD8⁺ dendritic cells, which in turn activate T cell responses (Backer et al, 2010). The absence of MMM in *Lxra*^{-/-} mice had no apparent effect on the sinus lining cells or the organization of B cell and T cell areas in the spleen, which rules out an involvement of MMM in the splenic structural organization during the steady-state (A-Gonzalez et al, 2013).

MZM interact with marginal zone B cells. They transfer blood-borne antigens to the B cells, which then migrate to the white pulp follicles and initiate germinal center reactions. SIGNR1 on MZM is a key molecule for marginal zone B cell-MZM interactions and in the absence of SIGNR1, the migration of the marginal zone B cells to the follicles is impaired (You et al, 2011). MZM further contribute to immune tolerance, which was demonstrated by their rapid clearance of intravenously injected apoptotic cells, to prevent immune activation towards dying cells (A-Gonzalez & Castrillo, 2018).

1.6.3 Splenic white pulp macrophages

Macrophages in the splenic white pulp predominantly phagocytose apoptotic and autoreactive B cells. WPM populate the spleen once the germinal centers become active after weaning, but little is known about their definitive origin (del Portillo et al, 2012). In the germinal center, F4/80-negative macrophages contain the phagocytosed bodies of apoptotic cells. Condensed chromatin structures are visible, which appear dark blue upon hematoxylin and eosin staining. A similar

macrophage population in lymph nodes are called tingible body macrophages (A-Gonzalez & Castrillo, 2018).

In the germinal centers in the white pulp, B cells are highly proliferative and undergo somatic hypermutation and affinity maturation after clonal selection. Autoreactive B cells are phagocytosed by the WPM (or tingible body macrophages in lymph nodes), which thus have an important function as homeostatic regulators (Rahman et al, 2010). The phagocytosis is assisted by soluble molecules (e.g Gas6, C1q) that are enriched in the splenic environment, therefore facilitating clearance of apoptotic cells. WPM themselves express high levels of phagocytic receptors, such as CD68, MerTK and Tim4 to mediate phagocytosis of apoptotic cells (Rahman et al, 2010; den Haan & Kraal, 2012).

1.7 Malaria

Despite numerous control and elimination programs, malaria is one of the world's major infectious diseases, causing more than 200 million new cases and 400,000 deaths annually (Kurup et al, 2019; Ozarslan et al, 2019). The causative agent is the *Plasmodium* parasite and an infection can lead to life-threatening complications. The protozoan parasite causes recurrent fever, the hallmark symptom of the disease, alongside headache and anemia, which can progress to more severe symptoms like acidosis, kidney failure, and cerebral malaria (Coban et al, 2018). The spread of drug-resistant parasites highlights the importance of identifying novel targets (Imai et al, 2015).

The complex development of human malaria into a clinical illness commences with the transition of the parasite from mosquito to human (Milner, 2018). The capability of relapsing from a dormant liver stage months to years after the initial mosquito-borne infection is central to the survival strategy of some parasite species (e.g. *P. vivax*) (Markus, 2018). On the contrary, selection pressure has evolved in humans toward mutations that favor sickle cell disease and enzyme

deficiencies, which confer a survival advantage through the intervention with typical parasite routes of transmission or differentiation within the human body (Perry, 2014). The clinical manifestation of malaria can vary and depends on the *Plasmodium* species as well as the host's innate and acquired immunity (Price et al, 2014).

Elimination strategies nowadays focus on the two prevalent human species *P. falciparum* and *P. vivax*. The burden of morbidity due to other species is less well understood (Perry, 2014). Upon infection, the asymptomatic liver stage of malaria precedes the symptomatic blood stage, when the parasites invade RBCs, causing severe symptoms including recurring fever, a hallmark symptom of the disease as well as headache, vomiting, and anemia. Chloroquine remains one of the first-line treatments because of its sustained efficacy, widespread availability, low cost, excellent safety, and tolerability profile (Price et al, 2014).

1.7.1 *Plasmodium* life cycle

The causative agent of malaria is the *Plasmodium* parasite, a protozoan organism that belongs to the large group of unicellular and mostly obligate endoparasites, called *Apicomplexa*. The *Plasmodium* parasite undergoes a complex life cycle that involves multiple morphologically distinct stages (Figure 7).

The parasite is transmitted by the female *Anopheles* mosquito. When an infected mosquito takes a blood meal, motile sporozoites are inoculated into the dermis, which facilitates access to the peripheral circulation. Trafficking through the blood allows the parasite to reach the liver and establish the asymptomatic liver-stage of infection (Hall et al, 2005). Sporozoites infiltrate hepatocytes and form a protective capsule for their transformation into multinucleated schizonts. Upon an active phase of differentiation and asexual intracellular replication, the syncytial-like schizonts are produced. This generation of thousands of merozoites within a membrane-bound vesicle is a short-lived, clinically silent process that occurs within the first week of the infection (Mota et al, 2001; Mawson, 2013).

The symptoms of malaria only begin with the first liver schizont rupture, when thousands of merozoites are released into the peripheral circulation (Milner, 2018). This initiates the symptomatic blood-stage of a malaria infection. Merozoites invade RBC and metabolize erythrocyte proteins when developing into highly proliferative trophozoites. Asexual reproduction inside RBC results in the formation of schizonts, which synchronously rupture from infected RBC to release daughter merozoites into the blood stream that invade new RBC (Ozarslan et al, 2019). This iterative cycle of invasion and synchronized rupture to release merozoite elicits recurrent cyclic fever, the hallmark clinical symptom of malaria pathology (Basu & Sahi, 2017).

To complete the transmission cycle of malaria parasites, the parasites undergo sexual reproduction. Therefore, in some infected RBC, the parasites develop into gametocytes instead of replicating asexually. These gametocytes circulate inside erythrocytes through the blood-stream and can be ingested by mosquitos. In the mosquito gut they form oocysts, which develop into high numbers of active sporozoites. The sporozoites travel to the salivary glands of the mosquito and a new cycle of infection begins upon a mosquito bite (Mawson, 2013).

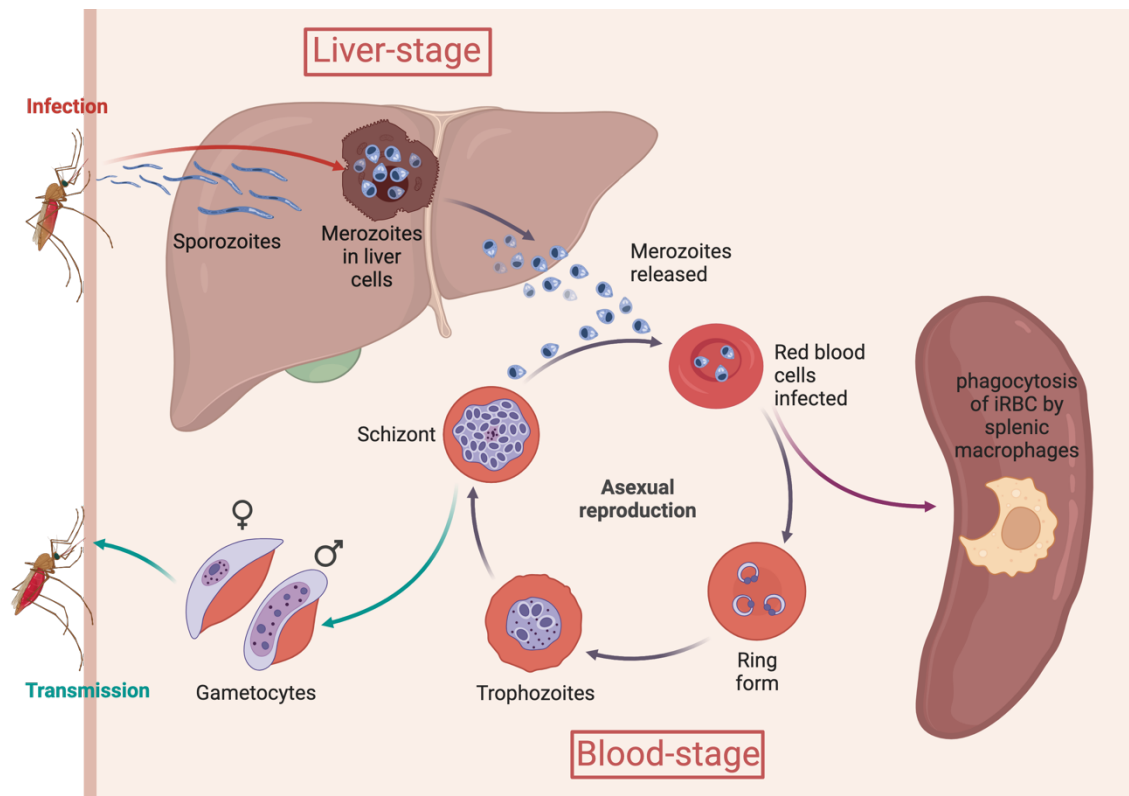


Figure 7: Plasmodium life cycle. Mosquitos transmit the parasite. Sporozoites manifest the asymptomatic liver-stage. During liver-stage malaria, the parasites differentiate inside hepatocytes into merozoites, which infect red blood cells (RBC) and undergo repeated cycles of asexual reproduction inside erythrocytes (ring form to trophozoites to schizonts and rupture of merozoites). During the blood-stage of malaria, circulating infected RBC can be cleared via phagocytosis by splenic macrophages. Some parasites differentiate into gametocytes, which fuse inside the mosquito gut and be transmitted to further hosts.

1.7.1.1 Hemozoin

Through repeated cycles of merozoites rupturing from infected RBC, erythrocyte and parasite debris is released. This includes hemozoin, which is called the “malaria pigment” or “malaria toxin” (Mawson, 2013). During the intra-erythroid trophozoite and schizont stages, almost 80 % of the cytoplasm components of host erythrocytes are consumed by the parasites. Digestive vacuoles inside the parasites are equipped with enzymes for the degradation of hemoglobin. The proteolytic degradation of hemoglobin yields amino acids for parasite growth, but

also free heme, which is toxic to the malaria parasite. They lack the enzyme heme-oxygenase, which detoxifies heme in vertebrates. Instead, they convert the heme monomer into an inert biocrystal (Coronado et al, 2014). The so called hemozoin is an undegradable crystal structure that is formed as a product of hemoglobin degradation by the parasites during a blood-stage malaria infection. It is associated to severe malaria and has implications for the host immune response (Pham et al, 2021). Hemozoin can activate the NF κ B inflammasome pathway and induce cytokine release by peripheral blood mononuclear cells.

It is predominantly macrophages in the spleen, liver and BM that ingest infected RBC and the free hemozoin that is released upon erythrocyte rupture. Although hemozoin has long been considered as nontoxic, it can contribute to malaria pathology by affecting macrophage function (Coronado et al, 2014). When macrophages ingest infected RBC that contain early ring-forms of the parasite and relatively little hemozoin, they can rapidly complete phagocytosis and proceed with the uptake of further particles. In contrast, when the macrophages phagocytose infected erythrocytes that contain the later schizont-stage of the parasites and greater amounts of hemozoin, they lose their functionality with respect to ingestion of parasitized erythrocytes, and fail to continue with the normal phagocytic cycle (Schwarzer et al, 1992). It is suggested that hemozoin has a toxic effect on macrophages and causes permanent damage to the normal function of the cells (Coronado et al, 2014; Schwarzer et al, 1992).

1.7.2 The bone marrow as a reservoir for *Plasmodium* parasites

While the highest parasitemia occurs during asexual replication in the circulating blood of the vertebrate host, a minor portion of the asexual blood-stage parasites make a developmental switch and differentiate into female and male gametocytes, the sexual parasite life stage that is infectious to mosquitos, thus essential for transmission (Mawson, 2013; Venugopal et al, 2020).

Immature gametocytes are preferentially found in the spleen, but also in the BM parenchyma, a niche that protects them from clearance during maturation and allows them to eventually invade erythroid precursor cells (De Niz et al, 2018). Unlike asexual schizont forms, the major fraction of immature gametocytes is enriched in the BM parenchyma. The hematopoietic niche of the BM is a major site of parasite growth and sex development, which takes up to ten days, dependent on the parasite species (Venugopal et al, 2020). Physiologically, erythropoiesis occurs in erythroblastic islands in the BM, which consist of a central macrophage surrounded by erythroid cells. During the maturation of erythroid cells, the erythroblastic islands move closer to the sinusoids, while the reticulocytes lose their nucleus and are eventually released into the sinusoidal lumen. Merozoites and young gametocytes home to the BM, leave the sinusoids, and enter the parenchyma, where they invade reticulocytes and develop in association with erythroblastic islands (Venugopal et al, 2020). The BM is suggested to be an important reservoir for gametocyte development and proliferation of malaria parasites (Obaldia et al, 2018). Parasites of all stages can persist with a very low level of peripheral parasitemia, without the development of symptoms in the host (Perry, 2014). A better understanding of the dynamics between parasite multiplication and gametocytogenesis is essential for the development of new tools to disrupt malaria transmission (Aguilar et al, 2014).

1.7.3 *Plasmodium* clearance in the spleen

The spleen is a crucial organ for the maintenance of blood homeostasis and the control of blood-borne infections (Borges Da Silva et al, 2015). The splenic structure is similar to large lymph nodes. It possesses efferent lymphatic vessels to collect antigens from the blood and is supplied with blood from the central splenic artery, which branches along with the splenic vein through the parenchyma (Charles A Janeway et al, 2001a). Along the marginal sinus, microbes, pathogens and soluble antigens are filtered from the blood by macrophages and dendritic cells to initiate immune responses (Steiniger, 2015).

The open circulation in the splenic red pulp provides an ideal environment to encounter blood-borne infectious agents. The importance of the filtering function of the spleen in the elimination of *Plasmodium* parasites becomes apparent in splenectomized mice, which show higher parasitemia and mortality (del Portillo et al, 2012). Upon infection with the malaria parasite, the majority of infected RBC are cleared by the macrophages in the spleen. During the initial phase of the infection, macrophages ingest merozoites, ruptured schizonts and trophozoites in the open circulation of the spleen.

It was further described, that antibodies bind to the surface of intact parasitized erythrocytes and that this opsonization leads to the internalization of infected RBC by macrophages *in vitro* (Mota et al, 1998). Evasion strategies of the parasites include the preferential infection of erythrocytes with high levels of CD47. CD47 is a marker of self and prevents the clearance by immune cells. *CD47^{-/-}* mice had lower parasitemia and showed a higher percentage of F4/80⁺ cells in the spleen as well as a higher percentage of phagocytosed infected erythrocytes (Banerjee et al, 2015). Antibody-independent mechanisms for the clearance of infected RBC include the retention of parasitized erythrocytes in the spleen, because they are less deformable when passing the filtering system of the spleen and therefore get phagocytosed (White, 2017). In an endpoint response of the host innate immune system to a *Plasmodium* infection, tissue macrophages undergo necroptosis to release inflammatory mediators and recruit monocytes and neutrophils (Lai et al, 2018).

Apoptosis is however the major pathway involved in splenic cell death during malaria progression, and its occurrence coincides with the systemic peak of pro-inflammatory cytokines (Dunst et al, 2017). Empty anatomical niches are replenished by infiltrating cells with different properties and phenotypes (A-Gonzalez & Castrillo, 2018). Splenic macrophages are replaced by infiltrating monocytes, a phenomenon that is associated with increased inflammation (Lai et al, 2018). The loss of resident macrophages correlates with multi-organ damage and worse disease outcomes, due to a loss of IL-10 secretion, which has anti-inflammatory effects (Gupta et al, 2016). Instead, high amounts of the pro-inflammatory cytokine TNF α are released, being one of the factors

responsible for the fever during infection (Randall & Engwerda, 2010). An imbalance between pro- and anti-inflammatory cytokines, growth factors and chemokines determines malaria disease severity (Langhorne et al, 2008). IL-6, TNF α and IFN γ have been reported to be increased in severe cases of malaria (Mawson, 2013). Excessive inflammation, particularly high systemic levels of TNF α and IFN γ lead to the clearance of uninfected RBC and thereby contribute to the development of anemia. Persistent high levels of inflammatory cytokines are associated with the suppression of hematopoiesis and the progression to severe malaria. Studies have suggested that severe malaria is largely caused by an overreaction of the host immune response and metabolic disorders (Lacerda-Queiroz et al, 2017). Complications due to an increased loss of splenic phagocytes upon exhaustion can be causative for the development cerebral malaria, acute respiratory stress syndrome, acute renal failure, acidosis, hypoglycemia, toxic shock and severe anemia (Randall & Engwerda, 2010; Gupta et al, 2016). It has recently been shown that renal epithelial cells can compensate for the loss of splenic macrophages and the onset of life-threatening malaria anemia through transcriptional reprogramming (Wu et al, 2023). Wu et al (2023) showed that renal epithelial cells acquire the capacity to store and recycle iron upon a malaria infection and thus partially take over the function of splenic erythrophagocytic RPMs, which maintain systemic iron homeostasis in steady-state.

Overall, the resolution of blood-borne infections including malaria is highly dependent on splenic macrophages. The distinct origin, heterogeneity, and respective functional involvement of each splenic macrophage population in the resolution of the disease is poorly understood and requires advanced transcriptomic and imaging techniques to elucidate relevant subtypes, interactions and pathways that could impede disease progression.

1.7.4 Human malaria

Over 200 *Plasmodium* species are known today, each infecting a certain range of hosts. *Plasmodium* species that naturally infect humans include *P. falciparum*, *P. vivax*, *P. malariae*, *P. ovale* and *P. knowlesi*. All are exclusively transmitted by anopheline mosquitos (Sato, 2021).

Between *Plasmodium* species that are infectious to humans, the parasite life cycle and susceptibility to drugs is rather similar. The synchronized rupture of erythrocytes causes severe symptoms in the host, including fever and anemia. The frequency of ruptures differs between species by 2 - 4 days (Sato, 2021).

P. falciparum and *P. vivax* are the most common species causing human malaria. While the former is more prevalent in African countries, the latter is more prevalent in Asia and Latin-American. The symptomatic blood-stage of the infection causes anemia, which is visually detectable by a pale skin, fatigue and nausea. *P. falciparum* can cause a more severe form of malaria, cerebral malaria, which is a potentially fatal complication (Rénia et al, 2012). *P. falciparum* infections can further lead to organ failure, with the kidney and the liver being especially affected (Oluwole et al, 2010).

P. vivax is known for its potential to form hypnozoites, a dormant form of the parasite that survives undetected in the blood of patients (Flannery et al, 2022). Recurrence due to recrudescence or relapse is often described in human patients although the parasites have been cleared from the blood. The parasites can persist undetected in the liver, blood and BM. Cases of *P. falciparum* persistence in the human body for more than 13 years have been described (Ashley & White, 2014).

Despite effective antimalarials and insecticides, people remain at high risk of severe malaria, especially on the African continent. Thalassemia and sickle-cell disease, which confer some degree of protection against a malaria infection are enriched in endemic areas (Hedrick, 2011). But increased movement of the

human population facilitates the import and spread into low-risk countries (Cibulskis et al, 2016).

The advent of both natural and chemical drugs has rendered malaria treatable, and the management of mosquito vectors through insecticides, along with patient treatment using medications like chloroquine, has significantly lessened the impact of malaria in contemporary times. However, despite these advancements, malaria persists as a widespread infectious disease, claiming the lives of hundreds of thousands of individuals, particularly children, worldwide each year (Sato, 2021).

1.7.5 Chloroquine

After decades of research, two vaccines have been recently approved by the World Health Organization after phase 3 clinical trials and showed 75 % efficacy (Dattoo et al, 2022). Long-term studies are however still ongoing and many people are not vaccinated yet and get infected. Infected patients can be treated with anti-malaria drugs that efficiently target the parasites. Five distinct classes of anti-malaria treatment have been described (Ross & Fidock, 2019) and categorize chloroquine in the class of 4-aminoquinolines (Table 1).

Table 1: Anti-malaria drugs.

Class	Drug
Endoperoxides	Artemisinin (and derivatives)
4-aminoquinolines	Chloroquine Quinine Mefloquine
Antifolates	Pyrimethamine Sulfadoxine
Naphthoquinones	Atovaquone
8-aminoquinoles	Primaquine Tafenoquine

Chloroquine was developed in the 1950's and has a high safety profile (Coban, 2020). It affects the erythrocytic stage of the malaria parasites, but was additionally described to have anti-viral, anti-bacterial and anti-cancer properties (Zhou et al, 2020). Some studies have shown that chloroquine binds to DNA- and RNA-structures, which explains why the drug can interfere with viral replication of Zika, influenza, herpes and SARS-CoV (Li et al, 2017). To target parasitic DNA in the nucleus, much higher concentrations than usually administered would be needed (Foley & Tilley, 1998). Instead, chloroquine targets the hemoglobin degradation pathway in *Plasmodium* parasites. During the intra-erythroid stage, the parasites express proteases for the degradation of hemoglobin and make use of the amino acids. This pathway generates free heme, which is toxic. The parasites therefore polymerize free heme to hemozoin in an acidic digestive vacuole. Chloroquine is a weak base and increases the pH of the vacuoles, which interferes with the degradation process (Lee et al, 2016). The drug was described to partially destroy the vacuoles, which leads to a loss of proteases and enzymes that are required for the detoxification of heme through the generation of hemozoin (Ch'ng et al, 2014). Blocking hemozoin formation leads to an accumulation of reactive products and heme mediated toxicity, which causes parasite death (Coban, 2020; Slater, 1993). Chloroquine was further assigned to have immunomodulatory modes of action and to inhibit autophagy, which are advantageous effects for the treatment of SARS-CoV and cancer (Zhou et al, 2020).

The genetic flexibility of the parasites, however, allows for a quick adaptation and the development of resistance (Sato, 2021). In *P. falciparum*, mutations in a specific reporter lead to the efflux of chloroquine from the digestive vacuoles (Valderramos & Fidock, 2006). The spread of chemo-resistant species makes it relevant to identify new targets. Other drugs, such as Primaquine, cause severe side effects, hence a safe and effective therapy for the cure of malaria is needed (Douglas et al, 2017).

1.7.6 Murine malaria

Malaria, a fatal disease, manifests a range of symptoms and severity levels, influenced by intricate host-parasite interactions. Studying the impact of parasite species on disease severity in human infections is challenging, but investigating the mechanisms leading to specific phenotypes can be accomplished using species of rodent malaria parasites. These species induce distinct symptoms in inbred mice, providing a valuable model for understanding the underlying processes (Lacerda-Queiroz et al, 2017). A drawback that needs to be considered however, is that the spleen and BM are active sites of erythropoiesis in mice, while in humans it only occurs in the BM (Safeukui et al, 2015).

P. falciparum and *P. vivax* are the prevalent species which cause human malaria. These species are not infectious to mice or other model organisms. Thus, mouse malaria species are used, which adequately mimic human pathologies of the disease. This study focuses on murine infections with *P. chabaudi* as well as *P. yoelii* and *P. berghei*.

1.7.6.1 *P. chabaudi*

P. chabaudi causes a mild but persistent infection in mice and features common human symptoms such as anemia, changes in body temperature and weight loss (Stephens et al, 2012). A significant conservation between genetic and phenotypic traits of human malaria parasites and rodent counterparts has been described (Walliker et al, 1971). The rodent *P. chabaudi* species was discovered in central Africa in the middle of the 20th century and resembles various characteristics of the human pathology. Wildtype *P. chabaudi*, unlike *P. yoelii*, is sensitive to chloroquine treatment and can be transmitted by mosquitos in the laboratory (Carter, 1972). The most commonly used species *P. chabaudi* AS is generally non-lethal, similar to human *P. falciparum* and *P. vivax* infections. Different from human *P. vivax*, which preferentially invades immature erythrocytes, *P. chabaudi* as well as *P. falciparum*, invade erythrocytes at all different developmental stages (Carter & Walliker, 1975). An infection with

P. chabaudi causes severe anemia, one of the major complications in human malaria, through dyserythropoiesis and phagocytosis of infected and non-infected RBC (Chang et al, 2004). In addition, splenomegaly and hypoglycemia are resembled with rodent *P. chabaudi* infections (Stephens et al, 2012). A downregulation of MHC molecules on dendritic cells has been described in human *P. falciparum* malaria in Kenya, which was also observed in *P. chabaudi* infections and affects the initiation of T cell responses (Urban et al, 2001). Human malaria is associated with the development of a Th1 response and characteristic IFN γ production by T cells and NK cells, which is resembled in *P. chabaudi* murine malaria (Langhorne et al, 1989; Ing & Stevenson, 2009). Also, a key role of the regulatory cytokine IL-10 in the reduction of severe symptoms was described in both, *P. falciparum* and *P. chabaudi* malaria (May et al, 2000). The contribution of malaria specific antibodies also shows similarities amongst species and antibody-mediated clearance of parasites is mostly mediated by antibodies of the IgG class (Meding & Langhorne, 1991).

Limitations of the murine *P. chabaudi* model include differences in the sequestration of the parasites. While human parasites are often sequestered in the brain, in the mouse the liver is the primary organ for *P. chabaudi* sequestration (Stephens et al, 2012). Both, *P. chabaudi* infected RBC and infected erythrocytes in humans, can adhere to the host endothelial cells, but in humans this is associated with cerebral malaria, while *P. chabaudi* infected RBC stay in the liver. Another major difference in the pathological symptoms is that mice develop hypothermia instead of fever (Stephens et al, 2012).

1.7.6.2 *P. yoelii*

P. yoelii produces self-limiting nonlethal parasitemia and is characterized by preferential infection of reticulocytes during blood-stage malaria. Upon infections with *P. yoelii* the clearance of co-infections with other pathogens is impaired (Zhang et al, 2012). The less frequently used *P. yoelii* YM infects both,

reticulocytes, and mature erythrocytes. This lethal species has been used to test vaccines (Wykes & Good, 2009; Rex et al, 2022).

1.7.6.3 *P. berghei*

Much knowledge about the mosquito stage of the *Plasmodium* life-cycle was gained from experimental models of *P. berghei*. It is a relevant model to study host-parasite interactions and immune responses in the host (Matz & Kooij, 2015). *P. berghei* is known to cause cerebral malaria in mice, similar to infection with human *P. falciparum* (Clark et al, 1990).

1.8 *Plasmodium* clearance by splenic red pulp macrophages

Venous cords and sinuses in the splenic red pulp mediate slow blood flow and allow for filtering of the blood and the elimination of infected RBC by macrophages (Borges Da Silva et al, 2015). A macrophage colony stimulating factor (M-CSF)-dependent type of RPM has been described as efficient phagocytes in the spleen, which produce inflammatory cytokines, such as TNF α and type I interferons in response to pathological stimuli. An M-CSF-independent RPM type produces high levels of prostaglandin E2, which strongly activated the M-CSF-dependent phagocytic macrophages and indicates a potential control mechanism of RPM phagocytic activity in the spleen (Rutherford & Schook, 1992).

Splenic RPM can further limit iron availability and uptake by *Plasmodium* through TLR-mediated release of lipocalin-2, which forms a complex with siderophores that are secreted by pathogens to collect iron (Flo et al, 2004). RPM themselves express high levels of heme-oxygenase-1 to degrade heme. The uptake of hemoglobin-bound heme via the CD163 receptor induces an increased level of heme-oxygenase-1 expression in macrophages (Pradhan et al, 2020). This enzyme confers a protective phenotype in macrophages and restrains the redox

activity of labile heme (Ramos et al, 2024). Microsatellite polymorphisms in the gene *Hmox1* encoding heme-oxygenase-1 are associated with an enhanced susceptibility to malaria (Mendonça et al, 2012).

Next to the regulation of iron availability, splenic RPM are suggested to control immune responses to blood-borne pathogens. They constitutively express PPAR γ , which restricts excessive immune responses to pathogens. Instead, RPM produce the anti-inflammatory cytokines transforming growth factor beta (TGF β) and IL-10 (Kurotaki et al, 2011).

RPM have a pivotal role in the control of blood-stage malaria. A proportion of RPM that exhibit strong labeling with F4/80, participate in the early clearance of *P. chabaudi* parasites, but this population sharply declines at the peak of parasitemia (Borges da Silva et al, 2015). RPM have a slow turnover and are usually maintained through local proliferation. However, upon the ingestion of infected RBC, they undergo cell death, most likely due to the toxic effects of hemozoin (Deshmukh & Trivedi, 2014). The loss of RPM can lead to intravascular hemolysis and the release of labile heme, which promotes the pathogenesis of severe forms of malaria (Gouveia et al, 2017; Lai et al, 2018). Labile heme has cytotoxic and pro-inflammatory effects (Gouveia et al, 2017) and was identified as a crucial regulator for the differentiation of circulating monocytes into macrophages (Pradhan et al, 2020). Circulating monocytes can differentiate into macrophages and substitute RPM by a more inflammatory phenotype (Hashimoto et al, 2013). Hemozoin, which is a disposal product from the digestion of hemoglobin by the parasites, can further trigger the NLRP3 inflammasome pathway during an acute malaria infection in bone marrow derived macrophages (BMDM) and leads to the production of the pro-inflammatory cytokines IL-1 β and IL-18 by macrophages (Kalantari et al, 2014).

The release of heat shock proteins (HSP) can also lead to the secretion of inflammatory cytokines. HSPs are released by cells upon stress and engage with TLR2 and TLR4 on macrophages (Borges Da Silva et al, 2015). *Plasmodium*

parasites have been described to release HSP homologues (Bianco et al, 1986). TLR2 and TLR4 can further recognize extracellular matrix components, such as fibronectin, which leads to macrophage activation (Okamura et al, 2001). Fibronectin is presumably secreted by splenic fibroblasts and is produced in higher amounts during malaria infection as a consequence of the changes in the splenic microarchitecture (Borges Da Silva et al, 2015).

Through extensive apoptotic cell death of splenocytes during malaria infection, macrophages release high mobility group box protein 1 (HMGB1), which can engage with TLR4 and further stimulate inflammatory responses in macrophages. Blocking of HMGB1 with a monoclonal antibody has been shown to prevent the development of severe sepsis (Qin et al, 2006). In humans, higher HMGB1 levels in the serum are associated with severe malaria. Abundant apoptosis of splenic cells is typical in rodent malaria at the peak of acute infection (Borges Da Silva et al, 2015; Elias et al, 2005).

1.9 Models to study the functional role of specific macrophage subtypes

To understand the role of macrophages in disease onset and progression, scientists have used administration of clodronate as a fast and feasible method to deplete macrophages. Its mode of action however is rather broad, as clodronate does not target specific organs or macrophage lineages, but also other myeloid cells (Moreno, 2018). Further, due to sudden cell death, clodronate induces a broad immune response (Weisser et al, 2012), which may be a confounding factor in any disease studied after or during this treatment. A more specific and inducible approach is the introduction of the diphtheria toxin receptor (DTR) expression via genetic methods and subsequent administration of diphtheria toxin. The chemical-induced ablation however triggers uncontrolled systemic inflammation, similar to clodronate, and thus does not represent homeostatic conditions (Miyake et al, 2007).

Instead, genetic engineering allows for the introduction of specific sequences and mutations into the mouse genome to target relevant pathways for a particular cell type or function (Hall et al, 2009). The utilization of this method became possible with the identification of homologous recombination and the isolation of embryonic stem cells. Homologous recombination, a DNA-repair mechanism, is utilized for gene editing, to incorporate a predetermined sequence or mutation. Using electroporation, this engineered construct can be introduced into isolated embryonic stem cells, which are then injected into the mouse blastocyst, giving rise to the formation of an embryo (Hall et al, 2009).

Complications in the design of genetic knockout models arise, when the gene product is essential for the normal function of the body and inactivation of the gene could be lethal or induce morphological or physiological abnormalities (Nelson, 1997). To circumvent the generation of developmentally lethal knockouts, Cre/loxP technology allows for the conditional depletion of target genes. Through the introduction of an inducible Cre-system, the depletion of a target gene can even be controlled in a temporal manner (Hayashi & McMahon, 2002). Careful interpretation of the target gene function is however always relevant, since unexpected compensatory or redundancy mechanisms can be activated and cloud the analysis of the designated gene function (Nelson, 1997).

1.9.1 Genetic depletion of the CD163 receptor

The CD163 receptor is expressed on tissue macrophages and contributes to homeostasis via the uptake of hemoglobin-haptoglobin complexes to prevent oxidative stress. Receptor mediated uptake has mostly been described in the spleen, liver and BM (Fabriek et al, 2005). CD163-expressing macrophages are associated with an anti-inflammatory phenotype, which is why their presence during the acute stage of malaria infection could counteract an inflammation-mediated parasite clearance (Skyttthe et al, 2020). On the other hand, parasite-induced hemolysis is a hallmark of malaria infection, which causes

high systemic levels of free hemoglobin and requires effective scavenging mechanisms (Mendonça et al, 2012). The CD163 receptor is crucial for the uptake of hemoglobin and thus to prevent oxidative stress caused by free heme (Kristiansen et al, 2001). To study the role and relevance of this receptor in an acute malaria infection and during the progression of the disease, a genetic CD163 receptor knockout mouse model can be used. In sepsis models, CD163-deficient mice showed reduced survival and higher abundance of pro-inflammatory cytokines, while IL-10 was reduced (Fujiwara et al, 2020).

1.9.2 Genetic depletion of Lxra

The liver x receptors (Lxr) are members of the nuclear receptor family of transcription factors that play key roles in the control of sterol homeostasis (Repa & Mangelsdorf, 2000). Lxra is encoded by the *Nr1h3* gene and Lxr β is encoded by the *Nr1h2* gene (A-Gonzalez et al, 2013). While Lxr β is ubiquitously expressed, Lxra is expressed by differentiated macrophages in the liver, intestine and splenic marginal zone (A-González & Castrillo, 2011). The nuclear receptors have largely redundant functions and regulate genes that are involved in lipid homeostasis and inflammation, but specifically Lxra has a pivotal role in the development of the splenic marginal zone (A-Gonzalez et al, 2013). Macrophage populations in the splenic marginal zone are characterized by the expression of CD169, SIGNR1 and MARCO (Kraal & Mebius, 2006). The expression of these characteristic surface receptors is lost in *Lxra* knockout (*Lxra*^{-/-}) mice, while splenic macrophages in other splenic compartments show a phenotype that is comparable to wildtype mice. Also, the structure of the splenic white pulp and red pulp develop normally and are clearly separated in *Lxra*^{-/-} mice. Thus, Lxra is presumably not involved in the signaling that is required for the development of the splenic red pulp and white pulp (A-Gonzalez et al, 2013).

But, the absence of macrophages in the splenic marginal zone in the *Lxra*^{-/-} model leads to abnormal responses to blood-borne pathogens. While MZM and MMM usually play a role in the capturing of blood antigens and the clearance of

circulating pathogens, this function is partially taken over by the macrophages in the splenic red pulp, indicating a high degree of plasticity (A-Gonzalez & Castrillo, 2018). In addition, the response of IgM antibodies during infections is decreased when *Lxra*-dependent macrophages are depleted. MMM and MZM signaling is important for the retention of marginal zone B cells and an early IgM response (A-Gonzalez et al, 2013).

The interplay between macrophages and their environment is crucial to determine the specific function of a macrophage subset. It was shown that an adoptive transfer with wildtype monocytes rescues the marginal zone microenvironment in *Lxra*^{-/-} mice (A-Gonzalez & Castrillo, 2018).

The loss of *Lxra* leads to peripheral lipid accumulation and mice showed symptoms of immune overreactions, which can culminate into systemic autoimmunity (Calkin & Tontonoz, 2012; A-Gonzalez et al, 2009). It was further shown that *Lxra* is important for the regulation of genes in cholesterol and fatty acid metabolism in the liver and intestine (Ulven et al, 2005). *Lxra*^{-/-} mice cannot express the *Cyp7a* gene, which leads to the accumulation of cholesterol in the liver and impaired hepatic function (Peet et al, 1998). *Lxra* might also play a role in the response to herpes viruses, since increased viral replication was detected in *Lxra*^{-/-} mice (Lange et al, 2019).

1.10 Macrophages and T cell activation upon blood-borne infections

T cells are adaptive immune cells that originate from HSC in the BM. They migrate to the thymus where they mature. T cells can be divided into different subtypes with distinctive important functions. Cytotoxic T cells are characterized by the expression of the co-receptor CD8 and recognize antigens presented on MHC class I. Upon activation, they can kill infected cells through the release of cytotoxic granules that contain perforin and granzyme (Junqueira et al, 2021). While almost all cells express MHC class I molecules, erythrocytes that have extruded their

nucleus do not display antigens via MHC class I on their surface (Murphy & Weaver, 2018). CD4 expressing T cells, called helper T cells, mount immune responses by recruiting and activating other immune cells. They recognize antigens presented on MHC class II molecules, which are expressed by specialized antigen-presenting cells. A variety of subclasses of T helper cells can be induced, dependent on the cytokine environment present at the time of activation and differentiation (Ivanova & Orekhov, 2015). Regulatory T cells on the other hand, are critical to mediate mechanism of immune tolerance and prevent excessive systemic inflammation.

The priming and activation of T cells is of crucial importance for long-term pathogen clearance and immunological memory formation. Yet, T cells require antigen-presenting cells to process and present peptide antigens for their activation. Splenic macrophages take up large amounts of blood-borne pathogens, which initiates a sequential process to generate antigens that are transferred to DC and presented to T cells for their activation (Malo et al, 2018). Thus, the interaction between macrophages, dendritic cells and T cells is of critical importance to engage the adaptive immune system and combat infections. Crosstalk along the macrophage - T cell - B cell axis leads to the production of antibodies, which can confer additional macrophage activity for more efficient parasite clearance (Krzych et al, 2014).

So far, malaria research mainly focuses on T cells and how they control the infection in a cytokine-dependent manner. Various intervention studies have aimed to sensitize T cells to target *Plasmodium*. Yet, splenic macrophages might play a crucial role in the generation of parasite-specific immunity through parasite uptake, antigen processing and transfer. The parasite hides from the immune system through its intracellular life-style within RBC that lack MHC expression, which impedes its recognition by cytotoxic T cells (Kurup et al, 2019). Recent studies suggest that CD8⁺ T cells undergo an antigen-mediated arrest in the splenic red pulp to locally deliver chemokines for monocyte activation, thereby mediating early protection (Boutet et al, 2021).

Activated CD8⁺ T cells might induce parasite clearance in the spleen through the expression of Fas-ligand, which activates Fas-receptor signaling on RBC, leading

to the exposure of phosphatidylserine on the surface. This, in turn, stimulates macrophages to phagocytose phosphatidylserine exposing cells (Imai et al, 2015). Elimination of both infected and uninfected erythrocytes in the spleen is, however, a frequent fatal complication that can lead to severe malarial anemia. Increased CD8⁺ T cell counts in the spleen are not only related to a reduction of the parasite load, but also associated with exacerbated hemoglobin loss and changed properties of uninfected erythrocytes (Safeukui et al, 2015; Lacerda-Queiroz et al, 2017). This suggests that CD8⁺ T cell-dependent parasite clearance causes erythrocyte removal in the spleen and, thus, anemia. Blood transfusions as a counter measure carry the risk of other infections (Safeukui et al, 2015). Observed phenotypes of high levels of pro-inflammatory cytokines and extensive splenic damage with dramatic reduction of splenic cell populations could be rescued in T cell depleted mice (Lacerda-Queiroz et al, 2017).

While the role of cytotoxic T cells in the immune response to blood-stage malaria remains controversial, CD4 T cells play a critical role in priming phagocytic cells to capture the parasite and activate B cells to produce functional antibodies (Kumar et al, 2020). Helper T cells orchestrate both humoral and cellular adaptive immune responses against pathogens. Their crosstalk with naïve B cells results in immunoglobulin class-switching, which is essential for the clearance of the parasites (Fernandez-Ruiz et al, 2017). The loss of INF γ producing CD4 T cells directly correlates with elevated parasite burdens (Kurup et al, 2019).

Another T cell lineage with immune surveillance activities are $\gamma\delta$ T-cells (Ribot et al, 2020). They sense phosphor-antigens on the surface of infected RBC and form immune synapses to lyse infected RBC in a degranulation-dependent manner to kill intracellular parasites (Junqueira et al, 2021). Phenotypic changes and increased numbers in malaria-exposed individuals suggest an important role of $\gamma\delta$ T cells in controlling blood-stage malaria (Lefebvre & Harty, 2021).

The development of a *Plasmodium* specific T-cell receptor (TCR) mouse model (Lau et al, 2014) allows us to describe the location and phenotype of malaria-

specific CD8 and CD4 T cells and their maintenance in the spleen (Fernandez-Ruiz et al, 2016). To advance prevention and treatment strategies, it remains to be investigated, which cellular and molecular responses of splenic macrophages are important to overcome blood-stage malaria and whether a continuous cross-talk of the innate and adaptive immune system alleviates resolution of the infection.

1.11 Vaccines

New sequencing technologies and novel bioinformatic approaches have improved the knowledge about malaria epidemiology, treatment and vaccine development. Vaccination strategies act against different stages of the disease and life-forms of the parasite. Pre-erythrocytic vaccines target sporozoites, thereby preventing the invasion of liver cells. Other vaccines block the invasion of erythrocytes by acting against merozoites (Price et al, 2014). Researchers have identified target antigens, which can be used as powerful adjuvants for the generation of a specific antibody response. However, so far, the generation of a sufficient antibody response to kill all parasites was not achieved (Good & Staniscic, 2020). Multiple vaccines are currently being evaluated in preclinical and clinical trials, with the main objective to induce humoral and cellular T cell responses, which are known to become exhausted during malaria (Roestenberg et al, 2011). Still, researchers face challenges when tackling the threat that this ancient parasite poses on millions of people (Price et al, 2014). The complex parasite life cycle, antigenic variability, insufficient knowledge about the immune responses triggered upon infection as well as the lack of adequate animal experimentation models are reasons why an effective vaccine against *Plasmodium* has been difficult to develop (Bergmann-Leitner et al, 2011).

Irradiation is a technique that attenuates pathogens and renders them non-infective (Targett & Fulton, 1965). Though the parasite cannot proliferate anymore after irradiation, it retains certain antigens on the surface. The

attenuation of *Plasmodium* parasites is also in the focus of research that aims for the development of vaccination strategies against malaria. While efforts to identify key target antigens for vaccination did not generate a sufficient antibody response, the application of irradiated sporozoites was promising in initial clinical trials (Good & Staniscic, 2020). Through heat inactivation or irradiation, the immunogenic properties of the pathogens are preserved and can trigger the development of specific immune responses (Frank et al, 2018). Radiation attenuated sporozoites as well as heat killed sporozoites have been shown to confer sterile immunity against the liver-stage of malaria, which is mediated by CD8 memory T cells (Ghilas et al, 2021). Recent advances have also been made in the development of mRNA-based vaccines against malaria (Ganley et al, 2023), which are safer and can confer effective protection.

1.12 The viral infection model of lymphatic choriomeningitis virus

The lymphocytic choriomeningitis virus (LCMV) is a member of the arenaviridae family of viruses. It is a single stranded RNA virus and received its name because of granularities that were observed with electron microscopy (Boldogh et al, 1996). The virus is mostly acquired via nasal inhalation. It enters the lung and replicates locally before entering the blood stream. This allows for dissemination into various organs for further replication. In the spleen the virus primarily infects dendritic cells and macrophages. Those specialized phagocytes process viral antigens and present them to T cells in the splenic T cell zones. This initiates a strong response of cytotoxic T cells in the host (Abdel-Hakeem, 2019). Ultimately LCMV reaches the meninges and choroid plexus, where the virus replicates to high titers. This causes an inflammatory response and eventually meningitis (Bonthius, 2012).

While rodents are a natural reservoir, in humans the virus causes neurological disorders, including meningitis and encephalitis. Acute LCMV can be diagnosed

through the isolation of the virus from the cerebrospinal fluid and especially children have a very poor prognosis. No effective antiviral therapy for LCMV has been developed to date (Bonthius, 2012).

1.13 Aims

1.13.1 Aim 1: Characterization of developmental origin and phenotypic identity of splenic macrophage subpopulations

The spleen is a pivotal organ to maintain homeostasis in the blood. Removal of aberrant erythrocytes and circulating pathogens happens predominantly through phagocytosis by macrophages.

The splenic macrophage compartment is quite diverse and at least four different macrophages subtypes have been identified in the spleen to date, and some of these subtypes have an unknown developmental origin. Studies so far have either focused on a particular subpopulation or described the overall relevance of splenic macrophages in a pathological context, but usually without considering their developmental origin and environmental niche within the spleen, which can have a pivotal impact on their function.

This study aims to

- (i) Identify and discriminate all splenic macrophage subpopulations simultaneously by characteristic surface markers via flow cytometry.
- (ii) Determine the developmental origin of different macrophage subtypes with novel fate-mapping models (Figure 8).

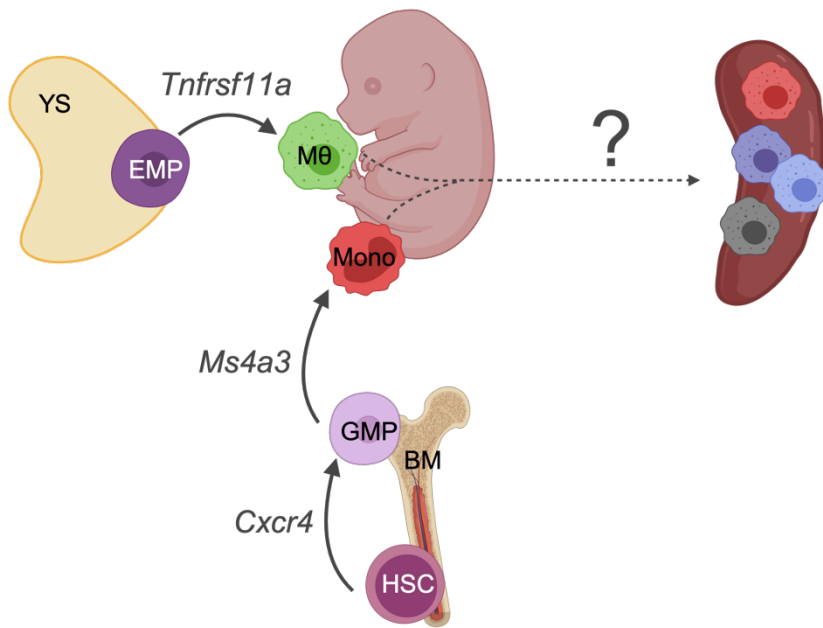


Figure 8: Developmental origin of splenic macrophages. Tissue macrophages are derived from either erythro-myeloid progenitors (EMP) in the yolk sac (YS) or from hematopoietic stem cells (HSC) from the bone marrow (BM). HSCs express *Cxcr4* and give rise to granulocyte-monocyte progenitors (GMP). GMPs upregulate *Ms4a3* when differentiating into monocytes. EMP-derived cells upregulate the core macrophage gene *Tnfrsf11a*, when differentiating into tissue macrophages (Mθ). The developmental origin of different macrophage populations in the spleen is not delineated in detail yet.

1.13.2 Aim 2: Characterization of the cellular and molecular changes amongst splenic macrophage subpopulations when challenged with blood-stage malaria

Malaria remains one of the major health issues worldwide. Most immunological research aimed at controlling malaria, focuses on the development of vaccines that activate the adaptive arms of the immune response.

However, here the focus is on innate immune cells of the myeloid lineage, which intervene immediately upon a pathogenic challenge. Macrophages in the spleen encounter and digest parasites rapidly due to their strategic position. It is known

that macrophages play a pivotal role in combatting pathogenic challenges, but the detailed dynamics of the different splenic macrophage subpopulations in the context of a malaria infection have not been delineated in detail. It is also known that splenic macrophages are depleted upon a *Plasmodium* infection and become replaced by monocytes, but how this affects their function and how the splenic environment and macrophage ontogeny changes long-term, after the resolution of the infection, remains largely unknown. This study primarily focuses on malaria infections with the murine *P. chabaudi* model, but also investigates other *Plasmodium* species and pathogens.

This study aims to

- (i) Follow the dynamics of each splenic macrophage population during an acute malaria infection and after the resolution, to identify which populations are exhausted, depleted, expanded, or replaced (Figure 9).
- (ii) Address the role of splenic macrophages in the scavenging of oxidative heme, a component of free hemoglobin, which is released upon parasite induced erythrolysis.
- (iii) Describe the developmental origin of each splenic macrophage subtype in the steady-state and compare this to the ontogeny of macrophages that refill the splenic niche upon malaria infection.
- (iv) Compare macrophage phenotypes during a malaria infection with the phenotype and dynamics of macrophage subtypes in viral and bacterial infections.
- (v) Identify changes in the transcriptional profile of macrophages upon malaria infection and find out which intercellular networks and intracellular signaling events are of relevance to prevent the systemic inflammation that leads to malaria-induced lethality (Figure 9).

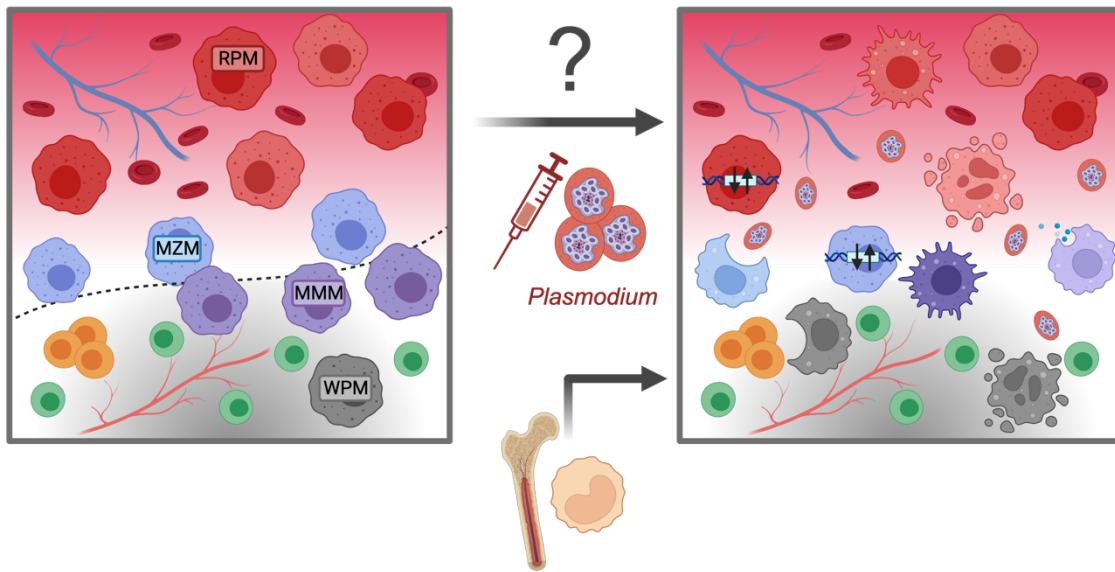


Figure 9: Cellular and molecular changes amongst splenic macrophages upon a malaria infection. Distinct environmental niches in the spleen are populated with distinct macrophage subtypes: Red pulp macrophages (RPM), marginal zone macrophages (MZM), marginal metallophilic macrophages (MMM), white pulp macrophages (WPM). Infections challenges such as a *Plasmodium* infection, have a severe impact on the splenic environment. It has to be determined, which splenic macrophages expand or are depleted upon the infection, which intracellular signaling pathways are differentially regulated and how the phenotype of infiltration cells with a different developmental origin impacts their function.

1.13.3 Aim 3: Genetic depletion of the CD163 receptor or marginal zone macrophages during a *P. chabaudi* infection to study the respective relevance and impact on malaria progression

Blood-stage malaria infection causes severe hemolysis and the release of free heme induces oxidative stress. The CD163 receptor on macrophages mediates uptake of hemoglobin and degradation of oxidative heme. The receptor is only expressed on certain subsets of macrophages, which are associated with an anti-inflammatory phenotype. The relevance of this receptor for the degradation of heme during the progression of malaria, has not been elucidated in detail to date. Macrophages in the splenic marginal zone are involved in the processing of antigens from the circulation. Their relevance and functional impact during the progression of a malaria infection has not been resolved in detail.

This study aims to

- (i) Investigate the impact of the loss of CD163 expression on macrophages during blood-stage malaria, with respect to parasite clearance, splenic architecture and environment (Figure 10).
- (ii) Investigate the relevance of Lxra-dependent splenic marginal zone macrophages on the progression of blood-stage malaria by comparing parasitemia in *Tnfrsf11a^{Cre}*, *Lxra^{fllox/fllox}* mice to wildtype controls and elucidate their relevance for the recovery of the splenic architecture after the acute infection (Figure 10).

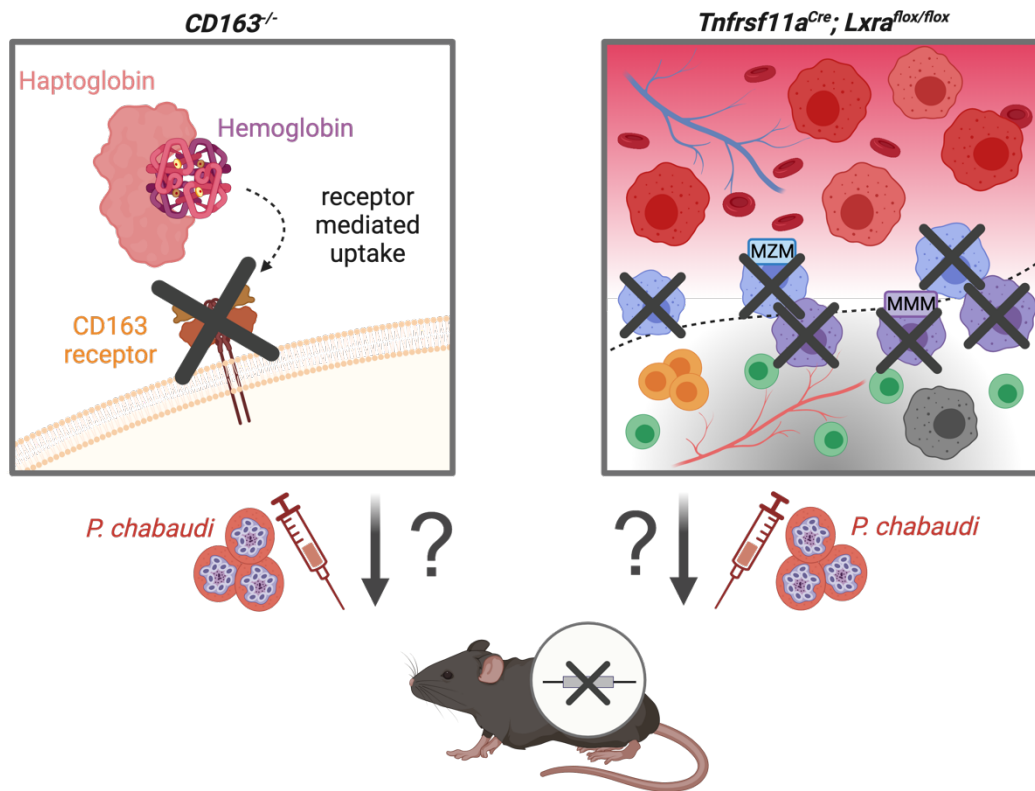


Figure 10: Genetic depletion of CD163 and $Lxra$ respectively to study functional impacts on malaria progression. The CD163 receptors mediates uptake of hemoglobin-haptoglobin complexes. The relevance of the receptor during blood-stage malaria upon a *P. chabaudi* infection is studied in a $CD163^{-/-}$ mouse model. Marginal zone macrophages (MZM) and marginal metallophilic macrophages (MMM) are located along the borders of the splenic red pulp and white pulp. The functional impact of their loss on the progression of *P. chabaudi* malaria is investigated with the $Tnfrsf11a^{Cre}; Lxra^{flox/flox}$ mouse model.

1.13.4 Aim 4: Follow the dynamics of myeloid and lymphoid cells in the bone marrow and blood, which compensate for the loss of effector cells in peripheral tissues during a blood-stage malaria infection

Malaria infection requires a fast and potent response of the immune system. Myeloid effector cells in peripheral organs form the first line of defense. They are however rapidly overwhelmed during the peak of parasitemia and require constant replenishment. Hematopoietic stem and progenitor cells in the bone marrow can adapt to challenges and increase their output and release new effector cells into the circulation to reach their target organs.

Emergency myelopoiesis has been described for various infectious diseases.

This study aims to

- (i) Describe the adaptations of hematopoietic stem and progenitor cells in the bone marrow to blood-stage malaria infection and delineate when the hematopoietic system normalizes its output.
- (ii) Track changes in the numbers of circulating myeloid and lymphoid cells during blood-stage malaria infection.

2 Materials and Methods

2.1 Materials

2.1.1 Devices

The following equipment and devices were used for experiments shown in this thesis:

Device	Company
Advia 2120i Hematology System	Siemens Healthcare
Aurora	Cytek Biosciences
AXIO Lab.A1	Carl Zeiss AG
Centrifuge 5810 R	Eppendorf SE
Centrifuge 5424	Eppendorf SE
Cryostat CM3050 S	Leica Biosystems
Dissection equipment	Fine Science Tools
Electrophoresis system	VWR
FACSAria™	BD Biosciences
FACSymphony	BD Biosciences
Freezer -80 °C	New Brunswick Scientific
Fridge 4 °C	Bosch
Gel Doc Imager	BioRad
LSM 880 Airyscan	Carl Zeiss AG
Mastercycler X50s	Eppendorf
Microscope Axio Lab.A1	Carl Zeiss AG
Neubauer Cell Counting Chamber	Paul Marienfeld GmbH & Co. KG
NextSeq2000 Sequencer	Illumina
Eppi Shaker (37 °C)	Eppendorf
37 °C incubator	BINDER
P3 50PE flowcell	Illumina
PCR cyclers	Applied Biosystems
Tapestation 2200 system	Agilent
2720 Thermal cycler	Applied Biosystems
Vortex	Scientific industries
Pipetboy Easypet 3	Eppendorf

2.1.2 Consumables

The following consumables and plasticware were used for experiments shown in this thesis:

Consumables	Company
1.5 ml Eppendorf tubes	Eppendorf
2.0 ml Eppendorf tubes	Eppendorf
15 ml Falcon tubes	Sarstedt, Inc.
50 ml Falcon tubes	Sarstedt, Inc.
5 ml Pipettes	BRAND
10 ml Pipettes	BRAND
1 ml syringes	Braun
6 well plate	VWR
96 well plate U-bottom	VWR
Pipet-tips (10 μ l, 200 μ l, 1000 μ l)	Sarstedt, Inc.
VWR cell strainer	Avantor™
FACS tubes	Sarstedt, Inc.
PAP pen	Biozol
Pasteur pipette	avantortm
Tubes 2.0 mL	TubeOne®
Tubes 1.5 mL	TubeOne®
Serological pipettes	Sarstedt, Inc.
Superfrost™Plus Adhesion	EpreDia
Microscope Slides	
Fluoromount G	Invitrogen
Disposable scalpel blade with plastic handle	RIBBEL®
Microtome blades	FEATHER
Micro cover glasses	BRAND
Microvette	Sarstedt, Inc.
ImmEdge Pen	Vector LABORATORIES
Tissue-Tek O.C.T. Compound	Sakura Finetek Germany GmbH

2.1.3 Reagents and Buffers

The following chemicals and reagents were used for experiments shown in this thesis:

Reagent	Company
Bovine serum albumin (BSA)	Sigma-Aldrich
Collagenase D	Sigma-Aldrich
4',6-Diamidino-2-phenylindole, diacetate (DAPI)	BioLegend
Dispase II powder	Thermo Fisher Scientific
DNase	Sigma-Aldrich
D-Sucrose	Thermo Fisher Scientific
Dulbecco's phosphate-buffered saline (DPBS, 10x, w/o Ca and Mg)	PAN-Biotech
Ethanol 100 %, molecular biology grade	Carl Roth
Ethylenediaminetetraacetic acid (EDTA)	Sigma-Aldrich
Fetal bovine serum (FBS), South America origin, 0.2 µm sterile filtered	PAN-Biotech
Fluoromount-G	Thermo Fisher Scientific
Formaldehyde 16 % (w/v)	Fisher Scientific
Giemsa solution	Merck
Hoechst 33258	Life Technologies
Narketan, ketamine hydrochloride	Vetoquinol
Normal goat serum (NGS)	VWR
PBS tablets (w/o Mg ²⁺ and Ca ₂₊)	Thermo Fisher Scientific
Protein Block, Serum-Free	Agilent Technologies
Rat serum (RS)	Thermo Fisher Scientific
Sodium chloride for anesthesia	Braun
Sphero Rainbow Calibration Particles (8 peaks)	BD Biosciences
SPRIBeads	Beckman-Coulter
Tamoxifen	Sigma-Aldrich
Tissue-tek O.C.T, Sakura Finetek	Thermo Fisher Scientific
Triton-X 100	Thermo Fisher Scientific
Xylazine	WDT-Markplatz

The following buffers and solutions were used for experiments shown in this thesis:

Buffer & solutions	Reagent and concentration
1x Phosphate-buffered saline (PBS)	PBS (10x) without Ca ²⁺ , Mg ²⁺ in Aqua Bidest
Antibody solution (for IF)	5 % BSA in PBS-T
Blocking solution (for IF)	5 % BSA 2 % NGS in PBS-T
Digestion buffer	1 mg/ml Collagenase 100 U/ml DNase 2.4 mg/ml Dispase 3 % FBS in PBS
FACS buffer	0.5 % w/v BSA 2 mM EDTA in PBS
Fc block	0.5 % CD16/32 (1:100) 2% RS in FACS buffer
Formaldehyde 4 % (w/v)	16 % Formaldehyde (w/v) in PBS
Iron stock solution (5 mM)	69.5 mg iron (II) sulfate heptahydrate In 50 ml ddH ₂ O
Narcotics	20 mg/ml Xylazine 100 mg/ml Ketamine in NaCl (0.9 %)
PBS-T	0.4 % Triton X-100 in PBS
Reagent A	3 g trichloroacetic acid in 3 ml ddH ₂ O add 7 ml HCl (37 %)
Reagent B1	15.6 g sodium acetate In 45 ml ddH ₂ O
Reagent B2	17 mg bathophenanthroline disulfonic acid 22 mg ascorbic acid In 5 ml ddH ₂ O
Red blood cell lysis buffer	0.1 mM EDTA 12 mM NaHCO ₃ 155 mM NH ₄ Cl in Aqua Bidest
Sucrose (30 %)	30 % sucrose (w/v) in PBS

2.1.4 Antibodies

The following antibodies were used for flow cytometry staining of the spleen shown in this thesis:

Antibody	Conjugate	Clone	Company	Dilution
F4/80	APC-Cy7	BM8	Biolegend	1:400
Tim4	BUV-563	RMT4-54	BD Biosciences	1:200
CD11b	BUV-661	M1/70	BD Biosciences	1:200
CD45	BUV-805	30-F11	BD Biosciences	1:800
CD163	BV421	S15049I	Biolegend	1:800
Ly6C	BV510	HK1.4	Biolegend	1:200
CD169	BV605	3D6.112	Biolegend	1:200
CD209b	BV711	22D1	BD Biosciences	1:50
Ly6G	Biotin	1A8	Biolegend	1:100
CD19	Biotin	6D5	Biolegend	1:100
NKp46	Biotin	29A1.4	Biolegend	1:100
TCR- β	Biotin	H57-597	Biolegend	1:100
Streptavidin	BV785	-	Biolegend	1:100
CD64	PerCP-Cy5.5	X54.5/7.1	Biolegend	1:50
MerTK	PE-Cy7	2B10C42	Biolegend	1:800
MARCO	APC	579511	R&D Systems	1:100
MHC class II	A-700	M5/113.15.2	Biolegend	1:200

The following antibodies were used for flow cytometry staining of the bone marrow shown in this thesis:

Antibody	Conjugate	Clone	Company	Dilution
NKp46	Biotin	29A1.4	Biolegend	1:200
TCR- β	Biotin	H57-597	Biolegend	1:200
CD19	Biotin	6D5	Biolegend	1:400
Gr1	Biotin	RB6-8C5	Biolegend	1:400
Ter119	Biotin	TER-119	Biolegend	1:100
Streptavidin	BV785	-	Biolegend	1:100
Kit (CD117)	BV711	2B8	Biolegend	1:200
Sca1	BV510	D7	Biolegend	1:100
CD48	AF647	HM48-1	Biolegend	1:200
CD150 (SLAM)	PE-Cy7	TC15- 12F12.2	Biolegend	1:400
CD16/32	APC Cy7	93	Biolegend	1:100
CD34	AF700	RAM43	BD Biosciences	1:100
CD135	BV421	A2F10	Biolegend	1:100
CD127	PerCP/Cy5.5	A7R34	Biolegend	1:100

The following antibodies were used for flow cytometry staining of the blood shown in this thesis:

Antibody	Conjugate	Clone	Company	Dilution
TCR- β	Biotin	H57-597	Biolegend	1:200
Streptavidin	BV785	-	Biolegend	1:100
XCR1	APC-Cy7	ZET	biolegend	1:200
CD172a	PE-Cy7	P84	Biolegend	1:400
CD115	APC	AFS98	Biolegend	1:200
CD11b	BUV661	M1/70	BD Biosciences	1:200
NKp46	BV711	29A1.4	Biolegend	1:50
Ly6C	BV510	HK1.4	Biolegend	1:200
CD11c	BV605	N418	Biolegend	1:200
CD19	BV421	6D5	Biolegend	1:200
Ly6G	PerCPCy5.5	1A8	Biolegend	1:200
MHC class II	AF700	M5/113.15.2	Biolegend	1:400

The following antibodies were used for labeling of the spleen to sort cells for single cell RNA sequencing shown in this thesis:

Antibody	Conjugate	Clone	Company	Dilution
NKp46	APC-Cy7	29A1.4	Biolegend	1:100
CD19	APC-Cy7	6D5	Biolegend	1:100
Ly6G	APC-Cy7	1A8	Biolegend	1:100
TCR- β	APC-Cy7	H57-597	Biolegend	1:100
Draq7	APC-Cy7	-	Biolegend	1:1000
CD45	APC	30-F11	Biolegend	1:200
CD11b	PE-Cy7	M1/70	Biolegend	1:800
CD64	PerCP-Cy5.5	X54-5/7.1	Biolegend	1:50
CD169	BV605	3F6-112	Biolegend	1:200
F4/80	BV421	BM8	Biolegend	1:400

The following antibodies were used for immunofluorescent staining shown in this thesis:

Antibody	Conjugate	Company	Dilution
Iba1 (rabbit)	-	Abcam	1:500
CD163	ATTO-647	Produced by Prof. Bajenoff group	1:400
CD169	Biotin	Miltenyi Biotec	1:400
F4/80 (rat)	-	BIO-RAD	1:300
YFP (rat)	-	Biotechnik Gerbu	1:1000
α -rabbit	AF488	Thermo Fisher Scientific	1:1000
α -rat	AF488	Thermo Fisher Scientific	1:1000
α -rat	AF647	Biolegend	1:1000
α -rat	AF555	Thermo Fisher Scientific	1:1000
Streptavidin	PE	Biolegend	1:500
Streptavidin	AF647	Biolegend	1:1000

2.1.5 Mouse strains

The following mouse strains were used for experiments shown in this thesis:

Mouse strain	Background	Description
Wildtype B6	B6/Jrcc	Non-transgenic wild-type mice
Tnfrsf11a ^{Cre} ; Ms4a3 ^{FlpO} ; Rosa26 ^{LSL-YFP} ; Rosa26 ^{LFL-tdTomato}	B6/Jrcc	Transgenic mice that express fluorescent reporter proteins
Cxcr4 ^{CreERT2} ; Rosa26 ^{LSL-tdTomato}	B6/Jrcc	Transgenic mice that express fluorescent reporter proteins upon tamoxifen administration
Tnfrsf11a ^{Cre} ; Lxra ^{flox/flox}	B6/Jrcc	Transgenic mice with conditional depletion of the nuclear receptor Lxra
CD163 ^{-/-}	B6/Jrcc	Generated by the LIMES GRC facility by knocking out the whole CD163 locus

2.1.5.1 PCR reagents

Reagent	Company
Taq-Polymerase Mastermix	VWR
Nuclease-free water	GE Healthcare
Sodium hydroxide	Merck
TRIS-Hydrochloride	AppliChem Panreac
DNA ladder	New England Biolabs

2.1.6 Pathogens

In this thesis, of the *P. chabaudi* species, the strain *P. chabaudi* AS was used and referred to as *P. chabaudi* in the following. *P. berghei* refers to the species *P. berghei* ANKA and *P. yoelii* refers to the species *P. yoelii* NL in this thesis.

The following pathogens were used for experiments shown in this thesis:

Pathogen	Description	Source
<i>P. chabaudi</i>	Plasmodium chabaudi AS	Prof. William Heath, Peter Doherty Institute, Melbourne (provided by Prof. Kevin Couper)
<i>P. berghei</i>	Plasmodium berghei ANKA	Prof. William Heath, Peter Doherty Institute, Melbourne (provided by Prof. Kevin Couper)
<i>P. yoelii</i>	Plasmodium yoelii NL	Prof. William Heath, Peter Doherty Institute, Melbourne (provided by Prof. Kevin Couper)
LCMV	Actue lymphocytic choriomeningitis virus	Prof. Laura Mackay and Prof. John Muller, Peter Doherty Institute, Melbourne

2.1.7 Software

The following software was used for the analysis of experiments shown in this thesis:

Software	Supplier
BD FACS Diva	BD Biosciences
Biorender	Science Suite Inc.
FlowJo	FlowJo, LLC
ImageJ (Fiji is just ImageJ)	NIH
Prism	GraphPad
Zen Blue	Zeiss
Zen Black	Zeiss

2.2 Methods

2.2.1 Experimental animals

2.2.1.1 Breeding

All mice were maintained on a C57BL/6 background and housed in SPF conditions. Animal procedures were performed in adherence to the project license 2020.A311 issued by the Landesamt für Natur, Umwelt und Verbraucherschutz (LANUV).

2.2.1.2 Genotyping

Upon weaning, the mice were ear-tagged. The tissue was used for genotyping and dissolved in 200 µl of 50 mM NaOH for 30 min at 95 °C. 20 µl of 1M TRIS-HCl (pH 8) were added for neutralization. After spinning for 5 min at full speed in an Eppendorf centrifuge, 1 µl of the supernatant was used for genotyping.

Per sample 1 µl of the isolated DNA was added to 9 µl of a master mix solution (consisting of 0.5 µl of each primer, 5 µl DreamTaq Green PCR Master Mix and H₂O to receive a total volume of 10 µl).

The genetic material was amplified in 35 cycles in a PCR cycler. Samples were applied on a 1.5 % agarose gel and separated via electrophoresis at 120 V for 30 min. The DNA was stained with the Sybr-safe dye for visualization via UV light.

Table 2: PCR Master-Mix

Reagent	Volume
Primer 1	0.5 μ l
Primer 2	0.5 μ l
Primer 3	0.5 μ l
Primer 4	0.5 μ l
DreamTaq Green PCR Master Mix	5 μ l
H2O	Top up to 10 μ l total volume (dependent on number of primers needed)
DNA	1 μ l

Table 3: PCR Primer for genotyping

Genotype	Primer sequence	Result
CD163 ^{-/-}	P1: TGA GAA TGC AGG TCC TGT TG P2: TGG ATG GTC CTT CCT TCT G P3: TGA TCA CAG TGC ATC ATG TC	516 bp: wt 690 bp: ko
Cxcr4- CreERT2	P1: AGT GAA ACC TCT GAG GCG TTT GGT P2: TAG AGC CTG TTT TGC ACG TTC ACC P3: TCT GAA CCC GTC CCA CTC AAC TTA	300 bp: wt 500 bp: Cre
Tnfrsf11a- Cre	P1: TCAAGG GTG ACA TCA TCG TGG T P2: ACT TCT CCA TGG TAG CCT CC P3: TAT GGG GGT GGG GTG ATA C	529 bp: wt 270 bp: Cre
Lxra-flox	P1: GGA TTT GGA GAA GGT AAA GTC TCC C P2: TGG ACT CAA GTG ATC TTG TCT CAG C P3: ATG CCT GAA AAG GGC ATC AGA TGC C	350 bp: wt 416 bp: flox 465 bp: del
Ms4a3- FlpO	P1: AGA GAA ATC ATC AGG GCA GAA AT P2: GAA AGG GGA ACA AGC GAA GAT P3: TTG GCG AGA GGG GAA AGAC	517 bp: wt 412 bp: FlpO
R26- FrtStop- tdTom	P1: ACG GGC AGT AGG GCT GAG P2: AGC CTG CCC AGA AGA CTC C P3: GGT GTT GGG TCG TTT GTT CA P4: TCT AGC TTG GGC TGC AGG T	402 bp: wt 290 bp: FrtStop-tdTom
R26- LoxStop- eYFP	P1: CTG GCT TCT GAG GAC CG P2: CAG GAC AAC GCC CAC ACA P3: AGG GCG AGG AGC TGT TCA P4: TGA AGT CGA TGC CCT TCA G	142 bp: wt 384 bp: LoxStop-eYFP
R26- LoxStop- tdTom	P1: AAG GGA GCT GCA GTG GAG TA P2: CCG AAA ATC TGT GGG AAG TC P3: GGC ATT AAA GCA GCG TAT CC P4: CTG TTC CTG TAC GGC ATG G	297 bp: wt 196 bp: LoxStop-tdTom

*(P = primer, wt = wildtype, ko = knockout, del = deleted, bp = base pair)

Table 4: PCR program

Steps	Temperature	Time	Repeats
1. Initial denaturation	95 °C	3 min	
2. Denaturation	95 °C	30 sec	
3. Primer annealing	60 °C	30 sec	x 35
4. Elongation	72 °C	30 sec	
5. Final extension	72 °C	5 min	

2.2.1.3 Generation of a CD163-depletion mouse model

The gene for the hemoglobin-receptor CD163 is located on chromosome 6 of the mouse and consists of 17 exons. For the generation of a conditional CD163 deficient mouse line, loxP-sites were introduced into the CD163 wildtype allele. For the introduction of the loxP sequence, the CRISPR/Cas9 technique was used. Guide RNA sequences were designed to target intron 1 for the introduction of the first loxP sequence. The second guide RNA was designed to target exon 17 and introduce the loxP-site close to the end of the CD163 coding sequence. A Cre-mediated recombination between the two loxP-sites would then lead to a depletion of almost the whole coding sequence of the CD163 gene.

In addition, two recognition sites for EcoRI on the 5' site and PstI on the 3' end were introduced, to test PCR products via restriction digest.

Oocytes were electroporated with the single guide RNAs, Cas9 and two oligos for homologous recombination, which contain the two loxP-sites. Surviving oocytes were transferred into pseudo-pregnant foster mothers and biopsies of the born pups were analyzed. Primer combinations P1 and P2 bind in intron 1 and exon 2, for the 5'-insertion site and the primer combinations P3 and P4 bind in exon 17 and downstream of exon 17, in the CD163 locus at the 3'-insterion site (Table 5).

Table 5: PCR primer to test the introduction of loxP-sites into the CD163 gene

Primer	Sequence
P1	TGAGAATGCAGGTCCTGTTG
P2	TCACCAGGAGCGTTAGTGAC
P3	TGATCACAGTGCATCATGTC
P4	TGGATGGTCCTTCCTTCTG

Some genotyping results remained inconclusive and were next analyzed with the primer combination P1 and P4. In case of a complete deletion of the region between the two CRISPR cutting sites, a 600 – 700 bp fragment was expected. This was indeed that case; in some pups the sequence between intron 1 and exon 17 was deleted and thus almost the entire coding sequence of CD163 (Figure 11). Mice with a heterozygous deletion of the CD163 gene were mated to generate a CD163 knockout line.

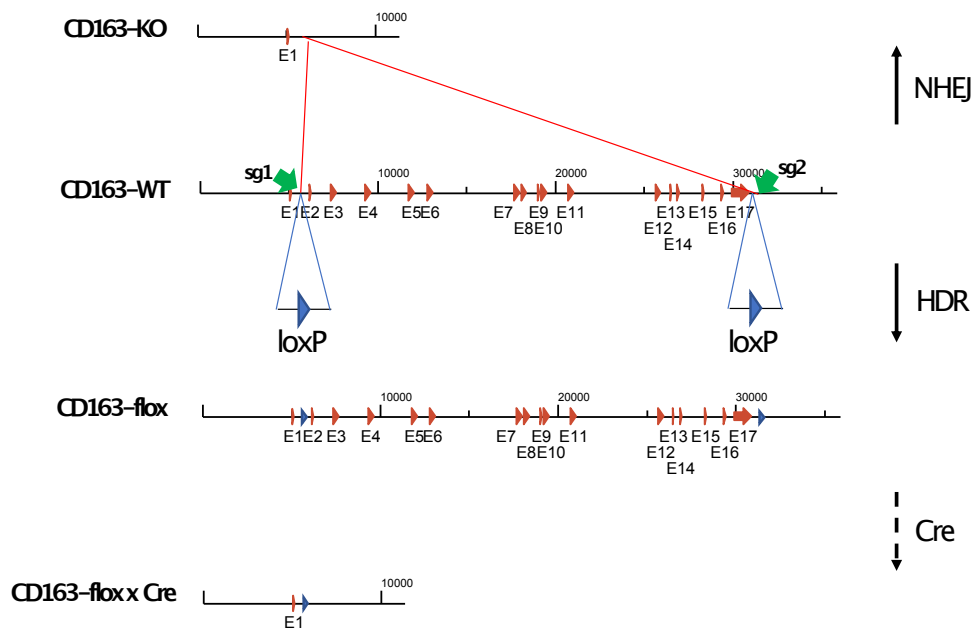


Figure 11: Genetic knockout of CD163. With the CRISPR/Cas9 technique, loxP-sites were introduced into intron 1 and exon 17 of the CD163 gene to generate a conditional depletion mode. A recombination of both target sites led to the genetic knockout of the CD163 gene.

2.2.2 Tamoxifen inducible fate-mapping

Mice that express an inducible Cre-recombinase (Cre^{ERT2}) require tamoxifen treatment to allow for the translocation of the Cre-recombinase to the nucleus and cleave its target sites.

Therefore, a tamoxifen solution of 10 mg/ml was prepared and dissolved in 90 % corn oil (v/v) and 10 % ethanol (v/v). The calculated amount of tamoxifen was first dissolved in the required volume of ethanol. To generate a homogenous solution, the tamoxifen and ethanol mix was placed into a 42 °C water bath for approximately 30 min (protected from light) and mixed regularly. When the tamoxifen was dissolved, the corn oil was added. The tamoxifen solution can be stored at 4 °C protected from the light for 4 - 6 weeks.

To induce Cre-activity, mice were *i.p.* injected with 100 µl of the tamoxifen solution for 5 consecutive days. Different injection sites on the lower abdomen, helped to prevent infections or inflammation.

In this study, tamoxifen injection was required to induce Cre-activity in the *Cxcr4*^{CreERT2}; *Rosa26*^{LSL-tdTomato} model.

The fate of HSC-derived cells that acquired tdTomato expression after tamoxifen treatment, was either followed over time, or mice were infected with *Plasmodium* parasites one month after tamoxifen administration to induce blood-stage malaria and follow the dynamics of HSC-derived cells (Figure 12).

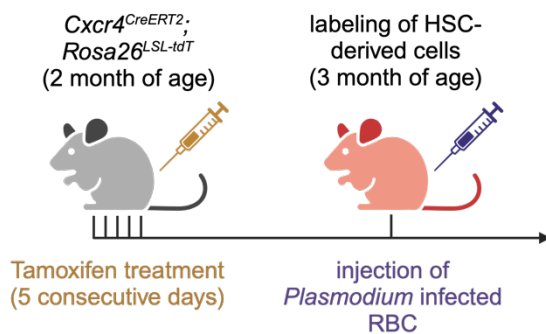


Figure 12: Tamoxifen treatment. At two months of age, mice of the *Cxcr4*^{CreERT2}; *Rosa26*^{LSL-tdTomato} line were treated with tamoxifen (*i.p.* injection of 100 µl per day of a 10 mg/ml stock) for five consecutive days. After four weeks, when mice were three months of age, HSC-derived cells should be labeled with tdTomato and mice were injected with *Plasmodium* parasites to induce blood-stage malaria.

2.2.3 Malaria

2.2.3.1 Infection of experimental animals from donor

Donor mice were intraperitoneal (*i.p.*) injected with 200 μ l of frozen blood aliquot that contains 1×10^8 infected RBC. Parasitemia was monitored from day 5 onwards (according to 2.2.3.2 Parasitemia). The donor mouse was sacrificed when the parasitemia reached 2 - 5 % and the blood was collected. The exact parasitemia at the time point of collection was determined and the blood cells were counted with a Neubauer counting chamber (1:2000 dilution in PBS).

Experimental mice were *i.p.* injected with a total volume of 200 μ l per mouse, containing 10,000 infected RBC from the donor mouse. Therefore, the amount of blood needed from the donor mouse was calculated and diluted with sterile PBS: the cell count (RBC/ml) was multiplied with the parasitemia value to obtain the amount of infected RBC per milliliter. This number was divided by 10,000 (the number of infected RBC to be injected per mouse). The calculated blood volume of the donor mouse was added to sterile PBS to obtain a total volume of 200 μ l. This dilution of infected RBC was *i.p.* injected into experimental mice. Control mice received an *i.p.* injection of 200 μ l of sterile PBS.

Parasitemia in experimental mice was monitored from day 5 onwards every 3 - 5 days in the first three weeks of the infection and every 5 - 7 days late later stages of the infection.

2.2.3.2 Parasitemia

To determine the parasitemia, drop of blood was collected from the mouse tail vein. The blood of one uninfected control was always collected in addition, as a reference for the blood of the malaria infected mice.

The vein was punctured with a needle (26 G) and the blood (1 - 5 μ l) collected in 100 μ l PBS in a 96-well plate or 1.5 ml tube. The DNA intercalating dye Hoechst was diluted 1:1000 in PBS from a 10 mg/ml stock. An equal volume (100 μ l) was added to the blood cell suspension, mixed and incubated at 37 °C for 1 h. 200 μ l FACS buffer were added and the cell suspension was filtered through a 70 μ m

strainer into a FACS tube. The samples were measured on the FACS Symphony machine (Figure 13). By forward and side scatter, small erythrocytes were selected. Single cells were gated on PE and FITC negativity to remove auto-fluorescent cells. Those cells were then gated on Hoechst positivity. Mature erythrocytes were not positive for Hoechst since they have extruded their nucleus. Only the genetic material of the intra-erythroid parasites showed Hoechst positivity. Additionally, some immature erythrocytes have not extruded their genetic material, but can be discriminated, because they were higher in the forward scatter position.

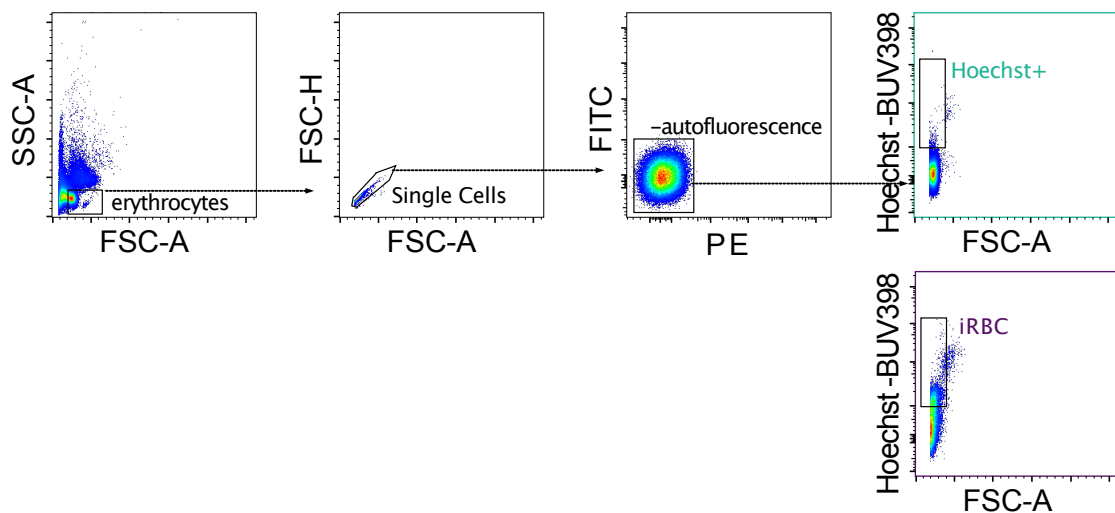


Figure 13: Gating strategy to determine parasitemia. Forward- and side-scatter low erythrocytes were gated. Autofluorescent cells were ruled out after gating on single cells. Hoechst intercalated into the parasitic DNA of infected erythrocytes. Uninfected controls were used to set the Hoechst⁺ gate, to determine the percentage of parasitemia in infected mice.

An alternative strategy to determine the parasitemia is to stain a blood smear with Giemsa. Blood was collected from the mouse tail vein of a control mouse and the infected animals (as described in: 2.2.3.2 Parasitemia). A drop of blood was placed close to one edge of a glass slide and a second glass slide was used to distribute the blood along the slide. Therefore, the second glass slide was placed

in an approximately 45° angle and moved with a constant speed along the surface of the glass slide containing the blood drop and dragging the liquid (Figure 14). The blood smear was air dried before methanol fixation. Slides were placed in a container with 100 % methanol for 2 min. Slides were then again air dried and placed in a container with 10 % Giemsa solution (1:10 diluted with water) for 5 - 10 min. Slides were then rinsed with water to remove stain and crystals and investigated with any standard light microscope. Blood smear of uninfected controls would not show Giemsa stain inside the erythrocytes, while characteristic dark stained structures of the parasites would be visible inside of infected erythrocytes (see results: Figure 23, C).

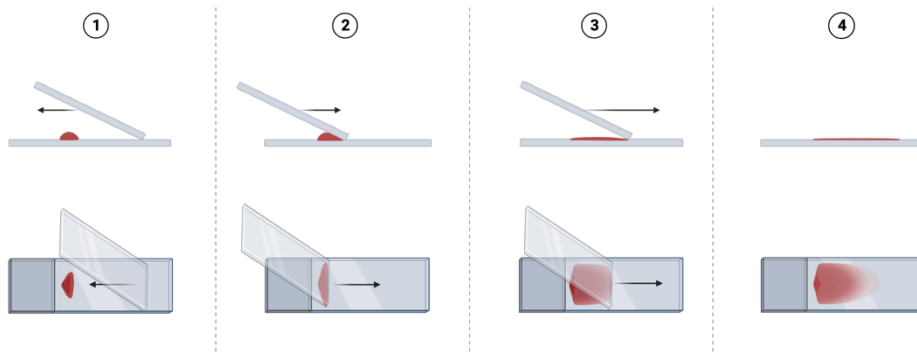


Figure 14: Blood smear. A drop of blood on a glass slide was distributed with an angled glass slied in a straight movement.

2.2.3.3 Chloroquine treatment

Mice were infected with the malaria parasites as described previously. At day 21 after the infection, the mice were *i.p.* injected with 200 μ l of a 4 mg/ml chloroquine solution (dissolved in sterile PBS). Afterwards mice received drinking water containing 6 mg/ml chloroquine for another 3 days.

2.2.4 LCMV

Spleens from mice that were infected with acute LCMV were received from Takahiro Asatsuma, Dr. Yannick Alexandre and Dr. Thomas Burn (University of Melbourne, Peter Doherty Institute) and processed with the standard flow cytometry protocol.

In short, the virus was replicated *in vitro* and the plaque forming units (PFU) were quantified to determine the viral titer. A dose of approximately 2×10^6 PFU was injected *i.p.* to develop an acute LCMV infection in mice.

2.2.5 Organ isolation

Mice were anesthetized with a mixture 120 mg/kg ketamine and 20 mg/kg xylazine. When mice did not respond with reflexes anymore the abdomen was opened. With a 26 G needle blood (>400 μ l) was collected from the heart with an EDTA-flushed 1 ml syringe and collected in a heparin-coated tube. Afterwards a minor cut in the left atrial appendage allows for the blood to flow out during perfusion. A 26 G needle is inserted into the left ventricle to perfuse the mouse systemically with 12 ml PBS. Next the spleen is collected in a PBS dish on ice and one leg is removed (both tibia and femur).

2.2.6 Flow Cytometry

2.2.6.1 Preparation of spleen tissue

The whole organ weight was determined and subsequently 30 - 40 mg of the spleen tissue were used for flow cytometry (exact weight determined). This spleen tissue was transferred into a 2 ml tube and 0.5 ml digestion mix (dispase, DNase, collagenase D) were added. The tissue was cut into small pieces with scissors and placed in a 37 °C shaker (900 rpm) for 30 min. The suspension was

transferred through a 100 µm strainer into a 50 ml tube and flushed with 7 ml FACS buffer. After a centrifugation step with 400 g for 5 min at 4 °C, the supernatant was discarded and the pellet resuspended in 1 ml RBC-lysis buffer and incubated for 5 min on ice. Approximately 7 ml FACS buffer were added and before spinning (400 g, 5 min, 4 °C). The pellet was resuspended in 50 µl Fc-blocking solution and incubated for 5 - 10 min on ice. The volume was determined and topped up at 200 µl with FACS buffer. 2 µl of this suspension were transferred into a new tube with 798 µl FACS buffer (1:400 dilution) and subsequently diluted with an equal volume of trypan blue (final 1:800 dilution) for counting with a Neubauer counting chamber. 100 µl of the remaining cell suspension were transferred into a 96-well plate (U-bottom) and topped with FACS buffer for spinning (400 g, 5 min, 4 °C). The supernatant was discarded, the pellet resuspended in 50 µl of the primary antibody mix and incubated for 30 min on ice. After topping up with FACS buffer the cells were pelleted (400 g, 5 min, 4 °C) and resuspended in 50 µl of the secondary antibody mix. After 30 min incubation on ice protected from light, FACS buffer was added and the suspension centrifuged (400 g, 5 min, 4 °C). The pellet was resuspended in 100 µl FACS buffer. Before measuring the labeled cells with a flow cytometer, the suspension was filtered through a 70 µm strainer and an equal volume of Hoechst was added (of a 1:5000 dilution from a 10 mg/ml stock).

2.2.6.2. Preparation of bone marrow

The bone was cleaned on the surface and muscle and tissue residues were removed. Tibia and femur were separated and cut open close to the edge on both sides. With a 10 ml syringe filled with FACS buffer and a 26 G needle, the bone marrow was flushed through a 70 µm strainer into a 50 ml tube. The suspension was centrifuged for 5 min at 4 °C with 400 g. The supernatant was discarded and the pellet resuspended in 1 ml RBC-lysis buffer and incubated for 5 min on ice. Approximately 7 ml FACS buffer were added and before spinning (400 g, 5 min, 4 °C). The pellet was resuspended in 50 µl Fc-blocking solution and incubated for 5 - 10 min on ice. The volume was determined and topped up at 200 µl with

FACS buffer. 2 μ l of this suspension were transferred into a new tube with 398 μ l FACS buffer (1:200 dilution) and subsequently diluted with an equal volume of trypan blue (final 1:400 dilution) for counting with a Neubauer counting chamber. 100 μ l of the remaining cell suspension were transferred into a 96-well plate (U-bottom) and topped with FACS buffer for spinning (400 g, 5 min, 4 °C). The supernatant was discarded, the pellet resuspended in 50 μ l of the primary antibody mix and incubated for 30 min on ice. After topping up with FACS buffer the cells were pelleted (400 g, 5 min, 4 °C) and resuspended in 50 μ l of the secondary antibody mix. After 30 min incubation on ice protected from light, FACS buffer was added and the suspension centrifuged (400 g, 5 min, 4 °C). The pellet was resuspended in 100 μ l FACS buffer. Before measuring the labeled cells with a flow cytometer, the suspension was filtered through a 70 μ m strainer and an equal volume of Hoechst was added (of a 1:5000 dilution from a 10 mg/ml stock).

2.2.6.3 Preparation of blood

Of the collected blood, 200 μ l were transferred into a 15 ml tube containing 3 ml RBC-lysis, mixed and incubated for 5 min on ice. After the addition of 7 ml FACS buffer, the suspension was centrifuged at 400 g, 4 °C for 5 min. The supernatant was aspirated and the pellet resuspended in 3 ml RBC-lysis buffer again. After adding 7 ml FACS buffer, the suspension was centrifuged (400 g, 4 °C, 5 min). The supernatant was aspirated and the pellet resuspended in 50 μ l FACS buffer. After an incubation for 5 - 10 min on ice, the volume was determined and topped up at 200 μ l with FACS buffer. 2 μ l of this suspension were transferred into a new tube with 18 μ l FACS buffer (1:20 dilution) and subsequently diluted with an equal volume of trypan blue (final 1:40 dilution) for counting with a Neubauer counting chamber. 150 μ l of the remaining cell suspension were transferred into a 96-well plate (U-bottom) and topped with FACS buffer for spinning (400 g, 5 min, 4 °C). The supernatant was discarded, the pellet resuspended in 50 μ l of the primary antibody mix and incubated for 30 min on ice. After topping up with FACS buffer the cells were pelleted (400 g, 5 min, 4 °C) and resuspended in 50 μ l of the secondary antibody mix. After 30 min incubation on ice protected from light, FACS

buffer was added and the suspension centrifuged (400 g, 5 min, 4 °C). The pellet was resuspended in 100 µl FACS buffer. Before measuring the labeled cells with a flow cytometer, the suspension was filtered through a 70 µm strainer and an equal volume of Hoechst was added (of a 1:5000 dilution from a 10 mg/ml stock).

2.2.6.4 Analysis of flow-cytometry data

Labeled cells were acquired with the BD Symphony flow cytometer and the Diva software. Exported data were analyzed with the FlowJo software.

2.2.7 Preparation of spleen tissue for imaging

2.2.7.1 Preparation of tissue for cryo-section

The spleen was collected and fixed in 4 % formaldehyde (in PBS) for 6 h while rotating at 4 °C. The tissue was washed three times with PBS for 10 min while rotating at 4 °C. The spleen tissue was then placed into a tube containing 30 % sucrose (in PBS) and the tube was placed upright overnight at 4 °C. The next day the tissue has sunk to the bottom of the tube and was transferred into a tissue mold and covered with OCT. For solidification, the block was placed on dry ice and subsequently stored at -80 °C.

The frozen OCT block containing the spleen tissue was cut with a Cryostat and 20 µm section were collected on superfrost glass slides. The slides were stored at -20 °C until used.

2.2.7.2 Antibody staining

The 20 µm spleen tissue sections that were collected on glass slides and stored at -20 °C were thawed at room temperature (RT). OCT was removed with forceps and a circle was drawn around the tissue with a PAPpen. Slides were placed into a wet dark chamber. Tissue was hydrated through the addition of PBS for 10 min. To permeabilize the spleen tissue, PBS-T was added two times for 10 min. Then

the protein-block solution (Agilent Technologies) was added and incubated at RT for 30 min. Slides were rinsed with PBS-T and the primary antibody mix, dissolved in PBS-T containing 5 % BSA, was added and incubated over night at 4 °C. Slides were rinsed with PBS-T the next day and washed three times for 5 min with PBS-T. Then the secondary antibody mix, dissolved in PBS-T containing 5 % BSA, was added and incubated for 2 h at RT. Slides were rinsed with PBS-T and washed for 10 min with PBS-T. Then PBS-T with DAPI (1:10,000 dilution of a 10 mg/ml stock) was added and incubated at RT for 10 min. Slides were subsequently washed with PBS-T for 10 min and air dried before mounting the tissue with Fluoromount G and a cover slide.

2.2.7.3 Microscopy and image analysis

Fluorescent antibody labeled spleen tissue was imaged with the confocal microscope LSM 880 Airyscan (Carl Zeiss) and the Zen-black software. Tile images were stitched with the Zen-blue software. Images were exported in the csv format and process with the Fiji software.

2.2.7.4 Immunohistochemistry (H&E)

Spleen tissue was fixed in 4 % formaldehyde (in PBS) for 6 h while rotating at 4 °C. The tissue was washed three times with PBS for 10 min while rotating at 4 °C. The spleen tissue was then placed into a 2 ml tube filled with 70 % ethanol for dehydration.

The fixed spleen tissue was processed by the histology core facility of the university clinic (UKB), embedded in paraffin, cut and stained with hematoxylin and eosin.

In short, tissue was mounted in paraffin. Paraffin blocks containing the spleen tissue were cut with a microtome (4 µm) and floating sections were collected on glass slides and dried.

In short, staining was performed according to Table 6.

Table 6: Hematoxylin and eosin staining.

Step	Reagent	Incubation time
1	Xylene	5 min
2	Xylene	5 min
3	100 % ethanol	2 min
4	100 % ethanol	2 min
5	96 % ethanol	2 min
6	90 % ethanol	2 min
7	80 % ethanol	2 min
8	70 % ethanol	2 min
9	H ₂ O	1 min
10	Hemalaun	3 min
11	H ₂ O	1 min rinse
12	Eosin	3 min
13	H ₂ O	1 min rinse
14	70 % ethanol	0.5 min
15	80 % ethanol	0.5 min
16	90 % ethanol	0.5 min
17	96 % ethanol	0.5 min
18	100 % ethanol	0.5 min
19	100 % ethanol	0.5 min
20	Xylene	0.5 min
21	Xylene	5 min

2.2.8 Iron assay

Spleen homogenates were generated by mincing approximately 10 mg of tissue in 200 μ l ddH₂O in a 1.5 ml tube. 50 μ l of Reagent A were added. Samples were hydrolyzed through heating the tubes at 65 °C for 18 h. Tubes were centrifuged at 3,000 g for 5 min at RT. 15 μ l of the supernatant were transferred into a 96 well plate containing 45 μ l ddH₂O per well if non-heme iron detection was desired. The remaining solution in the 1.5 ml tube was vortexed and boiled for 1 h at 140 °C for total iron detection. Tubes were centrifuged (3,000 g, 5 min, RT) to clarify the hydrolysate. 20 μ l of the tissue hydrolysate were transferred into a 96-well plate (clear flat-bottom) and 40 μ l ddH₂O were added. Reagent B1 and reagent B2 were mixed in a 9:1 ratio and 160 μ l were added on top of each sample in the 96-well plate. After an incubation for 10 min at RT, the absorbance was measured at 539 nm with a spectrometer.

2.2.9 Single-cell RNA-sequencing

2.2.9.1 Sorting of CD64⁺ macrophages

Spleens were collected from uninfected and *P. chabaudi* infected mice at day 90. Spleen cells were isolated, digested, and labeled with fluorescent antibodies according to the flow cytometry protocol.

The homogeneous cell suspension of splenocytes was subjected to sorting with the FACS Aria using a 100 μ m nozzle. Single, live, CD45⁺, CD64⁺ cells were selected for sorting (Figure 15) and collected in 100 μ l FACS buffer.

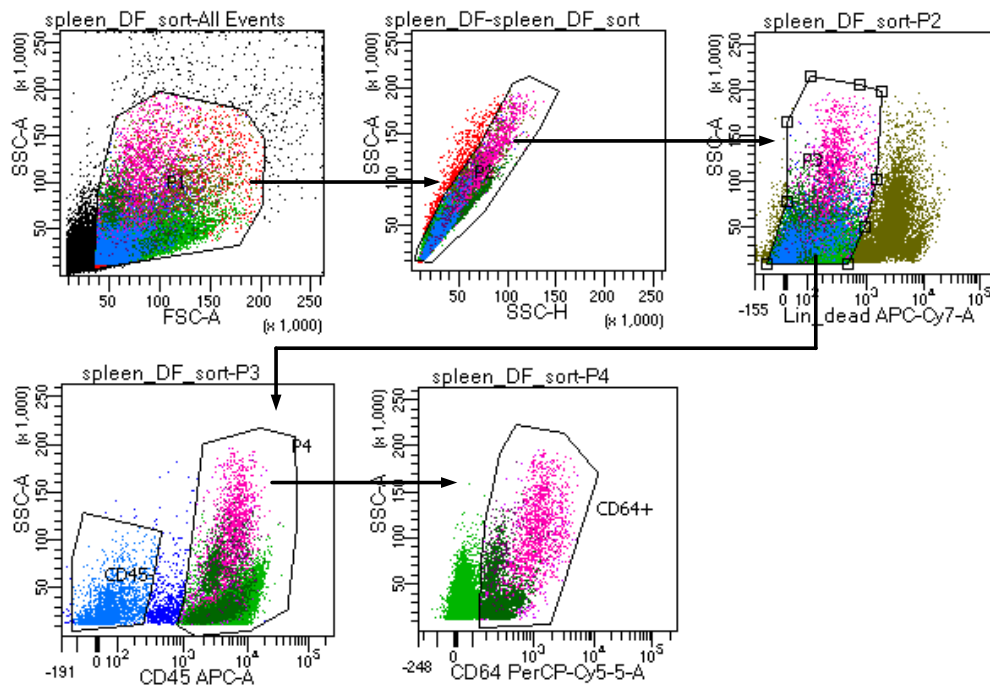


Figure 15: Sorting gate. Spleen homogenates were labeled with fluorescent antibodies and sorted with the FACS Aria. Gating on single, live, CD45⁺, CD64⁺ cells allowed for the collection of macrophages.

2.2.9.2 Single-cell library preparation and single-cell RNA-sequencing

This single-cell experiment was performed using 10x Genomics technology. Therefore, sorted cells were counted and the viability was examined by trypan

blue staining using a Neubauer counting chamber. Next, the cell suspension was adjusted to a concentration of 1000 cells/ μ l and processed by using the 10x Genomics Chromium Controller and the Chromium Next GEM Single cell 3' Reagent Kit v3.1 (Dual Index) (PN-1000268, 0x Genomics, Pleasanton, CA, USA) according to the standard manufacturer's protocol. The loaded cells were adjusted to 16,000 cells/sample to target a recovered cell number of 10,000 cells/sample for library preparation and sequencing.

The cDNA integrity and concentration measurements as well as the library concentration and size distribution were assessed using an Agilent high-sensitivity D5000 assay on a TapeStation 2200 system (Agilent Technologies). The cDNA libraries were quantified using a high-sensitivity dsDNA assay (Qubit, Thermo Fisher Scientific). In the final library preparation, amplified cDNA was fragmented, and size selected using SPRIselect magnetic beads (Beckman-Coulter) to purify for a library with a size distribution of 200 - 600 bp. After adaptor ligation and sample indexing, the final fragment size and concentration were measured and samples were pooled in an equimolar range. Samples were sequenced with a sequencing depth of > 30,000 reads/cell with 50 bp paired-end reads on an Illumina NextSeq2000 system.

2.2.9.3 Single-cell data alignment, read processing, data analysis and annotation

Raw data was demultiplexed and aligned to *Mus musculus* reference genome (mm10) along with the sequence for eYFP and tdTomato, using Cell Ranger-7.1.0 including the intronic reads (Alignment was performed by Dr. Lisa Maria Steinheuer). Count matrices were further processed using the R package Seurat (v4.0) starting with the evaluation of the sample quality and the appropriate filtering to exclude low-quality cells. The filtering criteria were set to 500-5,000 genes/cell, 25,000 transcripts/cell, and a mitochondrial gene content < 15 %. In addition, ribosomal genes were monitored (Figure 16). Next, highly abundant genes (Malat1, mitochondrial, ribosomal, hemoglobin and Gm genes) without biological relevance for this study were removed from the dataset. To generate a

UMAP following steps were performed: standard log-normalization, identification of variable genes, data scaling, linear dimensional reduction, and clustering. Afterward, using the SingleR package in R, processed data were used to assign different cell types in a UMAP. Based on the identified macrophage cluster a sub-clustering was performed. Splenic macrophage cluster were then assigned based on the expression of subtype specific marker genes: Adgre1 for RPM, SIGNR1 for MZM, CD169 for MMM, MerTK for WPM (Data analysis was performed by Dr. Nelli Blank-Stein)

Quality control and cut offs:

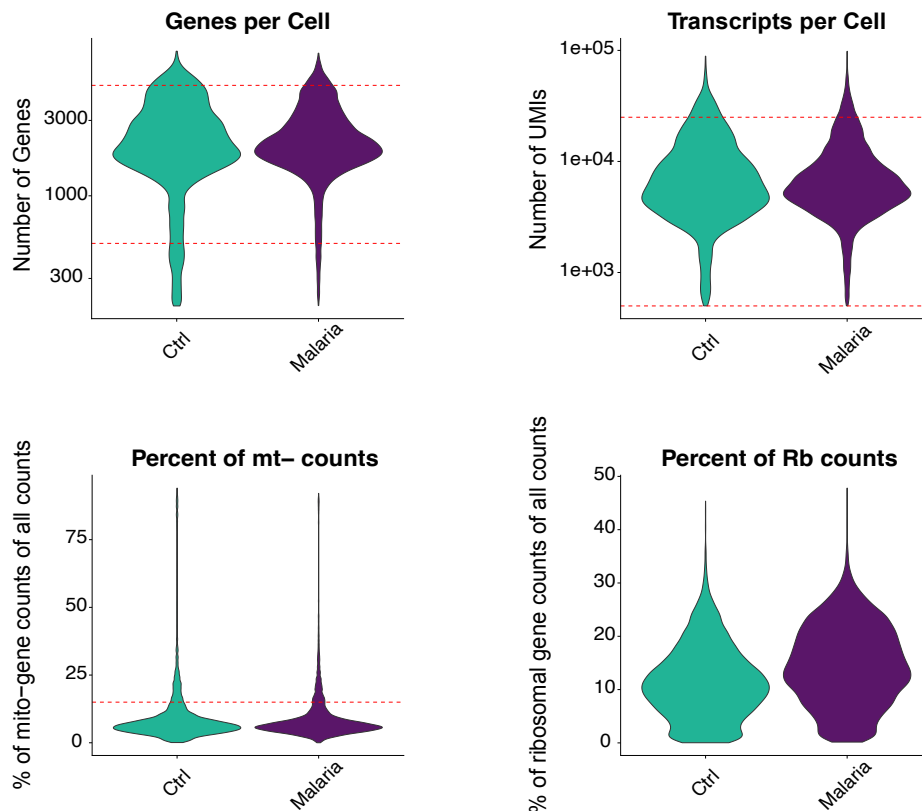


Figure 16: Quality control of single-cell RNA-sequencing data. The aligned data set was subjected to quality control and defined cut-offs were made, to select the cells that were further analyzed. Cut-offs were defined with 500 – 5,000 genes and 25,000 transcripts per cell and less than 15 % of mitochondrial genes. Percentage of ribosomal genes was monitored.

3 Results

3.1 Identification and ontogeny of splenic macrophage populations

The spleen is a secondary lymphoid organ, with one of its essential functions being to filter the blood. Thereby, it maintains a healthy composition of circulating erythrocytes. Aberrant or old RBCs are removed by spleen-resident phagocytes, the splenic macrophages. These macrophages also form the first line of defense against blood-borne infections, since they recognize, engulf and digest blood-borne pathogens. The composition of these splenic macrophages is very heterogeneous.

Extensive literature research led to the identification of characteristic markers for different splenic macrophage subpopulations (Figure 17). RPM are well described in the literature as F4/80 expressing macrophages (Kurotaki et al, 2015). The most characteristic marker for MZM is CD209b and CD169 for MMM (A-Gonzalez & Castrillo, 2018). Both populations express MARCO and Tim4, but MARCO is particularly highly expressed on MZM, as is Tim4 on MMM (Fujiyama et al, 2018). WPM have high levels of surface MerTK expression (A-Gonzalez & Castrillo, 2018). This was followed by a panel design that can be used on the BD FACSymphony and covers all relevant markers to distinguish splenic macrophages.

Upon isolation of splenocytes and antibody-staining for flow cytometry with the predefined panel of antibodies against relevant cell surface antigens, the aim was to characterize splenic RPM, MMM, MZM and WPM (Figure 18). To plot these data in two dimensions, 25,000 cells (live, CD45⁺, lineage negative, CD64⁺) were down-sampled and a non-linear dimensionality reduction technique was used to calculate similarities and proximities in a two-dimensional space, presented as uniform manifold approximation and projection (UMAP) (Becht et al, 2018).

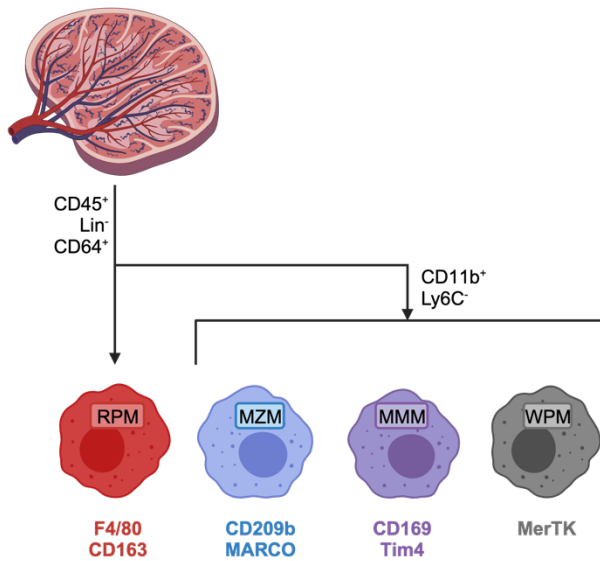


Figure 17: Relevant marker to distinguish splenic macrophages. Splenic macrophages are distinguishable from other cells via flow cytometry by the expression of CD45 and CD64 and the absence of CD19, TCRb, NKp46 and Ly6G (Lin). Characteristic for red pulp macrophages (RPM) is F4/80 expression and a heterogeneity amongst CD163 expression. Other splenic macrophages express CD11b, but are negative for Ly6C. Amongst them, marginal zone macrophages (MZM) express CD209b and MARCO, marginal metallophilic macrophages (MMM) express CD169 and Tim4, white pulp macrophages (WPM) express MerTK.

The generated UMAP was assessed for the expression of the predefined characteristic macrophage markers: F4/80, CD163, CD169, CD209b, MerTK and MARCO (Figure 18, A). Two distinct clusters showed high F4/80 expression, characteristic for RPM. These two clusters specifically differed in the expression of CD163. Thus, a new level of macrophage heterogeneity was defined to discriminate CD163⁺ and CD163⁻ RPM. No other clusters showed CD163 expression, except for the cluster that was assigned as CD163⁺ RPM. Splenic MMM and MZM are very similar, thus the highest intensity of their characteristic surface marker (CD169 and CD209b respectively) were found in close proximity in the UMAP. Based on those marker profiles, a gating strategy was developed and the gated macrophage populations overlaid with the calculated UMAP (Figure 18, B). This showed two distinct clusters of RPM; CD163⁺ and CD163⁻.

MMM and MZM clusters were in close proximity to each other and WPM and monocyte clusters were able to be distinguished.

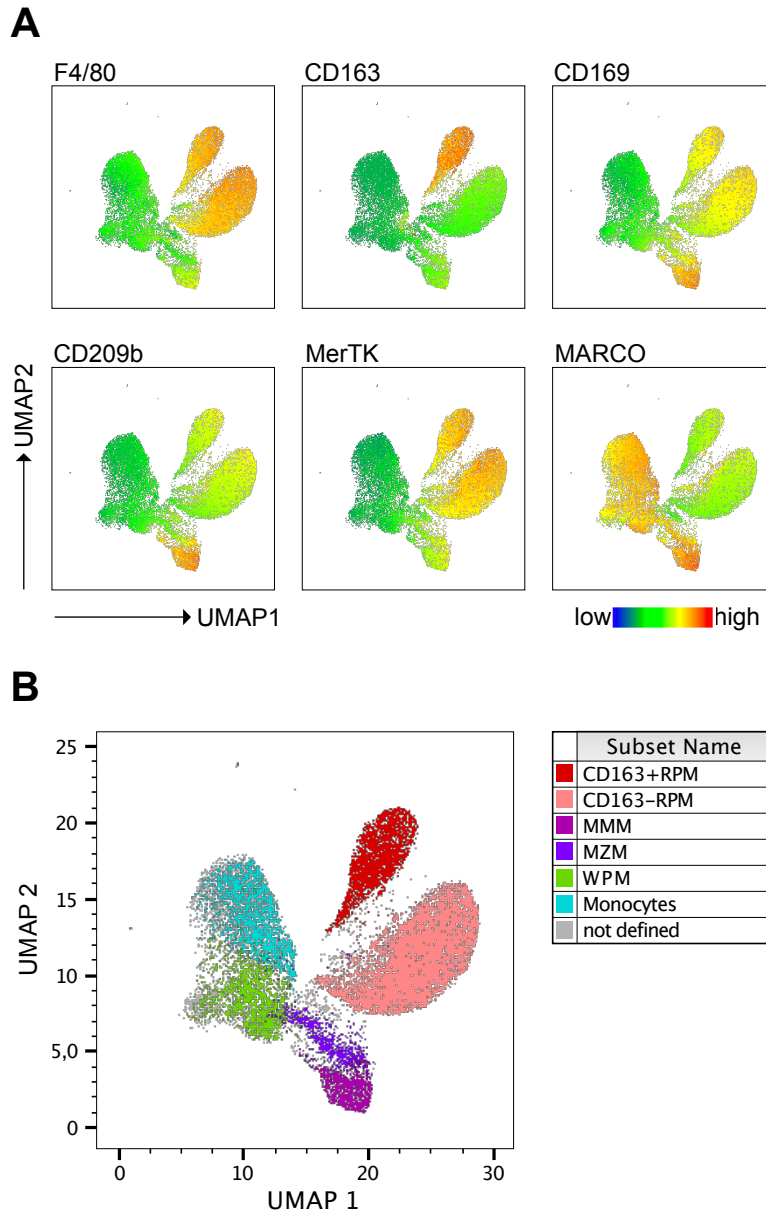


Figure 18: Identification of splenic macrophages via UMAP. Of all splenocytes, 25,000 live, CD45⁺, Lin⁻, CD64⁺ macrophages were down-sampled and the UMAP was calculated by FlowJo. (A) Expression intensity of characteristic splenic macrophage marker (F4/80, CD163, CD169, CD209b, MerTK, MARCO) on calculated UMAP. (B) Gating of distinct macrophage populations and identification of respective cluster (CD163⁺ red pulp macrophages (RPM), CD163⁻ RPM, marginal metallophilic macrophages (MMM), marginal zone macrophages (MZM), white pulp macrophages (WPM), monocytes) by layering on the UMAP.

A novel gating strategy was developed, which allows the discrimination of all splenic macrophage subsets. First, and similar to the down-sampled input that was used for the generation of the UMAP: single, live, CD45⁺, Lin⁻ cells were gated on CD64 expressing cells. The characteristic F4/80⁺ RPM were subdivided into CD163⁺ RPM and CD163⁻ RPM. CD163 expression was not detected in the CD11b⁺ population. From the CD11b⁺ population, Ly6C⁺ monocytes were excluded and CD169⁺/Tim4⁺ MMM, as well as MARCO⁺ MZM and MerTK⁺ WPM were identified (Figure 19).

Single, live, CD45⁺ cells:

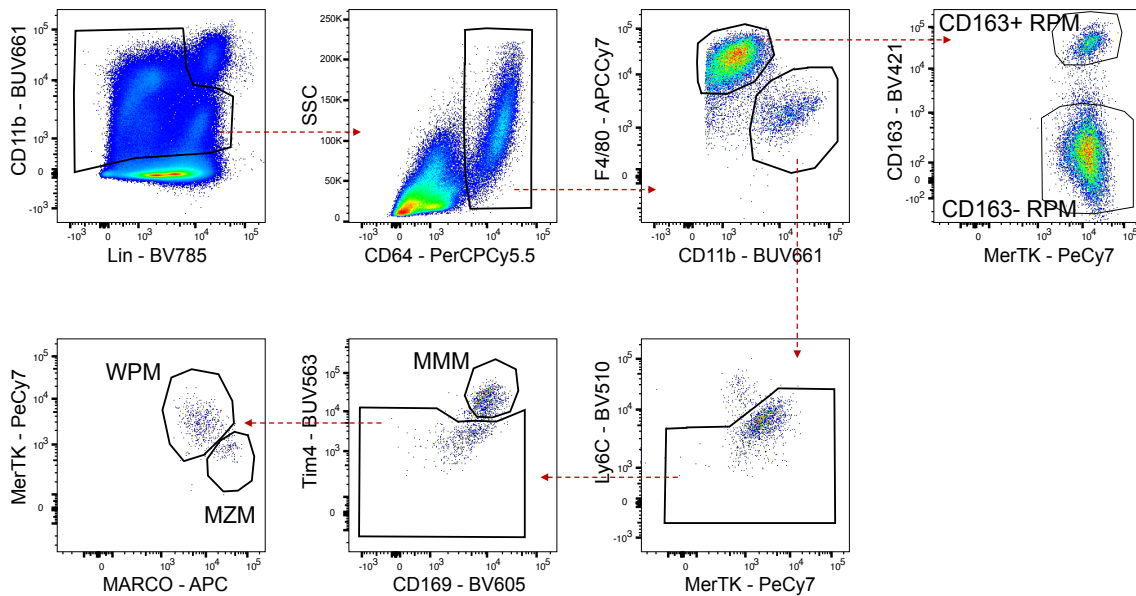


Figure 19: Gating strategy for splenic macrophages. The spleen tissue was digested and stained for flow cytometry. Single, live, CD45⁺, Lin⁻, CD64⁺ splenic cells comprise F4/80⁺ red pulp macrophages (RPM) differing in CD163 expression, CD169⁺ marginal metallophilic macrophages (MMM), MARCO⁺ marginal zone macrophages (MZM) and MerTK⁺ white pulp macrophages (WPM).

3.1.1 Splenic macrophage ontogeny

Splenic macrophages are a heterogeneous population, but their distinctive developmental origin has not been well described. An advanced technique to study the ontogeny of cells are genetically modified mouse models that induce the expression of a fluorescent reporter under the control of a lineage specific promoter. These so-called fate-mapper mice were used in this study to trace the developmental origin of macrophages in the spleen.

The *Cxcr4^{CreERT2}; Rosa26^{LSL-tdTomato}* mouse line is Tamoxifen inducible and labels LT-HSC. Thus, cells that have differentiated from BM-derived HSC express tdTomato (Mauel & Mass, 2024). Six months after Tamoxifen treatment, Ly6C⁺ circulating monocytes in the blood were analyzed. Since all circulating monocytes originate from BM-progenitors, these cells are a good readout for HSC labeling efficiency. Here, almost 100 % of circulating blood monocytes were tdTomato⁺, confirming that the reporter correctly labels cells of HSC origin. Within splenic macrophages, the percentage of tdTomato⁺, HSC-derived cells was much lower. Less than 50 % of splenic CD163⁺ RPM were tdTomato⁺ and approximately 60 % of CD163⁻ RPM (Figure 20).

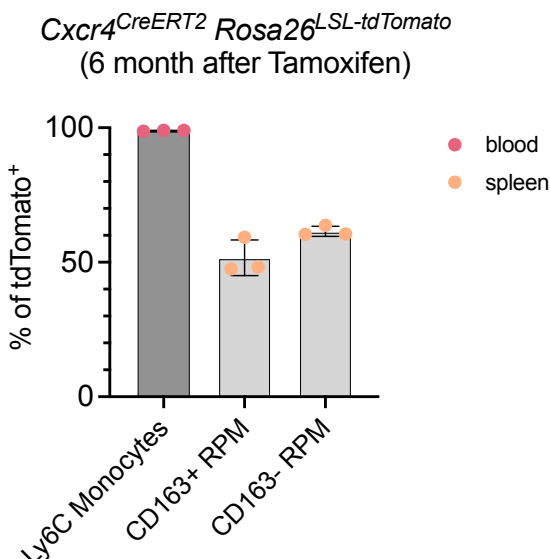


Figure 20: HSC-derived origin of splenic macrophages. Two months old *Cxcr4^{CreERT2}; Rosa26^{LSL-tdTomato}* mice were *i.p.* injected with tamoxifen for five consecutive days, to induce Cre-activity and label HSC-derived cells. Six months after tamoxifen administration, the percentage of tdTomato⁺ circulating blood

monocytes and splenic red pulp macrophages (RPM) was quantified via flow cytometry (n = 3).

With respect to the developmental origin of splenic macrophages, this indicated that approximately half of the splenic RPM population was HSC-derived in adult mice (at 8 months).

However, this did not allow for conclusions to be drawn about the developmental origin of the cells that were not labeled. Furthermore, the origin of splenic macrophages in young mice and aged mice could be dynamic and differ from observations seen in 8 months old animals.

Therefore, a novel fate-mapping mouse model was developed for this project, which will advance the study of macrophage ontogeny in many research focus areas.

The introduced *Tnfrsf11a^{Cre}; Rosa26^{LSL-YFP}; Ms4a3^{FlpO}; Rosa26^{FL-tdTomato}* model, called the double-fatemapper (see introduction chapter: 1.3.2.2 The double-fatemapper), labels *Tnfrsf11a* expressing EMP-derived cells with a YFP reporter and *Ms4a3* expressing HSC-derived cells with a tdTomato reporter (Figure 21). When tdTomato⁺ monocytes enter the tissue and differentiate into long-lived macrophages, they upregulate *Tnfrsf11a* and thus express both fluorescent reporter genes.

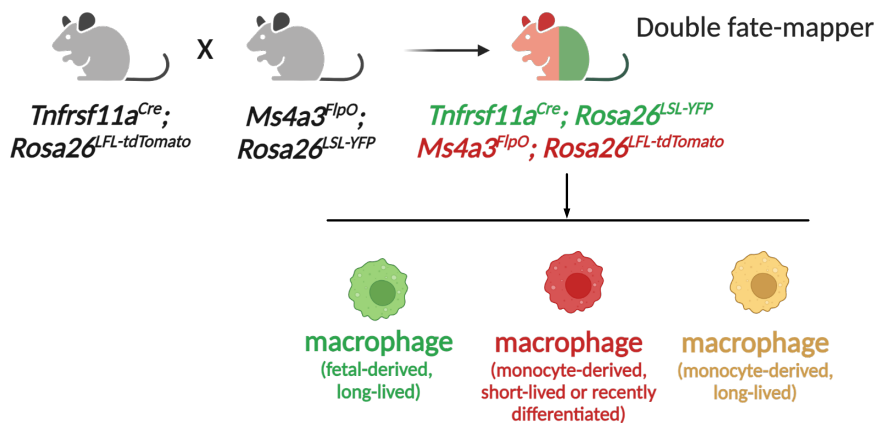


Figure 21: The double-fatemapper. EMP-derived cells express Cre under the control *Tnfrsf11a*, leading to YFP expression (green). HSC-derived cells express FlpO under the control of *Ms4a3*, leading to tdTomato expression (red). tdTomato positive monocytes upregulate *Tnfrsf11a*, when differentiating into macrophages and express both fluorescent proteins (yellow).

Using this model, the ontogeny of splenic RPM was investigated during early development and adulthood.

The contribution of EMP-derived progenitors (only YFP⁺) to the splenic CD163⁻ and CD163⁺ RPM compartments, was very high in unborn (E14.5) and juvenile mice (Figure 22, A). While approximately 90 % of the CD163⁻ RPM were YFP⁺ and thus derived from yolk sac progenitors during embryogenesis and within the first three weeks after birth, during early adulthood a trend was observed that indicated an influx of HSC-derived cells. These cells were positive for both fluorescent reporters, since they originated from tdTomato positive circulating monocytes and started to upregulate *Tnfrsf11a* when they entered the tissue and differentiated into long lived macrophages, which initiated the expression of YFP. On the other hand, CD163⁺ RPM were almost exclusively EMP-derived during embryogenesis and early adulthood. This population was almost 100 % positive for only YFP, with no contribution from HSC-derived progenitors in unborn and juvenile mice.

The composition of the macrophage compartment, in terms of developmental origin, is often transient and changes as a result of aging (Mass et al, 2023). The

ontogeny of splenic RPM populations was therefore studied in adulthood between three and 12 months after birth (Figure 22, B). For both the CD163⁻ and CD163⁺ RPM, a decrease in the proportion of EMP-derived macrophages during ageing and a steady influx of HSC-derived monocytes that differentiate into long-lived macrophages was observed. However, also during adulthood, the ontogeny of CD163⁻ and CD163⁺ RPM differs. While in one year old mice, only 50 % of the CD163⁻ RPM remain EMP-derived macrophages, the other half originated from BM-precursors that have differentiated into long lived CD163⁻ splenic RPM. For CD163⁺ RPM a similar trend was described, but a larger proportion of EMP-derived macrophages remained in the CD163⁺ RPM compartment during adulthood. While in young mice, almost all splenic CD163⁺ RPM were EMP-derived, in one year old mice, approximately 40 % were replaced by infiltrating monocytes that originated from HSC and 60 % were long-lived EMP-derived macrophages. The data suggested that in adult mice, cells of both origins could contribute to the pool of CD163⁺ RPM. It was evident that CD163⁺ RPM reached a plateau and the contribution of EMP- versus HSC-derived cells stabilized, while the dynamics of the CD163⁻ RPM was linear with ongoing replacement of EMP- by HSC-derived cells, as indicated by the opposing directions of the curves.

To validate these findings, spleen tissues were also collected for fixation and antibody labeling for fluorescent microscopy (Figure 22, C). Spleens from seven days old mice (P7) were compared with adult mice (8 weeks old). Labelling with an antibody that binds to CD169 highlighted the splenic marginal zone and yielded insight into the development of the splenic architecture. Staining with CD163 elucidated the newly discovered heterogeneity amongst splenic RPM. First, it was observed that the splenic architecture had not fully developed at P7. The dispersed CD169 signal indicated that the spleen had not yet separated into its red and white pulp areas. This separation was clearly visible in adult mice. Additionally, CD163⁺ macrophages were already present in the spleen at birth, but they only localized specifically in the red pulp in adult mice, once the marginal zone had properly developed. In accordance with the flow cytometry data, the CD163 signal co-localized with the YFP signal, but not with the tdTomato signal.

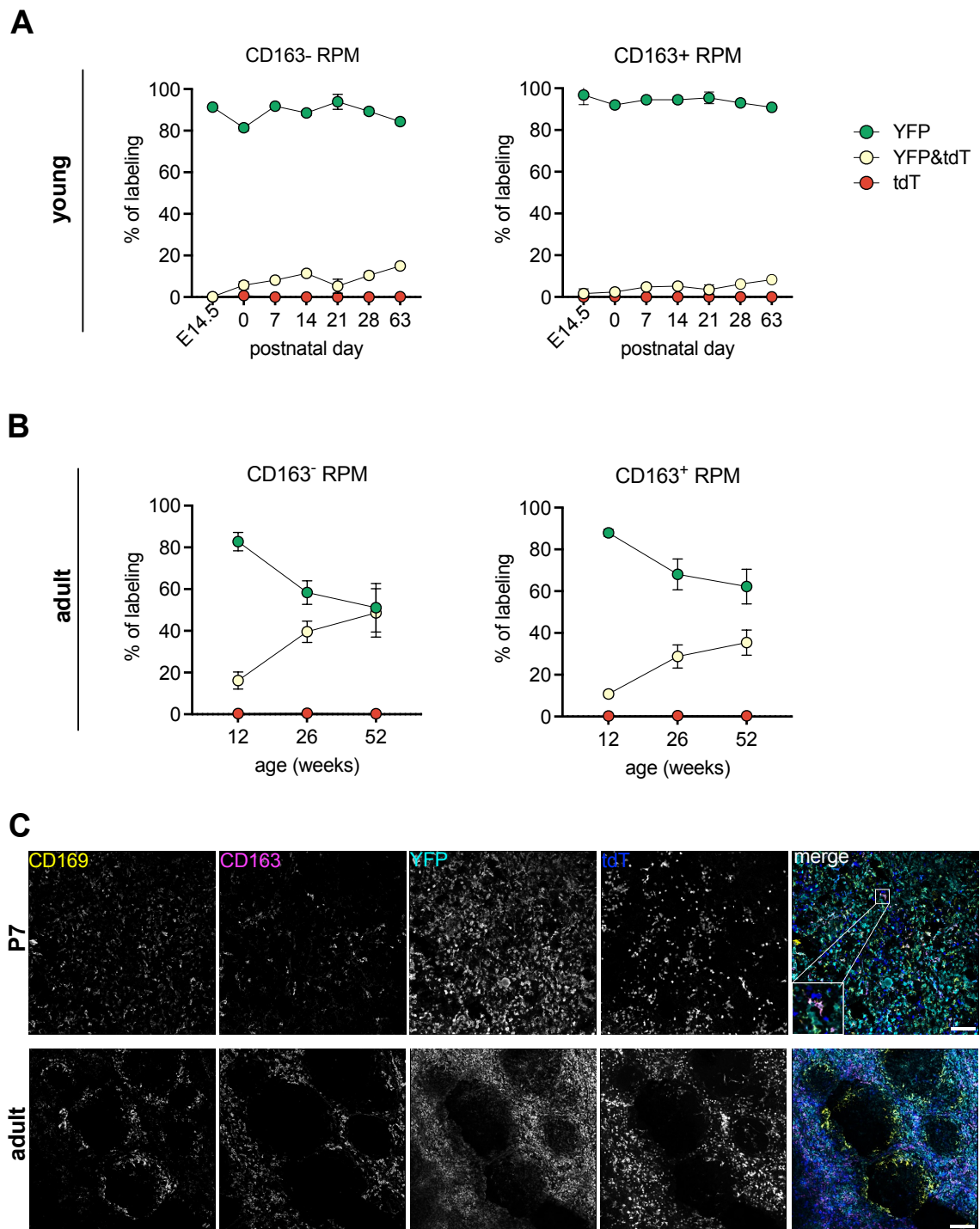


Figure 22: Developmental origin of splenic RPM. The *Tnfrsf11a^{Cre}; Rosa26^{LSL-YFP}; Ms4a3^{FlpO}; Rosa26^{LFL-tdTomato}* fate mapping model was used to study the ontogeny of splenic CD163⁻ and CD163⁺ red pulp macrophages (RPM) during embryogenesis until (A) early adulthood (n = 3 - 4) and in (B) adult mice (n = 4). EMP-derived cells were YFP⁺ (green), HSC-derived short-lived cells were tdTomato⁺ (red) and HSC-derived long-lived cells were YFP⁺ and tdTomato⁺ (yellow). (C) Spleen tissue was collected at day 7 after birth (P7) and 8 weeks of age (adult) for fixation and labeling with fluorescent antibodies. CD169 for splenic

marginal zone (yellow), CD163 for splenic RPM heterogeneity (magenta), YFP (cyan) and tdTomato (blue) as endogenous fluorescent reporter and merge. Inset on colocalization of CD163 and YFP signal. (representative for n = 2, scale bar = 100 μ m)

Taken together, a similar proportion of labelled HSC-derived splenic macrophages was observed with two different reporter mouse lines in adult mice. Of note, the cellular origin of splenic macrophages was dynamic and the proportions that originated from HSCs depended upon the age of the mice that were analyzed. In young mice, most splenic RPM originated from EMP-precursors. With respect to the novel discovery of a heterogeneity amongst splenic RPM, the double-fatemapper supported a difference in CD163⁺ and CD163⁻ RPM with respect to the dynamics of their developmental origin. CD163⁺ and CD163⁻ RPM showed similar, but not identical, ontogeny in both developmental origin and steady-state dynamics with replacement of EMP-derived cells by HSC-derived cells during physiological ageing.

3.2 The dynamics of splenic myeloid cells during blood-stage malaria

Blood-stage malaria causes severe symptoms, but it is still not completely understood how the splenic microenvironment and distinct cell compositions change during disease progression and what the functional impact of cellular loss and replacement by infiltrating cells is on parasite clearance and inflammation.

To investigate macrophage dynamics during and after the active stage of malaria, mice were infected with the *Plasmodium* species *P. chabaudi*, which mimics many features of human pathology. The mice were infected with a standard dose of 1×10^4 infected RBC per mouse via intraperitoneal injection. This led to the development of blood-stage malaria by day seven post-infection. The level of parasitemia was measured in the peripheral blood from 1 to 90 days after

infection (covering the period from acute infection until resolution) and the cellular composition of the spleen, BM and blood were also analyzed (Figure 23, A).

To monitor the progression of malaria infection, the proportion of red blood cells that were infected with parasites (infected RBC), termed parasitemia, was quantified via flow cytometry upon Hoechst staining of the blood sample every three to five days. Since mature erythrocytes extrude their nucleus, only the infected erythrocytes, carrying the genetic material of the parasites, bind Hoechst, therefore allowing for parasite infected RBC to be quantified via flow cytometry. The percentage parasitemia was calculated and showed the characteristic cyclic progression of malaria with repeated peaks of high parasitemia (Figure 23, B). Within the first two weeks, when the mice showed the most severe symptoms, the highest peaks in parasitemia were also observed. Once the mice had recovered from symptoms, parasites could not be detected after 56 days. The presence of the parasites was further validated on blood smears upon Giemsa staining and the typical ring structure of the parasites intra-erythroid stage was observed in infected RBC (Figure 23, C).

The experimental malaria model also exhibits severe splenomegaly (Figure 23, D), one of the complications of blood-borne infections. Two weeks after infection, the spleen was significantly enlarged as a result of the recruitment of effector cells during acute infection. This enlargement gradually normalizes after two months (Figure 23, E), although the organ still appears darker, compared to the control. This is most likely the result of hemozoin deposits, which are formed by the malaria parasite metabolizing heme (Sigala & Goldberg, 2014).

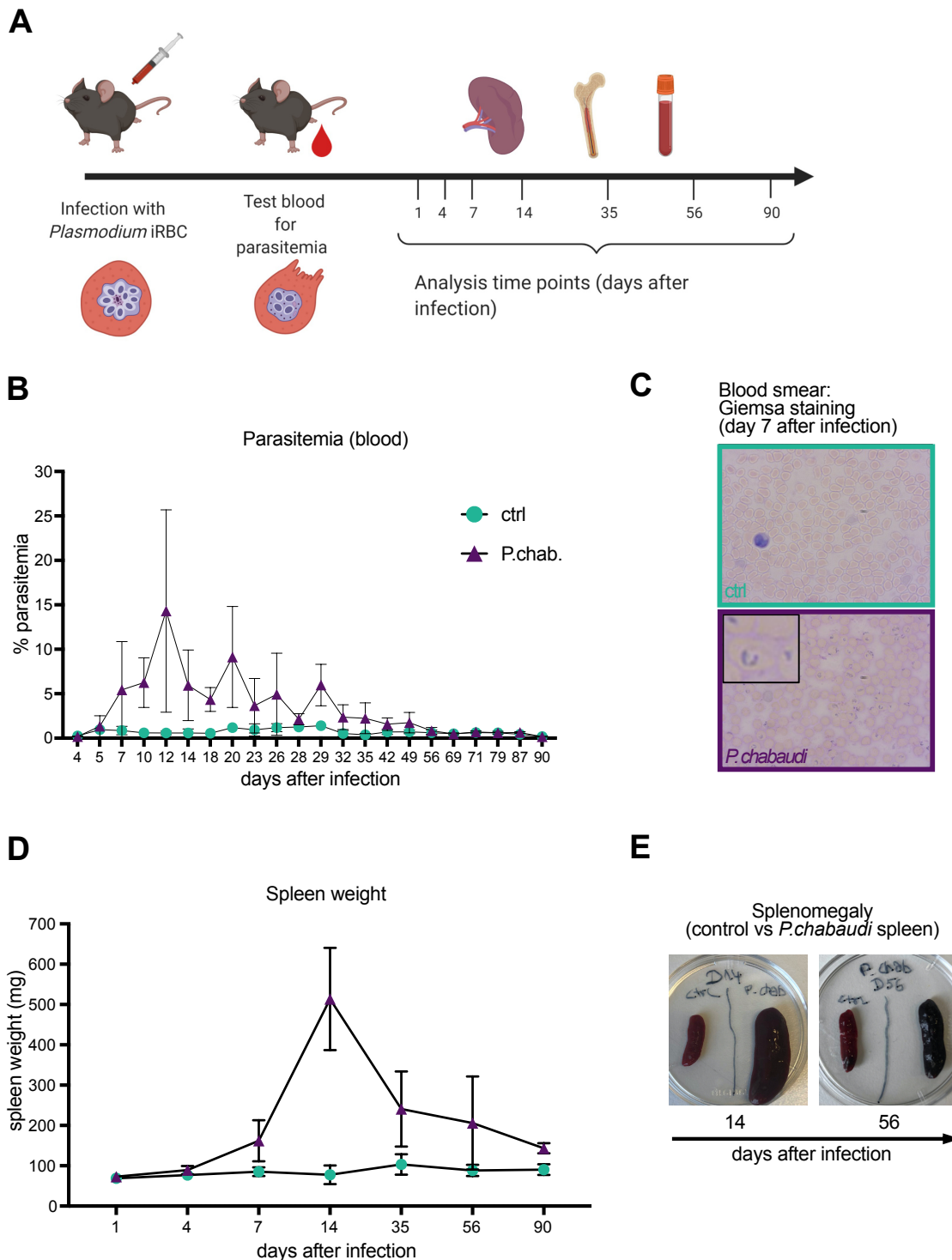


Figure 23: The *P. chabaudi* malaria model. (A) Experimental strategy: Mice were injected with *P. chabaudi* infected RBC to induce blood-stage malaria. Parasitemia was repeatedly tested on blood samples and spleen, BM and blood were analyzed at the indicated experimental days post infection. (B) Mice were infected with *P. chabaudi* blood-stage malaria. The percentage of infected RBC was quantified via flow cytometry upon Hoechst staining of blood samples of infected and control mice ($n > 9$). (C) Visualization of infected RBC on blood

smear upon Giemsa staining at day 7 after *P. chabaudi* infection showing parasites inside the erythrocytes, compared to uninfected control. (D) Spleens were isolated from experimental mice at indicated timepoints. Spleen weight indicating splenomegaly upon malaria infection (n = 3 - 9). (E) Pictures showing isolated spleens of control and *P. chabaudi* infected mice at day 14 after the infection with distinct splenomegaly, followed by normalization at day 56.

3.2.1 Loss of splenic CD163⁺ RPM upon *P. chabaudi* infection

With establishment of the *P. chabaudi* blood-stage malaria model, the impact of infection on splenic macrophages was investigated. Through the open circulation of the spleen, these innate phagocytes are in direct contact with the circulating blood, and thus infected erythrocytes. Spleens were collected at the respective experimental dates (Figure 24, A) and macrophages were isolated upon enzymatic digestion of splenic homogenates to prepare them for flow cytometry staining.

This revealed not only that there was a novel heterogeneity amongst splenic RPM, but also that the newly defined CD163⁺ RPM population was affected by malaria infection (Figure 24, A, B). The absolute number CD163⁺ RPM per gram of spleen decreased immediately after *P. chabaudi* administration and the population was entirely depleted within the first week of infection. This population remained absent throughout the time course of the experiment and did not recover after 90 days (Figure 24, C). In a preliminary experiment, CD163⁺ RPM were quantified 6 months after the infection with *P. chabaudi*, suggesting that CD163-expressing RPM did not recover long term after a malaria infection (Figure 24, D). On the other hand, the CD163⁻ RPM population expanded during the acute phase of the infection and remained elevated during the later stages of the time course. When the parasites were cleared from the circulation, as indicated by a decrease in parasitemia, the CD163⁻ RPM compartment recovered and the number of CD163⁻ RPM was found to be similar to the steady-state controls at day 90 (Figure 24, C).

Mechanistically, the CD163 receptor takes up hemoglobin/haptoglobin complexes, and is internalized, and then the receptor is recycled back to the cell surface. To determine if the loss of the CD163⁺ RPM population is due to a loss of the receptor from the cell surface, an intracellular flow cytometry assay was performed (Figure 24, E). While the receptor was identified on the cell surface and internalized in samples from uninfected control mice, CD163 expression was lost both on the extracellular surface and intracellularly upon malaria infection at day 7. The intracellular CD163-staining was performed for one cohort of mice; these preliminary data should help to decipher possible routes for the loss of the CD163 receptor on RPM.

Since the CD163 receptor is responsible for the uptake of heme and the recycling of iron, and a loss of the receptor could result in a change in the dynamics of iron in the spleen, the iron content in spleen homogenates at day 7 and day 14 of malaria infection was quantified and compared to uninfected controls. During acute malaria infection and specifically on day 14 (when the highest peak in parasitemia was observed), a significant loss in splenic iron was seen (Figure 24, F, tissue was collected and given to Daria Hirschmann to perform the iron assay).

Upon the obvious loss in CD163 expressing RPM detected via flow cytometry, these findings were validated by immunofluorescent imaging. Upon labeling of fixed tissue sections with antibodies conjugated to a fluorophore, control spleens were compared to the tissue during acute malaria (day 7) and after resolution of the infection (day 90). Labeling with Iba1, which is expressed by all macrophages, and with CD163 to examine RPM heterogeneity, as well as with CD169 for the MMM in the splenic marginal zone, highlighted two major pathologies in malaria (Figure 25, A). First, the CD163 signal was clearly detectable in control spleens and was distributed throughout the red pulp area. In accordance with the flow cytometry data, the CD163 signal was lost upon infection with *P. chabaudi* and did not return after the resolution of the infection.

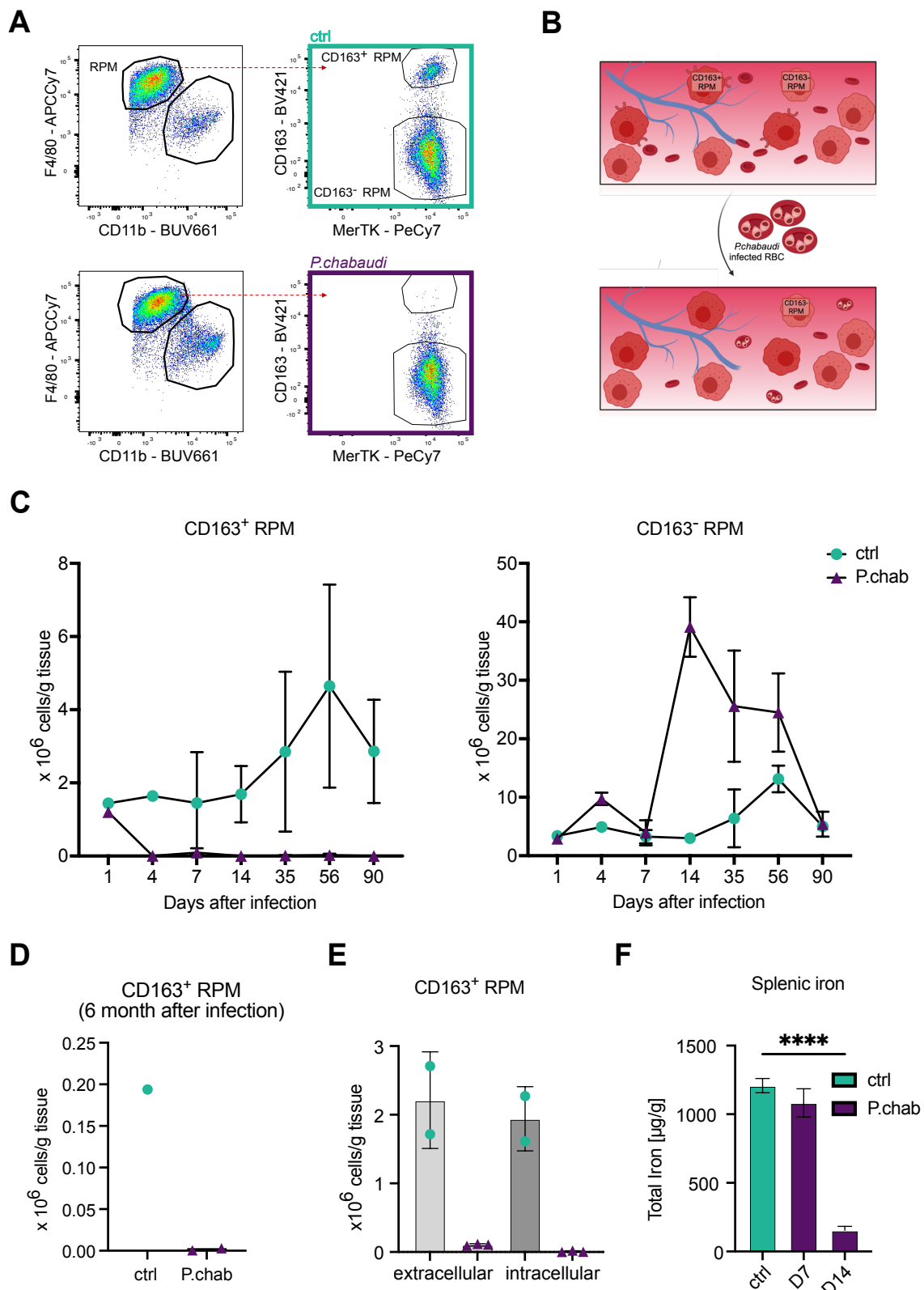


Figure 24: Loss of CD163⁺ RPM in *P. chabaudi* malaria. (A) Gating for splenic F4/80⁺ macrophages to distinguish CD163⁺ RPM in control (ctrl) vs. *P. chabaudi* (*P.chab*) infected mice at day 7 after malaria infection. (B) Model for loss of CD163 expression upon malaria infection. Heterogeneity of red pulp macrophages

(RPM) in terms of CD163 expression in steady-state and loss of CD163 expression in the presence of *Plasmodium* infected erythrocytes (C) At indicated timepoints after the infection with *P. chabaudi*, spleen tissue was collected for flow cytometry. Quantification of splenic CD163⁺ and CD163⁻ RPM at day 1 - 90 after malaria infection (day 1: n = 2, day 4: n = 2, day 7: n = 6, day 14: n = 8, day 35: n = 5, day 56: n = 6, day 90: n = 5). (D) In a preliminary experiment, spleen tissue was collected 6 months after the infection with *P. chabaudi* for flow cytometry analysis of CD163⁺ RPM. (E) Spleen tissue at day 7 after *P. chabaudi* infection was prepared for flow cytometry with the standard panel (including CD163-BV421), followed by permeabilization and intracellular staining with CD163-PE (n = 2 - 3). (F) Quantification of total iron content in spleen homogenates via colorimetric detection at day 7 (D7) and day 14 (D14) after infection (n = 3; statistics: p-values obtained using one-way ANOVA for multiple group comparison, ****p < 0.0001).

Additionally, F4/80-expressing RPM were evenly distributed throughout the red pulp in control spleens. Upon acute malaria infection (day 7), when the splenic integrity was lost with respect to the marginal zone, the F4/80 signal was diffusely distributed throughout the whole spleen tissue and the morphological shape of the RPM changed to a more rounded morphology, with fewer extensions from the cell body. After the resolution of the infection (day 90) the splenic environment recovered (Figure 25, B).

Second, the marginal zone, detectable by detection of CD169 expressing MMM, formed closed circular structures in control spleens. During acute phase of malaria (day 7), the marginal zone was open and fenestrated, indicating a temporal loss of the marginal zone integrity. However, 90 days after malaria infection, the marginal zone had regenerated (Figure 25, A, B).

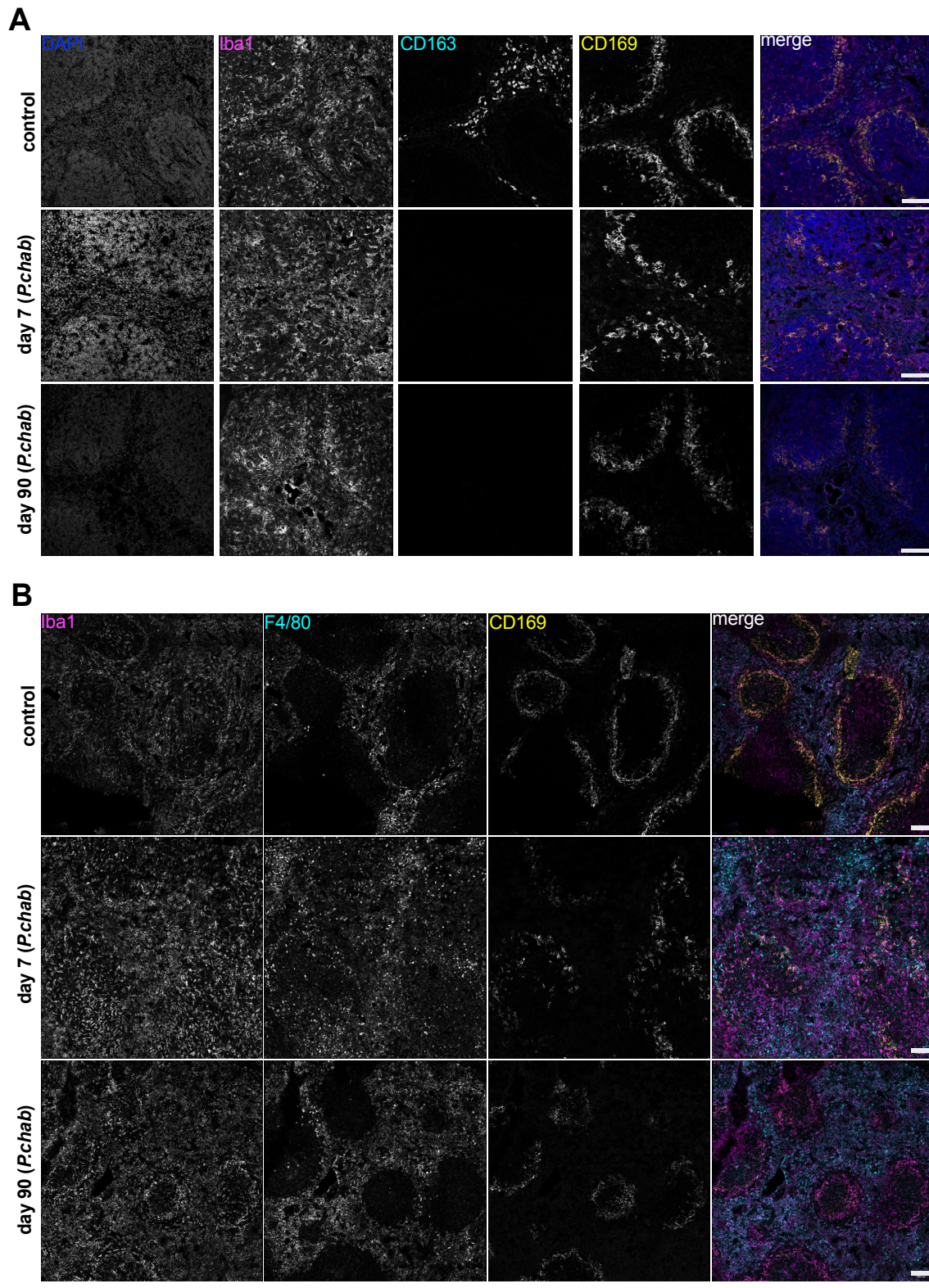


Figure 25: Expression of macrophage-specific markers in the spleen upon malaria with *P. chabaudi*. Immunostaining of spleen tissue: uninfected (ctrl), 7 days and 90 days after *P. chabaudi* infection. (A) Individual channels of DAPI for nuclear staining (blue), Iba1 for all macrophages (magenta), CD163 for

heterogeneity of RPM (cyan), CD169 for splenic marginal zone (yellow) and merge, showing loss of CD163 signal upon malaria infection. (B) Iba1 (magenta), CD169 (yellow) and F4/80 (cyan) for all RPM. (representative for n = 3, scale bar = 100 μ m)

One major function of the spleen is filtration of the blood, which mostly takes place in the red pulp. The above findings showed a severe impact of the blood-borne malaria infection on the splenic RPM. Since other splenic compartments and their resident macrophages are involved in the initiation of immune responses, changes in splenic MMM, MZM and WPM upon malaria were also investigated (Figure 26). All three macrophage populations showed a similar trend: they decreased in number relative to the amount of tissue assessed within the first week of infection and expanded later. The transient decrease of the macrophage populations during acute infection hinted towards an impact of malaria on splenic MMM, MZM and WPM (Figure 26, A). However, the uninfected controls also fluctuated similarly, indicating that the fluctuations may be technical in nature and associated with the difficulty of isolating these rare cell populations. Since infected mice suffer from severe splenomegaly, a spreading of the macrophages in the enlarged organ could cause fluctuations in the calculated number of cells per gram of tissue. Thus, the number of cells per spleen was also calculated (Figure 26, B). While the MMM population was rather stable in size via this calculation, MZM showed an infection related expansion after the acute phase of infection. WPM numbers decreased early after the infection and remained reduced until day 90 after *P. chabaudi* administration.

Previous experiments supported these findings, but the development of a flow cytometry panel to distinguish MMM, MZM and WPM was a laborious process and only the data analyzed with the final antibody panel (see Figure 19) were plotted here. Therefore, this analysis requires repetition with larger cohorts to assess the impact of a malaria infection on splenic MMM, MZM and WPM.

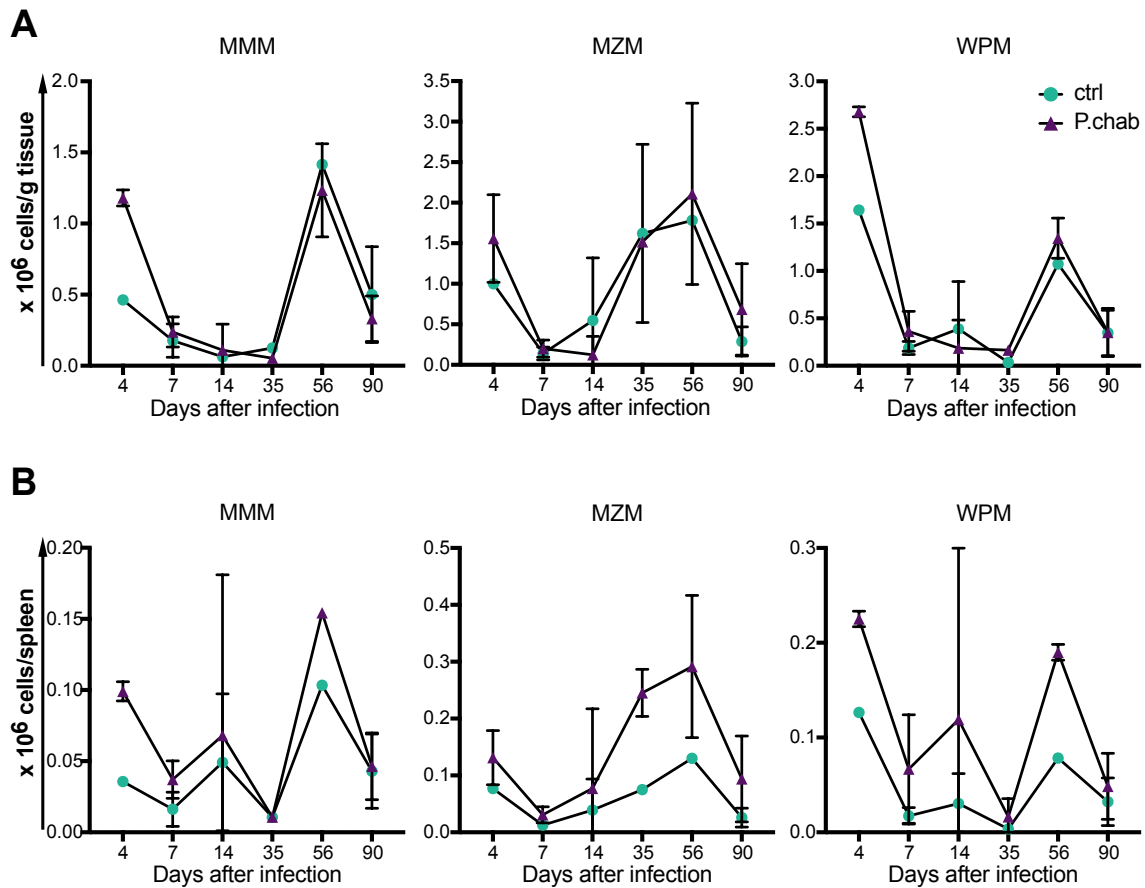


Figure 26: Dynamics of splenic marginal metallophilic macrophages, marginal zone macrophages and white pulp macrophages in *P. chabaudi* malaria infections. At the indicated timepoints after *P. chabaudi* infection, spleens were collected from mice for flow cytometry staining. Marginal metallophilic macrophages (MMM), marginal zone macrophages (MZM) and white pulp macrophages (WPM) were quantified in uninfected (ctrl) and malaria (*P.chab*) samples. (A) Quantified as cells per gram of tissue. (B) Quantified as cells per spleen. (day 4: n = 2, day 7: n = 5, day 14: n = 4, day 35: n = 3, day 56: n = 2, day 90: n = 5)

3.2.2 Loss of splenic CD163⁺ RPM upon malaria infection

To understand whether the disappearance of the CD163⁺ RPM is a phenomenon specific to infection with *P. chabaudi*, or a general consequence of malaria infection, the splenic cell composition was also examined after infection with other *Plasmodium* species. Mice were infected with 10⁴ infected RBC of either *P. yoelii*

or *P. berghei* and the spleens analyzed 7 days after infection (Figure 27, A). The parasitemia was followed over time and the mice developed an acute malaria infection within one week, indicated by increasing parasitemia and splenomegaly (Figure 27, B). Similar to what was observed after *P. chabaudi*, 7 days after infection with *P. yoelii* and *P. berghei*, the CD163⁺ RPM population could no longer be detected in the spleen of the infected mice, while the CD163⁺ RPM population was clearly detectable in controls (Figure 27, C). The relative numbers of CD163⁻ RPM were also reduced by day 7 (Figure 27, C), which aligned with the studies of *P. chabaudi*; an expansion of this population was only detected after day 14 (see Figure 24, C). CD163⁺ RPM were therefore depleted as a general consequence of malaria infection, irrespective of the parasite species used.

To determine if the CD163 expressing RPM were not detected due to shedding of the CD163-receptor, which is a common phenomenon upon infections and leads to an increase of CD163 in the serum (Droste et al, 1999; Etzerodt & Moestrup, 2013), serum of uninfected control mice as well as *P. yoelii* and *P. berghei* infected mice was collected at day 7 for an ELISA assay (Figure 27, D, serum was collected and given to Dr. Lynette Beattie to perform the ELISA assay). This assay showed a decrease in soluble CD163 in the serum of *P. yoelii* and *P. berghei* infected mice when compared to the steady-state serum concentration of CD163 in controls. Thus, shedding of the receptor was most likely not the cause of CD163⁺ RPM depletion during malaria infection.

Flow cytometry data were confirmed with immunofluorescent imaging of the same spleen tissues 7 days after *P. yoelii* or *P. berghei* infection respectively (Figure 27, E). Labeling with a Madcam1 fluorescent antibody showed that the signal of the vasculature located around the CD169 positive marginal zone. F4/80 binding identified RPM, localized in the splenic red pulp, which colocalized with the CD163 signal in the steady-state control spleens. Upon infection with *P. yoelii* or *P. berghei*, the CD163 signal was lost, validating the previous observations via flow cytometry.

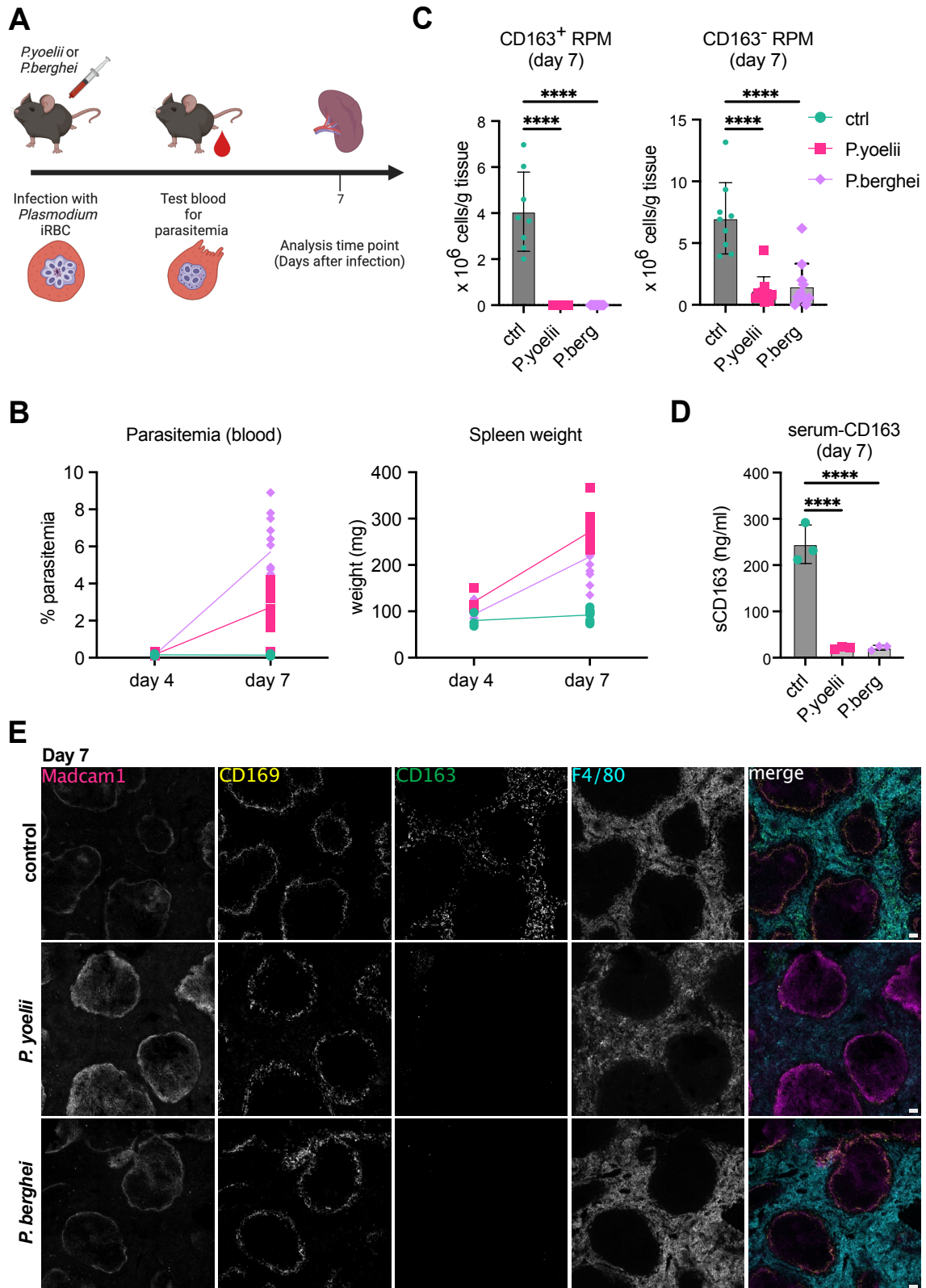


Figure 27: Loss of CD163 expressing RPM in malaria. (A) Experimental strategy. Mice were infected with *P. yoelii* or *P. berghei* blood-stage malaria respectively and the splenic macrophages were analyzed after 7 days. (B) The percentage of infected RBC (parasitemia) was quantified via flow cytometry after

Hoechst staining of blood samples and spleens were isolated from experimental mice at indicated timepoints. Spleen weight indicating splenomegaly upon malaria infection (n = 8 - 10). (C) At day 7 after the infection with *P. yoelii* or *P. berghei*, spleen tissue was collected for flow cytometry. Quantification of splenic CD163⁺ and CD163⁻ showed loss of CD163 expressing red pulp macrophages (RPM) (n = 8 - 10; statistics: p-values obtained using one-way ANOVA for multiple group comparison, ****p < 0.0001). (D) Collection of blood at day 7 after infection with *P. yoelii* or *P. berghei*. Quantification of soluble CD163 in serum via ELISA (n = 3; statistics: p-values obtained using one-way ANOVA for multiple group comparison, ****p < 0.0001). (E) Immunostaining of spleen tissue at day 7 after infection: uninfected (ctrl), *P. yoelii*, *P. berghei*. Individual channels of Madcam1 for vasculature (magenta), CD169 for splenic marginal zone (yellow), CD163 for heterogeneity of RPM (green), F4/80 for splenic RPM (cyan) and merge. (representative for n = 3, scale bar = 100 μm)

3.2.3 Parasite clearance by chloroquine and respective impact on splenic CD163⁺ RPM

After showing that malaria infection caused a lasting loss of CD163 expression on RPM, irrespective of the parasite species used, it was further assessed whether cure of the mice by chloroquine treatment, would lead to the repopulation with CD163 expressing RPM. Chloroquine prevents the parasites ability to detoxify metabolic side products, which consequently leads to the accumulation of these metabolic side products and killing of the parasites (Coban, 2020). To determine if complete clearance of the parasites would lead to repopulation of CD163⁺ RPM, mice were infected with the standard dose of *P. chabaudi* infected RBC and treated with chloroquine between day 21 and day 30 of infection (Figure 28, A). Parasitemia was monitored and showed that the mice developed acute malaria within the first two weeks of infection with a characteristic second peak one week later. However, administration of chloroquine cleared the parasites from the blood with no increase between day 22 and day 90 after the infection (Figure 28, B). In contrast, untreated mice showed reoccurring peaks of parasitemia until day 56 after initial *P. chabaudi* administration (see Figure 23, B).

At day 56 and day 90 after the initial *P. chabaudi* infection, splenic RPM were quantified via flow cytometry (Figure 28, C). Both at day 56 and day 90, when the mice were parasite free for at least one and two months respectively, CD163 expression could not be detected on splenic RPM. Thus, these preliminary data suggested that initial infection with live parasites caused a loss of CD163 expressing RPM, which did not recover after parasite clearance.

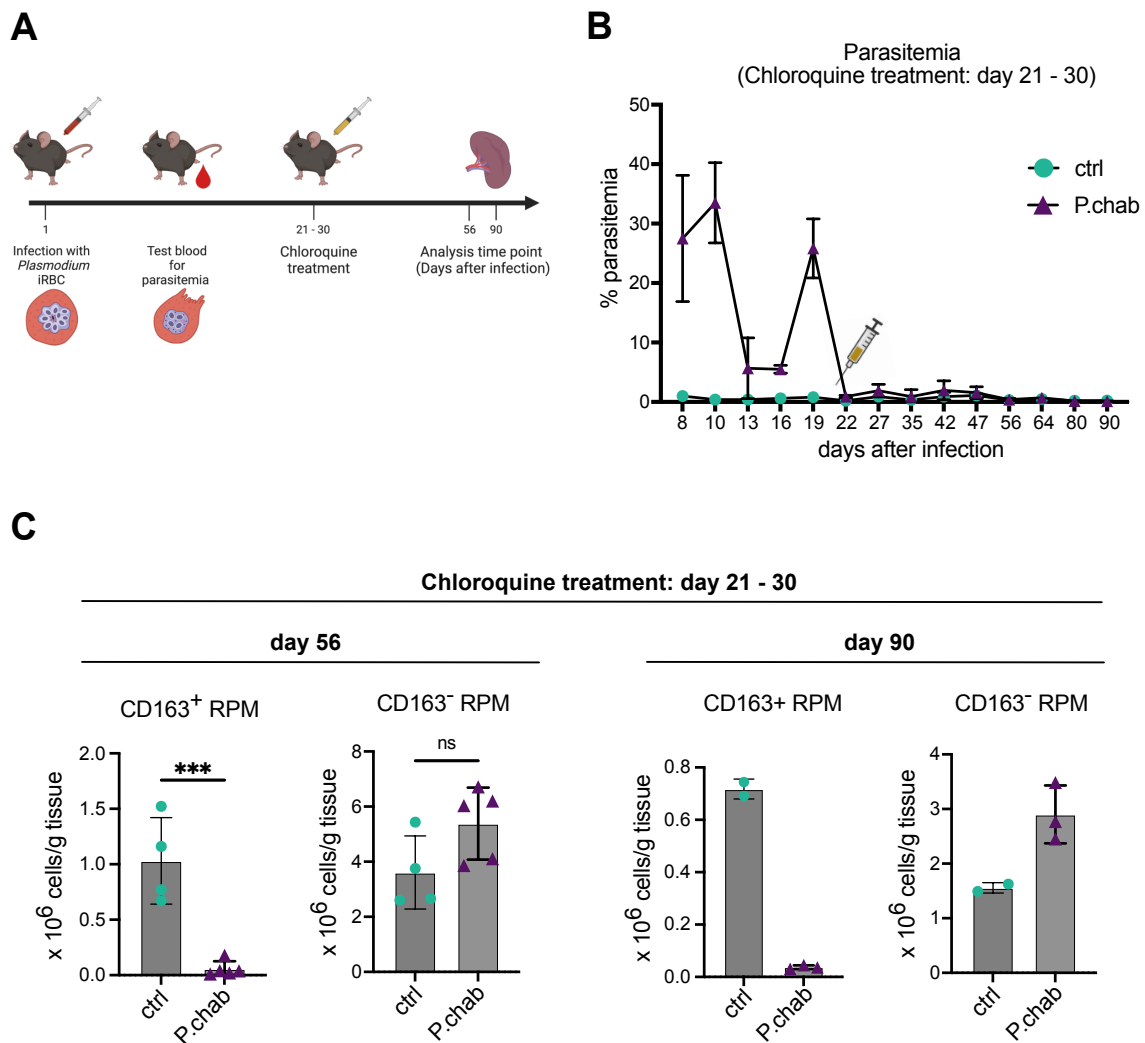


Figure 28: Parasite clearance with chloroquine does not rescue CD163 expression on RPM. (A) Experimental strategy: mice were infected with the standard dose of *P. chabaudi* and treated with chloroquine after day 21 to clear the parasites. Uninfected control mice that received a PBS injection were treated with the same dose of chloroquine. (B) Parasitemia was quantified via flow cytometry. Syringe indicates the start of the chloroquine treatment interval. (C) Splenic CD163⁺ and CD163⁻ red pulp macrophages (RPM) were quantified at day 56 (n = 4 - 5, two independent experiments, statistics: p-values obtained

using unpaired parametric t test, *** $p < 0.001$) and day 90 ($n = 2 - 3$, one experiment) after the infection.

3.2.4 CD163⁺ RPM dynamics in a viral infection model

Since it was shown in this study that blood-borne infection with malaria parasites caused a loss of CD163 expression in the splenic RPM population, the dynamics of CD163 expression on RPM was investigated in the context of other infection models.

A widely used viral infection model is infection with lymphocytic choriomeningitis virus (LCMV) (Rebejac et al, 2022). Here, mice were infected with the Armstrong species of LCMV, which causes an acute infection that is cleared within one week. CD163⁺ RPM were quantified one week, six weeks, and 20 weeks after the infection. Within the first week, the population of CD163 expressing RPM was reduced, but not depleted and the population did not recover 20 weeks after the infection (Figure 29, infections done by Takahiro Asatsuma, Dr. Yannick Alexandre, Dr. Thomas Burn who provided spleen tissue to perform flow cytometry analysis). Thus, infection with LCMV caused a reduction of CD163⁺ RPM, but not a complete depletion. On the other hand, CD163⁻ RPM were not affected by LCMV infection. Although a higher variability in the numbers of CD163⁻ RPM was detected one week after the infection, no significant changes were observed for CD163⁻ RPM between one and 20 weeks after LCMV infection (Figure 29).

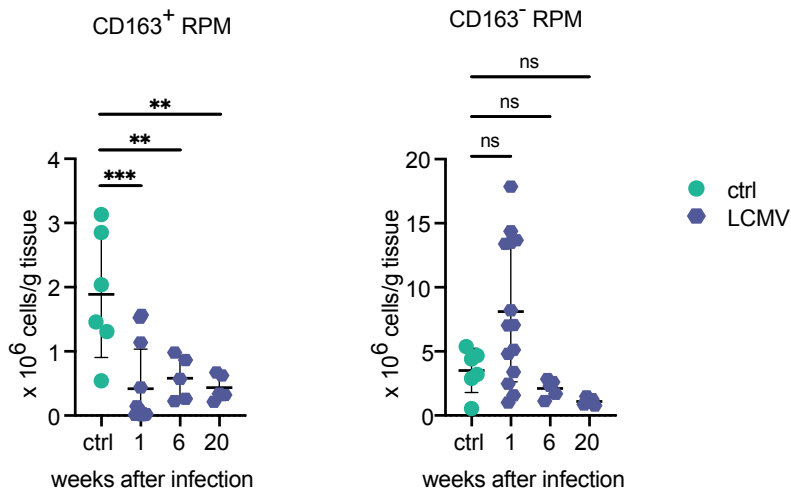


Figure 29: Viral infections cause a reduction, but not loss of splenic CD163⁺ red pulp macrophages. Mice were infected with acute lymphocytic choriomeningitis virus (LCMV). Between one and 20 weeks after the infection, splenic CD163⁺ and CD163⁻ RPM were quantified via flow cytometry (n = 5 - 6; statistics: p-values obtained using one-way ANOVA for multiple group comparison, **p < 0.01, ***p < 0.001).

3.2.5 Ontogeny of splenic macrophages in malaria

Since it was shown in this study that infection induces a reduction or a complete loss of CD163 expressing RPM, a detailed analysis of their developmental origin could explain why this population does not recover.

First, the previously introduced *Cxcr4*^{CreERT2}; *Rosa26*^{LSL-tdTomato} model was used to determine the fate of HSC-derived cells in the malaria model (Figure 30). After administration of tamoxifen to induce the expression of the fluorescent reporter in the HSC lineage, mice were infected with *P. chabaudi* to induce blood-stage malaria and analyzed 14, 35, 56, and 90 days after infection. On all analyzed time points after infection, Ly6C⁺ circulating monocytes in the blood were assessed for labeling with the fluorescent reporter tdTomato. Since circulating monocytes originate from HSC-derived progenitors, this was indicative of the labeling efficiency of the model. More than 80 % of the circulating monocytes expressed

tdTomato and were therefore labelled, as expected (Werner et al, 2020). The labeling of monocytes was similarly high in control and *P. chabaudi* infected mice (Figure 30). Comparing the labeling of RPM in the spleen between steady-state controls and *P. chabaudi* infected mice, it became evident, that the infection had a severe impact on the survival of resident macrophages, which led to a change in the ratio of EMP- to HSC-derived cells. Whilst amongst both CD163⁺ RPM and CD163⁻ RPM, only a minor percentage expressed tdTomato in steady-state conditions, indicative of HSC-derived ontogeny. During malaria infection, the labeling of CD163⁻ RPM with tdTomato reached almost 80 %, which was very close to the level of labeling of HSC-derived circulating monocytes in the blood (Figure 30). CD163⁺ RPM were depleted upon malaria infection; thus, only controls were visualized in the plot. Here however, it was observed in the steady-state control of both RPM populations, that the percentage of tdTomato⁺, thus HSC-derived cells, is not consistent, but dynamic and increased as the mice aged.

Mouse model:

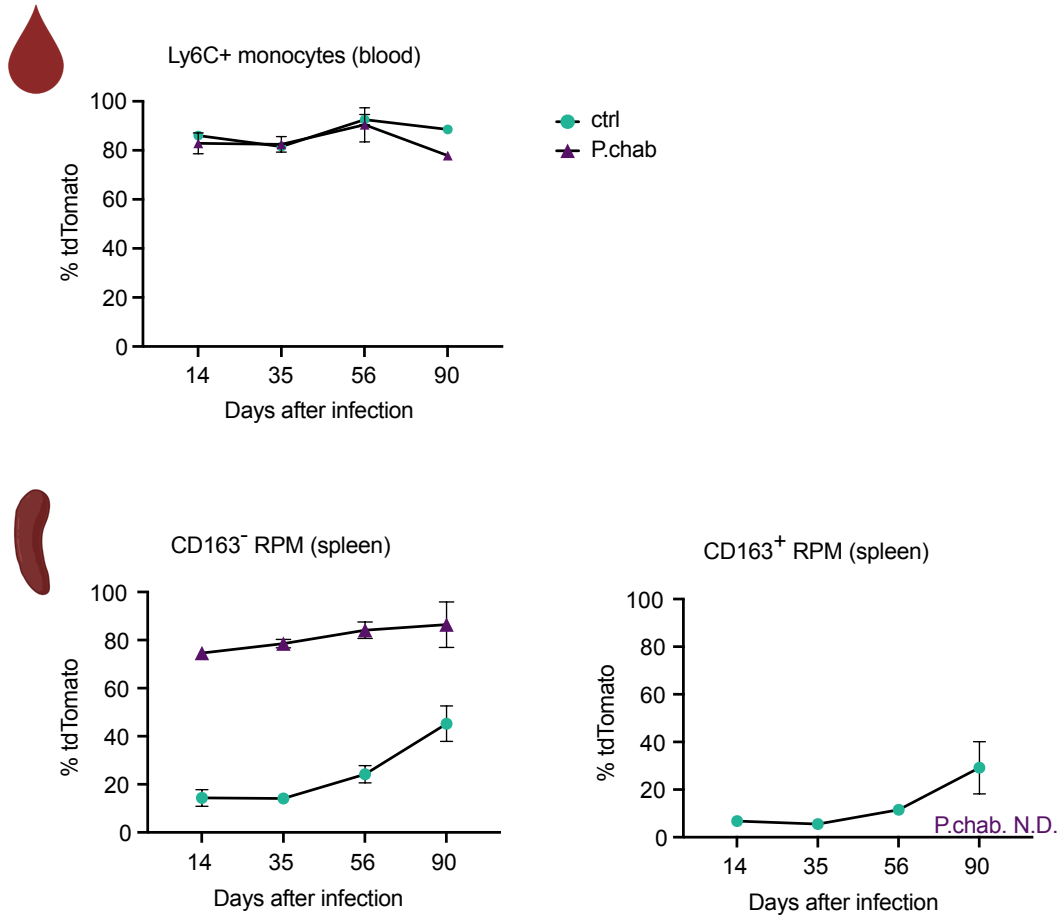


Figure 30: Quantification of HSC-derived circulating monocytes and splenic macrophages in malaria. The *Cxcr4^{CreERT2}; Rosa26^{LSL-tdTomato}* mouse model was used. Two months old mice were injected i.p. with Tamoxifen for five consecutive days to induce Cre-activity. One month later, the mice were injected with PBS (ctrl) or *P. chabaudi* (P.chab) to initiate blood-stage malaria. Between day 14 and day 90 after the infection, Ly6C⁺ monocytes in the blood as well as CD163⁺ and CD163⁻ red pulp macrophages (RPM) in the spleen were quantified for the expression of the fluorescent reporter tdTomato, indicative for an HSC-derived ontogeny (day 14: n = 3, day 35: n = 2, day 56: n = 4, day 90: n = 3).

To conclusively describe macrophage ontogeny in the blood-borne infection of *P. chabaudi* malaria, the novel double-fatemapper (DFM) mouse model (*Tnfrsf11a^{Cre}; Rosa26^{LSL-YFP}; Ms4a3^{FipO}; Rosa26^{LFL-tdTomato}*) (as introduced in

chapter: 1.3.2.2 The double-fatemapper) was used, which labels HSC-derived cells with tdTomato and EMP-derived cells with YFP (Figure 31). The tdTomato-positive, HSC-derived monocytes that enter the tissue and differentiate into long-lived macrophages acquire YFP labeling. In contrast, EMP-derived cells are YFP-positive only.

In the steady-state (PBS-injected control mice), the CD163⁺ RPM population was mostly derived from EMPs, indicated by the high labeling percentage of YFP⁺ cells (Figure 31). More than 80 % of splenic CD163⁺ were EMP-derived, with an age-related decrease throughout the three months experimental time course (up to day 90 after PBS administration). The contribution of HSC-derived, YFP and tdTomato double-positive cells, increased to above 20 % during the time course, but no tdTomato⁺ only CD163⁺ RPM were detected. A similar trend was observed in the splenic CD163⁻ RPM population, but the overall percentage of YFP⁺ cells was lower. In control mice, approximately 70 % of CD163⁻ RPM were EMP-derived. This percentage decreased to 60 % throughout the three-month experimental time course, while the contribution of HSC-derived, double-positive cells increased to approximately 40 %. Major changes in the dynamics of splenic RPM were observed upon the infection with *Plasmodium* parasites. Before the first major peak in parasitemia (between day 10 - 14, see Figure 23, B), a severe decrease in the percentage of EMP-derived splenic CD163⁻ RPM was seen. The contribution of EMP-derived, YFP⁺ cells to the splenic CD163⁻ RPM compartment decreased to 20 % within the first two weeks after infection and remained at that level. Simultaneously, a major influx of HSC-derived cells was observed. After 35 days of *P. chabaudi* infection, more than 80 % of the splenic CD163⁻ RPM were double-positive for YFP and tdTomato, indicating a strong influx of HSC-derived cells and differentiation of these cells into tissue macrophages upon infection.

Mouse model:

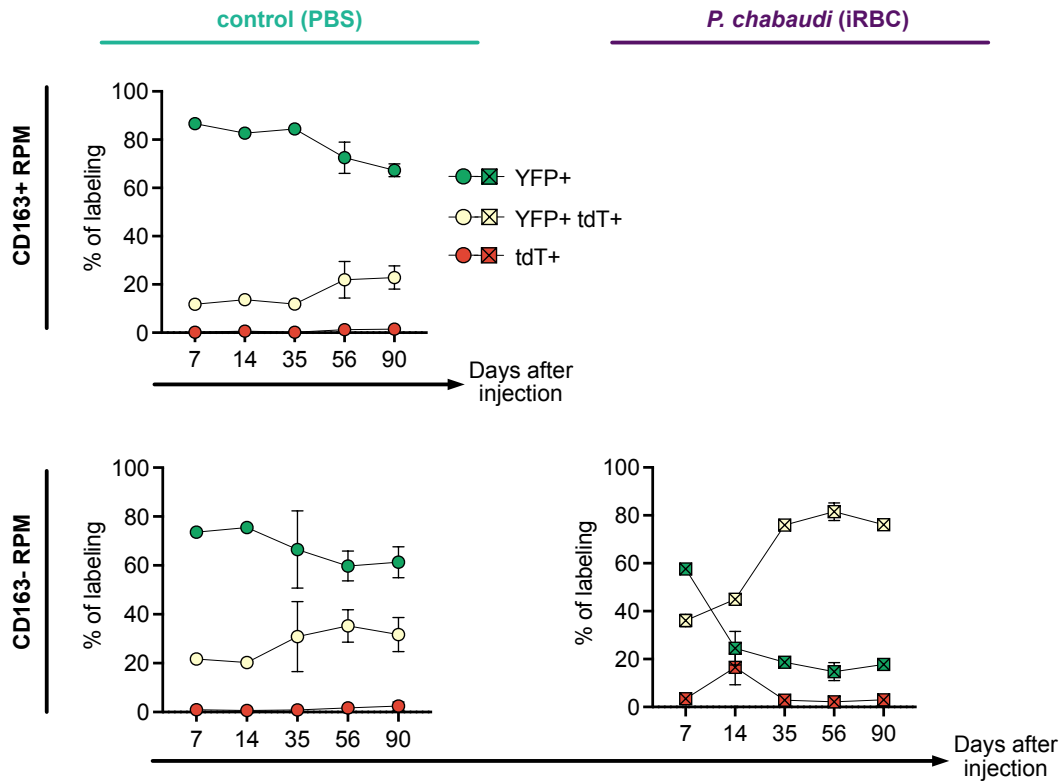


Figure 31: Quantification of HSC-derived and EMP-derived splenic red pulp macrophages in malaria. The *Tnfrsf11a^{Cre}; Rosa26^{LSL-YFP}; Ms4a3^{FlpO}; Rosa26^{LFL-tdTomato}* fate mapping model labels HSC-derived cells with tdTomato (red) and EMP-derived cells with YFP (green). The tdTomato⁺ HSC-derived cells acquire YFP labeling, when differentiating into long-lived tissue macrophages (yellow). Mice were injected with PBS as control or *P. chabaudi* infected RBCs to develop malaria. The ontogeny of splenic CD163⁺ and CD163⁻ red pulp macrophages (RPM) was described between day 7 and day 90 after the infection. Round data points for controls; squares for malaria. (day 7: n = 2, day 14: n = 3, day 35: n = 3, day 56: n = 5, day 90: n = 4)

With this model, other splenic macrophage populations were also assessed (Figure 32). Splenic MMM were mostly YFP⁺ (80 %) in the steady-state, with little contribution of HSC-derived (double-positive) cells and this was maintained

throughout the time course of the experiments. Upon infection with *P. chabaudi*, a decrease in the EMP-derived population was observed, with a simultaneous increase of HSC-derived (double-positive) cells. After 90 days of *P. chabaudi* infection, approximately 70 % of MMM were double-positive for YFP and tdTomato, indicating a strong turnover and influx of HSC-derived cells.

MZM, which populate the splenic marginal zone in close proximity to MMM, showed a different pattern in terms of their developmental origin. A major proportion of MZM was only tdTomato positive in controls, indicating a continuous influx and replacement by short-lived HSC-derived cells. Within the three-month experimental time course, more of these cells became tdTomato and YFP double-positive indicating differentiation into long-lived HSC-derived macrophages. The contribution of EMP-derived cells was small, with less than 10 % of MZM being YFP⁺ only. Upon the infection with *Plasmodium* parasites, no major changes in the developmental origin of the MZM were detected, but the percentage of tdTomato⁺ only, short-lived HSC-derived cells, remained elevated above 50 % throughout the experimental time course, indicating a constant influx of HSC-derived cells.

Splenic WPM in the steady-state (PBS-injected controls) were mostly HSC-derived. The proportion of YFP and tdTomato double-positive, long-lived macrophages increased over time and reached a peak of 60 %. The influx of short-lived tdTomato⁺ HSC-derived cells decreased from 40 % to 20 % within the experimental time course of 90 days. In control mice, between 20 % to 40 % of WPM were only YFP⁺, thus EMP-derived. When the mice were infected with *P. chabaudi*, the percentage of EMP-derived cells decreased below 20 % and more than 60 % of splenic WPM were YFP and tdTomato positive and thus long-lived HSC-derived macrophages. Long-term the percentage of only YFP⁺ WPM showed a trend of recovery and has increased to above 20 % at day 90 after the infection, which is more similar to the contribution of EMP-derived cells in the steady-state controls.

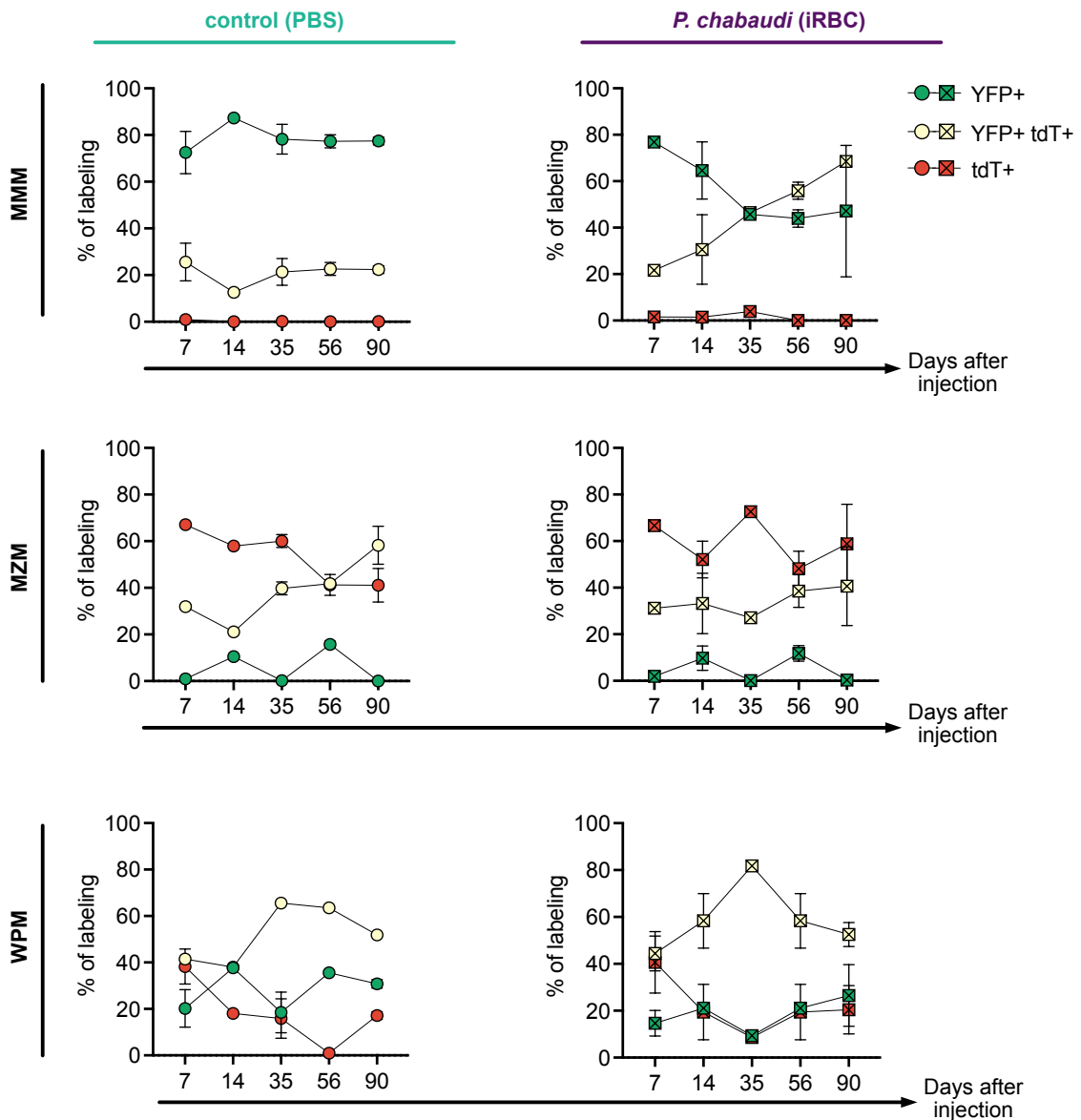


Figure 32: Quantification of HSC-derived and EMP-derived splenic macrophages in malaria. The *Tnfrsf11a*^{Cre}; *Rosa26*^{LSL-YFP}; *Ms4a3*^{FlpO}; *Rosa26*^{LFL-tdTomato} fate mapping model labels HSC-derived cells with tdTomato (red) and EMP-derived cells with YFP (green). The tdTomato⁺ HSC-derived cells acquire YFP labeling, when differentiating into long-lived tissue macrophages (yellow). Control mice were injected with PBS and infected mice with *P. chabaudi* infected RBCs. The ontogeny of splenic marginal metallophilic macrophages (MMM), marginal zone macrophages (MZM) and white pulp macrophages (WPM) was quantified between day 7 and day 90 after the infection. Round data points represent controls; squares represent infected mice. (day 7: n = 2, day 14: n = 2, day 35: n = 1, day 56: n = 3, day 90: n = 3)

Taken together these data clearly support the concept of heterogeneity amongst splenic macrophages with respect to their developmental origin, which can have major impacts on their physiological function and response to challenges.

3.2.6 Characterization of the transcriptional profile of splenic macrophages and changes upon a *P. chabaudi* infection via single-cell RNA-sequencing

This study has described a major impact on the cellular composition of the spleen and the ontogeny of splenic macrophages as a result of an infection with *P. chabaudi* blood-stage malaria. To further characterize this, the impact of a *P. chabaudi* infection on the transcriptome of cells in the spleen was studied via single-cell RNA-sequencing, to find out how the transcription profile changes in splenic macrophages and investigate how this might impact signaling and interaction pathways. Therefore, the previously described double-fatemapper mice (*Tnfrsf11a^{Cre}*; *Rosa26^{LSL-YFP}*; *Ms4a3^{FlpO}*; *Rosa26^{FL-tdTomato}*) were injected with either PBS as a control or with infected RBC to induce blood-stage malaria. Spleens from two mice per condition were collected at day 90 after the infection and sorted for CD64⁺ cells, to identify the macrophages (Figure 33, A, all data were analyzed by Dr. Nelli Blank-Stein).

After the quality control (cut-offs for number of genes, number of transcripts, number of mitochondrial genes) a UMAP was generated and the clusters were assigned a cellular identity (Figure 33, B). Although the cells were sorted for CD64⁺ macrophages, distinct clusters of B cells and T cells were visible. The macrophage cluster was selected and subclustered (Figure 33, B).

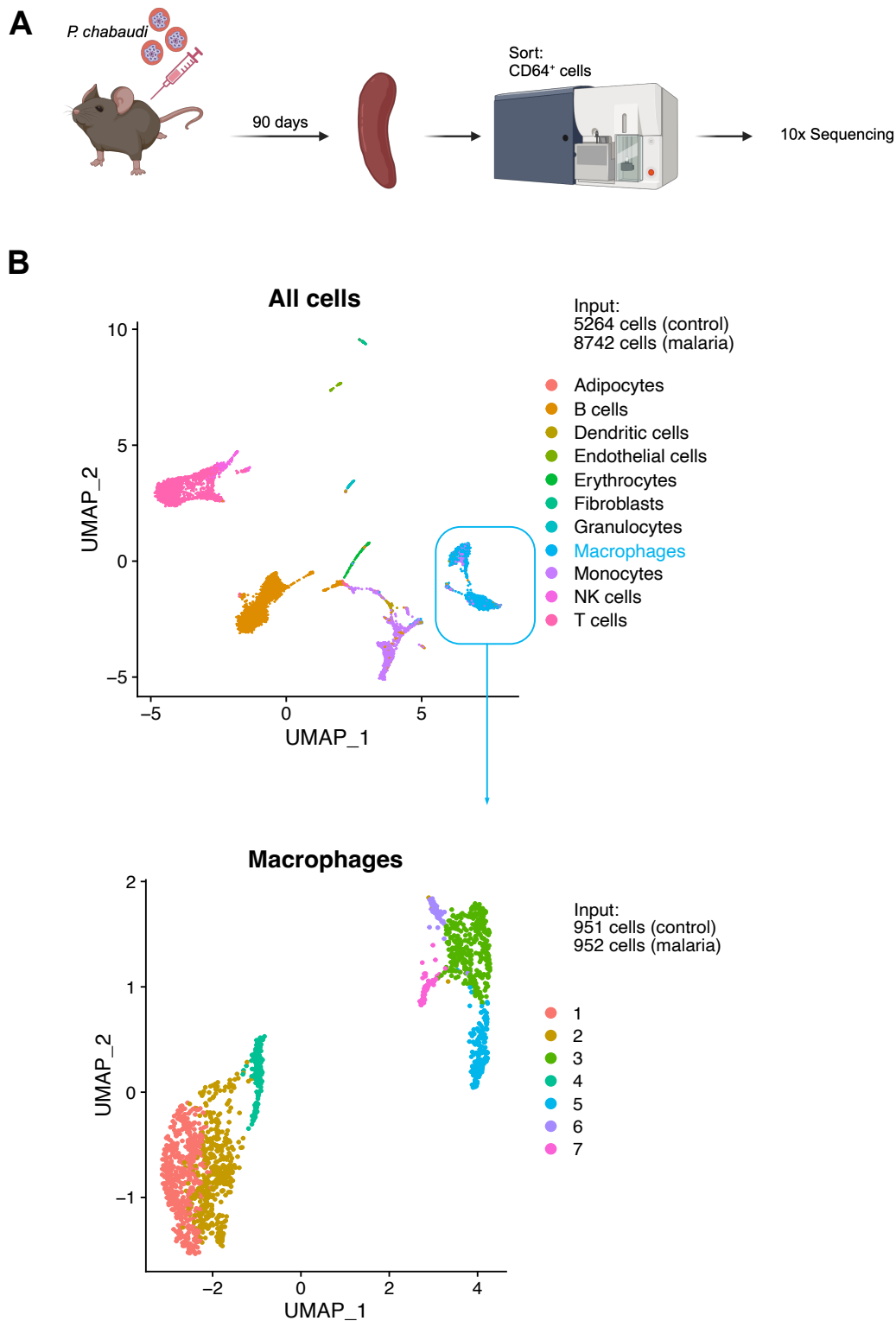


Figure 33: UMAP-clustering of CD64⁺ sorted cells. (A) Experimental strategy: *Tnfrsf11a*^{Cre}; *Rosa26*^{LSL-YFP}; *Ms4a3*^{FlpO} mice were administered PBS as control or infected with *P. chabaudi* to induce blood-stage malaria. After 90 days, spleens were collected and CD64⁺ cells were separated via cell sorting. The CD64⁺ fraction was subjected to a single-cell RNA-sequencing procedure (10x

Genomics). (B) Sorted CD64⁺ cells were aligned to a reference genome and after quality control, a UMAP was calculated from two control and two *P. chabaudi* infected mice (cellular input: in total 5264 cells of control samples and 8742 cells of *P. chabaudi* infected samples), resulting in 11 distinctive clusters. The clusters were assigned to their cellular identity (adipocytes, B cells, dendritic cells, endothelial cells, erythrocytes, fibroblasts, granulocytes, macrophages, monocytes, NK cells, T cells). The macrophage cluster was selected for subclustering (cellular input: in total 951 cells of control samples and 952 cells of *P. chabaudi* infected samples), resulting in 7 distinctive macrophage clusters.

According to chapter: 3.1 Identification and ontogeny of splenic macrophage populations), the relevant markers to discriminate splenic macrophages were identified within the macrophage populations and the expression profiles of those characteristic genes were visualized on a UMAP. Feature plots were separated to show cells from the controls and cells from the malaria samples. *Adgre1* is the gene locus encoding the characteristic macrophage antigen, F4/80. It is highly expressed by splenic RPM, but not by the other splenic macrophage populations (Borges Da Silva et al, 2015). Three out of the seven cell clusters showed high *Adgre1* expression (Figure 34). Examination of CD163 expression showed that it was particularly high in cluster 1. Within this cluster, the expression intensity of CD163 was not evenly distributed. The region of cluster 1, where CD163 expression was highest in the control, was absent in the malaria sample (Figure 34).

The two macrophage populations that populate the splenic marginal zone are similar but can be discriminated based on their expression of *Siglec1* (CD169), which is very characteristic for splenic MMM and expression of *CD209b* (SIGNR1), which is specifically found on MZM (Borges Da Silva et al, 2015). Cluster 3 showed high expression of *Siglec1* (Figure 34). A distinct region of that cluster disappeared in the malaria plot. While *Siglec1* expression was partially spreading to the neighboring cluster, *CD209b* expression was found specifically in cluster 6.

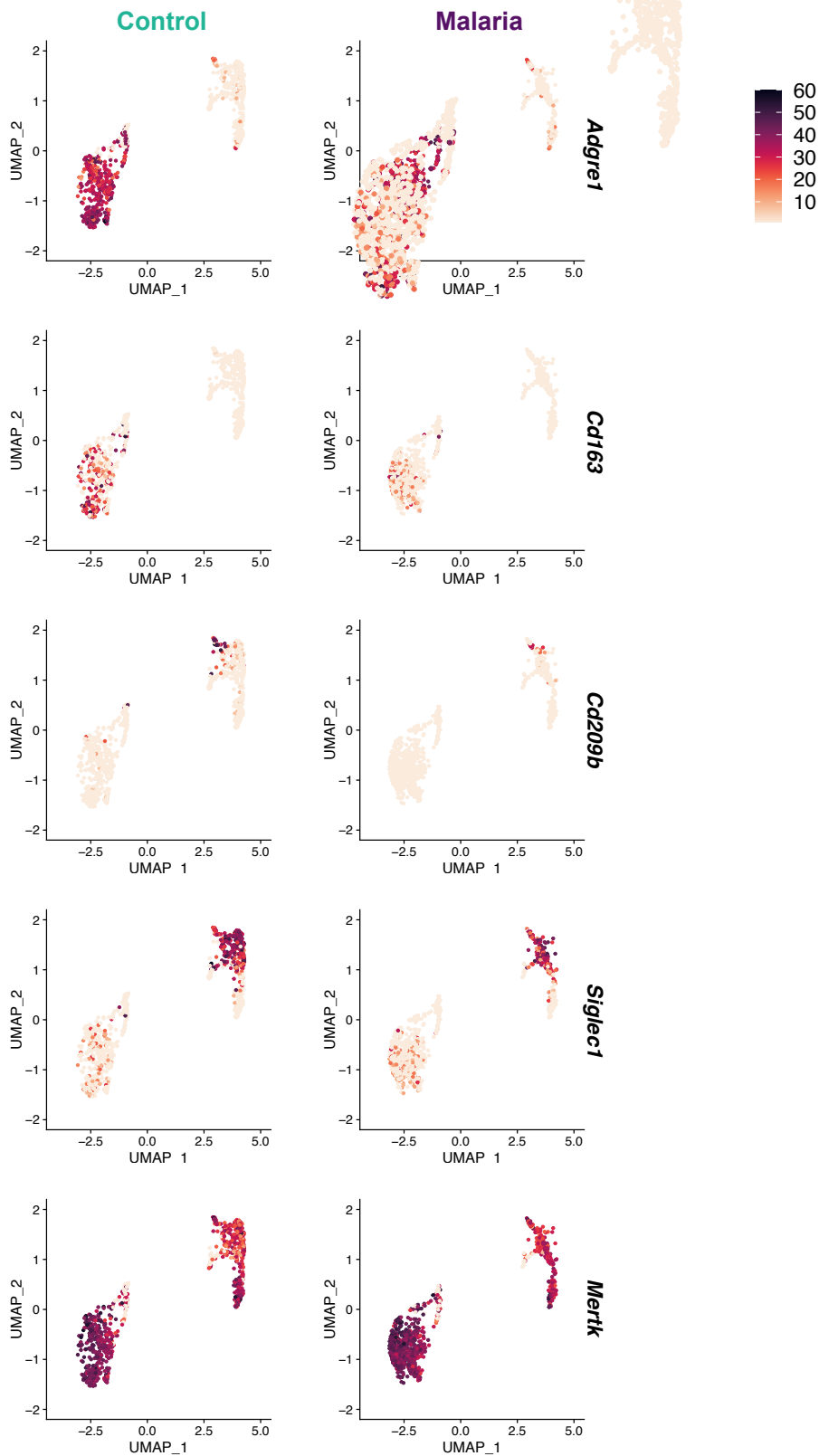


Figure 34: Feature plots showing expression of relevant macrophage genes for splenic macrophages. After 90 days, CD64⁺ cells were isolated from the spleen of uninfected (control) or *P. chabaudi* infected (malaria) mice for sorting and processed for single-cell RNA-sequencing. Data were aligned and a UMAP

generated. The macrophage cluster was selected and subclustered to discriminate different splenic macrophage subsets. Feature plots show expression profiles of relevant genes expressed in red pulp, marginal zone and white pulp macrophage, comparing between control and malaria: *Adgre1*, *Cd163*, *Siglec1*, *Cd209b* and *MerTK*.

Mertk is a receptor with important roles in normal macrophage physiology and is expressed by most macrophages (Anwar et al, 2009). Thus, *Mertk* expression was detected in all macrophage clusters. In the study presented here, it was used to discriminate WPM. High MerTK expression by splenic WPM has been described by others (A-Gonzalez & Castrillo, 2018). In this study, particularly the expression of *Mertk* in cluster 5 was relevant to identify WPM.

Feature plots of relevant marker genes for each splenic macrophage subpopulation allowed an estimation of the location of each subset within the UMAP. To specifically assign each cluster to a specific splenic macrophage population, the top 20 expressed genes of each cluster were evaluated. The most relevant genes amongst the top 20 genes, that were used to assign the UMAP clusters were visualized in a dot-plot (Figure 35, A).

Two clusters showed high *Adgre1* expression and were assigned as RPM. One of those clusters showed particularly high expression of *Cd163*, along with other macrophage genes (*Adam22*, *Pparg*, *Mrc1*) and was thus assigned as CD163⁺ RPM (Figure 35, B). In the second *Adgre1*-high cluster, *Spic* was specifically highly expressed, which is a key transcription factor expressed by cell that have committed to differentiate into red pulp macrophages (Kurotaki et al, 2015; Haldar et al, 2014). This cluster was assigned as CD163⁻ RPM (Figure 35, B). Further, high levels of expression of *Mertk* and *Hmox1* was detected in this cluster, characteristic for the highly phagocytic RPM. Another cluster that is closely related to the CD163⁻ RPM, was characterized by high expression of *Hmox1*.

While the three previously described populations cluster in close proximity, the other four clusters were quite distinct. *Timd4* expression was predominantly found

in two of the remaining clusters, which is characteristic for both splenic macrophage populations in the marginal zone. The additional expression of *Siglec1* allowed for the assignment of one of these two clusters as MMM (Figure 35, B). High expression of *CD209b* and *Marco* assigned the other cluster as MZM (Figure 35, B).

The expression of matrix metalloprotease genes (*Mmp14*) and complement genes (*C3*), together with the detection of *Cd4* genes allowed for the assignment of one macrophage cluster as WPM (Figure 35, B), which are located in the white pulp to phagocytose apoptotic B cells and T cells. The *Cd63* expressing cluster was assigned as monocytes (Figure 35, B).

In contrast to the flow cytometry data (see chapter: 3.2.1 Loss of splenic CD163⁺ RPM upon *P. chabaudi* infection and chapter 3.2.2 Loss of splenic CD163⁺ RPM upon malaria infection), the sequencing data showed that the cluster that was assigned as CD163⁺ RPM did not disappear after a malaria infection. However, there was a shift detected in the CD163⁺ RPM cluster upon the infection (see circles, Figure 35, B). While a high abundance of cells was detected in the lower corner of that cluster in control samples (where the highest CD163 expression was detected, see Figure 34), the majority of cells shifted upwards within the CD163⁺ RPM cluster upon infection with *P. chabaudi* and the dense area of CD163 expression that was present in the controls was not detected in the malaria samples.

To investigate the change in the CD163⁺ RPM cluster, the differentially regulated genes were compared between cells from the controls and cells from the malaria infected samples, specifically within the CD163⁺ RPM and the CD163⁻ RPM clusters respectively (Figure 36). The *Cd163* gene was found to be differentially expressed between the control and the malaria samples within the cluster designated as 'CD163⁺ RPM'. Next to *Cd163*, the metalloprotease gene *Adam22* was expressed at a higher level in cells from the control samples when compared to cells from the malaria samples.

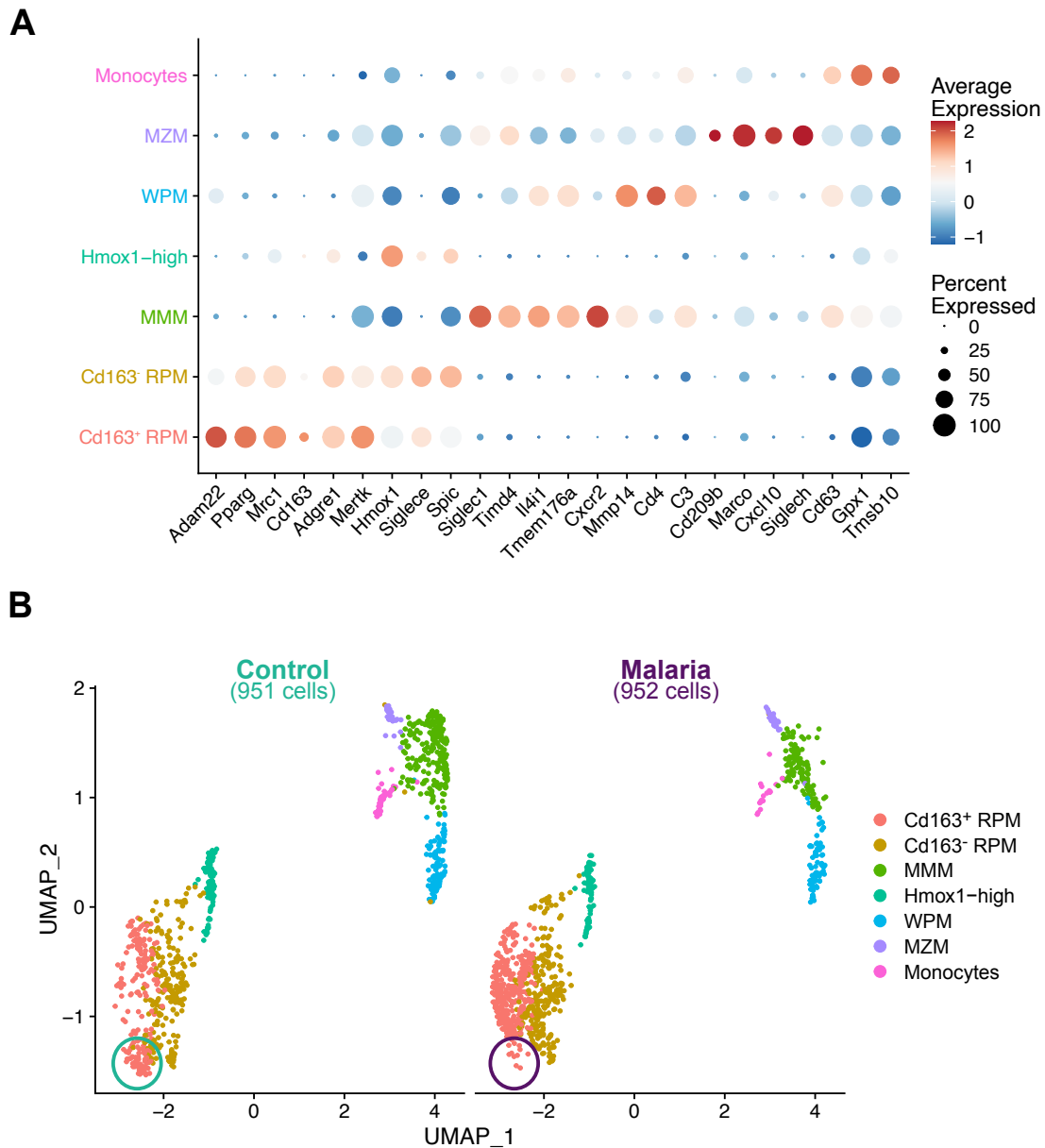


Figure 35: Assignment of UMAP clusters to splenic macrophage populations. Mice were injected with PBS (control) or infected with *P. chabaudi* (malaria). Cells were isolated from the spleen at day 90. CD64⁺ cells were sorted and processed for single-cell RNA-sequencing. Data were aligned and a UMAP generated. Of all cells, specifically the macrophage cluster was selected and subclustered to discriminate different splenic macrophage subsets. (A) Amongst the 20 most expressed genes of each cluster, the most characteristic genes were evaluated to assign the different splenic macrophage subtypes. (B) UMAP with annotation of splenic macrophages (CD163⁺ red pulp macrophages (RPM), CD163⁻ RPM, marginal metallophilic macrophages (MMM), Hmox1-high macrophages (Hmox1-high), white pulp macrophages (WPM), marginal zone macrophages (MZM) and Monocytes). Cellular input: in total 951 cells of control

samples and 952 cells of *P. chabaudi* infected samples. Circles indicate the area of highest CD163 expression.

In contrast, genes encoding proteins of the complement system (*C4b*), genes that are related to metabolic processes (*Akt3*) and genes that are involved in hematopoiesis (*Runx1*) and monocyte differentiation (*Cd74* as part of the MHC-complex) were increased in the CD163⁺ RPM cluster from the malaria samples (Figure 36).

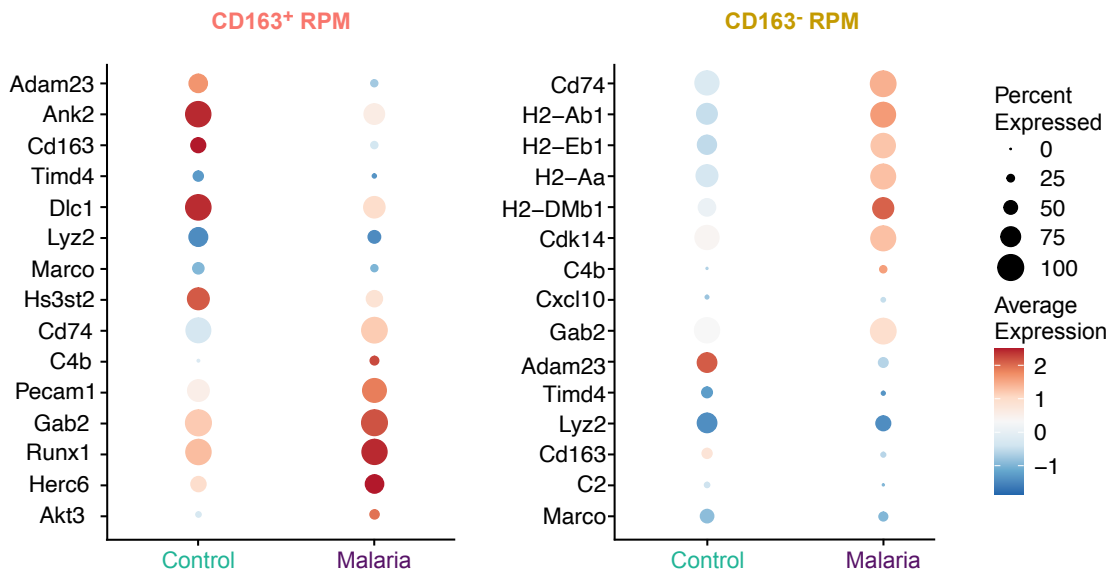


Figure 36: Differentially expressed genes in splenic red pulp macrophages populations upon malaria infection. Mice were injected with PBS (control) or infected with *P. chabaudi* (malaria). Cells were isolated from the spleen at day 90. CD64⁺ cells were sorted and processed for single-cell RNA-sequencing. Data were aligned and a UMAP generated. Of all cells, specifically the macrophage cluster was selected and subclustered to discriminate different splenic macrophage subsets. Of the CD163⁺ RPM and the CD163⁻ RPM cluster, differentially expressed genes were analyzed, comparing control and malaria samples.

Within the CD163⁻ RPM cluster, a variety of *H2* genes that encode subunits of the MHC class II complex were upregulated in the malaria samples (Figure 36).

In addition to the comparison of differentially expressed genes between control and malaria samples, the gene ontology (GO) terms for each splenic macrophage subtype were determined. GO terms were assigned to each macrophage cluster, but not discriminated between control and malaria samples, since the same clusters emerged in both conditions. GO term analysis associates genes to their molecular and biological functions. A variety of signaling regulatory pathways were assigned to the CD163⁺ RPM, including Ras-signaling, regulation of GTPase-activity and negative regulation of protein phosphorylation (Figure 37). Amongst the splenic macrophage populations, the CD163⁻ RPM were associated with apoptotic cell clearance as well as antigen processing and presentation. CD163⁻ RPM negatively regulate the production of IL-6 and were further associated to cytokine response pathways, TLR signaling and T-cell activation (Figure 37). Pathways related to antigen presentation via MHC were associated with MMM in addition to pathways that positively regulate T-cell mediated cytotoxicity (Figure 37). MZM were involved in cellular interaction pathways and the regulation of cell adhesion (Figure 37). Pathways involved in lymphocyte differentiation and activation were associated to WPM (Figure 37). In the Hmox1-high cluster, genes related to intracellular transport and biosynthesis were enriched (Figure 37). Monocytes were associated to interferon responses and catabolic processes (Figure 37).

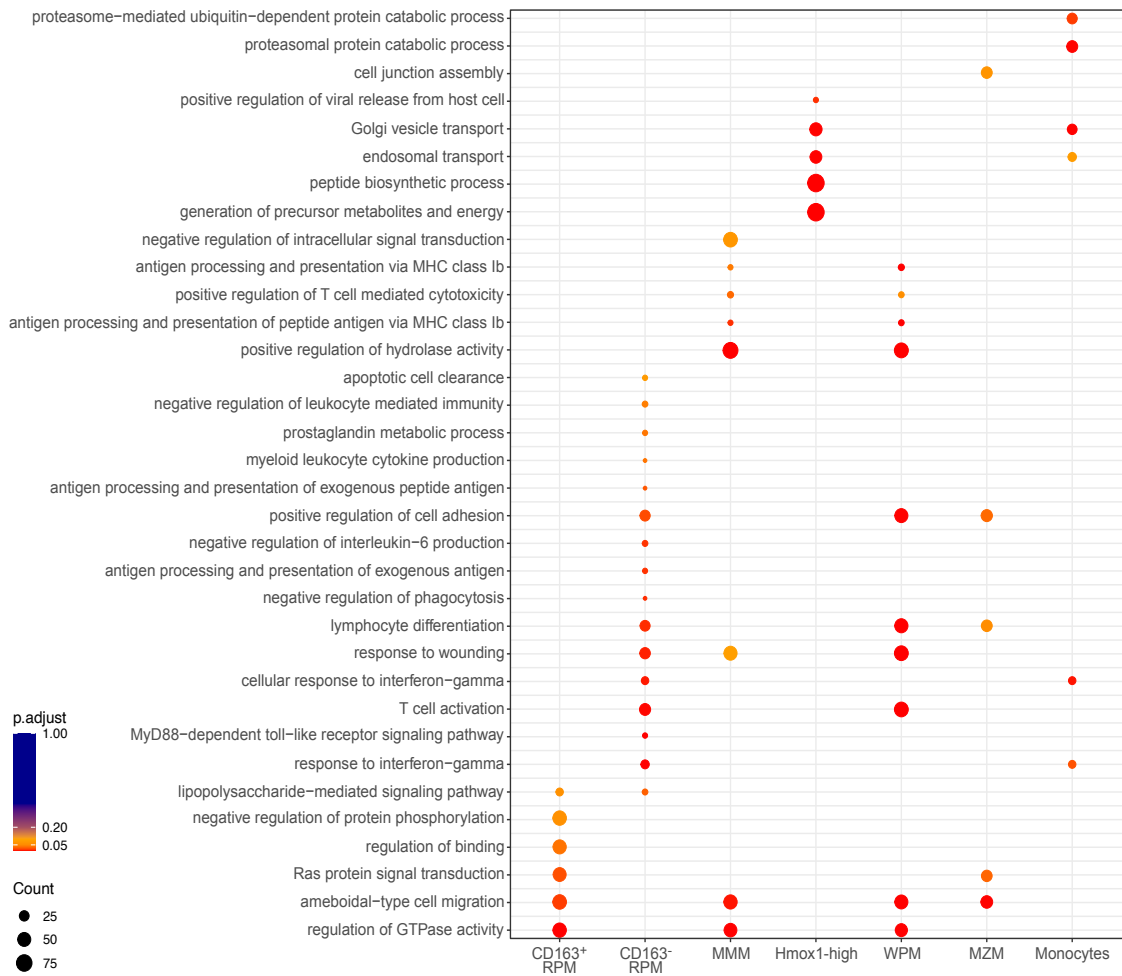


Figure 37: Gene ontology analysis of different splenic macrophages. Mice were injected with PBS (control) or infected with *P. chabaudi* (malaria). Cells were isolated from the spleen 90 days later. CD64⁺ cells were sorted and processed for single-cell RNA-sequencing. Data were aligned and a UMAP generated. The macrophage cluster was specifically selected and subclustered to discriminate seven different splenic macrophage subsets. Distinct gene ontology terms were assigned to each macrophage cluster (CD163⁺ red pulp macrophages (RPM), CD163⁻ RPM, marginal metallophilic macrophages (MMM), Hmox1-high macrophages, white pulp macrophages (WPM), marginal zone macrophages (MZM) and monocytes).

Since previous data in this study have shown that malaria infection has a severe impact on a subpopulation of splenic RPM, the *Adgre1*-positive RPM clusters were selected and further subclustered, which resulted in six distinctive clusters (Figure 38, A). Comparing the expression level of CD163 between control and

malaria samples in each cluster, showed first that CD163 was predominantly expressed in the control samples (Figure 38, B) and second that CD163 was expressed only in clusters 0, 1, 2 and 3 of the controls, but not in clusters 4 and 5 (Figure 38, B). Since the CD163-dependent heterogeneity of RPM was a central part of this study, it was next investigated how the CD163⁺ RPM population could be identified despite the loss of CD163 expression in malaria. Therefore, genes that were upregulated in the CD163-expressing clusters 0 - 3 were identified and selected for those that are not differentially regulated between control and malaria samples. A uniformly high expression in all CD163-expressing clusters in both control and malaria samples was detected for *Icam1* (Figure 38, C). The gene was not expressed in clusters 4 and 5, which were the CD163-negative clusters (Figure 38, C).

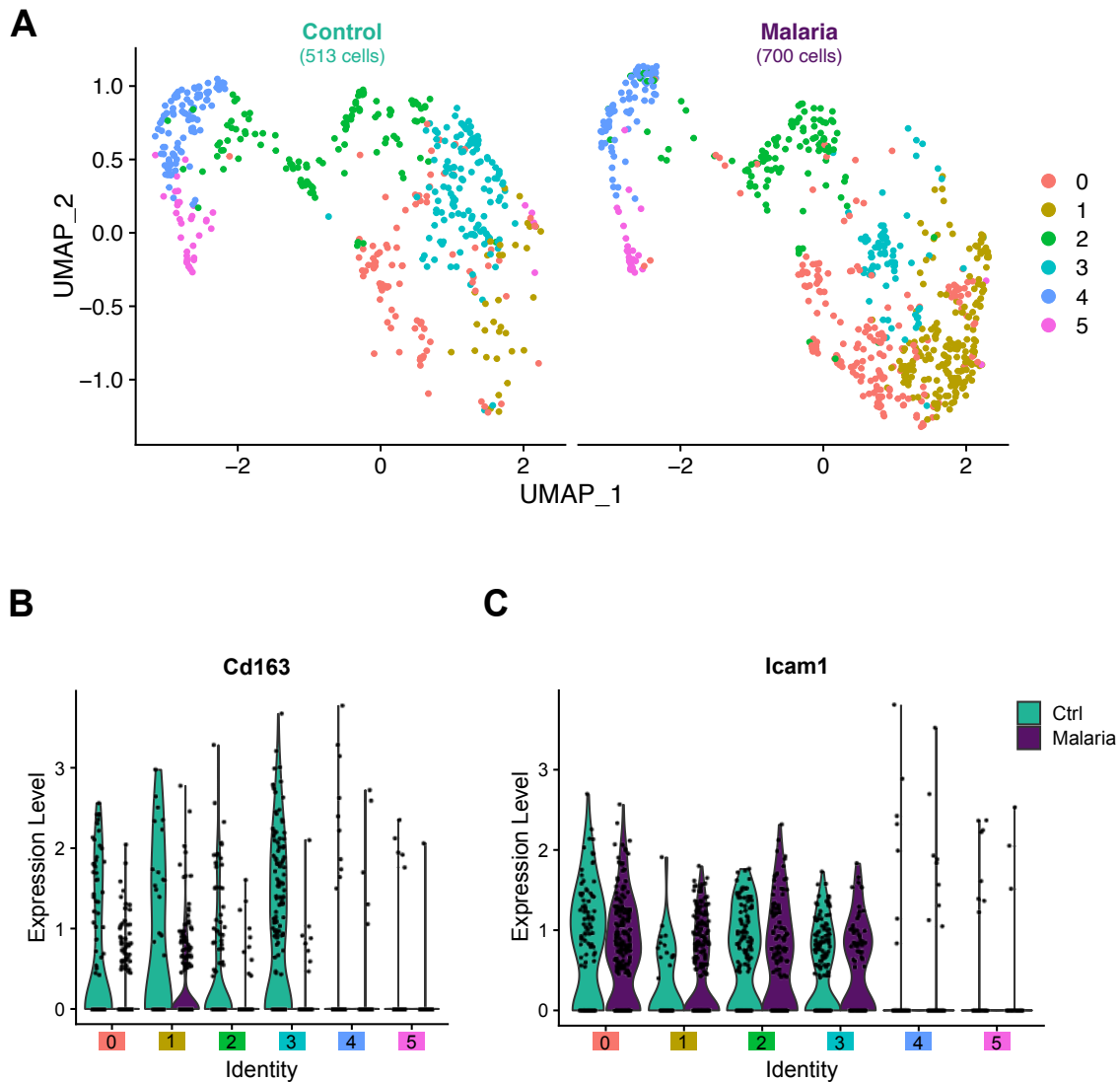


Figure 38: Subclustering of red pulp macrophages and comparison of differentially expressed genes. Mice were injected with PBS (control) or infected with *P. chabaudi* (malaria). Cells were isolated from the spleen at day 90. CD64⁺ cells were sorted and processed for single-cell RNA-sequencing. Data were aligned and a UMAP generated. The macrophage cluster was selected and subclustered to discriminate seven different splenic macrophage subsets. (A) The *Adgre1*-positive red pulp macrophage cluster was subjected to further subclustering (cellular input for RPM subclustering: 513 cells of control samples and 700 cells of *P. chabaudi* infected samples). (B) Expression of CD163 was compared between the control and the malaria samples in each cluster. (C) Within the CD163-expressing clusters, genes that are not differentially expressed between control and malaria conditions were identified. *Icam1* was conserved in all CD163-expressing clusters, in both (control and malaria) conditions.

3.3 Genetic depletion of CD163 receptor or macrophage populations in the splenic marginal zone and respective impact on malaria progression

A strategy to study the functional impact of specific macrophage populations or their signaling pathways, is the use of transgenic mouse models. These models allow for the depletion of specific cell populations or deletion of specific genes and, therefore, facilitate studies of the disease progression in the absence of a specific cell population or protein, allowing for conclusions to be drawn about the functional impact of these populations on parasite clearance and malaria disease progression.

3.3.1 Genetic depletion of the CD163 receptor and relevance for the maintenance and recovery of the splenic architecture in malaria

In this project, novel heterogeneity amongst splenic RPM was discovered and in chapter 3.2 (The dynamics of splenic myeloid cells during blood-stage malaria), it was shown that CD163 expression was lost on the CD163⁺ RPM subset upon malaria infection.

In order to understand the functional relevance of CD163 expression on RPM in the progression of malaria disease, a conditional depletion model for the CD163 receptor could be generated. A conditional depletion model for CD163 is not available to date. This model would facilitate the depletion of CD163 expression specifically in *Tnfrsf11a*-expressing cells (breeding with *Tnfrsf11a*^{Cre/+}). With the CRISPR/Cas9 technique for gene editing (Redman et al, 2016), two loxP-sites sited could be introduced into the CD163 wildtype allele. To this end, guide RNAs were designed to target intron 1 and exon 17 for the introduction of loxP-sites (detailed description see methods chapter: 2.2.1.3 Generation of a CD163-depletion mouse model). A recombination between the loxP-sites in intron 1 and

exon 17 would deplete a large proportion of the coding sequence of the CD163 gene. However, the generation of this model was not possible within the time-frame of this project.

Instead, a global genetic knockout model for the CD163 receptor was used and studied in the context of blood-stage malaria. The CD163-knockout mouse line was generated by introducing the flox-sites described above for the generation of the conditional knockout model. The large fragment between the two CRISPR target sites in intron 1 and exon 17 was deleted, resulting in the knockout of the CD163 allele. Mice with a homozygous deletion on both alleles were used in this study and termed CD163KO.

CD163KO mice were infected with *P. chabaudi* to induce blood-stage malaria or injected with PBS as controls. Fourteen days after infection, the spleen was collected and processed for immunofluorescent imaging with a confocal microscope (Figure 39, A). Parasitemia in CD163KO mice was monitored during the experimental time course of 14 days and compared to wildtype mice that were infected with *P. chabaudi* (Figure 39, B). Preliminary data suggest that the absence of CD163 did not have a major impact on parasitemia. In both wildtype and CD163KO mice, the parasitemia was above 20 %. However, the peak of parasitemia was slightly shifted and delayed in the CD163KO model.

The spleens of uninfected and *P. chabaudi* infected CD163KO mice were fixed and embedded in paraffin for staining with hematoxylin and eosin. In CD163KO mice that were injected with PBS (control), the splenic red pulp and white pulp were clearly separated and appeared similar to the spleen tissue of uninfected wildtype mice (Figure 39, C). Hematoxylin binds to nucleic acids and especially the lymphocyte rich white pulp was densely stained. Characteristic circular patches that describe the splenic white pulp were visualized. A total loss of spleen integrity was observed at day 14 after *P. chabaudi* infection in CD163KO mice (Figure 39, C) with the splenic white pulp and red pulp areas becoming totally intermingled.

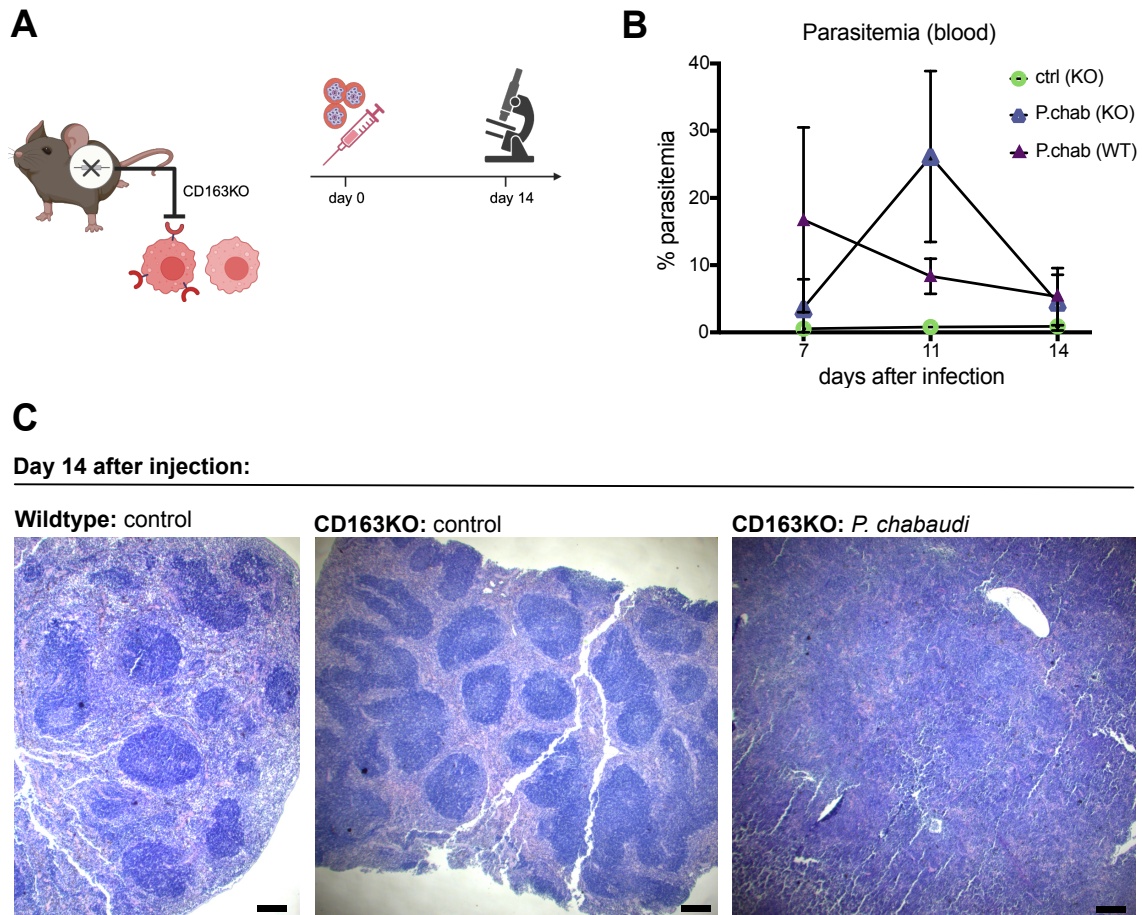


Figure 39: Impact of the absence of the CD163 receptor on splenic architecture and parasitemia in malaria. (A) Experimental strategy: CD163KO mice were infected with blood-stage malaria (*P. chabaudi*) and the spleen tissue collected at day 14 after the infection for immunofluorescence microscopy. (B) Blood was collected from day 7 to day 14 from uninfected (ctrl) and infected CD163KO mice (KO) and the parasitemia compared to infected wildtype mice (WT) ($n = 3$). (C) At day 14 after the infection, spleen tissue from wildtype and CD163KO mice was collected for fixation and hematoxylin & eosin staining. Control and *P. chabaudi* infected spleens were compared in CD163KO. (of two experiments: representative for $n = 2$, scale bar = 200 μm).

In the above-described experiment, infected and uninfected cohorts of wildtype and CD163KO mice were compared, both were either injected with PBS as control or infected with *P. chabaudi*. At day 14 after the injection, the spleens were collected from wildtype animals (WT) and CD163KO mice. Infected WT and CD163KO mice showed a similar degree of splenomegaly. The spleens were

fixed, labelled with antibody and imaged. Comparing the spleen tissue of uninfected controls between WT and CD163KO did not show clear differences in the splenic architecture, cellular composition and distribution (Figure 40, A). Iba1 labels macrophages in general and the signal was distributed throughout the spleen tissue equally in WT and CD163KO. F4/80 is specifically highly expressed on RPM in the spleen and was homogeneously distributed throughout the red pulp. Labeling with CD169 to detect the splenic marginal zone was clear in both the uninfected WT and CD163KO mice.

In contrast, when mice were infected with blood-stage malaria, the impact on the splenic architecture was more severe in CD163KO mice. As described before (see chapter: 3.2.1 Loss of splenic CD163⁺ RPM upon *P. chabaudi* infection), during the acute phase of a *P. chabaudi* malaria infection, the splenic marginal zone was disrupted in wildtype mice. A CD169 signal was visible, but the marginal zone was open and fenestrated and the separation between white and red pulp was disrupted as indicated by the F4/80 signal, which was detected throughout the spleen tissue and not specifically localized to the red pulp area (Figure 40, B). Similarly, the F4/80 signal was diffusely spread throughout the spleen tissue in the CD163KO model upon *P. chabaudi* infection. However, no CD169 signal could be detected in the spleens from the infected CD163KO mice at all. Thus, our preliminary studies show that in the spleen of mice that lack the expression of the CD163 receptor, an acute malaria infection may cause a loss of the marginal zone, which would otherwise be clearly detected upon labeling with a CD169 fluorescent antibody and confocal microscopy.

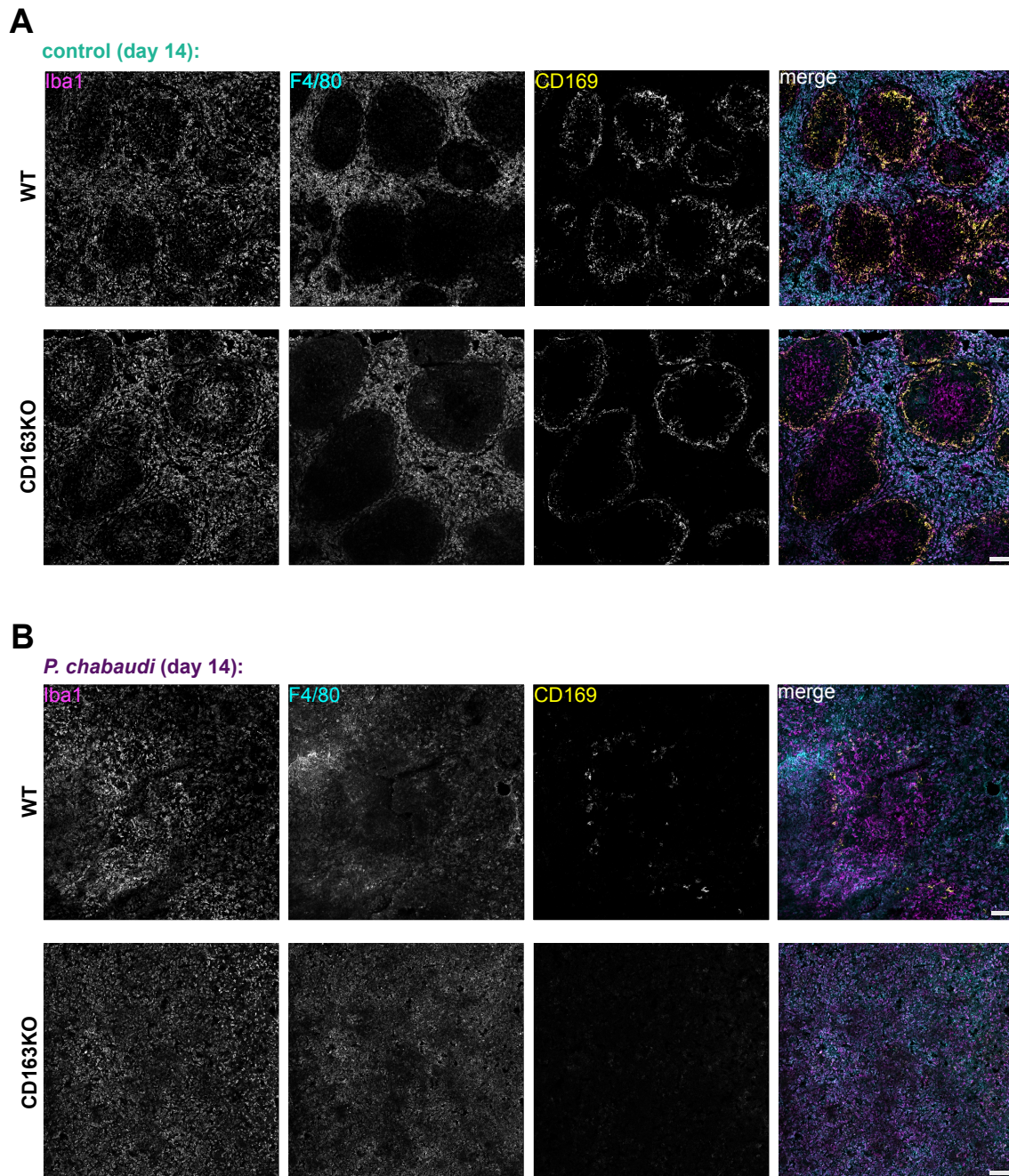


Figure 40: The absence of CD163 impacts the splenic marginal zone in malaria. Wildtype (WT) and CD163KO (genetic loss of the CD163 receptor) mice were infected with blood-stage malaria (*P. chabaudi*) and spleen tissue collected at day 14 after the infection for fixation, labeling with fluorescent antibodies and confocal imaging. Labeling with Iba1 for all macrophages (magenta), F4/80 for red pulp macrophages (cyan), CD169 for the splenic marginal zone (yellow) and merge. (A) Spleen tissue of uninfected WT and CD163KO mice. (B) Spleen tissue of *P. chabaudi* infected WT and CD163KO mice (of two experiments: representative for $n = 3$, scale bar = 100 μm).

3.3.2 The impact of the depletion of splenic marginal zone and marginal metallophilic macrophages on malaria progression

The data shown above suggested that there may be a connection between the splenic marginal zone and CD163 expression. The presence or absence of the CD163 receptor may have had an impact on the splenic marginal zone and the maintenance of its architecture. When the *Cd163* locus was depleted, resulting in all cells missing the CD163 protein, the marginal zone was no longer detected during acute malaria infection.

Therefore, it was further investigated if and how the absence of the splenic marginal zone macrophages (MZM and MMM) would impact malaria pathology and disease progression. Splenic MZM and MMM rely on the nuclear factor Lxr-alpha ($Lxr\alpha$) and a full knockout of *Lxra* causes a loss of both macrophage populations from the splenic marginal zone (A-Gonzalez et al, 2013). In this thesis, the *Tnfrsf11a^{Cre/+}; Lxra^{flox/flox}* mouse model (LxraKO) was generated and used to specifically deplete $Lxr\alpha$ -dependent macrophages. LxraKO mice were compared to littermate controls (*Tnfrsf11a^{+/+}; Lxra^{flox/flox}*, here LxraWT). Histological staining with hematoxylin and eosin of uninfected mice showed that the absence of macrophages in the marginal zone in steady-state conditions does not influence the splenic structure per se (Figure 41, upper panels). Spleen tissue of both, LxraWT and LxraKO, showed characteristic darker, circular white pulp areas, evenly distributed throughout the tissue in uninfected controls.

Day 14:

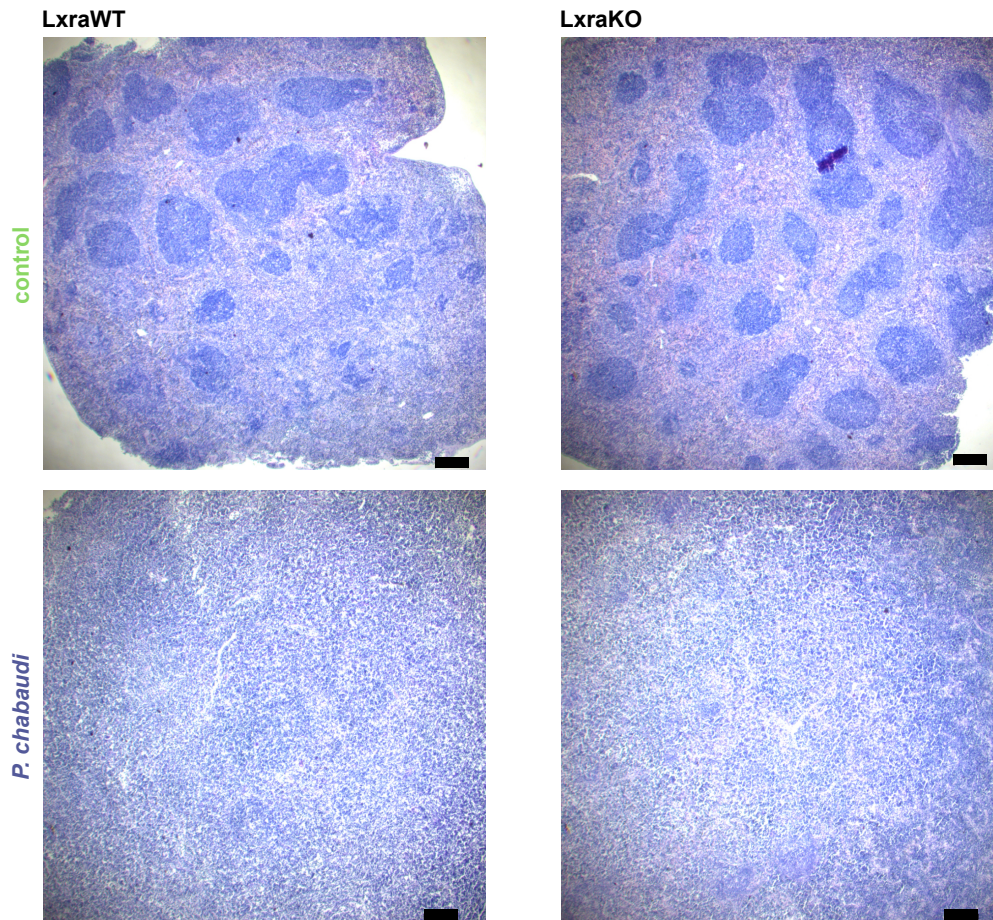


Figure 41: Spleen tissue in the absence of macrophages in the splenic marginal zone and impact of a *P. chabaudi* infection. Spleen tissue of LxraWT ($Tnfrsf11a^{+/+}$, $Lxra^{flox/flox}$) and LxraKO ($Tnfrsf11a^{Cre/+}$, $Lxra^{flox/flox}$) mice was collected for fixation and hematoxylin and eosin staining at day 14 after the injection of PBS (control) or the infection with *P. chabaudi* (of two experiments: representative for $n = 2$, scale bar = 200 μm).

LxraKO mice and littermate controls (LxraWT) were infected with *P. chabaudi* and the cellularity and structure of the spleen analyzed at day 14 and day 35 after blood-stage malaria infection (Figure 42, A). Parasitemia was monitored throughout the time course of the infection (Figure 42, B). The percentage of infected RBC was higher in LxraKO mice when compared to LxraWT littermates. In both, infected LxraWT and LxraKO mice, the highest peak in parasitemia was

detected at day 10 of the infection, but in LxraKO mice the parasitemia was above 30 %; almost 20 % higher than in LxraWT mice.

At day 14 after *P. chabaudi* infection, spleens were collected and analyzed via flow cytometry. Both macrophage populations in the splenic marginal zone, MZM and MMM, are characterized by high Tim4 expression. Thus, MZM and MMM in the Lxra-model were uniformly identified as Tim4⁺ macrophages. At day 14, no Tim4⁺ macrophages were detected in the spleen of either uninfected or *P. chabaudi* infected LxraKO mice (Figure 42, C). Thus, the genetic mouse model (LxraKO) efficiently depletes macrophages from the splenic marginal zone.

In littermate controls (LxraWT) that were not infected, the number of Tim4⁺ macrophages was significantly higher per gram of tissue as well as per gram of spleen compared to the numbers in uninfected LxraKO spleens (Figure 42, C). Upon *P. chabaudi* infection, the number of Tim4⁺ macrophages was significantly reduced in LxraWT compared to uninfected littermate controls. In particular, the total number of Tim4⁺ marginal zone macrophages per spleen showed that an acute *P. chabaudi* infection (at day 14) led to a reduction of this population. However, the comparison of total numbers of Tim4⁺ marginal zone macrophages in the infected LxraWT mice to LxraKO mice showed that the Tim4⁺ marginal zone macrophages were reduced, but not completely depleted in infected LxraWT mice. Monitoring the spleen weight at day 14 showed significant splenomegaly upon *P. chabaudi* infection (Figure 42, D). Comparing the spleen weight between infected LxraWT and LxraKO mice, revealed that splenomegaly was more prominent in LxraWT mice.

The spleen tissue of *P. chabaudi* infected LxraWT and LxraKO mice was additionally analyzed via immunofluorescent antibody labeling and confocal microscopy (Figure 43). Labeling of uninfected LxraWT spleens confirmed that the staining procedure visualized the circular marginal zone structure. CD169 labels the splenic marginal zone (specifically MMM). In *P. chabaudi* infected LxraWT spleens, CD169 expressing macrophages were detected, forming the marginal zone around the white pulp.

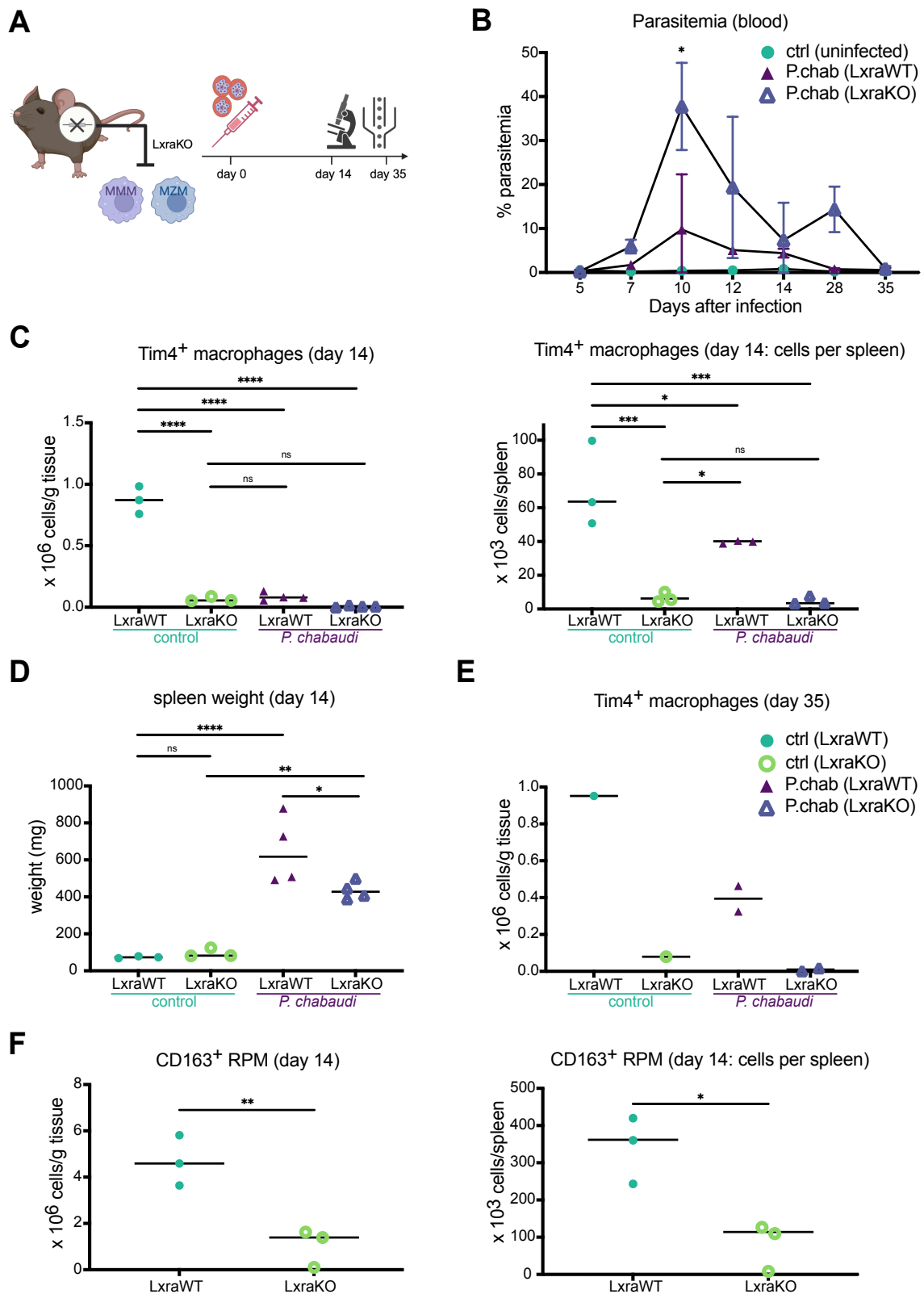


Figure 42: The impact of the absence of splenic marginal zone macrophage populations on the splenic architecture and cellularity during a malaria infection (A) Experimental strategy: Genetic depletion of *Lxra* (*Tnfrsf11a*^{Cre/+}, *Lxra*^{flox/flox}, here *LxraKO*) specifically depletes splenic marginal metallophilic

macrophages (MMM) and marginal zone macrophages (MZM). LxraKO mice and littermate controls (*Tnfrsf11a*^{+/+}, *Lxra*^{flox/flox}, here LxraWT) were infected with *P. chabaudi* to induce blood-stage malaria and spleen tissue was analyzed at day 14 and day 35 via confocal imaging and flow cytometry. (B) Blood was collected from uninfected and infected LxraWT and LxraKO mice to monitor the percentage of parasitemia. (n = 2 - 4, statistics: p-values obtained using unpaired parametric t test between infected LxraWT and LxraKO at day 10, *p < 0.05) (C) At day 14 after the infection, spleen tissue was collected and processed for antibody staining and flow cytometry analysis. In LxraWT and LxraKO mice, splenic MMM and MZM (Tim4⁺ macrophages) were quantified for cells per gram of tissue and cells per spleen via flow cytometry at day 14 after PBS injection (ctrl) or infection with *P. chabaudi* (P.chab) (n = 3 - 4, statistics: p-values obtained using one-way ANOVA for multiple group comparison, *p < 0.05, ***p < 0.001, ****p < 0.0001). (D) Spleen weight was compared between uninfected and infected LxraWT and LxraKO respectively, at day 14 (n = 3 - 4, statistics: p-values obtained using one-way ANOVA for multiple group comparison, *p < 0.05, **p < 0.01, ****p < 0.0001). (E) At day 35 after PBS injection (ctrl) or infection with *P. chabaudi* (P.chab) cell numbers between LxraWT and LxraKO were compared via flow cytometry analysis (n = 1 - 2). (F) In uninfected LxraWT and LxraKO spleens, the number of CD163⁺ RPM was determined per gram of tissue and per spleen (n = 3; statistics: p-values obtained using unpaired parametric t test, *p < 0.05, **p < 0.01).

As described for wildtype mice in previous chapters (see chapter: 3.2.1 Loss of splenic CD163⁺ RPM upon *P. chabaudi* infection and chapter: 3.2.2 Loss of splenic CD163⁺ RPM upon malaria infection), the integrity of the marginal zone was lost during acute malaria and was open and fenestrated in the infected LxraWT spleen. In contrast, in infected LxraKO mice, no CD169 signal was detectable.

Histological staining with hematoxylin and eosin confirmed the loss of splenic integrity upon *P. chabaudi* infection (Figure 41). In both, infected LxraWT and LxraKO spleens, no separation between the white and red pulp was visible, instead the tissue appeared homogeneous. A comparison between infected LxraWT and LxraKO spleens with histological hematoxylin and eosin staining showed a similar pathology, but differences in the cellularity and splenic integrity were detected more effectively by confocal microscopy.

After the acute phase of malaria, when parasitemia had been controlled, at day 35 after the infection (Figure 42, E), the Tim4⁺ macrophage population of the splenic marginal zone was recovering in LxraWT mice. In both, the uninfected and infected, LxraKO mice, no Tim4⁺ macrophages were detected in the splenic marginal zone at day 35 after the infection.

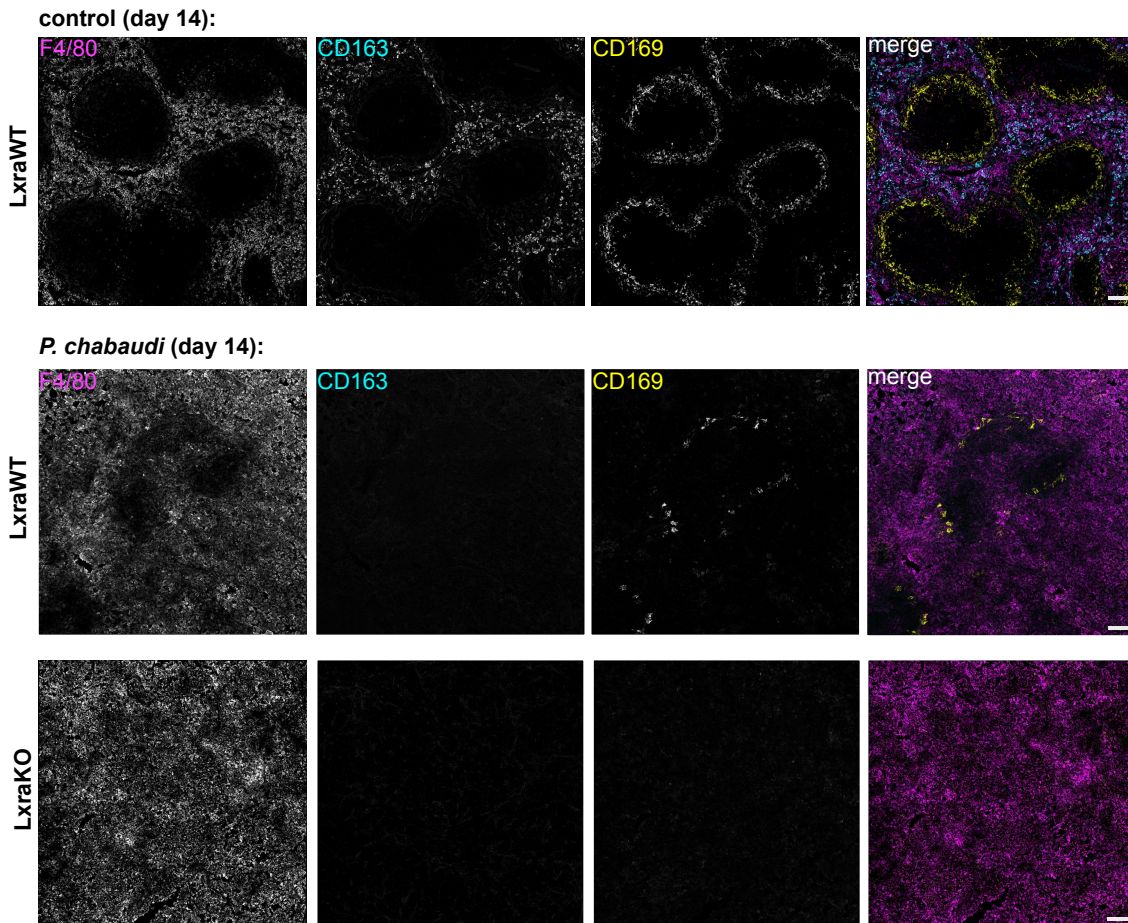


Figure 43: The absence of macrophages in the splenic marginal zone and impact on the splenic architecture upon *P. chabaudi* infection. Spleen tissue of LxraWT (*Tnfrsf11a*^{+/+}, *Lxra*^{flox/flox}) and LxraKO (*Tnfrsf11a*^{Cre/+}, *Lxra*^{flox/flox}) mice was collected for fixation and labeling with fluorescent antibodies at day 14 after the injection of PBS (control) or the infection with *P. chabaudi*. Labeling with F4/80 for red pulp macrophages (magenta), CD163 for splenic RPM subset (cyan), CD169 for the splenic marginal zone (yellow) and merge (of two experiments: representative for n = 3, scale bar = 100 μ m).

To investigate the impact of MZM and MMM depletion on other splenic macrophage populations, the numbers of CD163⁺ RPM were compared between uninfected LxraWT and LxraKO mice. A significant difference was detected: the numbers of CD163⁺ RPM were lower in the absence of splenic MZM and MMM (LxraKO) (Figure 42, F).

CD163 expression was further investigated in *P. chabaudi* infected mice upon fixation of the spleen tissue and labeling with fluorescent antibodies for confocal microscopy. Comparing LxraWT and LxraKO spleens at the peak of a malaria infection (day 14), showed a loss of the CD163 signal in both LxraWT and LxraKO tissue, while the signal was clearly detectable in LxraWT control spleen tissue (Figure 43). In contrast, the F4/80 signal, which is characteristic for RPM in the spleen, was abundantly detected in *P. chabaudi* infected LxraWT and LxraKO spleens.

3.4 The cellular dynamics in the bone marrow and blood during blood-stage malaria

In the blood-stage of malaria, circulating erythrocytes are infected with the *Plasmodium* parasite. These infected erythrocytes are mostly cleared through the filtering function of the spleen. However cellular loss needs to be compensated and thus the bone marrow stem and progenitor cells as well as circulating immune cells were further investigated in this study.

3.4.1 Stem- and progenitor cells in the bone marrow during blood-stage malaria

After birth, hematopoiesis is entirely shifted to the BM and the stem- and progenitor cells give rise to various immune cells. In the steady-state, short lived cells are constantly replaced through differentiation of BM-progenitors (Jagannathan-Bogdan & Zon, 2013). Upon need (for example during bleeding or

infections) the hematopoietic output can be increased and a higher number of progenitor cells differentiates and gives rise to effector cells, which can be mobilized towards the organs where their function is required (Hoggatt & Pelus, 2011).

An expansion of hematopoietic progenitor cells was also observed in the BM during the acute phase of infection with *P. chabaudi*. Infected mice that were previously analyzed for splenocytes in this project, were also investigated for the bone marrow progenitor cells via flow cytometry. Between one and 90 days after the infection with *P. chabaudi*, the BM was isolated and cells labeled with fluorescent antibodies. This allowed discrimination of granulocyte macrophage progenitors (GMP), multipotent progenitors 2, 3, 4 (MPP2, MPP3, MPP4) as well as short-term hematopoietic stem cells (ST-HSC) and long-term hematopoietic stem cells (LT-HSC) (Figure 44, A).

The BM cells of uninfected controls and *P. chabaudi* infected mice were compared (Figure 44, B). LT-HSC, which are at the top of the hematopoietic hierarchy, showed minor expansion at day four after the infection, but were otherwise not affected by the parasitic infection. Further down the hematopoietic hierarchy, ST-HSC expanded at day four, early after the infection, with the peak at day seven after the infection. All MPP populations expanded upon malaria infection. Similar to the ST-HSC, the peak of MPP expansion was observed at day seven after the infection, when the MPP compartments had multiplied compared to the cell numbers in uninfected controls. However, while ST-HSC already expanded at day four after the infection, MPP2 and MPP3 showed a distinct peak at day seven after the infection, with minimal deviation from controls at day four.

MPP4 on the other hand already expanded on day four of the infection. All MPPs normalized after two weeks and remained at the control level throughout the experimental time course. GMPs, which are further downstream the hematopoietic hierarchy and give rise to myeloid cells, did not show major infection-related deviations from the steady-state control cell numbers.

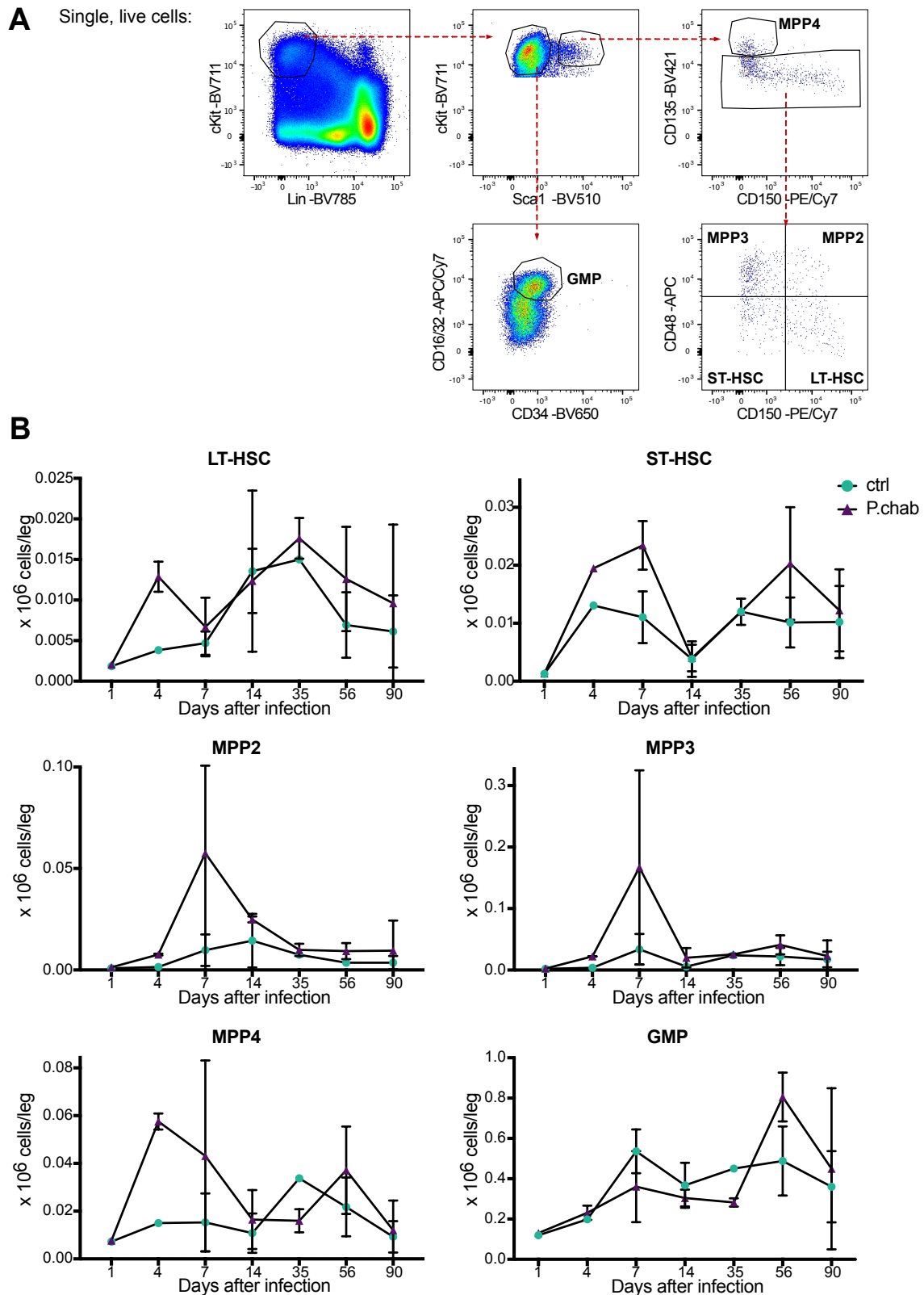


Figure 44: Quantification of stem- and progenitor cells in the bone marrow during a malaria infection. (A) Gating strategy to discriminate stem and progenitor cells in the bone marrow via flow cytometry: long-term hematopoietic stem cells (LT-HSC), short-term hematopoietic stem cells (ST-HSC), multipotent

progenitors (MPP2, MPP3, MPP4) and granulocyte macrophage progenitors (GMP). (B) At the indicated timepoints after *P. chabaudi* infection, the bone marrow was isolated from mice for labeling with fluorescent antibodies for flow cytometry staining. Stem- and progenitor cells were quantified in uninfected (ctrl) and *P. chabaudi* (P.chab) infected samples (day 1: n = 1, day 4: n = 2, day 7: n = 3, day 14: n = 4, day 35: n = 3, day 56: n = 6, day 90: n = 6).

3.4.2 Circulating immune cells in the blood during blood-stage malaria

Hematopoietic progenitor cells that differentiate in the bone marrow give rise to effector cells, which can be released into the circulation. The blood stream mostly consists of erythrocytes, but also carries immune cells that monitor the environment and can extravasate into the tissue (Charles A Janeway et al, 2001b). This process is tightly controlled and highly dynamic in the steady-state. This dynamic nature allows the hematopoietic system to adapt rapidly to challenges, such as infections, to contain and eliminate pathogens immediately. In the blood-borne infection model of *P. chabaudi* induced malaria, circulating lymphoid and myeloid cells were monitored. Blood was collected between day one and day 90 after the infection, from the previously described mice (that had been used for spleen and bone marrow analysis in this study). Immune cells in the blood were labeled with fluorescent antibodies for flow cytometry. This allowed a discrimination of B cells and T cells of the adaptive immune system as well as granulocytes, Ly6C⁺ classical monocytes, MHC class II⁺ monocytes and Ly6C^{low} patrolling monocytes of the innate immune system (Figure 45, A).

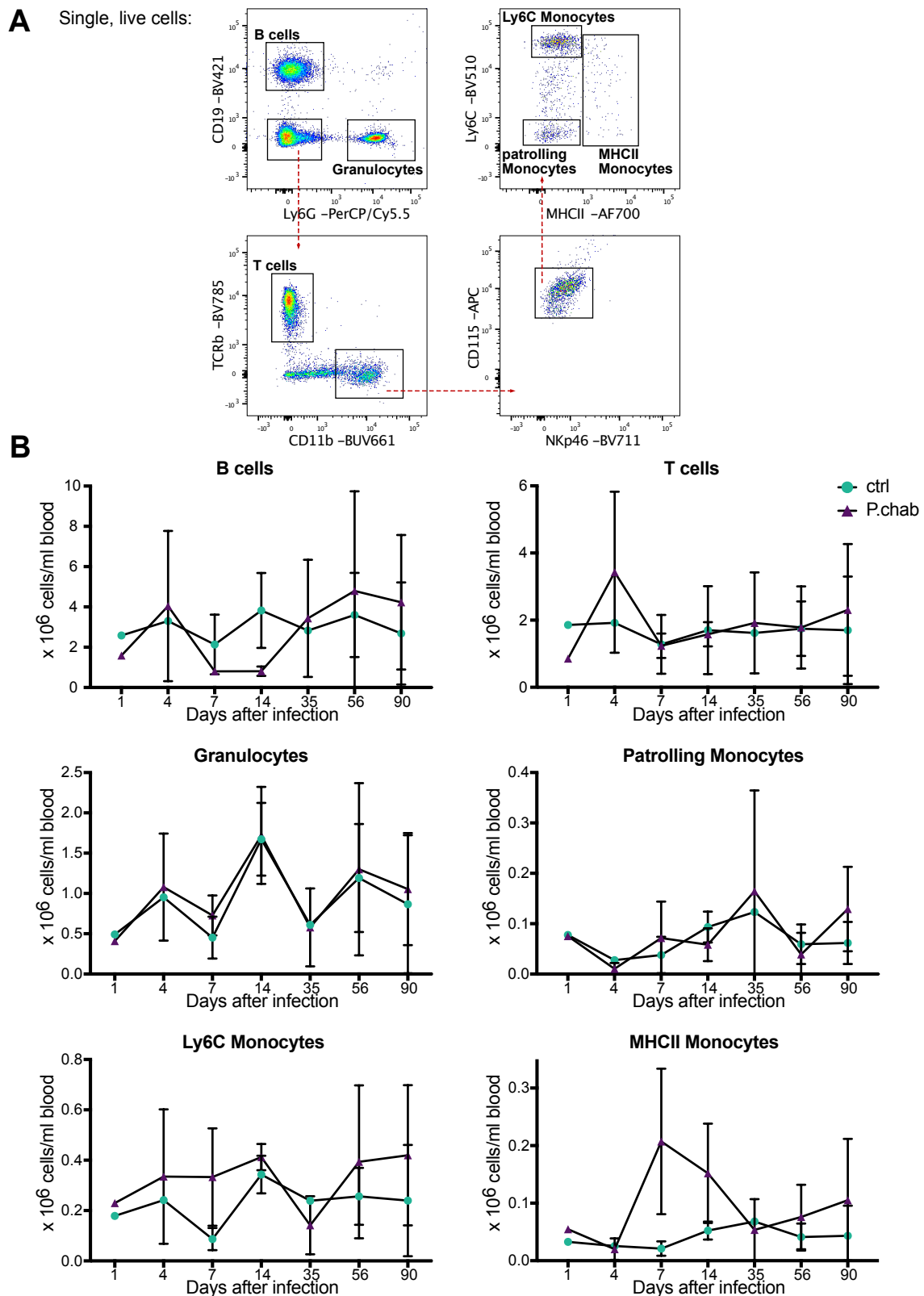


Figure 45: Quantification of lymphoid and myeloid immune cells in the blood during a malaria infection. (A) Gating strategy to discriminate B cells and T cells as well as granulocytes, patrolling monocytes, Ly6C monocytes and MHC class II monocytes in the blood. **(B)** At the indicated timepoints after *P. chabaudi*

infection, blood was collected from mice for labeling with fluorescent antibodies for flow cytometry staining. B cells and T cells of the adaptive immune system as well as granulocytes, patrolling monocytes, Ly6C⁺ monocytes and MHC class II⁺ monocytes of the innate immune system were quantified in *P. chabaudi* (P.chab) infected samples and compared to uninfected (ctrl) blood samples (day 1: n = 1, day 4: n = 2, day 7: n = 4, day 14: n = 4, day 35: n = 2, day 56: n = 6, day 90: n = 6).

Circulating immune cells in uninfected controls and *P. chabaudi* infected mice were compared (Figure 45, B). Regarding the adaptive immune system, B-cell and T-cell numbers were consistent in the blood of uninfected control mice. Upon infection with *P. chabaudi*, the counts of both adaptive immune cell populations became more unstable and fluctuated compared to controls, but no clear increase or decrease was observed during the acute phase of malaria and the progression of the disease.

Regarding the response of the myeloid immune cells, no major infection-related changes were detected in granulocytes and patrolling Ly6C^{low} monocytes. The amount of Ly6C^{high} monocytes in the blood was partially elevated upon the infection in comparison to the control group, but no distinct peak or high elevation was found. In contrast, a strong immune response was detected amongst MHC class II⁺ monocytes in the blood. The MHC class II⁺ monocyte population increased during the acute phase of the infection, with a peak at day seven and remained elevated after two weeks. One month after the infection the amount of circulating MHC class II⁺ monocyte had decreased and was similar to the uninfected controls until day 90 after the infection.

4 Discussion

Macrophages are innate immune cells that are essential for maintaining homeostasis in the body and play vital roles in combatting infections and diseases. It is an ongoing field of research to explore the full potential of this crucial, yet very heterogeneous cell type. Although the old dogma, that macrophages originate from HSCs and differentiate into a pro-inflammatory or anti-inflammatory phenotype, has been revised in the last decade, still much needs to be discovered. Macrophages are not one distinct cell population; depending on their tissue of residence and their developmental origin, they are attributed diverse functions and phenotypes (Mass & Gentek, 2021).

The spleen is an essential organ for maintaining homeostasis in the blood. Its main function is the filtration of the blood, to remove any harmful substances or pathogens (Cesta, 2006). This removal is mostly carried out by splenic macrophages, which phagocytose aberrant red blood cells and pathogens (A-Gonzalez & Castrillo, 2018).

The splenic macrophages are, however, quite heterogeneous. To date, at least four different macrophage populations have been described (Haan & Kraal, 2012). However, published research has mostly focused on only one particular sub-population of splenic macrophages at a time, but there is still a large knowledge gap, as the populations have not been characterized simultaneously and in great detail with respect to their developmental origin and function.

4.1 Characterization of splenic macrophages

In this study, cell surface markers expressed by splenic macrophages were identified. While most macrophages are characterized by the expression of F4/80, in the spleen it is specifically the RPM that express F4/80 at high levels. In the literature, splenic F4/80^{high} macrophages have so far been described as

RPM (Kurotaki et al, 2015). However, experiments in the context of this thesis have shown that RPM are not a homogeneous macrophage population that can simply be described by the expression of F4/80, as this population is heterogeneous. Splenic F4/80-positive RPM differ in their expression of the surface receptor CD163 and were thus subdivided into CD163⁺ RPM and CD163⁻ RPM in this study.

The important role of the CD163 receptor in iron recycling and homeostasis will make more detailed discrimination of splenic RPM relevant for future studies that assess RPM in homeostasis and disease. Single-cell RNA-sequencing analysis confirmed that both subpopulations have a similar expression profile, but significantly differ in the expression of CD163. Additionally, the RPM-specific *Spic* gene was expressed at a higher level in the CD163⁻ RPM population. Functionally, CD163⁺ RPM were assigned to various regulatory pathways, while CD163⁻ RPM were assigned to cytokine mediated signaling pathways and the response to IFN γ stimuli. This novel phenotypic and functional heterogeneity of splenic RPM is a central topic of this study.

Further, both macrophage subtypes that populate the marginal zone are very similar in their expression profile and both express a number of key surface markers. MZM and MMM express MARCO and Tim4, but MZM express MARCO at higher levels, while MMM express Tim4 at higher levels. To precisely distinguish these two very similar macrophage subsets, SIGNR1 and CD169 expression can be used. MZM are characterized by SIGNR1 expression (Koppel et al, 2008) and MMM are characterized by CD169 expression (Backer et al, 2010). Both macrophage subtypes that populate the marginal zone are less abundant than the RPM and thus an appropriate isolation strategy has to be applied to study them in detail (Fujiyama et al, 2019). In this study, enzymatic digestion and mechanical grinding were employed to allow isolation of these rare macrophages.

Macrophages in the splenic white pulp (WPM) have not yet been studied extensively. They are very similar to the so-called tingible body macrophages that

are found in the germinal centers of lymph nodes. These cells received their name due to the visible apoptotic bodies that were observed in their cytoplasm during phagocytosis of apoptotic lymphoid cells (Swartzendruber & Congdon; Gotur & Wadhwan, 2020). They do not express F4/80 but can be identified via CD68 expression (A-Gonzalez & Castrillo, 2018). CD68 is a common macrophage marker that is found in the lysosome and associated with phagocytotic activity (Chistiakov et al, 2016). Because of its relevance in the degradation of phagocytosed particles, CD68 is expressed on all splenic macrophages. Therefore, it was not used to specifically identify WPM in this study. Additionally, CD68 is a glycoprotein located in the lysosome and usually not transported to the cell surface. Thus, intracellular staining procedures would be required that include fixation of the cells. This can alter staining patterns through the masking of epitopes (Scalia et al, 2017). In the current study, the approach taken allowed for the identification of WPM via expression of CD64 and CD11b and, after the exclusion of MZM and MMM, they were described by MerTK expression (A-Gonzalez et al, 2009).

Based on the expression profiles of splenic macrophages, a novel gating strategy was developed that allowed for the discrimination of all splenic macrophage populations simultaneously via flow cytometry. In a related study (Fujiyama et al, 2018), the authors first compared a mechanical versus an enzymatic dissociation strategy and found that the enzymatic approach yielded a higher quantity of splenic macrophages and that only the enzymatic approach allowed for the isolation of marginal zone macrophages. Here, a combined approach of enzymatic digestion, followed by mechanical grinding was used and yielded even higher numbers of macrophages. The study of Fujiyama *et al* (2018) further identified CD11b⁺, F4/80^{low} MZM and MMM via differential expression of Tim4. They validated the cellular identity of MZM with a *CD19*^{-/-} model, showing a distinct reduction of MZM. The identity of MMM was validated with a *CD169*^{DTR} model, which caused a loss of the population identified as MMM. Here, a similar gating strategy was used; in addition, a large spectrum of antibodies for macrophage subtype-specific epitopes allowed for a more detailed discrimination

of MZM and MMM via SIGNR1 and CD169 expression, respectively. On the other hand, the heterogeneity of RPM was not addressed by Fujiyama *et al* (2018) and WPM were neglected.

Splenic macrophages subtypes do not only show phenotypic, but also functional differences. The anatomical location that a specific macrophage subtype populates and the functions they have at their site of residence, are related to their developmental origin (A-Gonzalez & Castrillo, 2018). The tools to study macrophage ontogeny and development are limited and have many pitfalls (Mass, 2018). Chemical targeting with clodronate in liposomes or diphtheria toxin induced uncontrolled systemic inflammation and thus does not represent homeostatic conditions (Chapman & Georas, 2013). Approaches using parabiosis or adoptive transfer after irradiation yield important insight on the origin of cells, but mainly allow for conclusions to be drawn about HSC-derived cells only (Yona *et al*, 2013). Genetic models that use the Cre/loxP system have evolved as important tools to describe cellular ontogeny in a spatiotemporal manner. Fate-mapping with the Cre/loxP system, using cell-specific promoters have so far only allowed tracing of cells of one origin at a time, i.e. either HSC-derived or EMP-derived cells. The discovery of the dual origin of tissue macrophages was a breakthrough in the field that allowed for the development of new tools to follow homeostatic kinetics and functions of macrophages of both origins. Therefore, the novel DFM-model was developed in this project, to study macrophage ontogeny in the spleen.

With the DFM-model, which labels EMP-derived cells with YFP and HSC-derived cells with tdTomato, it was shown that splenic RPM are almost exclusively EMP-derived during embryogenesis and in young mice. The EMP-derived origin of macrophages was also observed by others (Schulz *et al*, 2012), however, splenic RPM were so far considered as a homogenous population. Here, the distinct developmental origin of splenic CD163⁺ and CD163⁻ RPM was characterized. In prenatal and young mice, both CD163⁺ and CD163⁻ RPMs were

almost 100 % EMP-derived. By 3 weeks of age, the contribution of HSC-derived cells started to increase for CD163⁻ RPM, but not CD163⁺ RPM. This highlighted not only a difference amongst splenic RPM with respect to their expression of the surface receptor CD163, which is important for the spleen's function in iron homeostasis (Winn et al, 2020), but also deviating developmental trajectories. The anatomical location of CD163⁺ RPM also resolved in a temporal manner. While CD163⁺ RPM were distributed throughout the developing spleen tissue within the first week after birth, they localized specifically to the red pulp in juvenile mice (here shown at the age of 8 weeks). The homing of F4/80-expressing RPM to the red pulp was described to occur between postnatal day 14 and 21, when the red pulp and white pulp have segregated (A-Gonzalez & Castrillo, 2018). Since a heterogeneity of splenic RPM has not been considered in other research so far, F4/80-expressing RPM include both, the CD163⁺ and CD163⁻ RPM that were identified in this study. The study of Gonzalez & Castrillo (2018) supports the findings presented here: in mice that were younger than 14 days, both, the CD163⁺ and CD163⁻ RPM were distributed throughout the spleen tissue and, in juvenile mice older than 21 days, the splenic red and white pulp had segregated and both RPM populations were specifically located in the red pulp.

The heterogeneity in the development of macrophages has been described amongst resident macrophages in different tissues (Mass et al, 2016), but the novel DFM model allows for the discrimination of minor differences in the temporal development of particular subtypes of tissue macrophages. The difference between CD163⁺ and CD163⁻ splenic RPM is even more evident in adult mice. At three months of age, a distinct influx of HSC-derived cells to the splenic RPM compartment was observed, which reached an equilibrium after one year for CD163⁺ RPM, while for CD163⁻ RPM an ongoing trend of replacement by HSC-derived cells was observed. After one year, the influx of HSC-derived cells to the splenic CD163⁻ RPM compartment reached 50 %, while only approximately 35 % of the splenic CD163⁺ RPM were HSC-derived at that timepoint. The replacement of EMP-derived cells by monocyte-derived macrophages that originated from HSC was described for resident macrophage

populations in various tissues (Mass et al, 2023), but it has so far not been possible to study them at the resolution employed in the current study using the DFM-model. The infiltration of HSC-derived macrophages was shown for some macrophage subtypes in the lung (especially for interstitial macrophages) or in the gut for example (Maheshwari, 2022; Evren et al, 2020). Others, like microglia in the brain are not replaced by infiltrating monocytes (Ginhoux et al, 2010). Many studies have examined important organs, such as the brain (Werner et al, 2020), the liver (Mass et al, 2016) or the lung (Mass et al, 2023). Related studies used the *Ms4a3^{Cre}* mouse model to label HSC-derived monocytes and showed that their contribution to tissue macrophages was negligible after birth, but increased with age in the spleen (Liu et al, 2019). They, however, did not discriminate between the different splenic macrophage subtypes, which is now possible with the new panel and gating strategy that was developed in this study. Thus, this study yielded novel insight into the developmental origin and heterogeneity of splenic macrophages.

The replacement of splenic EMP-derived RPM by HSC-derived cells and the developmental heterogeneity amongst CD163⁺ and CD163⁻ RPM that was demonstrated with the novel DFM model, was further supported using the tamoxifen-inducible fate-mapping of *Cxcr4* expressing HSC-derived cells (Werner et al, 2020). In adult mice, 6 months after tamoxifen-mediated induction of Cre-expression, the percentage of labeled HSC-derived CD163⁻ RPM was higher than the percentage of CD163⁺ RPM. Overall, for both, the CD163⁺ and CD163⁻ RPM, the labeling frequency of HSC-derived cells in adult mice was about 10 % higher in the *Cxcr4*-model than in the DFM-model. The *Cxcr4*-Cre is inducible, but the high labeling frequency of almost 100 % of myeloid cells in the blood indicated a good labeling efficiency. In the DFM-model, labeling of HSC-derived cells is induced with the FlpO-recombinase; in contrast, the Cre-recombinase mediates labeling of HSC-derived cells in the *Cxcr4*-model. Different recombinase enzymes can differ in their recombination efficiency through different efficacy in the recognition of the target site and different cleavage potentials (Hara & Verma, 2019). Another difference between the two

models is the driver gene for recombinaise expression. *Cxcr4* is expressed by LT-HSC and thus targets all cells downstream of the hematopoietic hierarchy (Mauel & Mass, 2024; Werner et al, 2020), while *Ms4a3*, which is used to drive FlpO expression in the DFM, is expressed by GMP, further down the hematopoietic hierarchy (Liu et al, 2019). In addition, the driver gene itself can affect the level of recombinaise expression and thus the efficiency of recombination (Song & Palmiter, 2018; Hua et al, 2018).

Overall, both models support the same outcome: splenic RPM are a more heterogeneous population than described so far in regards to their ontogeny. High-dimensional flow cytometry revealed that phenotypically different RPM populations exist in the spleen and genetic fate-mapping highlighted deviating developmental trajectories among them. There is increasing evidence, that not only the developmental origin of a cell type dictates its function and phenotype, but that also the tissue environment can direct the phenotype of macrophages that integrate into a tissue. The micro-architectural niches of an organ can provide signals that direct macrophage function and EMP-derived, versus HSC-derived, macrophages that integrate into the same tissue niche might respond differently to the same signals (Mass et al, 2023).

Macrophages adapt to their tissue of residence and perform specific functions that are essential for organ homeostasis (Guilliams et al, 2020). Circulating monocytes, which can take up residency in any number of tissues can acquire functional specializations within a specific tissue, analogous to that of their resident EMP-derived counterparts (van de Laar et al, 2016). This supports the idea that the tissue niche confers tissue-specific identity (Guilliams et al, 2020). There is evidence that the establishment of tissue-specific macrophage niches are supported by other cells in that particular niche; for example the secretion of CSF-1 by endothelial cells in the lymph node is essential for formation of the functional network of different macrophage subtypes (Mondor et al, 2019). Due to these niche-specific functions and interactions, the macrophage network has been described as a dispersed homeostatic organ (Gordon & Plüddemann, 2017). The DFM-model showed that in the developing spleen, almost all RPM

were EMP-derived and only during adulthood, do HSC-derived cells partially replace them. The dynamics of HSC-derived cell replacement differed between CD163⁺ and CD163⁻ RPM, but in an intact splenic environment, infiltrating monocytes have the capacity to differentiate into both subpopulations, suggesting that the cells are equally capable of contributing to essential homeostatic functions.

4.1.3 Conclusions regarding aim 1

With respect to aim 1 (characterization of developmental origin and phenotypic identity of splenic macrophage subpopulations), a novel gating strategy to distinguish all macrophage subtypes in the spleen was established. Additionally, phenotypic differences and previously unappreciated heterogeneity within the splenic RPM compartment was identified with different developmental trajectories defined in the novel DFM-model.

For macrophage populations in other organs, it is likely that further ontogenetic and functional heterogeneity exists (Mass, 2018). The use of the novel DFM-model for the dissection of macrophage heterogeneity and origin will lead to a deeper understanding of the different phagocyte types that exist and has the potential to revolutionize research in the field of macrophage development in the context of disease.

4.2 Characterization of cellular and molecular changes of splenic macrophages upon malaria infection

4.2.1 Ontogeny and phenotype of splenic red pulp macrophages upon malaria infection and other perturbations

The above-described studies on splenic macrophages led to novel insight on the heterogeneity and developmental origin of splenic RPM. Analysis of the splenic compartment in homeostasis has shown that two distinct subpopulations of RPM co-exist in the splenic red pulp in the steady-state, which are mostly EMP-derived. Splenic RPM play an important function in the capture of circulating pathogens and the maintenance of iron homeostasis (Ganz, 2012). The presence of heme induces the expression of Spi-C, an important factor for RPM differentiation (Lavin et al, 2015; Haldar et al, 2014). Spi-C selectively controls the development of RPM and is not expressed by monocytes or dendritic cells. Genetic depletion of the gene (*Spic*^{-/-}) resulted in a defect in the development of RPM (Kohyama et al, 2009) with a total loss of F4/80-expressing cells in the spleen of *Spic*^{-/-} mice but normal appearance of MMM and MZM, when assessed by immunohistochemistry analysis. The loss of RPM could be rescued by Spi-C reconstitution through retroviral-mediated Spi-C expression. It was further shown *in vitro* that Spi-C expression induces VCAM1-expression, but not CD163 or heme-oxygenase (Kohyama et al, 2009).

Spi-C dependent RPM are early sentinels of malaria infection (Kim et al, 2012). In *Spic*^{-/-} mice, significantly lower levels of type I interferons were found in the spleen and plasma in response to *P. chabaudi* infection, when compared to *Spic*^{+/-} littermates. Progression and peaks of parasitemia were similar between *Spic*^{-/-} and *Spic*^{+/-} mice, as was the frequencies of neutrophils and F4/80⁺ macrophages in the splenic marginal zone. But the frequency of monocytes was higher in the blood and spleen 12 days after infection in the *Spic*^{-/-} model (Kim et al, 2012). The Spi-C dependent RPM were a central part of this study, but two phenotypically distinct subtypes of RPM were identified as part of this research. Thus, the focus

of this project was directed towards the differential impact of the above described CD163⁺ and CD163⁻ RPM on a malaria infection (see discussion chapter: 4.1 characterization of splenic macrophages), instead of considering Spi-C dependent RPM as a uniform population.

In blood-stage malaria, infected RBC pass the blood filtering system of the spleen and can be recognized and phagocytosed by the resident macrophages (Sengupta et al, 2019). The current study used the murine malaria model of *P. chabaudi* infection to mimic relevant aspects (e.g. anemia) of human pathology (Stephens et al, 2012) and investigate the role of splenic macrophages. Murine malaria models are indispensable to advance the understanding of malaria pathogenesis and pave the way to advance treatment and prevention strategies in humans (Li et al, 2001). Here it was shown that the model mimicked typical aspects of a malaria infection with respect to parasitemia and splenomegaly. Methodologically, parasitemia was quantified via flow cytometry, which is advantageous over microscopy due to the higher speed and reproducibility (Jun et al, 2012). Similar to other studies using the same infectious dose, the first peak of parasitemia was observed after day 10 of the infection and the second peak around day 20 (Fernandez-Ruiz et al, 2017). *P. chabaudi* infections exhibit features reminiscent of chronic human infection with *P. falciparum*, in which parasitemia can rebound over 30 days (Sheel & Engwerda, 2012). Shortly after the first and major peak of parasitemia, the spleen reached its maximal expansion. Splenomegaly is a common complication in malaria and can be caused by a prolonged elevation of anti-malaria antibodies in the spleen, along with massive immune cell recruitment (Leoni et al, 2015). The increase in spleen size is also caused by an expansion of the plasma volume and its sequestration in the spleen as a result of increased hemolysis caused by the parasites (Aldulaimi & Mendez, 2021; Ringelhann et al, 1973). After the acute infection, parasitemia is less prominent and the spleen reverts to a smaller size. While studies often focus on acute malaria infection, here the long-term effects were considered and it was shown that the splenic architecture recovered 90 days after the infection. However, the dark coloration that appeared in correlation with the

malaria infection remained. This is a result of hemozoin deposits in phagocytic cells of the liver and spleen (Bryceson et al, 1983). These hemozoin deposits can on the one hand cause chronic inflammation by triggering NOD-like receptor signaling and inflammasome activation, which leads to the production of large amounts of inflammatory cytokines, especially IL-1 β (Olivier et al, 2014). On the other hand hemozoin aggregates can limit the capacity of conventional dendritic cells to mount a robust T cell response (Pack et al, 2021). Macrophages engulf hemozoin deposits, but cannot dispose of it, which leads to an increase in cell volume (Lai et al, 2018). Larger amounts of hemozoin accumulation in phagocytes are associated with disease severity in human patients. The hemozoin deposits can persist for a long period of time and impair phagocytic activity - a core function of macrophages (Olivier et al, 2014). Upon subsequent infections, this compromises the innate immune response. In the context of this study, the phagocytic capacity of macrophages that had recovered from malaria infection could be compared to control groups upon the administration of apoptotic cells (Toussirot et al, 2021), to determine if phagocytic function is impaired.

In general, splenic RPM act as scavengers for senescent erythrocytes, but there is increasing evidence of a role for splenic RPM in the control of infections, such as blood-stage malaria (Borges Da Silva et al, 2015). Their main protective function is in the phagocytosis of pathogens from the circulation. Further, macrophages are equipped with a variety of pattern-recognition receptors and signaling through these receptors leads to the expression of pro-inflammatory genes and ultimately to the activation of the innate immune system (Campos et al, 2001). However, in this study, it was shown that splenic RPM are not a homogeneous population, but the macrophages in the red pulp are phenotypically different and can be further divided into at least two distinct subpopulations. Approximately one third of splenic RPM express the hemoglobin-binding receptor CD163, while two thirds of the RPM do not express the receptor in steady-state conditions. Each subtype responds differently to

blood-stage *P. chabaudi* infection. CD163⁺ RPM were no longer detected via flow cytometry early during the acute phase of the infection and the expression of CD163 did not recover long-term in this population. In contrast, CD163⁻ RPM expanded two weeks after the infection, remained elevated for two months and reverted to the numbers observed in control (uninfected) mice. A reason for the expansion of CD163⁻ RPM could be that malaria induced heme-stress is noxious for phagocytes; thus, they are excessively replenished by the influx of bone marrow-derived progenitors (Vallelian et al, 2022a). This is supported by a transfusion-based approach, to study erythrophagocytes in the spleen (Youssef et al, 2018). The injection of damaged RBCs led to increased erythrophagocytosis by splenic RPM, but consequently induced ferroptosis in this population within 24 h. This iron-dependent form of cell death was accompanied by increased ROS production and the release of chemokines that attract Ly6C^{high} monocytes to the spleen. Youssef et al (2018) showed that robust erythrophagocytosis leads to the depletion of RPMs in the spleen and is followed by a restoration of homeostasis through local proliferation and the recruitment of circulating monocytes. Since malaria causes severe damage to erythrocytes and requires efficient clearance, ferroptosis could explain the initial decline of RPMs. However, repeated peaks of parasitemia and RBC rupture make the recovery much more complex. The encounter of pathogens induces the local release of inflammatory cytokines, which leads to the upregulation of vascular endothelial adhesion molecules (Lai et al, 2018). Consequently, circulating monocytes can adhere more efficiently and extravasate into the spleen tissue to compensate for the loss of local macrophage populations.

Extensive studies using *P. chabaudi* to elucidate the impact of blood-stage malaria on splenic macrophages showed drastic and lasting changes amongst splenic RPM. CD163⁺ RPM disappeared early during an acute malaria infection and did not recover. Single-cell RNA-sequencing revealed that the cluster that was identified as CD163⁺ RPM in control samples remained upon malaria infection, but that the cells in this cluster did not express CD163 anymore after the infection. The question remained, whether this loss of CD163 expression was

specific to the *P. chabaudi* infection model or a general consequence of malaria infection. Other murine malaria species include *P. yoelii* and *P. berghei*. Upon infection with these parasite species, mice developed characteristic parasitemia and splenomegaly after 7 days. The splenic RPM were quantified via flow cytometry and showed a reduction of CD163⁻ RPM, as observed early following *P. chabaudi* infection, prior to the subsequent expansion of CD163⁻ RPM, seen after the first parasitemia peak on day 14. Complete depletion of CD163⁺ RPM was also observed during *P. yoelii* or *P. berghei* infection, mirroring the *P. chabaudi* infection model. This last finding indicates that the absence of CD163 expression on macrophages in the splenic red pulp generally occurs upon malaria infection and is not specific to a certain parasite species.

A closely related study used the *P. yoelii* infection model, and showed a rapid disappearance of F4/80⁺ tissue macrophages in the spleen before the first peak of parasitemia and an influx of CD11b⁺, Ly6C⁺ classical monocytes starting at day 4 after the infection (Lai et al, 2018). They demonstrated that these monocytes populated the empty splenic macrophage niche and their expression profile overlapped with the original F4/80⁺ cells. This study, however, did not discriminate between splenic RPM subtypes. The influx of monocytes and differentiation of these cells into F4/80⁺ macrophages is therefore most likely representative of the CD163⁻ RPM population and would support the idea that infiltrating monocytes, on a protein level, obtain only the phenotype of CD163⁻ RPM, but do not have the capacity to upregulate CD163 expression.

It was shown in the first part of this study, that the CD163⁺ RPM are mostly EMP-derived, thus the aim was to delineate the origin of splenic macrophages in the context of a malaria infection and address the influx of HSC-derived monocytes. In organs that are populated by EMP-derived tissue resident macrophages, these populations self-renew with minimal contribution by circulating monocytes (Perdiguero & Geissmann, 2016). This study showed that CD163-expressing RPM were predominantly EMP-derived in steady-state conditions. If the expression is lost upon challenge, incoming cells of a different origin might not be able to reconstitute the same phenotype and function, with respect to CD163 expression (as demonstrated by single-cell RNA-sequencing: CD163 expression is downregulated in the CD163⁺ RPM cluster upon infection). Steady-state data showed that a minor percentage of HSC-derived cells contributed to the pool of CD163⁺ cells upon aging. It is therefore likely that the splenic environment is altered through the infection (Meizlish et al, 2021) and does not provide necessary cues to induce CD163 expression irrespective of the cellular origin.

With two different mouse models (*Cxcr4*^{CreERT2}; *Rosa26*^{L^{SL}-tdTomato} & *Tnfrsf11a*^{Cre}; *Rosa26*^{L^{SL}-YFP}; *Ms4a3*^{FipO}; *Rosa26*^{L^{FL}-tdTomato}) that allow tracing of macrophage ontogeny, it was shown here that splenic RPM were mostly EMP-derived, with little contribution of HSC-derived cells in the steady-state. Upon challenge with malaria parasites, both models described a strong influx of HSC-derived cells into the splenic CD163⁻ RPM compartment, while CD163-expressing RPM were absent. The percentage of EMP-derived CD163⁻ RPM severely decreased within the first two weeks of the infection, while the contribution of HSC-derived cells rose above 80 % in both mouse models within the first few weeks after the *P. chabaudi* infection. The resident EMP-derived CD163⁻ RPM are likely to be depleted through the phagocytosis of parasitized erythrocytes. Recent studies that examined human spleen tissue (of patients that had undergone splenectomy upon malaria infection) demonstrate that intraerythrocytic malaria parasites accumulate in the spleen (Kho et al, 2021a, 2021b). In addition, malaria causes chronic heme-stress, which is noxious for macrophages (Vallelian et al, 2022a).

The research of Vallelian *et al* (2022) demonstrated that erythrophagocytes in the spleen require constant replenishment from bone marrow-derived progenitors upon erythrolysis. These infiltrating monocyte-derived cells have a higher capacity to metabolize heme and recycle iron. They described that heme activates NRF2 signaling, which shifts myeloid cell differentiation towards an antioxidant, iron-recycling macrophage phenotype at the expense of dendritic cells. Accordingly, splenic RPM were shown to be constantly replenished from BM-derived progenitors in this study. The investigation of the capacity of original and replenished RPM to process heme and recycle iron is a future direction suggested by the results presented in this study.

Related approaches used the *Kit^{MerCreMer}* fate-mapping model that labels early hematopoietic progenitors (Lai et al, 2018). Upon a *P. yoelii* infection, 80 % of the splenic F4/80⁺ macrophages were labeled at day 35. The same labeling percentage was detected after 90 days, indicating a long-term persistence of BM-replenished macrophages. The results of the *Kit^{MerCreMer}* model support the findings of this study and showed similar labeling percentages of HSC-derived cells after an infection. However, RPM heterogeneity was not assessed in the study of Lai *et al* (2018).

Upon systemic infections, such as malaria, the hematopoietic system adapts with enhanced cellular output and mobilization from the BM (Schultze et al, 2019). However, the large influx of HSC-derived cells into the spleen and the absence of CD163⁺ RPM might indicate that HSC-derived macrophages do not have the same capacity as EMP-derived cells to express this receptor. Thus, they differ from EMP-derived macrophages, which typically express CD163 and mostly self-maintain through local proliferation (Hashimoto et al, 2013), while recruited macrophages from the BM often do not manifest tissue-specific functions, but act as general immune sentinels (Mass, 2018). Transcriptional regulation that occurs during developmental pathways are linked to the function of macrophages (Schulz et al, 2012). Depletion of tissue macrophages by inflammation leaves the niche available and accessible to infiltrating monocytes (Guilliams & Scott, 2017). Repopulation with monocyte-derived cells following depletion due to *Plasmodium*

infection might result in a different functional and phenotypic profile of the newly recruited macrophages. Based on the data presented here, it is proposed that one reason that HSC-derived RPM do not express CD163 for at least 3 months after clearance of infection is that the infection alters the splenic macrophage niche and the RPM therefore do not receive the required cues to upregulate CD163 expression. Tissue-specific factors shape the function of splenic macrophages and it has been suggested that the macrophage niche of a tissue provides macrophage tropic factors (Guilliams et al, 2020). If the niche is disrupted and cannot produce those factors, then repopulation of specific macrophage populations or functions would be impaired.

The genetic fate-mapping models revealed distinct changes in the ontogeny of splenic macrophages upon malaria infection. Novel methodologies allowed for the characterization of tissue-specific macrophages and identified distinct subpopulations with different developmental trajectories and transcriptional programs (Mass et al, 2023). Single-cell RNA-sequencing allows for the characterization of cell types at a molecular level and deciphers minor differences amongst closely related cell populations. To assess lasting changes in the splenic macrophage compartment, splenocytes were isolated 90 days after *P. chabaudi* infection and compared to uninfected controls. For specific isolation of macrophages, CD64⁺ cells were sorted before sequencing. After the alignment to a mouse reference genome, the generated UMAP showed contamination with various other cell types, especially B cells and T cells. In the lymphocyte rich spleen tissue, it is likely that those cells were tightly associated with the CD64⁺ macrophages. *In vitro* studies have shown that T cells firmly adhere to the surface of macrophage in co-cultures (Chang et al, 2009).

Sub-clustering of the cells defined as macrophages resulted in seven clusters. Three clusters were in close proximity. A common feature amongst those three clusters was the expression of *Adgre1* (the gene encoding F4/80), a characteristic gene that is expressed at high levels by macrophages in the red pulp (A-Gonzalez & Castrillo, 2018). The three *Adgre1*-high RPM clusters were then classified in greater detail.

Other factors that regulate the development and survival of RPMs are Spi-C and heme-oxygenase-1 (Kurotaki et al, 2015). Spi-C is a PU.1-related transcription factor that selectively controls the development of RPM and is not expressed by monocytes or dendritic cells (Kohyama et al, 2009). RPM express genes that are involved in iron regulation at high levels, thus it is not surprising that *Hmox1* was upregulated in all RPM clusters, compared to the other splenic macrophage subtypes. Heme-oxygenase-1 catabolizes the degradation of cellular heme to free iron and is preferentially expressed in macrophages (Poss & Tonegawa, 1997), though it can be expressed by other cells in response to stressful conditions. For example, when the physiological integrity of RBCs becomes compromised upon a *Plasmodium*-infection, the cellular content can be released into the cytoplasm, including non-covalently bound heme. This can cause acute kidney injury, a common complication of malaria infections. Host defense strategies rely on tissue-damage control-mechanisms to detoxify labile heme, which can be achieved through the induction of heme-oxygenase-1 expression in renal proximal tubule epithelial cells (Ramos et al, 2019). Genetic depletion of the *Hmox1* gene specifically in those renal cells impaired the survival of *Plasmodium*-infected mice. Thus, heme-oxygenase-1 expression is critical in the control of malaria related systemic pathologies. The cluster that showed the most intense upregulation of *Hmox1* was classified as Hmox1-high macrophages.

Two cell clusters were identified as RPM by high expression of *Spic* and *Adgre1*. Several genes were upregulated in these two RPM cluster, including *Siglece* and *Mrc1*, which are both involved in the regulation of inflammatory responses to pathogens (Nielsen et al, 2020). In the context of this study, special focus was placed on the differential expression of CD163 in RPM. Single-cell RNA-sequencing revealed that CD163 expression was particularly upregulated in steady-state in one cluster. But, different from previous experiments presented in this study, which suggested a depletion of CD163⁺ RPM upon malaria infection, this cluster persisted upon infection, although the abundance of cells within that cluster was reduced compared to the steady-state controls. In addition, CD163

expression was not homogeneously distributed throughout this cluster in control samples and the area that showed highest expression of CD163 was diluted in the UMAP of the *P. chabaudi* infected sample. Therefore, it is suggested that the CD163⁺ RPM lose expression of CD163 upon infection, but the macrophage population itself persists and adapts to the parasite challenge via a phenotypic shift. Since both, the CD163⁺ RPM and the CD163⁻ RPM cluster persisted upon the infection, a simple conversion of CD163-expressing RPM to the CD163⁻ RPM population can be excluded. Instead, a CD163⁺-like RPM cluster persisted after malaria infection.

To further characterized the RPM populations, differentially expressed genes between the control and malaria sample in the CD163⁺ RPM cluster were evaluated. *CD163* was downregulated in the malaria samples, next to other characteristic macrophage genes, such as *Timd4* and *Marco*. Taken together, this describes a downregulation of several scavenging receptors on CD163⁺ RPM upon malaria infection and a phenotypic shift, which may be related to an influx of monocyte-derived macrophages, which occupy the niche. Fate-mapping data, using the powerful DFM mouse-model indicated a high influx of HSC-derived cells upon malaria infection. At the transcriptional level, a shift in the gene signatures of the CD163⁺ RPM cluster showed an upregulation of various genes related to hematopoiesis and monocyte differentiation upon infection. Thus, the splenic RPM niche might be repopulated upon malaria infection with cells that are similar, but cannot take over the original expression profile, which implies changes in the function of these macrophages.

Others have performed bulk RNA-sequencing 35 days after *P. yoelii* infection to determine if monocytes that infiltrate the spleen upon malaria infection could take over the gene expression pattern of the macrophages that they replaced (Lai et al, 2018). They defined a broad cluster of F4/80^{hi} macrophages that was similar between control and malaria samples. While they did not identify a specific cluster with high *Cd163* expression, they describe the upregulation of *Cd163/1* upon infection within the F4/80^{hi} cluster. The *Cd163/1* gene arose from duplication of the *CD163* gene, but does not possess measurable affinity for hemoglobin

complexes (Moeller et al, 2012). Others have described CD163L1 to be expressed on $\gamma\delta$ T-cells and downregulated upon malaria infection (Kumarasingha et al, 2020). Since lymphocytes were excluded, *Cd163l1* did not appear amongst the list of differentially expressed genes in this study.

To investigate if the splenic environment provides signaling to support the maintenance of CD163⁺ RPM, the CD45⁻ splenocytes could be sorted and analyzed via single-cell RNA-sequencing. CD45⁻ cells include fibroblasts and stromal cells (Sikora et al, 2021), which can provide signals to regulate macrophage polarization (Bruch-Oms et al, 2023). Signaling molecules that are released by cells in the splenic environment could interact with upstream regulators of the CD163 gene, which include PPAR- γ , KLF4 and HIF-1 α (Ritter et al, 2000).

Regarding their gene ontology, CD163⁺ RPM were shown here to be involved in a variety of regulatory processes. CD163-expressing macrophages possess strong anti-inflammatory potential and take part in the downregulation of inflammatory responses (Kowal et al, 2011). During blood-stage malaria infection, pro-inflammatory cytokines play a pivotal role in controlling parasite growth and elimination. However, prolonged elevated levels of such cytokines can induce secondary pathologies (Popa & Popa, 2021). Therefore, initial downregulation of the expression of the immunoregulatory CD163 receptor could be advantageous to ensure a fast inflammatory response and enhancement of parasite clearance.

The detected loss of CD163-expressing macrophages upon *P. chabaudi* infection by flow cytometry did not align with the single-cell RNA-sequencing data, which showed a changed, but persistent cluster of CD163⁺-like RPM. Therefore, splenic RPM were subjected to sub-clustering. Comparing the expression of *Cd163* between the control and malaria samples showed high levels of CD163 expression only in the controls. Of the six RPM subclusters, cluster 3 showed the highest expression level of CD163 and this cluster was noticeably sparse in the malaria sample. Overall, CD163-expression was detected in four clusters and

absent in the other two clusters. Since the sequencing data revealed that a CD163⁺-like RPM population persisted upon malaria infection, but CD163 was not expressed, CD163 alone does not suffice to discriminate splenic RPMs after infection. Therefore, the four clusters that showed CD163-expression, were screened for another marker that is specifically expressed by CD163-expressing cells, but not by CD163⁻ RPM and not affected by the infection. *Icam-1* was specifically upregulated in all CD163-expressing clusters, but not in the CD163-negative clusters. Additionally, *Icam-1* expression was not influenced by the infection, but uniformly expressed in control and malaria conditions. Thus *Icam-1* is proposed as an additional surface marker to discriminate splenic RPM and may allow for the identification of CD163⁺-like RPM in malaria.

The cluster that was assigned as CD163⁻ RPM showed a similar expression profile to the CD163⁺ RPM cluster for most genes. Genes that were differentially expressed included lower expression of *Cd163* and the highest expression of *Spic* within the CD163⁻ RPM clusters. Other studies have shown that splenic RPM specifically express *Spic*, while the expression level in all other macrophages (including alveolar macrophages, microglia, Langerhans cells, Ly6C⁺ blood monocytes) is very low (Kurotaki et al, 2015). In this cluster of classical RPM, the abundance of cells increased upon malaria infection.

A comparison of differentially expressed genes in the CD163⁻ RPM cluster between control and malaria samples revealed a distinct upregulation of genes involved in the assembly of MHC complexes upon infection. MHC class II molecules on the surface of antigen presenting cells can bind parasite proteins and regulate a malaria-specific CD4 T-cell response (Draheim et al, 2017). Other studies that examined macrophage signatures after the resolution of zymosan-induced peritonitis showed a similar upregulation of MHC class II related genes (Stables et al, 2011). Clinical research, focusing on infection with *P. vivax* in humans, showed a relationship between a genetic polymorphism of MHC genes and the host resistance or susceptibility to a malaria infection (Lima-Junior & Pratt-Riccio, 2016).

Gene ontology terms support an association of CD163⁻ RPM with antigen processing and presentation. MHC class II mediated signaling not only triggers lymphocyte activation, but also transduces intracellular signals in antigen presenting cells that lead to the production of inflammatory cytokines (Al-Daccak et al, 2004). CD163⁻ RPM were also associated with the GO term for responsiveness to IFN γ signaling. This would also activate macrophages and induce the production of cytokines (Schroder et al, 2004). Thus, two pathways converge in the production of pro-inflammatory cytokines, which mediate the recruitment and activation of immune cells. Additionally, IFN γ signaling leads to the upregulation of MHC class I molecules, which promotes NK cell activity and regulates Th1 cell activation (Bhat et al, 2018).

Overall, single-cell RNA-sequencing data with respect to GO terms suggest that CD163⁻ RPM process pathogenic antigens and can function as antigen presenting cells that mediate inflammatory responses as well as the recruitment and activation of other immune cells. Thus, they are proposed to play an important role in the defense against pathogens, including malaria parasites. To validate the functions that were assigned to splenic RPM based on the sequencing results, the cells could be isolated and incubated with the model antigen ovalbumin to investigate T lymphocyte activation *in vitro* (Muntjewerff et al, 2020). Others have shown ovalbumin-specific T-cell activation in a mouse model that was depleted for dendritic cells (Schliehe et al, 2011).

The sequencing data further support the concept that splenic RPM are diverse and differentially regulate immune responses towards infections. In accordance with the previous research of this study, a subpopulation of RPM was identified that was characterized by high expression levels of CD163. Sequencing analysis then showed that this particular macrophage population persists upon a malaria infection, but downregulates the expression of CD163. Therefore, the addition of Icam-1 to the flow cytometry panel is proposed for future experiments to identify the CD163⁺-like RPM population in malaria.

4.2.1.3 Cure of *Plasmodium* infection does not recover CD163 expression on RPM

The data presented have shown that CD163 expressing RPMs themselves persist after a malaria infection, but fail to re-express CD163, however, the reason for this was still to be clarified. If residual parasites persist after clearance of the acute infection and prevent re-expression of CD163 on macrophages, then drug treatment to remove all remaining parasites might allow for the re-expression of CD163. Therefore, *P. chabaudi* infected mice were treated with chloroquine after the acute infection, to eliminate all parasites, and splenic macrophages followed over a time course of 90 days to determine if CD163 expression on RPM appeared again.

Following the parasitemia in this study showed an efficient clearance of the parasites upon chloroquine treatment. After two characteristic peaks of parasitemia within the first three weeks of the infection, chloroquine treatment clearly removed all parasites from the circulation, as parasitemia was indistinguishable from controls upon treatment. Minor deviations in the parasitemia at day 56 between the parasitemia curves of the control mice and the infected animals in the preliminary experiment may be the result of dysregulated erythropoiesis upon parasite-induced anemia (Dumarchey et al, 2022). Enhanced production of erythrocytes leads to the presence of immature erythroid cells in the circulation that have not yet extruded their nucleus (Buttarelo & Buttarelo, 2016) and will therefore intercalate Hoechst, which renders them indistinguishable from parasitized erythrocytes in this assay.

Splenic RPM were followed for one month (day 56 after initial *P. chabaudi* infection) and two months (day 90 after initial *P. chabaudi* infection) after chloroquine mediated clearance of the parasites. Interestingly, removal of the parasites did not rescue CD163 protein expression on the surface of RPM, in the preliminary experiment conducted. The expression of the scavenging receptor remained lost even long after chloroquine treatment and lasting clearance of parasitemia. This suggests that the exposure of splenic RPM to malaria parasites

may have a lasting impact on CD163 expression. This may be because the splenic environment is remodeled by the infection in such a way that the tissue niche actively suppresses CD163 expression on the macrophages. Newly incoming cells might therefore not have the capacity to resemble the original phenotype of the CD163⁺ RPM. That the tissue niche impacts macrophage function and phenotype has been demonstrated by others, showing that cell-cell interactions in the respective niche imprint tissue-specific identities of macrophages (Bonnardel et al, 2019). Bonnardel *et al* (2019) showed that repopulation of Kupffer cells to an empty niche in the liver, requires endothelial cells in the liver to release chemokines and adhesion molecules for the engraftment of monocytes. Subsequently, factors provided by hepatocytes are essential for the acquisition of the Kupffer cell-specific phenotype. In the context of this study, investigating alterations in the signaling of splenic stromal cells, could yield insight into changes of the splenic niche that impact macrophage function and phenotype.

4.2.1.4 Splenic RPM dynamics upon viral perturbations

Since the impact of malaria infection on splenic CD163-expressing RPM was so profound, it remained to be determined whether other systemic infections had the same impact on the splenic RPM populations.

LCMV is a commonly used model to study the impact of viral infection on the immune system. In the applied model of acute LCMV infection, viral titers usually decrease between day 4 and day 6 after infection (Müller et al, 2002). Thus, viral particles are rapidly cleared. Here, the effect of an LCMV infection on splenic RPM was investigated between one and 20 weeks after infection. A clear effect of viral infection on splenic CD163⁺ RPM was observed, while no significant changes were detected for CD163⁻ RPM throughout the time-course. Compared to uninfected controls, the number of CD163-expressing RPM was reduced in the spleen one week after the infection and this reduction lasted for 20 weeks. Thus,

upon LCMV infection, the expression of CD163 by splenic RPM was not entirely depleted, in contrast to the complete loss in the malaria infection models, but the number of CD163-expressing RPM was reduced and did not recover to control numbers long after the virus was cleared. Other studies have shown a tropism of the virus for the splenic marginal zone, with the viral titer being lower in genetic mouse models that have a disrupted splenic marginal zone (Müller et al, 2002). Thus, LCMV infection has an impact on the splenic RPM population, but these cells are not the primary target of the virus. In contrast, in a blood-stage malaria infection, the splenic RPM are involved in the phagocytosis of aberrant or parasitized erythrocytes. This could explain the differential impact of LCMV and *Plasmodium* infection on the phenotype of splenic RPM. However, the fact that the numbers of CD163⁺ RPM were lower after LCMV infection and did not recover to control levels, supports the idea that once this specific cell type is altered, the source of origin or the necessary environmental cues differ and are not sufficient to stimulate CD163 expression on RPM.

Others have shown that pro-inflammatory mediators, such as IFN γ and TNF α suppress the expression of CD163 (Buechler et al, 2000). For the acute LCMV infection-model used in this study, it has been described that the inflammatory cytokine response peaks after 24 - 48 h and normalizes after 78 h (Norris et al, 2013). This could explain the observed reduction of CD163-expressing cells in the acute LCMV-model. In contrast, the presence of inflammatory cytokines remains elevated in response to an ongoing malaria infection (Popa & Popa, 2021). Buechler *et al* (2000) further showed that anti-inflammatory cytokines, such as IL-10, lead to the upregulation of *Cd163* mRNA abundance. CD163 is assigned a functional role in anti-inflammatory immune responses. Therefore, a suppression of CD163-expression in the presence of pathogens could be advantageous for a persistent immune response.

4.2.1.5 Mechanisms of CD163 loss

Having shown that CD163 expression was reduced or lost upon infections and cannot be detected on the surface of macrophages after the resolution of the infection, pathways that could be responsible for the initial loss of CD163 were investigated. Blood-stage malaria causes severe hemolysis, making scavenging of free heme extremely relevant to prevent oxidative stress. The physiological mechanism by which the CD163 receptor scavenges free heme is via binding of a hemoglobin-haptoglobin complex, followed by endocytosis and recycling of iron. The receptor itself is then transported back to the cell surface under physiological conditions to capture further heme (Schaer et al, 2006). One possibility for the detected loss of the CD163 receptor is therefore, that the receptor persistently binds the hemoglobin-complex, which is present at high levels in the spleen upon malaria infection and is thus constantly internalized and not detectable on the cell surface. However, neither by labeling of fixed spleen tissue with fluorescent antibodies for imaging, nor by intracellular flow cytometry could the CD163 receptor be detected. Thus, internalization can be excluded as a reason for the loss of CD163.

Further downstream in the hemoglobin-CD163 pathway, heme is degraded by the enzyme heme-oxygenase to harmless byproducts and iron (Schaer et al, 2007). Byproducts are bilirubin, a pigment with antioxidant properties that can scavenge free radicals and carbon monoxide, which can act as a signaling molecule to modulate inflammation (Yang & Wang, 2022). Iron can be stored in a ferritin complex until utilized for the hemoglobin synthesis (Zhang *et al*, 2021). The iron content in the spleen tissue was followed in this study and was significantly decreased two weeks after *P. chabaudi* infection. This was mostly likely due to severe anemia, which is a common complication in malaria. Next to enhanced erythrocyte clearance in the spleen, dyserythropoiesis in the BM is a protective mechanism to deprive parasites of their replicative niche and required metabolites. Together, these factors both contribute to malaria anemia and thus the availability of heme and its bound iron (White, 2022; Spottiswoode et al, 2014). The destruction of RBCs is reversed and hemoglobin levels start to rise

as soon as the infection is controlled, otherwise patients require blood transfusions to prevent iron deficiencies, hypoxia and susceptibility to secondary infections (Spottiswoode et al, 2014). It would therefore be relevant to investigate the iron content later than 14 days post-infection, when the acute phase has passed and the parasites are controlled. Here, no major parasitemia peaks were detected after day 35, therefore an evaluation of the iron content at day 35 and day 56 after the infection could yield useful insight. Additionally, the iron content in other organs could be measured. If iron recycling is reduced in the spleen due to CD163 loss upon malaria infection, other organs might compensate and show increased iron deposits. A study that used a similar *P. chabaudi* infection-model, revealed the kidney as a promising candidate (Wu et al, 2023). Similar to the findings presented here, they showed that the iron content in the spleen decreased during the first peak of parasitemia, accompanied by a loss of circulating RBCs (anemia) and a reduction of RPMs. Wu *et al* (2023) further quantified the iron content in the kidneys and found a marked increase. They propose a re-allocation of the iron-storage to the kidney, while the iron-recycling capacity of splenic macrophages was overloaded during acute malaria infection. Sequencing data showed an upregulation of iron-regulatory genes in renal proximal tubule epithelial cells and *in vitro* studies confirmed that the presence of labile heme induced the expression of ferroportin 1 in those cells. Genetic depletion of ferroportin 1 in renal epithelial cells was associated with an increased mortality upon *P. chabaudi* infection. Wu et al (2023) revealed that renal epithelial cells undergo transcriptional re-programming and contribute to iron-recycling to prevent life-threatening malaria anemia. They further propose that iron is subsequently delivered to erythroblast islands in the spleen, thus the investigation of the splenic iron contents at later timepoints as well as the quantification of the iron content in the kidneys is a proposed future direction for this project.

Having excluded an internalization as the reason for the loss of the hemoglobin/haptoglobin-binding receptor CD163 on the surface of RPM and showing a reduction of the total iron content in the spleen upon infection, the role

of the malaria-toxin hemozoin on the expression of CD163 could be further investigated. Throughout the experimental time-course of 90 days, the dark coloration of hemozoin deposits persisted in the spleen. Either hemozoin deposits in the splenic environment negatively influence signaling pathways that would induce CD163 expression, or hemozoin might interact directly with the receptor and confer toxicity to the cells. Methods to follow hemozoin include immunohistochemical assays or flow cytometry with specific hemozoin-binding antibodies (Rebelo et al, 2013). The presence of hemozoin has been proposed as an indicator for malaria severity and new chip-based devices allow for a quick quantification in the sera of human patients (Baptista et al, 2022).

Another possibility for the loss of CD163-expression on RPM could be the shedding of the receptor from the macrophage surface. Shedding of CD163 and thus, increased concentrations of soluble CD163, have been reported in human malaria cases (Kusi et al, 2008). High serum levels were associated with a downregulation of inflammation and consequently a reduction of disease severity. Comparing the amount of soluble CD163 in the serum of uncomplicated patients with severe malaria patients showed that the concentration was higher in uncomplicated patients (Kusi et al, 2008). High concentrations of soluble CD163 might thus induce anti-inflammatory responses and avoid further complications during the infection. It was however not determined if CD163 was lost on macrophages at the site of inflammation in uncomplicated patients or if the receptor was still attached to the macrophage surface in patients with severe malaria, reflecting ongoing levels of higher inflammation (Kusi et al, 2008).

With the murine malaria model used in this study, the CD163 receptor was lost on splenic macrophages. Quantification of soluble CD163 in the serum of malaria infected mice 7 days after infection revealed that the concentration was lower in infected mice when compared to controls. However, it was shown by others that high expression of CD163 on macrophages is a characteristic response in the tissue to early-stage inflammation (Etzerodt & Moestrup, 2013), thus it would be relevant to analyze the serum at an earlier timepoint after the infection and

quantify soluble CD163. In addition, a quantitative analysis of soluble or membrane-bound CD163 in other tissues, which harbor CD163-expressing macrophages, such as the liver (Nielsen et al, 2020), would help to draw a systemic picture of CD163 dynamics upon malaria infection.

The soluble form of CD163 may be a biomarker for inflammatory diseases and the cell surface bound receptor on macrophages could be a therapeutic target for drug delivery, to direct macrophages in inflammatory diseases (Etzerodt & Moestrup, 2013). Next to chronic inflammation, cancer research has also begun to focus on macrophages as targets for immunotherapy. While macrophages in general show a high plasticity and comprise numerous types with different functions, the tumor microenvironment is rich in CD163-expressing macrophages (Park et al, 2016). Thus, CD163 targeting antibodies could direct tumoricidal drugs to CD163-expressing macrophages, as demonstrated in proof of principle pre-clinical studies with high efficiency and low toxicity (Skytthe et al, 2020). The CD163 receptor is therefore an exciting target for future research with many applications. Stimulating expression of the anti-inflammatory receptor CD163 after the acute phase of a malaria infection, could be advantageous and enhance tissue recovery and accelerate the return to its homeostatic state. *In vitro*, CD163 expression can be induced on monocytes upon stimulation with glucocorticoids, but not by treatment with IL-4, GM-CSF or IFN γ (Van Den Heuvel et al, 1999).

Splenic RPM play a critical role in the elimination of pathogens during malaria infection (Sengupta et al, 2019). This study has shown that RPM are heterogeneous and differentially impacted by infection. The loss of the CD163 receptor on splenic RPM could have adverse effects during subsequent infections.

To demonstrate whether CD163⁺ RPM have a homeostatic function that is related to iron homeostasis or whether their loss impairs immune function, mice that have recovered from a malaria episode could be re-infected with either another *Plasmodium* species or with another parasite, for example *Leishmania*. In comparison to a control group with naïve spleen tissue, this would yield insight

into the relevance of expression of CD163 by splenic RPM. Parasitemia read-outs would indicate if mice that lack CD163 expression after a malaria-infection, have a disadvantage and cannot clear pathogens with the same efficiency as control groups that have CD163⁺ RPM in the spleen.

4.2.2 Ontogeny and phenotype of splenic macrophages in the marginal zone and white pulp upon *P. chabaudi* infection

4.2.2.1. Marginal zone macrophages and marginal metallophilic macrophages

Spleen resident macrophages confer early defense against *Plasmodium* parasites (del Portillo et al, 2012). MZM and MMM are strategically located around the splenic marginal sinus, where infected RBC enter. They are considered important mediators of the adaptive immune response, because of their involvement in the processing and transfer of antigens to support humoral immune responses (Kraal & Mebius, 2006).

In particular, MZM are required for the maturation and regulation of germinal center B cells (Pirgova et al, 2020). In experimental animal hosts, the humoral immune response during the first peak of parasitemia relies on an adequate priming of B cells by antigen presenting cells (Meding & Langhorne, 1991).

Splenic MZM were identified via single-cell transcriptomics based on their expression of *Cd209b* and *Marco*. In addition, *Cxcl10* and *Siglech* were upregulated. *Cxcl10* is upregulated in response to IFN γ stimuli and in turn recruits further immune cells (Lee et al, 2009). Siglec-H is involved in the recognition and clearance of apoptotic cells and thereby helps to maintain immune tolerance (Schmitt et al, 2016). Gene ontology analysis uncovered that MZM modulate the assembly of cell junctions and positively regulate adhesion. Thereby, they likely provide structural support and modulate stability and plasticity within the tissue

(Collinet & Lecuit, 2013). MZM might play an important part in the regeneration of the splenic architecture after an acute malaria infection and are not directly involved in the clearance of the parasites, but rather act as secondary mediators that interact with lymphoid cells.

In the single-cell RNA-sequencing data, MMM were identified via the expression of signature genes for MMM identity: *Siglec1* and *Timd4* (den Haan & Kraal, 2012). The bulk of cells in the MMM cluster shifted location between the control and malaria samples, suggesting that *P. chabaudi* infection may have a lasting impact on the gene expression trajectories of MMM. Gene ontology terms revealed that MMM are predominantly involved in processing and presentation of antigens via MHC class I and the regulation of T-cell mediated cytotoxicity. That MMM can take up antigens and transfer them to CD8⁺ dendritic cells, which in turn activate T cells, has been demonstrated in other studies (Backer et al, 2010). Due to their strategic position at the marginal sinus, MMM can rapidly internalize blood-borne pathogens. Their close proximity to lymphocyte rich zones then favors a rapid activation of an adaptive immune response (Borges Da Silva et al, 2015).

The majority of MMM were EMP-derived, while MZM were shown by the DFM-model to be a very transient population with permanent influx of short-lived HSC-derived cells. Others claim that MMM and MZM only appear in the spleen between postnatal day 7 - 14 (A-Gonzalez & Castrillo, 2018). In contrast, our data show that a significant proportion of MMM are EMP-derived in steady-state. Immunofluorescent imaging analysis further showed the presence of CD169⁺ MMM already at postnatal day 7. In accordance with others, immunofluorescence analysis showed that the MMM only locate specifically in the splenic marginal zone after 3 - 4 weeks of age (A-Gonzalez et al, 2013).

The ontogeny of MMM is rather stable in the steady-state, but upon infection, the proportion of EMP-derived cells decreases, while HSC-derived cells infiltrate and differentiate to long-lived MMM. A transient loss of the marginal zone integrity was

shown via immunofluorescence analysis with fewer CD169⁺ cells and a fenestrated and disrupted structure of the marginal zone during the acute phase of malaria infection. This correlated with the loss of EMP-derived cells and an influx of HSC-derived cells. Therefore, it is likely that incoming cells are able to take over the position and function of MMM and restore the structure of the splenic marginal zone long-term. Others have shown that adoptive transfer of BM-derived cells could rescue the splenic marginal zone in a mouse model of genetically depleted marginal zone macrophages (A-Gonzalez et al, 2013).

Related studies showed a similar loss of the splenic integrity at day 10 after a *P. chabaudi* infection (Cadman et al, 2008). In addition, they showed that the splenic architecture was partially protected after *P. chabaudi* infection in *TLR4*^{-/-} and *TLR9*^{-/-} mice, compared to infected wildtype controls. It was hypothesized that infected RBC contain hemozoin, which is recognized by TLR9 and that membrane proteins of the parasite can be recognized by TLR2 and TLR4. They and others (Togbe et al, 2007) claim that a loss of TLR-expression is not associated with increased susceptibility to malaria infection, but instead that the receptor knockout can prevent changes in the spleen structure. While TLR-signaling mediates the release of inflammatory cytokines and thereby the recruitment of cells, it would be advisable to investigate if the knockout mice are protected from severe splenomegaly. Further, alterations in the splenic microenvironment contribute to lower B cell and T cell responses (Cadman et al, 2008). Considering the functional involvement of MMM in the processing of antigens for the initiation of adaptive immune responses (according to the single-cell RNA-sequencing data of this study), the importance of the splenic marginal zone integrity could be further investigated. If TLR-knockout mice protect the integrity of the marginal zone and thus MMM, the T cell response to a malaria-infection could be monitored with parasite-specific tetramers and compared to wildtype infected mice.

4.2.2.2 White pulp macrophages

One of the main functions of WPM is the phagocytosis of apoptotic lymphocytes. This prevents the presence of apoptotic cells, which can activate inflammatory reactions (den Haan & Kraal, 2012). The detection of CD4 genes in the WPM UMAP-cluster could be a result of their phagocytic uptake of T cells. The cellular components, including the genetic material, might not have been fully degraded and were captured by the sequencing method. It is also possible that T cells firmly attach to the macrophage surface and contaminate the sample (Hodne & Weltzien, 2015). The expression of CD4 has furthermore been described on nonlymphoid cells, especially on monocytes (Baba et al, 2006), which could give rise to CD4-expressing WPM in the spleen. Complement related genes and metalloproteases were also upregulated in WPM. The activation of the complement system triggers an enzymatic cascade that results in the covalent attachment of complement proteins to the surface of pathogens, which subjects them to phagocytosis. Complement components can further act as chemo-attractants to recruit phagocytes (Charles A Janeway et al, 2001c).

Gene ontology analysis suggested that WPM are involved in the processing and presentation of antigens as well as in the differentiation of lymphocytes and the activation of T cells. The strategic location of WPM in the B cell and T cell zones in the spleen allows for tight interactions.

Macrophages found in the white pulp of the spleen are similar to tingible body macrophages found in the germinal centers of the lymph node. They can capture antigens to initiate lymphocyte effector functions (den Haan & Kraal, 2012). In the lymph node follicles, germinal center reactions eventually lead to a specific humoral immune response, but also cause cell death of maturing B cells. The main task of tingible body macrophages is the clearance of those apoptotic B cells to prevent necrosis and autoimmune activation through the release of intracellular self-antigens. Tingible body macrophages are non-migratory and capture cell fragments via cytoplasmic processes. Similar to the WPM in the spleen, they are characterized by high expression of the phagocytosis receptor MerTK. The functional relevance of the receptor was demonstrated in *Mertk*^{-/-} mice, by impaired clearance of apoptotic cells (Grootveld et al, 2023).

Lineage tracing with a CD169-reporter mouse line showed labeling of tingible body macrophages, but no expression of CD169 (Grootveld et al, 2023). Thus, the authors assume that tingible body macrophages originate from long-lived lymph node-resident cells that express MerTK, CD68 and Cx3cr1. Similar to the WPM in this project, they identified lymph node tingible body macrophages as CD11b⁺, CD169⁻, MerTK⁺ cells. Grootveld *et al* (2023) further showed the majority of tingible body macrophages were derived from non-CCR2-expressing tissue-resident cells in the lymph node, but that CCR2-expressing cells can contribute to the pool of tingible body macrophages. The high plasticity of macrophages however, made it difficult to study the dynamics upon immunization and germinal center formation.

The novel DFM mouse model used in this project is advantageous for the delineation of macrophage fates and origins. It was shown that WPM originate mostly from HSC-derived cells and differentiate into long-lived macrophages in the spleen. Others claim that the HSC-derived WPM only appear in the white pulp when the germinal centers form in the spleen after weaning upon contact with the external environment (A-Gonzalez & Castrillo, 2018). Together with the insight of Grootveld et al (2023), that tingible body macrophages originate from a CD169-expressing precursor and the findings of this project that CD169⁺ splenic MMM are mostly EMP-derived, this could hint towards a so far unrecognized developmental trajectory of splenic WPM, which might diverge from EMP-derived CD169⁺ precursor cells and populate the white pulp after birth. The DFM model showed that the majority of WPM originate from HSC-derived cells that differentiate into long-lived tissue resident cells, similar to the CCR2-dependent replenishment of tingible body macrophages by monocyte-derived cells, which was described by Grootveld et al (2023). But the detected 30 - 40 % of EMP-derived WPM in steady-state, could originate from a similar EMP-derived precursor as splenic CD169⁺ MMM.

In comparing the WPM population in steady-state controls to the ontogeny of WPM upon *P. chabaudi* infection, no major differences were detected. Since the number of WPM varied in the control groups, repeating the experiments with larger cohorts would allow for more precise conclusions about the impact of

malaria infection on splenic WPM. A trend of recovery of EMP-derived WPM was described after the acute phase of the infection (after day 35). When the splenic architecture begins to recover, the distinct environmental niches that support macrophage maintenance and function (Guilliams & Scott, 2017) may reestablish to support the recovery of EMP-derived WPM to steady-state levels.

4.2.3 Conclusions regarding aim 2

The dynamics of splenic macrophages during blood-stage malaria were described. Focusing on RPM, the expression of the hemoglobin-binding receptor CD163, which facilitates the downstream recycling of iron, was lost upon infection, but sequencing data showed that this population persisted. Icam-1 was predicted as an additional surface-marker to identify this population in future experiments. The CD163-negative RPM population became successively replaced by HSC-derived cells during the course of the infection.

Focusing on macrophages in the splenic white pulp and marginal zone, their developmental origin could be resolved with the novel DFM-model. The EMP-derived origin of most MMM in steady-state was demonstrated and a new developmental trajectory was proposed for WPM.

4.3 Delineating macrophage interaction and signaling pathways in malaria via the genetic depletion of receptors or sub-populations

As already mentioned, macrophages play crucial roles during homeostatic tissue processes and in the management of infections (Ponzoni et al, 2018). The genetic depletion of a specific macrophage subtype or an important signaling molecule, allows for the study of their respective role in diseases in greater detail (Hua et al, 2018).

4.3.1 Genetic depletion of the CD163 receptor on macrophages in the context of *P. chabaudi* infection

The previous chapter clearly demonstrated a profound impact of the infection with blood-stage *P. chabaudi* and other murine parasite species on splenic RPM, causing a loss of CD163 expression on RPM. Therefore, a global CD163-knockout mouse model (CD163KO) was used to study the relevance of the absence of CD163 on malaria progression. Preliminary experiments in which parasitemia was compared between CD163KO and wildtype animals revealed that the absence of CD163 expression may not have a major impact on the clearance of parasites from the circulation. The peak of parasitemia was comparable between CD163KO and wildtype mice with respect to the degree of parasitemia, but preliminary studies indicated a temporal shift (because the first peak appeared delayed in CD163KO compared to wildtype infected mice). These data suggest that the CD163 receptor may not be involved in the clearance of parasites themselves, but might rather be important to clear malaria-associated debris, mostly free heme (Onofre et al, 2009). *Plasmodium* parasites cause enhanced hemolysis and the release of free heme which is associated with oxidative stress and inflammation (Mooney et al, 2018). In cases of human *P. falciparum* malaria, individuals with higher levels of regulatory molecules,

including IL10 and CD163, show less severe disease progression and monocytes isolated from those individuals exhibited attenuated inflammatory cytokine responses upon re-exposure to the parasites *in vitro* (Guha et al, 2020).

Thus, it is reasonable to propose that the degree of parasitemia is similar between wildtype and CD163KO mice, as the receptor does not directly participate in the clearance of the parasites, but has anti-inflammatory properties through the binding of hemoglobin and thus preventing oxidative damage by free heme (di Masi et al, 2020). This is an important function in the context of blood-borne infections and has significant relevance for the resolution of the disease and the recovery of the physiological conditions in the host.

The absence of CD163 expression did not have an impact on the splenic structure in steady-state conditions. The marginal zone was clearly visible and separated the white pulp from the red pulp with the F4/80 signal for splenic RPM evenly distributed throughout the red pulp in immunofluorescent images.

In contrast, preliminary experiments suggest that the absence of CD163 expression might have an impact on the anatomical structure of the spleen upon *P. chabaudi* malaria infection. During the acute infection, at day 14 after the administration of *P. chabaudi*, the marginal zone was not detected in immunofluorescent imaging of the spleen of CD163KO mice. Wildtype mice that were infected with the same batch of parasites showed the previously described disrupted and fenestrated appearance of the marginal zone, but the CD169 signal was still detectable.

It remains to be investigated if the splenic marginal zone of CD163KO mice recovers at later timepoints. In wildtype animals it was shown that the marginal zone had recovered and formed a closed circular structure around the splenic white pulp area again 90 days after *P. chabaudi* infection. These data hint toward an important homeostatic function of the CD163 receptor that supports the splenic microenvironment, which warrants further investigation.

To further investigate the functional relevance of the CD163 receptor in the spleen, in terms of hemoglobin scavenging function, wildtype and CD163KO mice

could be challenged with a chemical to induce hemolysis (Martin Shetlar & Allen, 1985). Phenylhydrazine has been used in other studies to induce acute hemolysis and follow iron levels in serum and tissue (Masaratana et al, 2012). Preliminary data suggested that the CD163 receptor might not be directly relevant for the clearance of parasites. Instead, it is proposed to prevent oxidative damage by free heme through the binding and uptake of hemoglobin-haptoglobin complexes (Thomsen et al, 2013), which are increased in the circulation upon a malaria infection due to hemolytic events (White, 2018). A *Plasmodium* infection causes a transient depletion of erythrophagocytic macrophages (Wu et al, 2023), which leads to intravascular hemolysis and the release of non-covalently bound heme. When heme is only loosely associated to plasma proteins, this fails to control the redox activity of its contained iron (Gouveia et al, 2017). Labile heme has been described to catalyzes the pathogenesis of severe malaria (Wu et al, 2023) and patients with severe malaria have a significantly higher concentration of labile heme compared to uncomplicated cases (Ramos et al, 2024). Although the affinity of the CD163 receptor is towards hemoglobin-complexes, the persistent absence of the receptor upon a malaria infection, could have a severe impact on iron metabolism and subsequent hemolytic diseases in patients. In the proposed model, CD163KO mice would mimic the post-malaria phenotype and chemically induced hemolysis might challenge the CD163-mediated scavenging pathway. In comparison to wildtype mice that express CD163, this assay would reveal if other redundant mechanisms can compensate for the loss of CD163 expression or if CD163 is important for controlling responses to secondary complications that induce hemolysis, such as a repeated malaria episode.

Other studies have investigated the relevance of CD163 on different diseases. In a collagen-induced arthritis model, CD163KO mice had higher arthritis scores and prolonged disease progression (Svendsen et al, 2020). Upon bacterial challenge with *S. aureus*, CD163KO mice were more susceptible to the infection (Fabriek et al, 2009). And in a model of allergic dermatitis CD163KO mice showed stronger inflammation. Thus, the regulatory and anti-inflammatory properties of

the CD163 receptor might leave individuals more susceptible to secondary infection when the receptor is lost upon blood-stage malaria infection.

4.3.2 Depletion of Lxra-dependent macrophages in the splenic marginal zone in the context of *P. chabaudi* infection

Since *P. chabaudi* infection in wildtype and CD163KO mice indicated that CD163 may have an impact on the integrity of the splenic marginal zone, the function of the splenic marginal zone was tested in a conditional knockout mouse model for the Lxra-dependent MMM and MZM. It was previously reported that the macrophages in the splenic marginal zone (MMM and MZM) specifically rely on the nuclear receptor Lxra, while other splenic macrophages are not affected by the absence of Lxra (A-Gonzalez et al, 2013). Different from the aforementioned study, which used a global Lxra knockout, here a conditional knockout that depletes Lxra specifically in *Tnfrsf11a*-expressing tissue macrophages was used (*Tnfrsf11a*^{Cre/+}; *Lxra*^{flox/flox}: here LxraKO).

In the absence of MMM and MZM (LxraKO) the parasitemia was higher compared to *P. chabaudi* infected littermate controls (*Tnfrsf11a*^{+/+}; *Lxra*^{flox/flox}: here LxraWT). Thus, the marginal zone macrophage populations might have a direct impact on the clearance of *Plasmodium* parasites. Although the main parasite scavenging function is assigned to splenic RPM, MMM and MZM play an important role in infectious diseases (Borges Da Silva et al, 2015). The SIGNR1 receptor, expressed on MZM binds yeast particles and bacteria and can activate the classical complement pathway (Kang et al, 2006). The scavenger receptor MARCO is expressed on different macrophage populations but is especially highly expressed on MZM. MARCO mediates the uptake of gram-negative bacteria and enhances phagocytosis activity (Chen et al, 2010). Removal of MMM and MZM with low dose clodronate liposomes in a *Listeria* infection model, showed that both marginal zone macrophage populations are dispensable as

antigen-presenting cells for the initiation of T cell responses (Aichele et al, 2003). On the other hand, their strategic location at the interface between the bloodstream and lymphocyte-rich zones in the spleen, makes them suitable for bridging the innate and adaptive immune responses. Splenic MMM for instance transfer antigens to CD8 α ⁺ dendritic cells and collaborate to activate cytotoxic T cells (Backer et al, 2010).

The involvement of MMM in the initiation of an adaptive immune response could be an explanation for the higher parasitemia in LxraKO mice. The major peak in parasitemia is observed 10 days after the *P. chabaudi* infection. Upon first antigen encounter it takes approximately one week until effector T cells are primed, expand and accumulate at the site of infection (Sun et al, 2023). Because this pathway is intact in LxraWT mice, the adaptive control of parasitemia might be better than in LxraKO littermates. The pathway of MMM-mediated antigen transfer for the priming of an adaptive immune response is impaired in LxraKO mice which could be an explanation for higher parasitemia.

Both MMM and MZM express high levels of Tim4, which was used for their identification in the Lxra model of this study. In LxraWT uninfected control mice, stable counts of Tim4⁺ marginal zone macrophages were detected. Both Tim4⁺ splenic marginal zone macrophage populations were absent in LxraKO mice, irrespective of the treatment (PBS or infected with *P. chabaudi*). Minimal residual cell numbers that were detected via flow cytometry in uninfected LxraKO, could result from the conditional depletion model, which might differ from a global knockout model as it is not 100 % efficient. Immunofluorescent images confirmed the absence of the marginal zone macrophages in LxraKO mice 14 days after *P. chabaudi* infection, while a dim signal of the disrupted marginal zone was visible in infected LxraWT mice.

Surprisingly, the absence of marginal zone macrophages in the steady-state also had an impact on CD163 expression on RPM. The numbers of CD163⁺ RPM in uninfected controls were significantly reduced in LxraKO mice compared to

LxraWT mice. It can be postulated that splenic macrophages in the red pulp and marginal zone may influence each other. Macrophage-macrophage interactions with anti-inflammatory properties have been demonstrated in other studies (Nakamura et al, 2023). Nakamura *et al* (2023) showed that acetylcholine signaling in the spleen enhances macrophage interactions, which in turn reduces TNF α signaling and has protective effects towards inflammatory kidney diseases.

An intact macrophage network is crucial for an adequate innate immune response upon infection. This study has shown that the loss of a specific subtype of macrophages within the spleen can impact the progression and recovery of diseases, such as *P. chabaudi*-induced blood-stage malaria. Understanding these pathways in detail will help to stimulate or suppress specific pathways in order to ameliorate the disease outcome.

4.3.3 Conclusions regarding aim 3

Genetic depletion of the CD163-receptor had no impact on parasitemia, which suggested that the receptor is not primarily involved in parasite clearance during malaria infection. Instead, the absence of the receptor had an impact on the recovery of the integrity of the splenic marginal zone upon infection. The depletion of both marginal zone macrophage populations on the other hand resulted in reduced numbers of CD163⁺ RPM in steady-state and higher parasitemia upon malaria infection.

4.4 The cellular dynamics in the bone marrow and blood during blood-stage malaria

In blood-stage malaria, infected red blood cells are mostly removed when they pass through the spleen. Challenges, such as malaria infection, require an adaptation of the hematopoietic output from the bone marrow to ensure efficient elimination of the pathogens (Fanti et al, 2023).

4.4.1 Adaptation of stem- and progenitor cells in the bone marrow to blood-stage infection with *P. chabaudi*

Hematopoiesis is a tightly regulated process with a controlled output in physiological conditions. LT-HSC comprise the top of the hematopoietic hierarchy and are mostly quiescent, but have the capacity to self-renew or differentiate. They can give rise to the whole repertoire of hematopoietic cells (Zhao & Baltimore, 2015). Unique adaptations of LT-HSC protect the lifelong production of blood cells (Zhao et al, 2023).

Comparing the LT-HSC population in the BM between *P. chabaudi* infected mice and uninfected controls revealed that parasitic infection does not have a major impact on LT-HSC. Similar studies of systemic infections showed that LT-HSC do not expand in a sepsis model (Fanti et al, 2023). A minimal rise of LT-HSC was observed at day 4 after *P. chabaudi* infection. It has been shown that HSC are vulnerable to ferroptosis (Zhao et al, 2023). An increase in iron ions, as a result of parasite induced hemolysis, could cause oxidative stress in LT-HSC, but they quickly revert to their quiescent state. Overall, the LT-HSC niche is well protected from inflammatory challenges. Their quiescent state is required to prevent exhaustion of LT-HSC and ensure maintenance of the whole hematopoietic system (Singh et al, 2020).

The necessary cellular output to satisfy the increased demand of effector cells must therefore be delivered by cells further downstream the hematopoietic

hierarchy. ST-HSC expand between day 4 and day 7 after infection with *P. chabaudi* and normalize after two weeks. This correlates with the expansion of all multipotent progenitor populations. MPP2 and MPP3 expand with a peak at day 7 after the infection. The temporal delay of MPP expansion reflects the hematopoietic hierarchy. ST-HSC expand already at day 4 after the infection. They give rise to MPPs, which expand one week after *P. chabaudi* infection and normalize after two weeks. In a model of a systemic bacterial infection, it was similarly demonstrated that MPPs further downstream the hematopoietic hierarchy respond to the infection and proliferate to enhance the release of effector cells (Fanti et al, 2023).

Downstream the hematopoietic hierarchy, MPPs give rise to CMPs, from which MEPs and GMPs emerge (Paudel et al, 2022). In many bacterial infections, emergency granulopoiesis occurs and leads to an expansion of GMPs, to sustain the high neutrophil demand in peripheral tissues. Since the intracellular malaria parasites might not primarily require a neutrophil response, this could explain why the GMP population did not expand upon *P. chabaudi* infection.

In general, the hematopoietic system rapidly adapts to acute infections. The state of emergency hematopoiesis was described in inflammation, bleeding and radiation (Boettcher & Manz, 2017). Various stimuli then increase the hematopoietic output. Next to paracrine signaling in the stem cell niche, the expansion of progenitor cells in the BM can be induced by inflammatory cytokines, such as TNF α and IL-6 (Bernad et al, 1994). IL-1 signaling, which is dispensable for homeostatic hematopoiesis, drives emergency myelopoiesis in acute infections (Mantovani et al, 2019). The bias towards myelopoiesis and the enhanced output of innate immune cells happens at the expense of lymphoid cells and erythrocytes (Zhao & Baltimore, 2015). Therefore, it is likely that emergency myelopoiesis during an acute malaria episode is one of the reasons for the lasting anemia, as one of the main complications during a malaria infection.

Overall, a rapid response of stem- and progenitor cells following infection allows for early intervention and containment of pathogens. But the activation of the stem- and progenitor cells can have short- and long-term impacts on the preservation of the stem cell niche (Essers et al, 2009).

4.4.2 The impact of *P. chabaudi* blood-stage malaria on circulating immune cells in the blood

During the blood-stage of malaria infection, the parasites proliferate inside erythrocytes and are recognized and cleared by the blood filtering function of the spleen. The blood is also the route of transport for delivery of effector cells to infectious sites and organs. Progenitors in the bone marrow provide the hematopoietic output for those effector cells, which are mobilized and enter the circulation (Paudel et al, 2022).

Upon *P. chabaudi* infection, no major changes in the numbers of circulating lymphocytes were detected in comparison to uninfected controls. The spleen is the critical organ for parasite clearance during a blood-stage malaria infection. It is likely that B cells and T cells are activated and proliferate locally in the spleen, because the spleen itself is a secondary lymphoid organ. Thus, antigen presentation and lymphocyte priming takes place in the parenchyma (Lewis et al, 2019). Both a cellular and humoral adaptive immune response are essential to limit the progression to severe malaria. An immune response of CD8⁺ cytotoxic T-cells, depends on the help of CD4⁺ T-cells (Fernandez-Ruiz et al, 2017; Bedoui et al, 2016). CD4⁺ T-cells play a central role during the erythrocytic stage of the infection and the elimination of infected RBC. They produce IFN γ to control the acute infection and support the activation of a protective B-cell response (Perez-Mazliah & Langhorne, 2014).

Furthermore, circulating granulocytes did not differ in the blood of *P. chabaudi* infected mice when compared to steady-state controls. The most abundant type of granulocytes are neutrophils. In general, neutrophils are involved in the defense of bacterial and fungal infections, while less abundant eosinophils respond to parasites. It has been described that the neutrophil response to *Plasmodium* parasites compromises their antibacterial functions, rendering patients more susceptible to secondary infections (Pollenus et al, 2022).

It has been described in previous chapters that splenic macrophages are strongly impacted by blood-stage malaria infection. While certain populations changed, or lost expression of key molecules, others expanded during the progression of the disease. Spleen resident macrophages themselves have been reported to be involved in signaling that leads to the recruitment of effector cells during acute immune responses (Borges Da Silva et al, 2015). For example, MMM take up apoptotic cells, whereupon they release CCL22, which recruits regulatory T cells and dendritic cells (Ravishankar et al, 2014). In a sepsis model, it was shown that myelopoiesis is controlled by IL-3, which causes higher production of monocytes in the bone marrow (Schultze et al, 2019). Circulating monocytes were followed in the blood stream during *P. chabaudi* infection. Monocytes are heterogeneous (Menezes et al, 2016); classical Ly6C⁺ monocytes can upregulate MHCII during their maturation and are critical during inflammatory responses, while patrolling monocytes maintain vascular homeostasis (Narasimhan et al, 2019). Patrolling and classical Ly6C⁺ monocytes in the blood were not affected by *P. chabaudi* malaria infection. In contrast, MHCII monocytes expand within the first week of the infection and only normalize after one month. The expansion of MHCII monocytes in the blood correlates with the time course of precursor expansion in the bone marrow. Precursor cells in the bone marrow proliferate within the first week of infection and subsequently the number of circulating monocytes increases in the blood. A significant proportion of these monocytes might extravasate into the spleen and replace the red pulp macrophages, which expand between day 14 and day 56 after the infection. Phagocytes in the spleen have been reported to be constantly replenished by bone marrow derived progenitors

during a malaria infection (Vallelian et al, 2022a). The adaptation to an increased monocyte output might shift differentiation trajectories in the bone marrow at the expense of dendritic cells and contribute to secondary immunodeficiencies (Vallelian et al, 2022a).

4.4.3 Conclusions regarding aim 4

LT-HSC were not affected by the parasitic infection. Downstream the hematopoietic hierarchy, ST-HSC and MMPs expanded early after the infection and quickly normalized within two weeks. In the circulation this led to increased numbers of MHCII⁺ monocytes until day 35 after *P. chabaudi* infection.

5 Conclusion

In summary, this thesis has resolved the different developmental origins of distinct macrophage subtypes in the spleen with a novel fate-mapping model and identified a so far unrecognized CD163-dependent heterogeneity amongst splenic RPM.

Splenic CD163⁺ and CD163⁻ RPM showed different developmental trajectories and responded differently to the challenge of a malaria infection. While CD163-expressing macrophages were depleted early after the infection with different murine *Plasmodium* species, CD163⁻ RPM were replenished by HSC-derived cells. Shedding and internalization were excluded as a reason for the loss of the CD163 receptor. The expression of the CD163 receptor could not be rescued by curing the mice with chloroquine. A viral infection model demonstrated a lasting reduction instead of an entire depletion of CD163 expression. Transcriptomic data validated a downregulation of CD163 expression in malaria, but a persistent cell CD163⁺ RPM-like population.

Genetic depletion of the CD163 receptor did not have an impact on parasitemia, but did affect the splenic micro-architecture. Thus, the CD163 receptor, which is involved in iron recycling pathways, might rather have homeostatic functions that support tissue maintenance and homeostasis than being involved in pathogen clearing.

The fact that splenic macrophage subsets populate the organ at different developmental stages and originate from different progenitors leads to the assumption that splenic macrophage turnover during malaria progression and the resulting repopulation by cells of different origins could impact organ function and affect disease progression.

Changes in the splenic macrophage niche due to the infection might not enable infiltrating cells that replenish the empty niche to express the CD163 receptor. CD163 is assigned anti-inflammatory properties and the presence of the receptor is associated with better prognosis in human malaria. Having identified this novel heterogeneity in the splenic RPM population and their distinct developmental

origin, this knowledge could help to exploit CD163 as a new target and potentially restore its expression to amelioration of disease.

It is likely that the absence of the CD163 receptor is advantageous during the early acute phase of infections, to ensure an inflammatory response and recruitment of effector cells for efficient elimination of pathogens. But the receptor might be relevant for tissue recovery after an episode of severe inflammation. Thus, enhancing or promoting CD163 expression after peak parasitemia could support the recovery to a homeostatic state and prevent lasting tissue injuries.

References

- Abdel-Hakeem MS (2019) Viruses Teaching Immunology: Role of LCMV Model and Human Viral Infections in Immunological Discoveries. *Viruses* 11
- A-Gonzalez N, Bensinger SJ, Hong C, Beceiro S, Bradley MN, Zelcer N, Deniz J, Ramirez C, Díaz M, Gallardo G, *et al* (2009) Apoptotic cells promote their own clearance and immune tolerance through activation of LXR. *Immunity* 31: 245
- A-González N & Castrillo A (2011) Liver X receptors as regulators of macrophage inflammatory and metabolic pathways. *Biochim Biophys Acta* 1812: 982–994
- A-Gonzalez N & Castrillo A (2018) Origin and specialization of splenic macrophages. *Cell Immunol* 330: 151–158
- A-Gonzalez N, Guillen JA, Gallardo G, Diaz M, De La Rosa J V., Hernandez IH, Casanova-Acebes M, Lopez F, Tabraue C, Beceiro S, *et al* (2013) The nuclear receptor LXR α controls the functional specialization of splenic macrophages. *Nat Immunol* 14: 831–839
- Aguilar R, Magallon-Tejada A, Achtman AH, Moraleda C, Joice R, Cisteró P, Li Wai Suen CSN, Nhabomba A, Macete E, Mueller I, *et al* (2014) Molecular evidence for the localization of plasmodium falciparum immature gametocytes in bone marrow. *Blood* 123: 959–966
- Aichele P, Zinke J, Grode L, Schwendener RA, Kaufmann SHE & Seiler P (2003) Macrophages of the Splenic Marginal Zone Are Essential for Trapping of Blood-Borne Particulate Antigen but Dispensable for Induction of Specific T Cell Responses. *The Journal of Immunology* 171: 1148–1155

- Al-Daccak R, Mooney N & Charron D (2004) MHC class II signaling in antigen-presenting cells. *Curr Opin Immunol* 16: 108–113
- Aldulaimi S & Mendez AM (2021) Splenomegaly: Diagnosis and Management in Adults. *Am Fam Physician* 104: 271–276
- Álvarez-Aznar A, Martínez-Corral I, Daubel N, Betsholtz C, Mäkinen T & Gaengel K (2020) Tamoxifen-independent recombination of reporter genes limits lineage tracing and mosaic analysis using CreERT2 lines. *Transgenic Res* 29: 53–68
- Anwar A, Keating AK, Joung D, Sather S, Kim GK, Sawczyn KK, Brandão L, Henson PM & Graham DK (2009) Mer tyrosine kinase (MerTK) promotes macrophage survival following exposure to oxidative stress. *J Leukoc Biol* 86: 73
- Ashley EA & White NJ (2014) The duration of Plasmodium falciparum infections. *Malar J* 13
- Baba T, Ishizu A, Iwasaki S, Suzuki A, Tomaru U, Ikeda H, Yoshiki T & Kasahara M (2006) CD4⁺/CD8⁺ macrophages infiltrating at inflammatory sites: a population of monocytes/macrophages with a cytotoxic phenotype. *Blood* 107: 2004–2012
- Backer R, Schwandt T, Greuter M, Oosting M, Jüngerkes F, Tütting T, Boon L, O'Toole T, Kraal G, Limmer A, *et al* (2010) Effective collaboration between marginal metallophilic macrophages and CD8⁺ dendritic cells in the generation of cytotoxic T cells. *Proc Natl Acad Sci U S A* 107: 216–221
- Banerjee R, Khandelwal S, Kozakai Y, Sahu B & Kumar S (2015) CD47 regulates the phagocytic clearance and replication of the Plasmodium yoelii malaria parasite. *Proc Natl Acad Sci U S A* 112: 3062–3067

- Baptista V, Peng WK, Minas G, Veiga MI & Catarino SO (2022) Review of Microdevices for Hemozoin-Based Malaria Detection. *Biosensors (Basel)* 12
- Basu S & Sahi PK (2017) Malaria: An Update. *Indian J Pediatr* 84: 521–528 doi:10.1007/s12098-017-2332-2 [PREPRINT]
- Becht E, McInnes L, Healy J, Dutertre CA, Kwok IWH, Ng LG, Ginhoux F & Newell EW (2018) Dimensionality reduction for visualizing single-cell data using UMAP. *Nature Biotechnology* 2018 37:1 37: 38–44
- Bedoui S, Heath WR & Mueller SN (2016) CD4(+) T-cell help amplifies innate signals for primary CD8(+) T-cell immunity. *Immunol Rev* 272: 52–64
- Bergmann-Leitner ES, Legler PM, Savranskaya T, Ockenhouse CF & Angov E (2011) Cellular and humoral immune effector mechanisms required for sterile protection against sporozoite challenge induced with the novel malaria vaccine candidate CeTOS. *Vaccine* 29: 5940–5949
- Bernad A, Kopf M, Kulbacki R, Weich N, Koehler G & Gutierrez-Ramos JC (1994) Interleukin-6 is required in vivo for the regulation of stem cells and committed progenitors of the hematopoietic system. *Immunity* 1: 725–731
- Bhat MY, Solanki HS, Advani J, Khan AA, Keshava Prasad TS, Gowda H, Thiyagarajan S & Chatterjee A (2018) Comprehensive network map of interferon gamma signaling. *J Cell Commun Signal* 12: 745
- Bianco AE, Favaloro JM, Burkot TR, Culvenor JG, Crewther PE, Brown G V., Anders RF, Coppel RL & Kemp DJ (1986) A repetitive antigen of Plasmodium falciparum that is homologous to heat shock protein 70 of Drosophila melanogaster. *Proc Natl Acad Sci U S A* 83: 8713–8717

- Le Blanc S, Garrick MD & Arredondo M (2012) Heme carrier protein 1 transports heme and is involved in heme-Fe metabolism. *Am J Physiol Cell Physiol* 302
- Boettcher S & Manz MG (2017) Regulation of Inflammation- and Infection-Driven Hematopoiesis. *Trends Immunol* 38: 345–357
- Boldogh I, Albrecht T & Porter DD (1996) Persistent Viral Infections. *Medical Microbiology*
- Bonnardel J, T'Jonck W, Gaublomme D, Browaeys R, Scott CL, Martens L, Vanneste B, De Prijck S, Nedospasov SA, Kremer A, *et al* (2019) Stellate Cells, Hepatocytes, and Endothelial Cells Imprint the Kupffer Cell Identity on Monocytes Colonizing the Liver Macrophage Niche. *Immunity* 51: 638-654.e9
- Bonthius DJ (2012) Lymphocytic choriomeningitis virus: An under-recognized cause of neurologic disease in the fetus, child, and adult. *Semin Pediatr Neurol* 19: 89
- Borges da Silva H, Fonseca R, Cassado A dos A, Machado de Salles É, de Menezes MN, Langhorne J, Perez KR, Cuccovia IM, Ryffel B, Barreto VM, *et al* (2015) In vivo approaches reveal a key role for DCs in CD4+ T cell activation and parasite clearance during the acute phase of experimental blood-stage malaria. *PLoS Pathog* 11
- Borges Da Silva H, Fonseca R, Pereira RM, Cassado AA, Álvarez JM & D'Império Lima MR (2015) Splenic macrophage subsets and their function during blood-borne infections. *Front Immunol* 6 doi:10.3389/fimmu.2015.00480 [PREPRINT]
- Boutet M, Benet Z, Guillen E, Koch C, M' S, Soudja H, Delahaye F, Fooksman D & Lauvau G (2021) Memory CD8 + T cells mediate early pathogen-specific

protection through localized delivery of chemokines and IFN γ to clusters of inflammatory monocytes. *bioRxiv*: 2021.03.01.433468

Brender E, Burke A & Glass RM (2005) The spleen. *J Am Med Assoc* 294: 2660

Bronte V & Pittet MJ (2013) The spleen in local and systemic regulation of immunity. *Immunity* 39: 806

Bruch-Oms M, Olivera-Salguero R, Mazzolini R, del Valle-Pérez B, Mayo-González P, Beteta Á, Peña R & García de Herreros A (2023) Analyzing the role of cancer-associated fibroblast activation on macrophage polarization. *Mol Oncol* 17: 1492–1513

Bryceson A, Fakunle YM, Fleming AF, Crane G, Hutt MSR, de Cock KM, Greenwood BM, Marsden P & Rees P (1983) Malaria and splenomegaly. *Trans R Soc Trop Med Hyg* 77: 879

Buechler C, Ritter M, Orsó E, Langmann T, Klucken J & Schmitz G (2000) Regulation of scavenger receptor CD163 expression in human monocytes and macrophages by pro- and antiinflammatory stimuli. *J Leukoc Biol* 67: 97–103

Buffet PA, Safeukui I, Deplaine G, Brousse V, Prendki V, Thellier M, Turner GD & Mercereau-Puijalon O (2011) The pathogenesis of *Plasmodium falciparum* malaria in humans: insights from splenic physiology. *Blood* 117: 381–392

Busch K, Klapproth K, Barile M, Flossdorf M, Holland-Letz T, Schlenner SM, Reth M, Höfer T & Rodewald H-R (2015) Fundamental properties of unperturbed haematopoiesis from stem cells in vivo. *Nature* 518: 542–546

- Buttarelo M & Buttarelo M (2016) Laboratory diagnosis of anemia: are the old and new red cell parameters useful in classification and treatment, how? *Int J Lab Hematol* 38: 123–132
- Cadman ET, Abdallah AY, Voisine C, Sponaas AM, Corran P, Lamb T, Brown D, Ndungu F & Langhorne J (2008) Alterations of Splenic Architecture in Malaria Are Induced Independently of Toll-Like Receptors 2, 4, and 9 or MyD88 and May Affect Antibody Affinity. *Infect Immun* 76: 3924
- Calkin AC & Tontonoz P (2012) Transcriptional integration of metabolism by the nuclear sterol-activated receptors LXR and FXR. *Nat Rev Mol Cell Biol* 13: 213–224
- Campos MAS, Almeida IC, Takeuchi O, Akira S, Valente EP, Procópio DO, Travassos LR, Smith JA, Golenbock DT & Gazzinelli RT (2001) Activation of Toll-Like Receptor-2 by Glycosylphosphatidylinositol Anchors from a Protozoan Parasite. *The Journal of Immunology* 167: 416–423
- Carter R (1972) Effect of PABA on chloroquine resistance in *Plasmodium berghei yoelii*. *Nature* 238: 98–99
- Carter R & Walliker D (1975) New observations on the malaria parasites of rodents of the Central African Republic - *Plasmodium vinckei petteri* subsp. nov. and *Plasmodium chabaudi* Landau, 1965. *Ann Trop Med Parasitol* 69: 187–196
- Cesta MF (2006) Normal Structure, Function, and Histology of the Spleen. *Toxicol Pathol* 34: 455–465
- Cesta MF (2016) Normal Structure, Function, and Histology of the Spleen: <http://dx.doi.org/10.1080/01926230600867743> 34: 455–465

Chang DT, Colton E, Matsuda T & Anderson JM (2009) Lymphocyte adhesion and interactions with biomaterial adherent macrophages and foreign body giant cells. *J Biomed Mater Res A* 91: 1210–1220

Chang KH, Tam M & Stevenson MM (2004) Inappropriately low reticulocytosis in severe malarial anemia correlates with suppression in the development of late erythroid precursors. *Blood* 103: 3727–3735

Chapman TJ & Georas SN (2013) Adjuvant effect of diphtheria toxin after mucosal administration in both wild type and diphtheria toxin receptor engineered mouse strains. *J Immunol Methods* 0: 122–126

Charles A Janeway J, Travers P, Walport M & Shlomchik MJ (2001a) Summary to Chapter 11.

Charles A Janeway J, Travers P, Walport M & Shlomchik MJ (2001b) The components of the immune system.

Charles A Janeway J, Travers P, Walport M & Shlomchik MJ (2001c) The complement system and innate immunity.

Chen Y, Wermeling F, Sundqvist J, Jonsson AB, Tryggvason K, Pikkarainen T & Karlsson MCI (2010) A regulatory role for macrophage class A scavenger receptors in TLR4-mediated LPS responses. *Eur J Immunol* 40: 1451–1460

Chiba Y, Mizoguchi I, Hasegawa H, Ohashi M, Orii N, Nagai T, Sugahara M, Miyamoto Y, Xu M, Owaki T, *et al* (2018) Regulation of myelopoiesis by proinflammatory cytokines in infectious diseases. *Cell Mol Life Sci* 75: 1363–1376

- Chistiakov DA, Killingsworth MC, Myasoedova VA, Orekhov AN & Bobryshev Y V. (2016) CD68/macrosialin: not just a histochemical marker. *Laboratory Investigation* 2017 97:1 97: 4–13
- Ch'ng JH, Lee YQ, Gun SY, Chia WN, Chang ZW, Wong LK, Batty KT, Russell B, Nosten F, Renia L, *et al* (2014) Validation of a chloroquine-induced cell death mechanism for clinical use against malaria. *Cell Death Dis* 5
- Christensen JL, Wright DE, Wagers AJ & Weissman IL (2004) Circulation and Chemotaxis of Fetal Hematopoietic Stem Cells. *PLoS Biol* 2
- Cibulskis RE, Alonso P, Aponte J, Aregawi M, Barrette A, Bergeron L, Fergus CA, Knox T, Lynch M, Patouillard E, *et al* (2016) Malaria: Global progress 2000 - 2015 and future challenges. *Infect Dis Poverty* 5
- Clark IA, Ilschner S, MacMicking JD & Cowden WB (1990) TNF and Plasmodium berghei ANKA-induced cerebral malaria. *Immunol Lett* 25: 195–198
- Coban C (2020) The host targeting effect of chloroquine in malaria. *Curr Opin Immunol* 66: 98
- Coban C, Lee MSJ & Ishii KJ (2018) Tissue-specific immunopathology during malaria infection. *Nat Rev Immunol* 18: 266–278 doi:10.1038/nri.2017.138 [PREPRINT]
- Collinet C & Lecuit T (2013) Stability and dynamics of cell-cell junctions. *Prog Mol Biol Transl Sci* 116: 25–47
- Coronado LM, Nadovich CT & Spadafora C (2014) Malarial Hemozoin: From target to tool. *Biochim Biophys Acta* 1840: 2032

- Dan J, Deng H, Xia Y, Zhan Y, Tang N, Wang Y & Cao M (2022) Application of the FLP/LoxP-FRT recombination system to switch the eGFP expression in a model prokaryote. *Open Life Sci* 17: 172
- Datoo MS, Natama HM, Somé A, Bellamy D, Traoré O, Rouamba T, Tahita MC, Ido NFA, Yameogo P, Valia D, *et al* (2022) Efficacy and immunogenicity of R21/Matrix-M vaccine against clinical malaria after 2 years' follow-up in children in Burkina Faso: a phase 1/2b randomised controlled trial. *Lancet Infect Dis* 22: 1728–1736
- Deshmukh R & Trivedi V (2014) Phagocytic uptake of oxidized heme polymer is highly cytotoxic to macrophages. *PLoS One* 9
- Douglas NM, Poespoprodjo JR, Patriani D, Malloy MJ, Kenangalem E, Sugiarto P, Simpson JA, Soenarto Y, Anstey NM & Price RN (2017) Unsupervised primaquine for the treatment of *Plasmodium vivax* malaria relapses in southern Papua: A hospital-based cohort study. *PLoS Med* 14
- Draheim M, Wlodarczyk MF, Crozat K, Saliou J, Alayi TD, Tomavo S, Hassan A, Salvioni A, Demarta-Gatsi C, Sidney J, *et al* (2017) Profiling MHC II immunopeptidome of blood-stage malaria reveals that cDC1 control the functionality of parasite-specific CD4 T cells. *EMBO Mol Med* 9: 1605–1621
- Droste A, Sorg C & Högger P (1999) Shedding of CD163, a novel regulatory mechanism for a member of the scavenger receptor cysteine-rich family. *Biochem Biophys Res Commun* 256: 110–113
- Dumarchey A, Lavazec C & Verdier F (2022) Erythropoiesis and Malaria, a Multifaceted Interplay. *Int J Mol Sci* 23

- Dunst J, Kamena F & Matuschewski K (2017) Cytokines and chemokines in cerebral malaria pathogenesis. *Front Cell Infect Microbiol* 7: 324 doi:10.3389/fcimb.2017.00324 [PREPRINT]
- Elias RM, Sardinha LR, Bastos KRB, Zago CA, da Silva APF, Alvarez JM & Lima MRD (2005) Role of CD28 in polyclonal and specific T and B cell responses required for protection against blood stage malaria. *J Immunol* 174: 790–799
- Essers MAG, Offner S, Blanco-Bose WE, Waibler Z, Kalinke U, Duchosal MA & Trumpp A (2009) IFN α activates dormant haematopoietic stem cells in vivo. *Nature* 458: 904–908
- Etzerodt A & Moestrup SK (2013) CD163 and Inflammation: Biological, Diagnostic, and Therapeutic Aspects. *Antioxid Redox Signal* 18: 2352
- Etzerodt A, Rasmussen MR, Svendsen P, Chalaris A, Schwarz J, Galea I, Møller HJ & Moestrup SK (2014) Structural Basis for Inflammation-driven Shedding of CD163 Ectodomain and Tumor Necrosis Factor- α in Macrophages. *J Biol Chem* 289: 778
- Evren E, Ringqvist E & Willinger T (2020) Origin and ontogeny of lung macrophages: from mice to humans. *Immunology* 160: 126
- Fabrick BO, Bruggen R Van, Deng DM, Ligtenberg AJM, Nazmi K, Schornagel K, Vloet RPM, Dijkstra CD & Van Den Berg TK (2009) The macrophage scavenger receptor CD163 functions as an innate immune sensor for bacteria. *Blood* 113: 887–892
- Fabrick BO, Dijkstra CD & van den Berg TK (2005) The macrophage scavenger receptor CD163. *Immunobiology* 210: 153–160

- Fanti AK, Busch K, Greco A, Wang X, Cirovic B, Shang F, Nizharadze T, Frank L, Barile M, Feyerabend TB, *et al* (2023) Flt3- and Tie2-Cre tracing identifies regeneration in sepsis from multipotent progenitors but not hematopoietic stem cells. *Cell Stem Cell* 30: 207-218.e7
- Feil S, Krauss J, Thunemann M & Feil R (2014) Genetic inducible fate mapping in adult mice using tamoxifen-dependent Cre recombinases. *Methods Mol Biol* 1194: 113–139
- Fernandez-Ruiz D, Lau LS, Ghazanfari N, Jones CM, Ng WY, Davey GM, Berthold D, Holz L, Kato Y, Enders MH, *et al* (2017) Development of a Novel CD4 + TCR Transgenic Line That Reveals a Dominant Role for CD8 + Dendritic Cells and CD40 Signaling in the Generation of Helper and CTL Responses to Blood-Stage Malaria . *The Journal of Immunology* 199: 4165–4179
- Fernandez-Ruiz D, Ng WY, Holz LE, Ma JZ, Zaid A, Wong YC, Lau LS, Mollard V, Cozijnsen A, Collins N, *et al* (2016) Liver-Resident Memory CD8+ T Cells Form a Front-Line Defense against Malaria Liver-Stage Infection. *Immunity* 45: 889–902
- Flannery EL, Kangwanrangsang N, Chuenchob V, Roobsoong W, Fishbaugher M, Zhou K, Billman ZP, Martinson T, Olsen TM, Schäfer C, *et al* (2022) Plasmodium vivax latent liver infection is characterized by persistent hypnozoites, hypnozoite-derived schizonts, and time-dependent efficacy of primaquine. *Mol Ther Methods Clin Dev* 26: 427
- Flo TH, Smith KD, Sato S, Rodriguez DJ, Holmes MA, Strong RK, Akira S & Aderem A (2004) Lipocalin 2 mediates an innate immune response to bacterial infection by sequestering iron. *Nature* 432: 917–921

- Foley M & Tilley L (1998) Quinoline antimalarials: mechanisms of action and resistance and prospects for new agents. *Pharmacol Ther* 79: 55–87
- Frank R, Gabel M, Heiss K, Mueller AK & Graw F (2018) Varying immunizations with Plasmodium radiation-attenuated sporozoites alter tissue-specific CD8+ T cell dynamics. *Front Immunol* 9: 28
- Fujiwara Y, Ohnishi K, Horlad H, Saito Y, Shiraishi D, Takeya H, Yoshii D, Kaieda S, Hoshino T & Komohara Y (2020) CD163 deficiency facilitates lipopolysaccharide-induced inflammatory responses and endotoxin shock in mice. *Clin Transl Immunology* 9
- Fujiyama S, Nakahashi-Oda C, Abe F, Wang Y, Sato K & Shibuya A (2018) Identification and isolation of splenic tissue-resident macrophage subpopulations by flow cytometry. *Int Immunol* 31: 51–56
- Fujiyama S, Nakahashi-Oda C, Abe F, Wang Y, Sato K & Shibuya A (2019) Identification and isolation of splenic tissue-resident macrophage subpopulations by flow cytometry. *Int Immunol* 31: 51
- Ganley M, Holz LE, Minnell JJ, de Menezes MN, Burn OK, Poa KCY, Draper SL, English K, Chan STS, Anderson RJ, *et al* (2023) mRNA vaccine against malaria tailored for liver-resident memory T cells. *Nat Immunol* 24: 1487–1498
- Ganz T (2012) Macrophages and systemic iron homeostasis. *J Innate Immun* 4: 446–453
- Ganz T (2016) Macrophages and Iron Metabolism. *Microbiol Spectr* 4
- Gentek R, Ghigo C, Hoeffel G, Bulle MJ, Msallam R, Gautier G, Launay P, Chen J, Ginhoux F & Bajénoff M (2018) Hemogenic Endothelial Fate Mapping

Reveals Dual Developmental Origin of Mast Cells. *Immunity* 48: 1160-1171.e5

Gentek R, Molawi K & Sieweke MH (2014) Tissue macrophage identity and self-renewal. *Immunol Rev* 262: 56–73

Ghilas S, Enders MH, May R, Holz LE, Fernandez-Ruiz D, Cozijnsen A, Mollard V, Cockburn IA, McFadden GI, Heath WR, *et al* (2021) Development of Plasmodium-specific liver-resident memory CD8+ T cells after heat-killed sporozoite immunization in mice. *Eur J Immunol* 51: 1153–1165

Ginhoux F, Greter M, Leboeuf M, Nandi S, See P, Gokhan S, Mehler MF, Conway SJ, Ng LG, Stanley ER, *et al* (2010) Fate mapping analysis reveals that adult microglia derive from primitive macrophages. *Science* 330: 841–845

Ginhoux F, Lim S, Hoeffel G, Low D & Huber T (2013) Origin and differentiation of microglia. *Front Cell Neurosci* 7: 46040

Gomez Perdiguero E, Klapproth K, Schulz C, Busch K, Azzoni E, Crozet L, Garner H, Trouillet C, De Bruijn MF, Geissmann F, *et al* (2015) Tissue-resident macrophages originate from yolk-sac-derived erythro-myeloid progenitors. *Nature* 518: 547–551

Good MF & Staniscic DI (2020) Whole parasite vaccines for the asexual blood stages of Plasmodium. *Immunol Rev* 293: 270–282

Gorak PMA, Engwerda CR & Kaye PM Dendritic cells, but not macrophages, produce IL-12 immediately following *Leishmania donovani* infection.

Gordon S (2016) Elie Metchnikoff, the Man and the Myth. *J Innate Immun* 8: 223

- Gordon S & Plüddemann A (2017) Tissue macrophages: Heterogeneity and functions. *BMC Biol* 15 doi:10.1186/s12915-017-0392-4 [PREPRINT]
- Gotur S & Wadhwan V (2020) Tingible body macrophages. *J Oral Maxillofac Pathol* 24: 418
- Gouveia Z, Carlos AR, Yuan X, Aires-da-Silva F, Stocker R, Maghzal GJ, Leal SS, Gomes CM, Todorovic S, Iranzo O, *et al* (2017a) Characterization of plasma labile heme in hemolytic conditions. *FEBS J* 284: 3278–3301
- Grootveld AK, Kyaw W, Panova V, Lau AWY, Ashwin E, Seuzaret G, Dhenni R, Bhattacharyya ND, Khoo WH, Biro M, *et al* (2023) Apoptotic cell fragments locally activate tingible body macrophages in the germinal center. *Cell* 186: 1144
- Guha R, Mathioudaki A, Doumbo S, Doumtabe D, Skinner J, Arora G, Siddiqui S, Li S, Kayentao K, Ongoiba A, *et al* (2020) Plasmodium falciparum malaria drives epigenetic reprogramming of human monocytes toward a regulatory phenotype. *bioRxiv*: 2020.10.21.346197
- Guilliams M, Ginhoux F, Jakubzick C, Naik SH, Onai N, Schraml BU, Segura E, Tussiwand R & Yona S (2014) Dendritic cells, monocytes and macrophages: a unified nomenclature based on ontogeny. *Nat Rev Immunol* 14: 571
- Guilliams M & Scott CL (2017) Does niche competition determine the origin of tissue-resident macrophages? *Nature Reviews Immunology* 2017 17:7 17: 451–460
- Guilliams M, Thierry GR, Bonnardel J & Bajenoff M (2020) Establishment and Maintenance of the Macrophage Niche. *Immunity* 52: 434–451

- Gupta P, Lai SM, Sheng J, Tetlak P, Balachander A, Claser C, Renia L, Karjalainen K & Ruedl C (2016) Tissue-Resident CD169+ Macrophages Form a Crucial Front Line against Plasmodium Infection. *Cell Rep* 16: 1749–1761
- den Haan JMM & Kraal G (2012) Innate Immune Functions of Macrophage Subpopulations in the Spleen. *J Innate Immun* 4: 437–445
- Haan JMM den & Kraal G (2012) Innate Immune Functions of Macrophage Subpopulations in the Spleen. *J Innate Immun* 4: 437
- Haldar M, Kohyama M, So AYL, Kc W, Wu X, Briseño CG, Satpathy AT, Kretzer NM, Arase H, Rajasekaran NS, *et al* (2014a) Heme-mediated SPI-C induction promotes monocyte differentiation into iron-recycling macrophages. *Cell* 156: 1223
- Hall B, Limaye A & Kulkarni AB (2009) Overview: Generation of Gene Knockout Mice. *Current protocols in cell biology / editorial board, Juan S Bonifacino . [et al]* CHAPTER: Unit
- Hall N, Karras M, Raine JD, Carlton JM, Kooij TWA, Berriman M, Florens L, Janssen CS, Pain A, Christophides GK, *et al* (2005) A comprehensive survey of the Plasmodium life cycle by genomic, transcriptomic, and proteomic analyses. *Science* (1979) 307: 82–86 doi:10.1126/science.1103717 [PREPRINT]
- Hara T & Verma IM (2019) Modeling Gliomas Using Two Recombinases. *Cancer Res* 79: 3983
- Hashimoto D, Chow A, Noizat C, Teo P, Beasley MB, Leboeuf M, Becker CD, See P, Price J, Lucas D, *et al* (2013) Tissue-resident macrophages self-maintain

locally throughout adult life with minimal contribution from circulating monocytes. *Immunity* 38: 792–804

Hayashi S & McMahon AP (2002) Efficient recombination in diverse tissues by a tamoxifen-inducible form of Cre: A tool for temporally regulated gene activation/inactivation in the mouse. *Dev Biol* 244: 305–318

Hedrick PW (2011) Population genetics of malaria resistance in humans. *Heredity (Edinb)* 107: 283–304

Van Den Heuvel MM, Tensen CP, Van As JH, Van Den Berg TK, Fluitsma DM, Dijkstra CD, Döpp EA, Droste A, Van Gaalen FA, Sorg C, *et al* (1999) Regulation of CD163 on human macrophages: cross-linking of CD163 induces signaling and activation. *J Leukoc Biol* 66: 858–866

Hodne K & Weltzien FA (2015) Single-Cell Isolation and Gene Analysis: Pitfalls and Possibilities. *Int J Mol Sci* 16: 26832

Hoeffel G & Ginhoux F (2018) Fetal monocytes and the origins of tissue-resident macrophages. *Cell Immunol* 330: 5–15

Hoggatt J & Pelus LM (2011) Mobilization of hematopoietic stem cells from the bone marrow niche to the blood compartment. *Stem Cell Res Ther* 2: 13

Hu G, Su Y, Kang BH, Fan Z, Dong T, Brown DR, Cheah J, Wittrup KD & Chen J (2021) High-throughput phenotypic screen and transcriptional analysis identify new compounds and targets for macrophage reprogramming. *Nat Commun* 12: 773

Hua L, Shi J, Shultz LD & Ren G (2018) Genetic Models of Macrophage Depletion. *Methods Mol Biol* 1784: 243

- Hume DA (2008) Differentiation and heterogeneity in the mononuclear phagocyte system. *Mucosal Immunol* 1: 432–441
- Humphreys BD & Dirocco DP (2014) Lineage-tracing methods and the kidney. *Kidney Int* 86: 481–488 doi:10.1038/ki.2013.368 [PREPRINT]
- Hutter H (2006) Fluorescent reporter methods. *Methods Mol Biol* 351: 155–173
- Imai T, Ishida H, Suzue K, Taniguchi T, Okada H, Shimokawa C & Hisaeda H (2015) Cytotoxic activities of CD8⁺ T cells collaborate with macrophages to protect against blood-stage murine malaria. *Elife* 2015: 1–49
- Ing R & Stevenson MM (2009) Dendritic cell and NK cell reciprocal cross talk promotes gamma interferon-dependent immunity to blood-stage *Plasmodium chabaudi* AS infection in mice. *Infect Immun* 77: 770–782
- Ivanova EA & Orekhov AN (2015) T Helper lymphocyte subsets and plasticity in autoimmunity and cancer: An overview. *Biomed Res Int* 2015 doi:10.1155/2015/327470 [PREPRINT]
- Jacome-Galarza CE, Percin GI, Muller JT, Mass E, Lazarov T, Eitler J, Rauner M, Yadav VK, Crozet L, Bohm M, *et al* (2019) Developmental origin, functional maintenance and genetic rescue of osteoclasts. *Nature* 568: 541–545
- Jagannathan-Bogdan M & Zon LI (2013) Hematopoiesis. *Development* 140: 2463
- Jun G, Lee JS, Jung YJ & Park JW (2012) Quantitative Determination of Plasmodium Parasitemia by Flow Cytometry and Microscopy. *J Korean Med Sci* 27: 1137
- Junqueira C, Polidoro RB, Castro G, Absalon S, Liang Z, Sen Santara S, Crespo Â, Pereira DB, Gazzinelli RT, Dvorin JD, *et al* (2021) $\gamma\delta$ T cells suppress

Plasmodium falciparum blood-stage infection by direct killing and phagocytosis. *Nat Immunol* 22: 347–357

Kalantari P, DeOliveira RB, Chan J, Corbett Y, Rathinam V, Stutz A, Latz E, Gazzinelli RT, Golenbock DT & Fitzgerald KA (2014) Dual engagement of the NLRP3 and AIM2 inflammasomes by plasmodium-derived hemozoin and DNA during malaria. *Cell Rep* 6: 196–210

Kang YS, Do Y, Lee HK, Park SH, Cheong C, Lynch RM, Loeffler JM, Steinman RM & Park CG (2006) A Dominant Complement Fixation Pathway for Pneumococcal Polysaccharides Initiated by SIGN-R1 Interacting with C1q. *Cell* 125: 47–58

Kang YS, Kim JY, Bruening SA, Pack M, Charalambous A, Pritsker A, Moran TM, Loeffler JM, Steinman RM & Park CG (2004) The C-type lectin SIGN-R1 mediates uptake of the capsular polysaccharide of *Streptococcus pneumoniae* in the marginal zone of mouse spleen. *Proc Natl Acad Sci U S A* 101: 215–220

Kanitakis J, Morelon E, Petruzzo P, Badet L & Dubernard JM (2011) Self-renewal capacity of human epidermal Langerhans cells: observations made on a composite tissue allograft. *Exp Dermatol* 20: 145–146

Kapila V, Wehrle CJ & Tuma F (2023) Physiology, Spleen. *StatPearls*

Kho S, Qotrunnada L, Leonardo L, Andries B, Wardani PAI, Fricot A, Henry B, Hardy D, Margyaningsih NI, Apriyanti D, *et al* (2021a) Evaluation of splenic accumulation and colocalization of immature reticulocytes and *Plasmodium vivax* in asymptomatic malaria: A prospective human splenectomy study. *PLoS Med* 18

- Kho S, Qotrunnada L, Leonardo L, Andries B, Wardani PAI, Fricot A, Henry B, Hardy D, Margyaningsih NI, Apriyanti D, *et al* (2021b) Hidden Biomass of Intact Malaria Parasites in the Human Spleen. *New England Journal of Medicine* 384: 2067–2069
- Kim CC, Nelson CS, Wilson EB, Hou B, DeFranco AL & DeRisi JL (2012) Splenic Red Pulp Macrophages Produce Type I Interferons as Early Sentinels of Malaria Infection but Are Dispensable for Control. *PLoS One* 7: 48126
- Kim H, Kim M, Im SK & Fang S (2018) Mouse Cre-LoxP system: general principles to determine tissue-specific roles of target genes. *Lab Anim Res* 34: 147
- Kim I, He S, Yilmaz ÖH, Kiel MJ & Morrison SJ (2006) Enhanced purification of fetal liver hematopoietic stem cells using SLAM family receptors. *Blood* 108: 737–744
- Kissa K & Herbomel P (2010) Blood stem cells emerge from aortic endothelium by a novel type of cell transition. *Nature* 464: 112–115
- Kjærgaard AG, Rødgaard-Hansen S, Dige A, Krog J, Møller HJ & Tønnesen E (2014) Monocyte expression and soluble levels of the haemoglobin receptor (CD163/sCD163) and the mannose receptor (MR/sMR) in septic and critically ill non-septic ICU patients. *PLoS One* 9
- Kohyama M, Ise W, Edelson BT, Wilker PR, Hildner K, Mejia C, Frazier WA, Murphy TL & Murphy KM (2009) Critical role for Spi-C in the development of red pulp macrophages and splenic iron homeostasis. *Nature* 457: 318
- Kondo H, Saito K, Grasso JP & Aisen P (1988) Iron metabolism in the erythrophagocytosing Kupffer cell. *Hepatology* 8: 32–38

- Kondo M (2010) Lymphoid and myeloid lineage commitment in multipotent hematopoietic progenitors. *Immunol Rev* 238: 37
- Koppel EA, Litjens M, van den Berg VC, van Kooyk Y & Geijtenbeek TBH (2008) Interaction of SIGNR1 expressed by marginal zone macrophages with marginal zone B cells is essential to early IgM responses against *Streptococcus pneumoniae*. *Mol Immunol* 45: 2881–2887
- Kowal K, Silver R, Sławińska E, Bielecki M, Chyczewski L & Kowal-Bielecka O (2011) CD163 and its role in inflammation. *Folia Histochem Cytobiol* 49: 365–374
- Kraal G & Mebius R (2006) New Insights into the Cell Biology of the Marginal Zone of the Spleen. *Int Rev Cytol* 250: 175
- Kristiansen M, Graversen JH, Jacobsen C, Sonne O, Hoffman HJ, Law SKA & Moestrup SK (2001) Identification of the haemoglobin scavenger receptor. *Nature* 409: 198–201
- Krzych U, Zarling S & Pichugin A (2014) Memory T cells maintain protracted protection against malaria. *Immunol Lett* 161: 189–195
- Kumar R, Loughland JR, Ng SS, Boyle MJ & Engwerda CR (2020) The regulation of CD4+ T cells during malaria. *Immunol Rev* 293: 70–87 doi:10.1111/imr.12804 [PREPRINT]
- Kumar S & Bandyopadhyay U (2005) Free heme toxicity and its detoxification systems in human. *Toxicol Lett* 157: 175–188
- Kumarasingha R, Ioannidis LJ, Abeysekera W, Studniberg S, Wijesurendra D, Mazhari R, Poole DP, Mueller I, Schofield L, Hansen DS, *et al* (2020)

Transcriptional Memory-Like Imprints and Enhanced Functional Activity in $\gamma\delta$ T Cells Following Resolution of Malaria Infection. *Front Immunol* 11

Kurotaki D, Kon S, Bae K, Ito K, Matsui Y, Nakayama Y, Kanayama M, Kimura C, Narita Y, Nishimura T, *et al* (2011) CSF-1-dependent red pulp macrophages regulate CD4 T cell responses. *J Immunol* 186: 2229–2237

Kurotaki D, Uede T & Tamura T (2015) Functions and development of red pulp macrophages. *Microbiol Immunol* 59: 55–62

Kurup SP, Butler NS & Harty JT (2019) T cell-mediated immunity to malaria. *Nat Rev Immunol* 19: 457–471 doi:10.1038/s41577-019-0158-z [PREPRINT]

Kusi KA, Gyan BA, Goka BQ, Dodoo D, Obeng-Adjei G, Troye-Blomberg M, Akanmori BD & Adjimani JP (2008) Levels of Soluble CD163 and Severity of Malaria in Children in Ghana. *Clin Vaccine Immunol* 15: 1456

van de Laar L, Saelens W, De Prijck S, Martens L, Scott CL, Van Isterdael G, Hoffmann E, Beyaert R, Saeys Y, Lambrecht BN, *et al* (2016) Yolk Sac Macrophages, Fetal Liver, and Adult Monocytes Can Colonize an Empty Niche and Develop into Functional Tissue-Resident Macrophages. *Immunity* 44: 755–768

Lacerda-Queiroz N, Riteau N, Eastman RT, Bock KW, Orandle MS, Moore IN, Sher A, Long CA, Jankovic D & Su XZ (2017) Mechanism of splenic cell death and host mortality in a *Plasmodium yoelii* malaria model. *Sci Rep* 7

Lai SM, Sheng J, Gupta P, Renia L, Duan K, Zolezzi F, Karjalainen K, Newell EW & Ruedl C (2018a) Organ-Specific Fate, Recruitment, and Refilling Dynamics of Tissue-Resident Macrophages during Blood-Stage Malaria. *Cell Rep* 25: 3099-3109.e3

- Lang F, Lang E & Filler M (2012) Physiology and pathophysiology of eryptosis. *Transfus Med Hemother* 39: 308–314
- Lange PT, Jondle CN, Darrah EJ, Johnson KE & Tarakanova VL (2019) LXR Alpha Restricts Gammaherpesvirus Reactivation from Latently Infected Peritoneal Cells. *J Virol* 93
- Langhorne J, Gillard S, Simon B, Slade S & Eichmann K (1989) Frequencies of CD4+ T cells reactive with *Plasmodium chabaudi chabaudi*: distinct response kinetics for cells with Th1 and Th2 characteristics during infection. *Int Immunol* 1: 416–424
- Langhorne J, Ndungu FM, Sponaas AM & Marsh K (2008) Immunity to malaria: more questions than answers. *Nat Immunol* 9: 725–732
- Larsson A, Hult A, Nilsson A, Olsson M & Oldenborg PA (2016) Red blood cells with elevated cytoplasmic Ca(2+) are primarily taken up by splenic marginal zone macrophages and CD207+ dendritic cells. *Transfusion (Paris)* 56: 1834–1844
- Lau LS, Fernandez-Ruiz D, Mollard V, Sturm A, Neller MA, Cozijnsen A, Gregory JL, Davey GM, Jones CM, Lin YH, *et al* (2014) CD8+ T Cells from a Novel T Cell Receptor Transgenic Mouse Induce Liver-Stage Immunity That Can Be Boosted by Blood-Stage Infection in Rodent Malaria. *PLoS Pathog* 10
- Lavin Y, Mortha A, Rahman A & Merad M (2015) Regulation of macrophage development and function in peripheral tissues. *Nat Rev Immunol* 15: 731
- Lee EY, Lee ZH & Song YW (2009) CXCL10 and autoimmune diseases. *Autoimmun Rev* 8: 379–383

- Lee MSJ, Igari Y, Tsukui T, Ishii KJ & Coban C (2016) Current status of synthetic hemozoin adjuvant: A preliminary safety evaluation. *Vaccine* 34: 2055–2061
- Lefebvre MN & Harty JT (2021) $\gamma\delta$ T cells burst malaria's bubble. *Nat Immunol* 22: 270–272 doi:10.1038/s41590-021-00879-4 [PREPRINT]
- Leoni S, Buonfrate D, Angheben A, Gobbi F & Bisoffi Z (2015) The hyper-reactive malarial splenomegaly: a systematic review of the literature. *Malar J* 14
- Lewis SM, Williams A & Eisenbarth SC (2019) Structure-function of the immune system in the spleen. *Sci Immunol* 4
- Li C, Seixas E & Langhorne J (2001) Rodent malarias: the mouse as a model for understanding immune responses and pathology induced by the erythrocytic stages of the parasite. *Med Microbiol Immunol* 189: 115–126
- Li C, Zhu X, Ji X, Quanquin N, Deng YQ, Tian M, Aliyari R, Zuo X, Yuan L, Afridi SK, *et al* (2017) Chloroquine, a FDA-approved Drug, Prevents Zika Virus Infection and its Associated Congenital Microcephaly in Mice. *EBioMedicine* 24: 189–194
- Li Z, Liu S, Xu J, Zhang X, Han D, Liu J, Xia M, Yi L, Shen Q, Xu S, *et al* (2018) Adult Connective Tissue-Resident Mast Cells Originate from Late Erythro-Myeloid Progenitors. *Immunity* 49: 640-653.e5
- Lima-Junior J da C & Pratt-Riccio LR (2016) Major Histocompatibility Complex and Malaria: Focus on Plasmodium vivax Infection. *Front Immunol* 7: 1
- Liu R, Zhang X, Nie L, Sun S, Liu J & Chen H (2023) Heme oxygenase 1 in erythropoiesis: an important regulator beyond catalyzing heme catabolism. *Ann Hematol* 102: 1323–1332

- Liu Z, Gu Y, Chakarov S, Bleriot C, Kwok I, Chen X, Shin A, Huang W, Dress RJ, Dutertre CA, *et al* (2019) Fate Mapping via Ms4a3-Expression History Traces Monocyte-Derived Cells. *Cell* 178: 1509-1525.e19
- Maheshwari A (2022) The Phylogeny, Ontogeny, and Organ-specific Differentiation of Macrophages in the Developing Intestine. *Newborn (Clarksville, Md)* 1: 340
- Malo CS, Huggins MA, Goddery EN, Tolcher HMA, Renner DN, Jin F, Hansen MJ, Pease LR, Pavelko KD & Johnson AJ (2018) Non-equivalent antigen presenting capabilities of dendritic cells and macrophages in generating brain-infiltrating CD8 + T cell responses. *Nat Commun* 9
- Mantovani A, Dinarello CA, Molgora M & Garlanda C (2019) IL-1 and related cytokines in innate and adaptive immunity in health and disease. *Immunity* 50: 778
- Markus MB (2018) Biological concepts in recurrent Plasmodium vivax malaria. *Parasitology* 145: 1765–1771
- Martin Shetlar by D & Allen H (1985) Reactions of hemoglobin with phenylhydrazine: a review of selected aspects. *Environ Health Perspect* 64: 265
- Masaratana P, Latunde-Dada GO, Patel N, Simpson RJ, Vulont S & McKie AT (2012) Iron metabolism in hepcidin1 knockout mice in response to phenylhydrazine-induced hemolysis. *Blood Cells Mol Dis* 49: 85–91
- di Masi A, De Simone G, Ciaccio C, D'Orso S, Coletta M & Ascenzi P (2020) Haptoglobin: From hemoglobin scavenging to human health. *Mol Aspects Med* 73

- Mass E (2018) Delineating the origins, developmental programs and homeostatic functions of tissue-resident macrophages. *Int Immunol* 30: 493–501 doi:10.1093/intimm/dxy044 [PREPRINT]
- Mass E, Ballesteros I, Farlik M, Halbritter F, Günther P, Crozet L, Jacome-Galarza CE, Händler K, Klughammer J, Kobayashi Y, *et al* (2016) Specification of tissue-resident macrophages during organogenesis. *Science* (1979) 353
- Mass E & Gentek R (2021) Fetal-Derived Immune Cells at the Roots of Lifelong Pathophysiology. *Front Cell Dev Biol* 9: 356
- Mass E & Lachmann N (2021) From macrophage biology to macrophage-based cellular immunotherapies. *Gene Ther*: 1–4
- Mass E, Nimmerjahn F, Kierdorf K & Schlitzer A (2023) Tissue-specific macrophages: how they develop and choreograph tissue biology. *Nat Rev Immunol* 23: 1
- Matz JM & Kooij TWA (2015) Towards genome-wide experimental genetics in the in vivo malaria model parasite *Plasmodium berghei*. *Pathog Glob Health* 109: 46
- Mauel K & Mass E (2024) Fate-Mapping of Hematopoietic Stem Cell-Derived Macrophages. *Methods in Molecular Biology* 2713: 139–148
- Mawson AR (2013) The pathogenesis of malaria: a new perspective. *Pathog Glob Health* 107: 122
- May J, Lell B, Luty AJF, Meyer CG & Kremsner PG (2000) Plasma interleukin-10:Tumor necrosis factor (TNF)-alpha ratio is associated with TNF promoter variants and predicts malarial complications. *J Infect Dis* 182: 1570–1573

- Mechnikov II (1988) Immunity in Infective Diseases. *Rev Infect Dis* 10: 223–227
- Meding SJ & Langhorne J (1991) CD4+ T cells and B cells are necessary for the transfer of protective immunity to *Plasmodium chabaudi chabaudi*. *Eur J Immunol* 21: 1433–1438
- Meizlish ML, Franklin RA, Zhou X & Medzhitov R (2021) Tissue Homeostasis and Inflammation. <https://doi.org/10.1146/annurev-immunol-061020-053734> 39: 557–581
- Mendonça VRR, Luza NF, Santos NJG, Borges VM, Gonçalves MS, Andrade BB & Barral-Netto M (2012) Association between the Haptoglobin and Heme Oxygenase 1 Genetic Profiles and Soluble CD163 in Susceptibility to and Severity of Human Malaria. *Infect Immun* 80: 1445
- Menezes S, Melandri D, Anselmi G, Perchet T, Loschko J, Dubrot J, Patel R, Gautier EL, Hugues S, Longhi MP, *et al* (2016) The Heterogeneity of Ly6Chi Monocytes Controls Their Differentiation into iNOS+ Macrophages or Monocyte-Derived Dendritic Cells. *Immunity* 45: 1205
- Milner DA (2018) Malaria Pathogenesis. *Cold Spring Harb Perspect Med* 8
- Miyake Y, Asano K, Kaise H, Uemura M, Nakayama M & Tanaka M (2007) Critical role of macrophages in the marginal zone in the suppression of immune responses to apoptotic cell-associated antigens. *Journal of Clinical Investigation* 117: 2268–2278
- Moeller JB, Nielsen MJ, Reichhardt MP, Schlosser A, Sorensen GL, Nielsen O, Tornøe I, Grønlund J, Nielsen ME, Jørgensen JS, *et al* (2012) CD163-L1 is an endocytic macrophage protein strongly regulated by mediators in the inflammatory response. *J Immunol* 188: 2399–2409

- Mohandas N & An X (2012) Malaria and human red blood cells. *Med Microbiol Immunol* 201: 593–598
- Møller HJ, Kazankov K, Rødgaard-Hansen S, Nielsen MC, Sandahl TD, Vilstrup H, Moestrup SK & Grønbæk H (2017) Soluble CD163 (sCD163): Biomarker of Kupffer Cell Activation in Liver Disease. 321–348
- Mondor I, Baratin M, Lagueyrie M, Saro L, Henri S, Gentek R, Suerinck D, Kastenmuller W, Jiang JX & Bajénoff M (2019) Lymphatic Endothelial Cells Are Essential Components of the Subcapsular Sinus Macrophage Niche. *Immunity* 50: 1453-1466.e4
- Monvoisin A, Alva JA, Hofmann JJ, Zovein AC, Lane TF & Iruela-Arispe ML (2006) VE-cadherin-CreERT2 transgenic mouse: A model for inducible recombination in the endothelium. *Developmental Dynamics* 235: 3413–3422
- Mooney JP, Barry A, Gonçalves BP, Tiono AB, Awandu SS, Grignard L, Drakeley CJ, Bottomley C, Bousema T & Riley EM (2018) Haemolysis and haem oxygenase-1 induction during persistent ‘asymptomatic’ malaria infection in Burkinabé children. *Malar J* 17: 1–11
- Moreno SG (2018) Depleting macrophages in vivo with clodronate-liposomes. In *Methods in Molecular Biology* pp 259–262. Humana Press Inc.
- Mosser DM, Hamidzadeh K & Goncalves R (2020) Macrophages and the maintenance of homeostasis. *Cell Mol Immunol* 18: 579–587 doi:10.1038/s41423-020-00541-3 [PREPRINT]
- Mota MM, Brown KN, Holder AA & Jarra W (1998) Acute Plasmodium chabaudi chabaudi Malaria Infection Induces Antibodies Which Bind to the Surfaces of

Parasitized Erythrocytes and Promote Their Phagocytosis by Macrophages In Vitro. *Infect Immun* 66: 4080

Mota MM, Thathy V, Nussenzweig RS & Nussenzweig V (2001) Gene targeting in the rodent malaria parasite *Plasmodium yoelii*. *Mol Biochem Parasitol* 113: 271–278

Müller S, Hunziker L, Enzler S, Bühler-Jungo M, Di Santo JP, Zinkernagel RM & Mueller C (2002) Role of an intact splenic microarchitecture in early lymphocytic choriomeningitis virus production. *J Virol* 76: 2375–2383

Muntjewerff EM, Meesters LD & van den Bogaart G (2020) Antigen Cross-Presentation by Macrophages. *Front Immunol* 11: 1276

Murphy K & Weaver C (2018) *Janeway Immunologie* Springer Berlin Heidelberg

Nakamura Y, Matsumoto H, Wu CH, Fukaya D, Uni R, Hirakawa Y, Katagiri M, Yamada S, Ko T, Nomura S, *et al* (2023) Alpha 7 nicotinic acetylcholine receptors signaling boosts cell-cell interactions in macrophages effecting anti-inflammatory and organ protection. *Commun Biol* 6

Narasimhan PB, Marcovecchio P, Hamers AAJ & Hedrick CC (2019) Nonclassical Monocytes in Health and Disease. <https://doi.org/10.1146/annurev-immunol-042617-053119> 37: 439–456

Nelson RJ (1997) The use of genetic ‘knockout’ mice in behavioral endocrinology research. *Horm Behav* 31: 188–196

Nielsen MC, Hvidbjerg Gantzel R, Clària J, Trebicka J, Møller HJ & Grønbaek H (2020) Macrophage Activation Markers, CD163 and CD206, in Acute-on-Chronic Liver Failure. *Cells* 9

- De Niz M, Meibalan E, Mejia P, Ma S, Brancucci NMB, Agop-Nersesian C, Mandt R, Ngotho P, Hughes KR, Waters AP, *et al* (2018) Plasmodium gametocytes display homing and vascular transmigration in the host bone marrow. *Sci Adv* 4
- Norris BA, Uebelhoer LS, Nakaya HI, Price AA, Grakoui A & Pulendran B (2013) Polyphasic innate immune responses to acute and chronic LCMV infection: Innate immunity to acute & chronic viral infection. *Immunity* 38: 309–321
- Obaldia N, Meibalan E, Sa JM, Ma S, Clark MA, Mejia P, Moraes Barros RR, Otero W, Ferreira MU, Mitchell JR, *et al* (2018) Bone marrow is a major parasite reservoir in plasmodium vivax infection. *mBio* 9
- Okabe Y & Medzhitov R (2016) Tissue biology perspective on macrophages. *Nat Immunol* 17: 9–17 doi:10.1038/ni.3320 [PREPRINT]
- Okamura Y, Watari M, Jerud ES, Young DW, Ishizaka ST, Rose J, Chow JC & Strauss JF (2001) The extra domain A of fibronectin activates Toll-like receptor 4. *J Biol Chem* 276: 10229–10233
- Okreglicka K, Iten I, Pohlmeier L, Onder L, Feng Q, Kurrer M, Ludewig B, Nielsen P, Schneider C & Kopf M (2021) PPAR γ is essential for the development of bone marrow erythroblastic island macrophages and splenic red pulp macrophages. *J Exp Med* 218
- Olivier M, Van Den Ham K, Shio MT, Kassa FA & Fougerey S (2014) Malarial pigment hemozoin and the innate inflammatory response. *Front Immunol* 5
- Oluwole O, Sia S & Mohammed M (2010) Plasmodium Falciparum-Induced Kidney and Liver Dysfunction in Malaria Patients in Freetown, Sierra Leone. *Sierra Leone Journal of Biomedical Research* 2: 70–74

- Onofre G, Kolácková M, Jankovicová K & Krejsek J (2009) Scavenger receptor CD163 and its biological functions. *Acta Medica (Hradec Kralove)* 52: 57–61
- Ozarslan N, Robinson JF & Gaw SL (2019) Circulating Monocytes, Tissue Macrophages, and Malaria. *J Trop Med* 2019
- Pack AD, Schwartzhoff P V., Zacharias ZR, Fernandez-Ruiz D, Heath WR, Gurung P, Legge KL, Janse CJ & Butler NS (2021) Hemozoin-mediated inflammasome activation limits long-lived anti-malarial immunity. *Cell Rep* 36: 109586
- Palis J (2016) Hematopoietic stem cell-independent hematopoiesis: emergence of erythroid, megakaryocyte, and myeloid potential in the mammalian embryo. *FEBS Lett* 590: 3965–3974
- Palis J, Robertson S, Kennedy M, Wall C & Keller G (1999) Development of erythroid and myeloid progenitors in the yolk sac and embryo proper of the mouse. *Development* 126: 5073–5084
- Park JY, Sung JY, Lee J, Park YK, Kim YW, Kim GY, Won KY & Lim SJ (2016) Polarized CD163+ tumor-associated macrophages are associated with increased angiogenesis and CXCL12 expression in gastric cancer. *Clin Res Hepatol Gastroenterol* 40: 357–365
- Parroche P, Lauw FN, Goutagny N, Latz E, Monks BG, Visintin A, Halmen KA, Lamphier M, Olivier M, Bartholomeu DC, *et al* (2007) Malaria hemozoin is immunologically inert but radically enhances innate responses by presenting malaria DNA to Toll-like receptor 9. *Proc Natl Acad Sci U S A* 104: 1919–1924

- Parwaresch MR & Wacker H -H (1984) Origin and Kinetics of Resident Tissue Macrophages: Parabiosis studies with radiolabelled leucocytes. *Cell Prolif* 17: 25–39
- Paudel S, Ghimire L, Jin L, Jeansonne D & Jeyaseelan S (2022) Regulation of emergency granulopoiesis during infection. *Front Immunol* 13
- Peet DJ, Turley SD, Ma W, Janowski BA, Lobaccaro JMA, Hammer RE & Mangelsdorf DJ (1998) Cholesterol and bile acid metabolism are impaired in mice lacking the nuclear oxysterol receptor LXR alpha. *Cell* 93: 693–704
- Perdiguero EG & Geissmann F (2016) The development and maintenance of resident macrophages. *Nat Immunol* 17: 2–8
- Perez-Mazliah D & Langhorne J (2014) CD4 T-Cell Subsets in Malaria: TH1/TH2 Revisited. *Front Immunol* 5
- Perry GH (2014) Parasites and human evolution. *Evolutionary Anthropology: Issues, News, and Reviews* 23: 218–228
- Pham TT, Lamb TJ, Deroost K, Opdenakker G & Van den Steen PE (2021) Hemozoin in Malarial Complications: More Questions Than Answers. *Trends Parasitol* 37: 226–239
- Pirgova G, Chauveau A, MacLean AJ, Cyster JG & Arnon TI (2020) Marginal zone SIGN-R1+ macrophages are essential for the maturation of germinal center B cells in the spleen. *Proc Natl Acad Sci U S A* 117: 12295–12305
- Pollenus E, Gouwy M & Van den Steen PE (2022) Neutrophils in malaria: The good, the bad or the ugly? *Parasite Immunol* 44

- Ponzoni M, Pastorino F, Di Paolo D, Perri P & Brignole C (2018) Targeting Macrophages as a Potential Therapeutic Intervention: Impact on Inflammatory Diseases and Cancer. *International Journal of Molecular Sciences* 2018, Vol 19, Page 1953 19: 1953
- Popa GL & Popa MI (2021) Recent Advances in Understanding the Inflammatory Response in Malaria: A Review of the Dual Role of Cytokines. *J Immunol Res* 2021
- del Portillo HA, Ferrer M, Brugat T, Martin-Jaular L, Langhorne J & Lacerda MVG (2012) The role of the spleen in malaria. *Cell Microbiol* 14: 343–355 doi:10.1111/j.1462-5822.2011.01741.x [PREPRINT]
- Poss KD & Tonegawa S (1997) Reduced stress defense in heme oxygenase 1-deficient cells. *Proc Natl Acad Sci U S A* 94: 10925
- Pradhan P, Vijayan V, Gueler F & Immenschuh S (2020) Interplay of Heme with Macrophages in Homeostasis and Inflammation. *Int J Mol Sci* 21
- Price RN, von Seidlein L, Valecha N, Nosten F, Baird JK & White NJ (2014) Global extent of chloroquine-resistant *Plasmodium vivax*: A systematic review and meta-analysis. *Lancet Infect Dis* 14: 982–991
- Qin S, Wang H, Yuan R, Li H, Ochani M, Ochani K, Rosas-Ballina M, Czura CJ, Huston JM, Miller E, *et al* (2006) Role of HMGB1 in apoptosis-mediated sepsis lethality. *J Exp Med* 203: 1637–1642
- Rahman ZSM, Shao W-H, Khan TN, Zhen Y & Cohen PL (2010) Impaired apoptotic cell clearance in the germinal center by Mer-deficient tingible body macrophages leads to enhanced antibody-forming cell and germinal center responses. *J Immunol* 185: 5859

- Ramos S, Carlos AR, Sundaram B, Jeney V, Ribeiro A, Gozzelino R, Bank C, Gjini E, Braza F, Martins R, *et al* (2019) Renal control of disease tolerance to malaria. *Proc Natl Acad Sci U S A* 116: 5681–5686
- Ramos S, Jeney V, Figueiredo A, Paixão T, Sambo MR, Quinhentos V, Martins R, Gouveia Z, Carlos AR, Ferreira A, *et al* (2024) Targeting circulating labile heme as a defense strategy against malaria. *Life Sci Alliance* 7
- Randall LM & Engwerda CR (2010) TNF family members and malaria: Old observations, new insights and future directions. *Exp Parasitol* 126: 326–331
- Ravishankar B, Shinde R, Liu H, Chaudhary K, Bradley J, Lemos HP, Phillip C, Tanaka M, Munn DH, Mellor AL, *et al* (2014) Marginal zone CD169+ macrophages coordinate apoptotic cell-driven cellular recruitment and tolerance. *Proc Natl Acad Sci U S A* 111: 4215–4220
- Rebejac J, Eme-Scolan E, Arnaud Paroutaud L, Kharbouche S, Teleman M, Spinelli L, Gallo E, Roussel-Queval A, Zarubica A, Sansoni A, *et al* (2022) Meningeal macrophages protect against viral neuroinfection. *Immunity* 55: 2103-2117.e10
- Rebelo M, Sousa C, Shapiro HM, Mota MM, Grobusch MP & Hänscheid T (2013) A Novel Flow Cytometric Hemozoin Detection Assay for Real-Time Sensitivity Testing of *Plasmodium falciparum*. *PLoS One* 8: 61606
- Redman M, King A, Watson C & King D (2016) What is CRISPR/Cas9? *Arch Dis Child Educ Pract Ed* 101: 213
- Rénia L, Howland SW, Claser C, Gruner AC, Suwanarusk R, Teo TH, Russell B & Lisa NP (2012) Cerebral malaria: Mysteries at the blood-brain barrier. *Virulence* 3: 193

- Repa JJ & Mangelsdorf DJ (2000) The role of orphan nuclear receptors in the regulation of cholesterol homeostasis. *Annu Rev Cell Dev Biol* 16: 459–481
- Rex DAB, Patil AH, Modi PK, Kandiyil MK, Kasaragod S, Pinto SM, Tanneru N, Sijwali PS & Prasad TSK (2022) Dissecting Plasmodium yoelii Pathobiology: Proteomic Approaches for Decoding Novel Translational and Post-Translational Modifications. *ACS Omega* 7: 8246–8257
- Ribot JC, Lopes N & Silva-Santos B (2020) $\gamma\delta$ T cells in tissue physiology and surveillance. *Nat Rev Immunol*: 1–12 doi:10.1038/s41577-020-00452-4 [PREPRINT]
- Rieger MA, Hoppe PS, Smejkal BM, Eitelhuber AC & Schroeder T (2009) Hematopoietic cytokines can instruct lineage choice. *Science* 325: 217–218
- Rieger MA & Schroeder T (2012) Hematopoiesis. *Cold Spring Harb Perspect Biol* 4
- Ringelmann B, Miller H & Konotey Ahulu FI (1973) The origin of anaemia in tropical splenomegaly syndrome. *Acta Med Acad Sci Hung* 30: 331–341
- Ritter M, Buechler C, Langmann T, Orso E, Klucken J & Schmitz G (2000) The Scavenger Receptor CD163: Regulation, Promoter Structure and Genomic Organization. *Pathobiology* 67: 257–261
- Roestenberg M, Teirlinck AC, McCall MBB, Teelen K, Makamdop KN, Wiersma J, Arens T, Beckers P, Van Gemert G, Van De Vegte-Bolmer M, *et al* (2011) Long-term protection against malaria after experimental sporozoite inoculation: An open-label follow-up study. *The Lancet* 377: 1770–1776
- Ross LS & Fidock DA (2019) Elucidating Mechanisms of Drug-Resistant Plasmodium falciparum. *Cell Host Microbe* 26: 35–47

- Rutherford MS & Schook LB (1992) Differential immunocompetence of macrophages derived using macrophage or granulocyte-macrophage colony-stimulating factor. *J Leukoc Biol* 51: 69–76
- Safeukui I, Gomez ND, Adelani AA, Burte F, Afolabi NK, Akondy R, Velazquez P, Holder A, Tewari R, Buffet P, *et al* (2015) Malaria induces anemia through CD8+ T Cell-dependent parasite clearance and erythrocyte removal in the spleen. *mBio* 6
- Sato S (2021) Plasmodium—a brief introduction to the parasites causing human malaria and their basic biology. *J Physiol Anthropol* 40
- Scalia CR, Boi G, Bolognesi MM, Riva L, Manzoni M, DeSmedt L, Bosisio FM, Ronchi S, Leone BE & Cattoretti G (2017) Antigen Masking During Fixation and Embedding, Dissected. *Journal of Histochemistry and Cytochemistry* 65: 5
- Schaer CA, Schoedon G, Imhof A, Kurrer MO & Schaer DJ (2006) Constitutive Endocytosis of CD163 Mediates Hemoglobin-Heme Uptake and Determines the Noninflammatory and Protective Transcriptional Response of Macrophages to Hemoglobin. *Circ Res* 99: 943–950
- Schaer DJ, Alayash AI & Buehler PW (2007) Gating the radical hemoglobin to macrophages: the anti-inflammatory role of CD163, a scavenger receptor. *Antioxid Redox Signal* 9: 991–999
- Schliehe C, Redaelli C, Engelhardt S, Fehlings M, Mueller M, van Rooijen N, Thiry M, Hildner K, Weller H & Groettrup M (2011) CD8- dendritic cells and macrophages cross-present poly(D,L-lactate-co-glycolate) acid microsphere-encapsulated antigen in vivo. *J Immunol* 187: 2112–2121

- Schmitt H, Sell S, Koch J, Seefried M, Sonnewald S, Daniel C, Winkler TH & Nitschke L (2016) Siglec-H protects from virus-triggered severe systemic autoimmunity. *J Exp Med* 213: 1627
- Schroder K, Hertzog PJ, Ravasi T & Hume DA (2004) Interferon-gamma: an overview of signals, mechanisms and functions. *J Leukoc Biol* 75: 163–189
- Schultze JL, Mass E & Schlitzer A (2019) Emerging Principles in Myelopoiesis at Homeostasis and during Infection and Inflammation. *Immunity* 50: 288–301
- Schulz C, Perdiguero EG, Chorro L, Szabo-Rogers H, Cagnard N, Kierdorf K, Prinz M, Wu B, Jacobsen SEW, Pollard JW, *et al* (2012) A lineage of myeloid cells independent of myb and hematopoietic stem cells. *Science* (1979) 335: 86–90
- Schwarzer E, Turrini F, Ulliers D, Giribaldi G, Ginsburg H & Arese P (1992) Impairment of macrophage functions after ingestion of Plasmodium falciparum-infected erythrocytes or isolated malarial pigment. *J Exp Med* 176: 1033–1041
- Scott CL & Guilliams M (2018) The role of Kupffer cells in hepatic iron and lipid metabolism. *J Hepatol* 69: 1197–1199 doi:10.1016/j.jhep.2018.02.013 [PREPRINT]
- Seidman JS, Troutman TD, Sakai M, Gola A, Spann NJ, Bennett H, Bruni CM, Ouyang Z, Li RZ, Sun X, *et al* (2020) Niche-Specific Reprogramming of Epigenetic Landscapes Drives Myeloid Cell Diversity in Nonalcoholic Steatohepatitis. *Immunity* 52: 1057-1074.e7
- Sengupta A, Sarkar S, Keswani T, Mukherjee S, Ghosh S & Bhattacharyya A (2019) Impact of autophagic regulation on splenic red pulp macrophages during cerebral malarial infection. *Parasitol Int* 71: 18–26

- Shapouri-Moghaddam A, Mohammadian S, Vazini H, Taghadosi M, Esmaeili SA, Mardani F, Seifi B, Mohammadi A, Afshari JT & Sahebkar A (2018) Macrophage plasticity, polarization, and function in health and disease. *J Cell Physiol* 233: 6425–6440 doi:10.1002/jcp.26429 [PREPRINT]
- Sheel M & Engwerda CR (2012) The diverse roles of monocytes in inflammation caused by protozoan parasitic diseases. *Trends Parasitol* 28: 408–416
- Sigala PA & Goldberg DE (2014) The Peculiarities and Paradoxes of Plasmodium Heme Metabolism. <https://doi.org/10.1146/annurev-micro-091313-103537> 68: 259–278
- Sikora M, Śmieszek A & Marycz K (2021) Bone marrow stromal cells (BMSCs CD45-/CD44+/CD73+/CD90+) isolated from osteoporotic mice SAM/P6 as a novel model for osteoporosis investigation. *J Cell Mol Med* 25: 6634
- Singh S, Jakubison B & Keller JR (2020) Protection of hematopoietic stem cells from stress-induced exhaustion and aging. *Curr Opin Hematol* 27: 225–231
- Skytthe MK, Graversen JH & Moestrup SK (2020) Targeting of CD163+ Macrophages in Inflammatory and Malignant Diseases. *Int J Mol Sci* 21: 1–31
- Slater AFG (1993) Chloroquine: Mechanism of drug action and resistance in plasmodium falciparum. *Pharmacol Ther* 57: 203–235
- Song AJ & Palmiter RD (2018) Detecting and Avoiding Problems When Using the Cre/lox System. *Trends Genet* 34: 333
- Spottiswoode N, Duffy PE & Drakesmith H (2014) Iron, anemia and hepcidin in malaria. *Front Pharmacol* 5

- Stables MJ, Shah S, Camon EB, Lovering RC, Newson J, Bystrom J, Farrow S & Gilroy DW (2011) Transcriptomic analyses of murine resolution-phase macrophages. *Blood* 118
- Steiniger BS (2015) Human spleen microanatomy: Why mice do not suffice. *Immunology* 145: 334–346
- Stephens R, Culleton RL & Lamb TJ (2012) The contribution of *Plasmodium chabaudi* to our understanding of malaria. *Trends Parasitol* 28: 73
- Stremmel C, Schuchert R, Wagner F, Thaler R, Weinberger T, Pick R, Mass E, Ishikawa-Ankerhold HC, Margraf A, Hutter S, *et al* (2018) Yolk sac macrophage progenitors traffic to the embryo during defined stages of development. *Nat Commun* 9
- Summers KM, Bush SJ & Hume DA (2020) Network analysis of transcriptomic diversity amongst resident tissue macrophages and dendritic cells in the mouse mononuclear phagocyte system. *PLoS Biol* 18
- Sun L, Su Y, Jiao A, Wang X & Zhang B (2023) T cells in health and disease. *Signal Transduction and Targeted Therapy* 2023 8:1 8: 1–50
- Svendsen P, Etzerodt A, Deleuran BW & Moestrup SK (2020) Mouse CD163 deficiency strongly enhances experimental collagen-induced arthritis. *Sci Rep* 10
- Swartzendruber C & Congdon CC ELECTRON MICROSCOPE OBSERVATIONS ON TINGIBLE BODY MACROPHAGES IN MOUSE SPLEEN.
- Targett GAT & Fulton JD (1965) Immunization of rhesus monkeys against *Plasmodium knowlesi* malaria. *Exp Parasitol* 17: 180–193

- Testa U, Pelosi E & Peschle C (1993) The transferrin receptor. *Crit Rev Oncog* 4: 241–276
- Theurl I, Hilgendorf I, Nairz M, Tymoszuk P, Haschka D, Asshoff M, He S, Gerhardt LMS, Holderried TAW, Seifert M, *et al* (2016) On-demand erythrocyte disposal and iron recycling requires transient macrophages in the liver. *Nat Med* 22: 945
- Thomsen JH, Etzerodt A, Svendsen P & Moestrup SK (2013) The haptoglobin-CD163-heme oxygenase-1 pathway for hemoglobin scavenging. *Oxid Med Cell Longev* 2013
- Togbe D, Schofield L, Grau GE, Schnyder B, Boissay V, Charron S, Rose S, Beutler B, Quesniaux VFJ & Ryffel B (2007) Murine cerebral malaria development is independent of toll-like receptor signaling. *Am J Pathol* 170: 1640–1648
- Toussirot E, Bonnefoy F, Vauchy C, Perruche S & Saas P (2021) Mini-Review: The Administration of Apoptotic Cells for Treating Rheumatoid Arthritis: Current Knowledge and Clinical Perspectives. *Front Immunol* 12: 630170
- Trzebanski S & Jung S (2020) Plasticity of monocyte development and monocyte fates. *Immunol Lett* 227: 66–78
- Ulven SM, Dalen KT, Gustafsson JÅ & Nebb HI (2005) LXR is crucial in lipid metabolism. *Prostaglandins Leukot Essent Fatty Acids* 73: 59–63
- Underhill DM, Gordon S, Imhof BA, Núñez G & Bousso P (2016) Élie Metchnikoff (1845–1916): celebrating 100 years of cellular immunology and beyond. *Nature Reviews Immunology* 2016 16:10 16: 651–656

- Urban BC, Mwangi T, Ross A, Kinyanjui S, Mosobo M, Kai O, Lowe B, Marsh K & Roberts DJ (2001) Peripheral blood dendritic cells in children with acute *Plasmodium falciparum* malaria. *Blood* 98: 2859–2861
- Valderramos SG & Fidock DA (2006) Transporters involved in resistance to antimalarial drugs. *Trends Pharmacol Sci* 27: 594–601
- Vallelian F, Buzzi RM, Pfefferlé M, Yalamanoglu A, Dubach IL, Wassmer A, Gentinetta T, Hansen K, Humar R, Schulthess N, *et al* (2022a) Heme-stress activated NRF2 skews fate trajectories of bone marrow cells from dendritic cells towards red pulp-like macrophages in hemolytic anemia. *Cell Death & Differentiation* 2022 29:8 29: 1450–1465
- Vallelian F, Buzzi RM, Pfefferlé M, Yalamanoglu A, Dubach IL, Wassmer A, Gentinetta T, Hansen K, Humar R, Schulthess N, *et al* (2022b) Heme-stress activated NRF2 skews fate trajectories of bone marrow cells from dendritic cells towards red pulp-like macrophages in hemolytic anemia. *Cell Death Differ* 29: 1450
- Venugopal K, Hentzschel F, Valkiūnas G & Marti M (2020) *Plasmodium* asexual growth and sexual development in the haematopoietic niche of the host. *Nat Rev Microbiol* 18: 177–189 doi:10.1038/s41579-019-0306-2 [PREPRINT]
- Waas B & Maillard I (2017) Fetal hematopoietic stem cells are making waves. *Stem Cell Investig* 2017 doi:10.21037/sci.2017.03.06 [PREPRINT]
- Walliker D, Carter R & Morgan S (1971) Genetic recombination in malaria parasites. *Nature* 232: 561–562
- Weaver LK, Pioli PA, Wardwell K, Vogel SN & Guyre PM (2007) Up-regulation of human monocyte CD163 upon activation of cell-surface Toll-like receptors. *J Leukoc Biol* 81: 663–671

- Weisser SB, van Rooijen N & Sly LM (2012) Depletion and reconstitution of macrophages in mice. *Journal of Visualized Experiments*
- Weledji EP (2014) Benefits and risks of splenectomy. *Int J Surg* 12: 113–119
- Wen Y, Lambrecht J, Ju C & Tacke F (2021) Hepatic macrophages in liver homeostasis and diseases-diversity, plasticity and therapeutic opportunities. *Cell Mol Immunol* 18: 45–56 doi:10.1038/s41423-020-00558-8 [PREPRINT]
- Werner Y, Mass E, Ashok Kumar P, Ulas T, Händler K, Horne A, Klee K, Lupp A, Schütz D, Saaber F, *et al* (2020a) Cxcr4 distinguishes HSC-derived monocytes from microglia and reveals monocyte immune responses to experimental stroke. *Nat Neurosci* 23: 351–362
- White NJ (2017) Malaria parasite clearance. *Malar J* 16
- White NJ (2018) Anaemia and malaria. *Malar J* 17: 371
- White NJ (2022) What causes malaria anemia? *Blood* 139: 2268–2269
- Willekens FLA, Werre JM, Kruijt JK, Roerdinkholder-Stoelwinder B, Groenen-Döpp YAM, Van Den Bos AG, Bosman GJCGM & Van Berkel TJC (2005) Liver Kupffer cells rapidly remove red blood cell-derived vesicles from the circulation by scavenger receptors. *Blood* 105: 2141–2145
- Wilson A, Laurenti E, Oser G, van der Wath RC, Blanco-Bose W, Jaworski M, Offner S, Dunant CF, Eshkind L, Bockamp E, *et al* (2008) Hematopoietic stem cells reversibly switch from dormancy to self-renewal during homeostasis and repair. *Cell* 135: 1118–1129

- Winn NC, Volk KM & Hasty AH (2020) Regulation of tissue iron homeostasis: the macrophage “ferrostat”. *JCI Insight* 5: 132964
- Wong SH, Francis N, Chahal H, Raza K, Salmon M, Scheel-toellner D & Lord JM (2009) Lactoferrin is a survival factor for neutrophils in rheumatoid synovial fluid. *Rheumatology (Oxford)* 48: 39
- Wu Q, Sacomboio E, Valente de Souza L, Martins R, Kitoko J, Cardoso S, Ademolue TW, Paixão T, Lehtimäki J, Figueiredo A, *et al* (2023) Renal control of life-threatening malarial anemia. *Cell Rep* 42
- Wykes MN & Good MF (2009) What have we learnt from mouse models for the study of malaria? *Eur J Immunol* 39: 2004–2007
- Yang Q & Wang W (2022) The Nuclear Translocation of Heme Oxygenase-1 in Human Diseases. *Front Cell Dev Biol* 10
- Yap YJ, Wong PF, AbuBakar S, Sam SS, Shunmugarajoo A, Soh YH, Misbah S & Ab Rahman AK (2023) The clinical utility of CD163 in viral diseases. *Clin Chim Acta* 541
- Yona S, Kim KW, Wolf Y, Mildner A, Varol D, Breker M, Strauss-Ayali D, Viukov S, Guilliams M, Misharin A, *et al* (2013) Fate mapping reveals origins and dynamics of monocytes and tissue macrophages under homeostasis. *Immunity* 38: 79
- Yosef N, Vadakkan TJ, Park JH, Poché RA, Thomas JL & Dickinson ME (2018) The phenotypic and functional properties of mouse yolk-sac-derived embryonic macrophages. *Dev Biol* 442: 138–154

- You Y, Myers RC, Freeberg L, Foote J, Kearney JF, Justement LB & Carter RH (2011) Marginal Zone B Cells Regulate Antigen Capture by Marginal Zone Macrophages. *J Immunol* 186: 2172
- Youssef LA, Rebbaa A, Pampou S, Weisberg SP, Stockwell BR, Hod EA & Spitalnik SL (2018) Increased erythrophagocytosis induces ferroptosis in red pulp macrophages in a mouse model of transfusion. *Blood* 131: 2581
- Zhang N, Yu X, Xie J & Xu H (2021) New Insights into the Role of Ferritin in Iron Homeostasis and Neurodegenerative Diseases. *Mol Neurobiol* 58: 2812–2823
- Zhang Y, Qi Y, Li J, Liu S, Hong L, Lin T, Long C & Su XZ (2012) A new malaria antigen produces partial protection against Plasmodium yoelii challenge. *Parasitol Res* 110: 1337–1345
- Zhao J, Jia Y, Mahmut D, Deik AA, Jeanfavre S, Clish CB & Sankaran VG (2023) Human hematopoietic stem cell vulnerability to ferroptosis. *Cell* 186: 732-747.e16
- Zhao JL & Baltimore D (2015) Regulation of Stress-Induced Hematopoiesis. *Curr Opin Hematol* 22: 286
- Zhou W, Wang H, Yang Y, Chen ZS, Zou C & Zhang J (2020) Chloroquine against malaria, cancers and viral diseases. *Drug Discov Today* 25: 2012